

Alma Mater Studiorum – Università di Bologna

DOTTORATO DI RICERCA IN  
SCIENZE BIOTECNOLOGICHE, BIOCOMPUTAZIONALI,  
FARMACEUTICHE E FARMACOLOGICHE

Ciclo 33

**Settore Concorsuale:** 03/D1-CHIMICA E TECNOLOGIE FARMACEUTICHE,  
TOSSICOLOGICHE E NUTRACEUTICO-ALIMENTARI

**Settore Scientifico Disciplinare:** CHIM/08-CHIMICA FARMACEUTICA

SMALL MOLECULES EXPLOITING EMERGING THERAPEUTIC  
OPPORTUNITIES FOR BREAST CANCER TREATMENT

**Presentata da:** Jessica Caciolla

**Coordinatore Dottorato**

Maria Laura Bolognesi

**Supervisore**

Silvia Gobbi

**Esame finale anno 2021**

## *Preface*

This thesis describes the research performed during three years of PhD study. The main project has been carried out at the Department of Pharmacy and Biotechnology, Alma Mater Studiorum-University of Bologna (Italy), under the supervision of Prof. Silvia Gobbi, and is focused on the design and synthesis of small molecules targeting multiple pathways involved in the development of estrogen dependent breast cancer. In the last year of PhD, I spent six months at the VU University of Amsterdam (The Netherlands), under the supervision of Prof. Iwan De Esch, working in a project focused on the development of potential ligands for histamine H<sub>4</sub>-receptor, potentially involved in triple negative breast cancer.

The thesis is divided into four chapters: chapter 1 is an introduction on estrogen dependent breast cancer and different targets involved in its progression.

In chapter 2, the main therapies currently used to fight this disease and the state of the art of drug development in this research field, as well as recently emerged treatment strategies, are discussed.

Chapter 3 reports the different design approaches used for the main project, the synthetic strategies, the biological evaluation (where available) and the experimental procedures applied to obtain the desired molecules.

Chapter 4 is focused on the project carried out in Amsterdam. After a brief introduction on histamine and histamine receptors and ligands, the design and the synthesis of the newly developed compounds is described.

I would like to mainly thank Prof. Silvia Gobbi and all the research group involved in the main project of this thesis, in particular Prof. Alessandra Bisi, Prof. Angela Rampa, Prof. Federica Belluti and Dr. Francesca Seghetti for their support and encouragement. I would also like to thank to Dr. Alessandra Magistrato and Angelo Spinello (International School for Advanced Studies (SISSA), Trieste, Italy) for the computational studies, and Prof. Nadia Zaffaroni and Silvia Martini (Istituto Nazionale dei Tumori, Milano, Italy) for the biological evaluation of the synthesized compounds. Finally, I would like to thank Prof. Iwan De Esch and Dr. Maikel Wijtmans for the great experience at VU University in Amsterdam.

# Table of contents

<b>ABSTRACT</b> .....	I
<b>1. INTRODUCTION</b> .....	1
1.1 BREAST CANCER .....	1
1.2 ESTROGENS.....	3
1.3 THE AROMATASE ENZYME .....	5
1.4 ESTROGEN RECEPTORS .....	8
<b>2. ENDOCRINE THERAPY FOR ER+ BREAST CANCER</b> .....	11
2.1 SERMs .....	11
2.1.1 Development of SERMs: state of the art.....	15
2.2 SERDs.....	18
2.2.1 Development of oral SERDs: state of the art .....	19
2.3 AROMATASE INHIBITORS .....	23
2.3.1 Development of non-steroidal AIs: state of the art .....	26
2.3.2 Development of steroidal AIs: state of the art.....	34
2.4 NEW APPROACHES FOR ER+ BREAST CANCER TREATMENT .....	42
2.4.1 Potential allosteric modulation of aromatase .....	43
2.4.2 Multipotent agents targeting both aromatase and ERs.....	49
<b>3. DESIGN AND SYNTHESIS OF NEW POTENTIAL AGENTS FOR THE TREATMENT OF ER+ BREAST CANCER</b> .....	53
3.1 POTENTIAL ALLOSTERIC OR DUAL-ACTING AROMATASE MODULATORS .....	53
3.1.1 Design and synthesis of alkoxyated imidazolymethylxanthenes.....	53
3.1.2 Design and synthesis of alkoxyated imidazolymethylbenzophenones .....	62
3.1.3 Experimental procedures.....	66
3.2 DESIGN AND SYNTHESIS OF POTENTIAL MULTITARGET AGENTS.....	74
3.2.1 Design and synthesis of potential AIs/SERMs: bisphenols derivatives.....	74
3.2.2 Design and synthesis of potential AIs/SERMs: tricyclic derivatives.....	88
3.2.3 Design and synthesis of potential AIs/SERDs .....	93
3.2.4 Experimental procedures.....	97
<b>4. DESIGN AND SYNTHESIS OF HISTAMINE H<sub>4</sub> LIGANDS POTENTIALLY USEFUL IN THE MANAGEMENT OF TRIPLE NEGATIVE BREAST CANCER</b> .....	121
4.1 HISTAMINE AND HISTAMINE RECEPTORS.....	121

4.1.1 H <sub>1</sub> Receptor (H <sub>1</sub> R) and ligands .....	123
4.1.2 H <sub>2</sub> Receptor (H <sub>2</sub> R) and ligands .....	124
4.1.3 H <sub>3</sub> Receptor (H <sub>3</sub> R) and ligands .....	125
4.1.4 The H <sub>4</sub> Receptor (H <sub>4</sub> R) .....	125
4.2 H <sub>4</sub> R AND BREAST CANCER.....	127
4.3 H <sub>4</sub> R LIGANDS .....	128
4.3.1 H <sub>4</sub> R agonists.....	128
4.3.2 H <sub>4</sub> R antagonists.....	129
4.4 DESIGN AND SYNTHESIS OF POTENTIAL H <sub>4</sub> R LIGANDS.....	132
4.4.1 Experimental procedures.....	136
<b>5. LIST OF ABBREVIATIONS.....</b>	<b>159</b>
<b>6. REFERENCES.....</b>	<b>161</b>

## ABSTRACT

Among the different types of breast cancer (BC), the estrogen receptor positive (ER+) subtype, which requires estrogens for its growth and proliferation, is the most common, while triple negative BC, characterized by the absence of ER, progesterone receptor and human epidermal growth factor receptor 2, often leads to poor prognosis.

First-line therapies for the treatment of ER+ BC act either by suppressing estrogen production, through the inhibition of aromatase (AR) enzyme, or by blocking estrogen prooncogenic activity, *via* the modulation/degradation of ERs. The serious side effects and the intrinsic or acquired resistance phenomena that arise with prolonged use of these drugs limit their therapeutic application, stimulating the search for new strategies to face this disease. In this context, the development of dual acting aromatase inhibitors, able to target both the orthosteric and the recently identified allosteric pockets of AR could be an opportunity to fight ER+ BC. Another promising strategy could be the development of multitarget compounds, targeting both AR and ERs.

In this scenario, here we designed and synthesized two series of new xanthenes or more flexible benzophenones as potential dual acting aromatase inhibitors. Moreover, inspired from tamoxifen metabolites and a literature compound endowed with activity on both AR and ER, different structurally related series of potential multitarget compounds were developed. The biological results showed that some of the new molecules were promising candidates for further development.

It was recently observed that the lately discovered histamine H<sub>4</sub> receptor is expressed in human breast tissue, displaying a key role in biological processes mediated by histamine such as cell proliferation, senescence, and apoptosis in malignant cells, representing a potential target in triple negative BC. Thus, a broad series of methyl quinazoline sulfonamides, carrying different functional groups on the sulfonamide moiety, were designed and synthesized as potential H<sub>4</sub> receptor ligands.

## 1. INTRODUCTION

Breast cancer (BC) is the most common cancer among women and, according to Breast Cancer Facts and Figures 2019-2020, it is estimated that 1 in 8 women (13 %) will develop invasive breast cancer in her lifetime, and 1 in 39 women (3 %) will die from this disease.<sup>1</sup> The prolonged use of first-line therapies currently employed to fight this disease is hampered by the development of severe side effects and intrinsic or acquired resistance. In this scenario, many researchers have focused their interest on the development of new strategies to overcome these drawbacks.

### 1.1 BREAST CANCER

BC is a group of diseases characterized by uncontrolled change and proliferation of breast tissue cells forming masses and lumps. Although the risks of getting BC increase with age, the incidence rate is slower after menopause, because a high percentage of BC is estrogen dependent (ER+) and requires the presence of these hormones for proliferation, and in post-menopausal women there is a drastic decrease in circulating estrogens levels.<sup>2</sup> Other factors that have an impact on BC incidence are menstrual state, age at first pregnancy, race, hormonal therapies and life style. Women who have early first menarche or late menopause have a major risk of getting BC in their lifetime. Likewise, women who have their first pregnancy before 20 years old have a 30-40 % lower risk of BC compared with women who have their first child at the age of 30 or later. The incidence of BC also varies with race, the white population have a higher risk compared with American African and Hispanics. Among exogenous risk factors, life style and hormone replacement therapy (HRT) are the most important, and wrong diet, abuse of alcohol and a sedentary life, that lead to an excessive weight, increase the incidence of BC.<sup>2,3</sup>

BCs can be subdivided into two large groups: in situ carcinoma and invasive carcinoma; in situ carcinoma is further classified in ductal (DCIS) and lobular (LCIS). DCIS is the most common and, usually, it is a precursor of invasive BC, while LCIS is considered as a benign condition in which the risk of developing cancer is greater but there is no progression to invasive cancer.<sup>1</sup> Regarding invasive

BC, although in 40-75 % of cases it is invasive carcinoma of No Special Type (NST), the remaining part is characterized by “special” histological subtypes and is divided into different groups: invasive lobular, tubular, mucinous and metaplastic carcinoma and carcinoma with medullary, neuroendocrine or apocrine features.<sup>4</sup>

A further classification of BC is based on histological tumors grade, that is the degree of differentiation of tumor tissues. The Nottingham Grading System (NGS), the grading system approved by World Health Organization (WHO), American Joint Committee on Cancer (AJCC) and other professional bodies, classifies tumors in different degrees considering three morphological features: degree of tubule or gland formation, nuclear pleomorphism and mitotic count. Tumors of grade 1 have well-differentiated tissues with high degree of tubule formation (> 75 %), a mild degree of nuclear pleomorphism and low mitotic count, those of grade 2 are characterized by moderate differentiation and those of grade 3 by low differentiation with no tubule formation (< 10 %).<sup>5</sup>

Finally, expression of certain markers such as estrogen receptor (ER), progesterone receptor (PR) and overexpression of human epidermal growth factor receptor 2 (HER2) have been used to classify BCs into different molecular subtypes. There are four main molecular groups: luminal A, luminal B, HER2-enriched and basal like. *Luminal A* is the most common type of BC and it is ER and/or PR positive and HER negative. Thanks to the presence of these markers, it is the tumor with the most favorable prognosis as it usually responds positively to endocrine therapy. *Luminal B* is ER and/or PR positive and HER positive with high levels of protein Ki67 (an indicator associated with tumor cell proliferation and growth). This type of cancer grows faster than Luminal A cancers and, for this reason, its prognosis is slightly worse. *HER2-enriched* is ER and PR negative and HER positive. In the past, it had the worst prognosis because it tends to grow faster than luminal cancers but, to date, the use of targeted therapies has improved the life prospects for these patients. *Basal-like* is ER, PR and HER2 negative and it is also called triple negative BC. This kind of tumor spreads and grows faster than the other cancers and it has poor prognosis; it is more common between black women. This molecular classification is important because it allows to predict prognosis and potential response to endocrine therapy.<sup>1, 3, 6</sup>

## 1.2 ESTROGENS

Estrogens are a group of steroids characterized by a 18C central core. Their peculiarity with respect to other steroid hormones is the presence in their structure of an aromatic ring with a phenol group at C3. The most common estrogens in humans are estrone (E1), characterized by a ketone group at C17, 17 $\beta$ -estradiol (E2), with a hydroxyl group at C17, and 17 $\beta$ ,16 $\alpha$ -estriol (E3) that presents two hydroxyl groups at C16 and C17 (Figure 1).

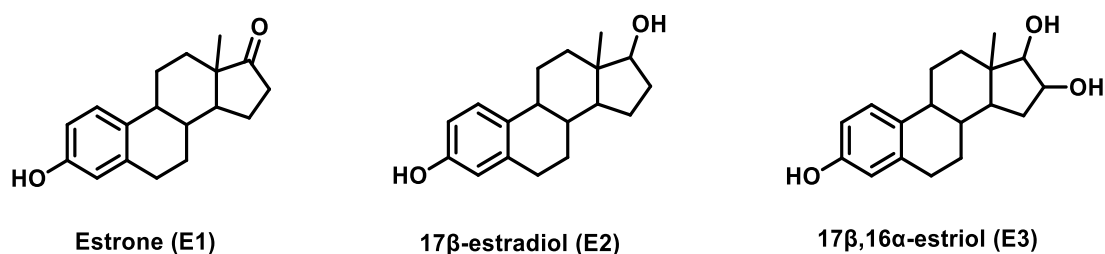


**Figure 1.** Structures of the most common estrogens.

Estrogens, like all steroid hormones, are synthesized from cholesterol in a process called steroidogenesis (Figure 2), in which 27C cholesterol is metabolized by a wide array of enzymes to give C21-, C19- or C18-steroids.<sup>7</sup> In the first phase, that represents the rate-limiting step of this biosynthetic process, cholesterol is converted into pregnenolone (P5) by the cholesterol side-chain cleavage enzyme (P450<sub>scc</sub>, CYP11A1), a cytochrome P450 located within the mitochondria that hydrolyzes the side chain of cholesterol in a three-steps process. The transport of cholesterol from the cytosol within the mitochondria is regulated by steroidogenic acute regulatory protein (StAR), a 37 kDa transport protein mainly present in steroid-producing cells. It has been observed that each StAR molecule can carry only one molecule of cholesterol at a time through the mitochondrial membrane, but every StAR molecule is responsible for the transport of more than 100 molecules of cholesterol.<sup>8</sup> P5 can be converted first to 17 $\alpha$ -hydroxypregnenolone and then to dehydropiandrosterone (DHEA) by 17 $\alpha$ -hydroxylase (P450<sub>c17</sub>, CYP17A1), or to progesterone by 3 $\beta$ -hydroxysteroid dehydrogenase (3 $\beta$ -HSD2). Then, DHEA and progesterone are both converted to androstendione (ASD) by the

action of  $3\beta$ -HSD2 or CYP17A1, respectively. ASD is further transformed into the two most common estrogens in the body, E1 and E2, by the action of two enzymes:  $17\beta$ -hydroxysteroid dehydrogenase and aromatase (AR, CYP19A1).  $17\beta$ -hydroxysteroid dehydrogenase ( $17\beta$ -HSD3/5) is responsible for the conversion of ASD into testosterone (TST) and of E1 into E2 ( $17\beta$ -HSD1), while AR converts ASD into E1 and TST into E2.

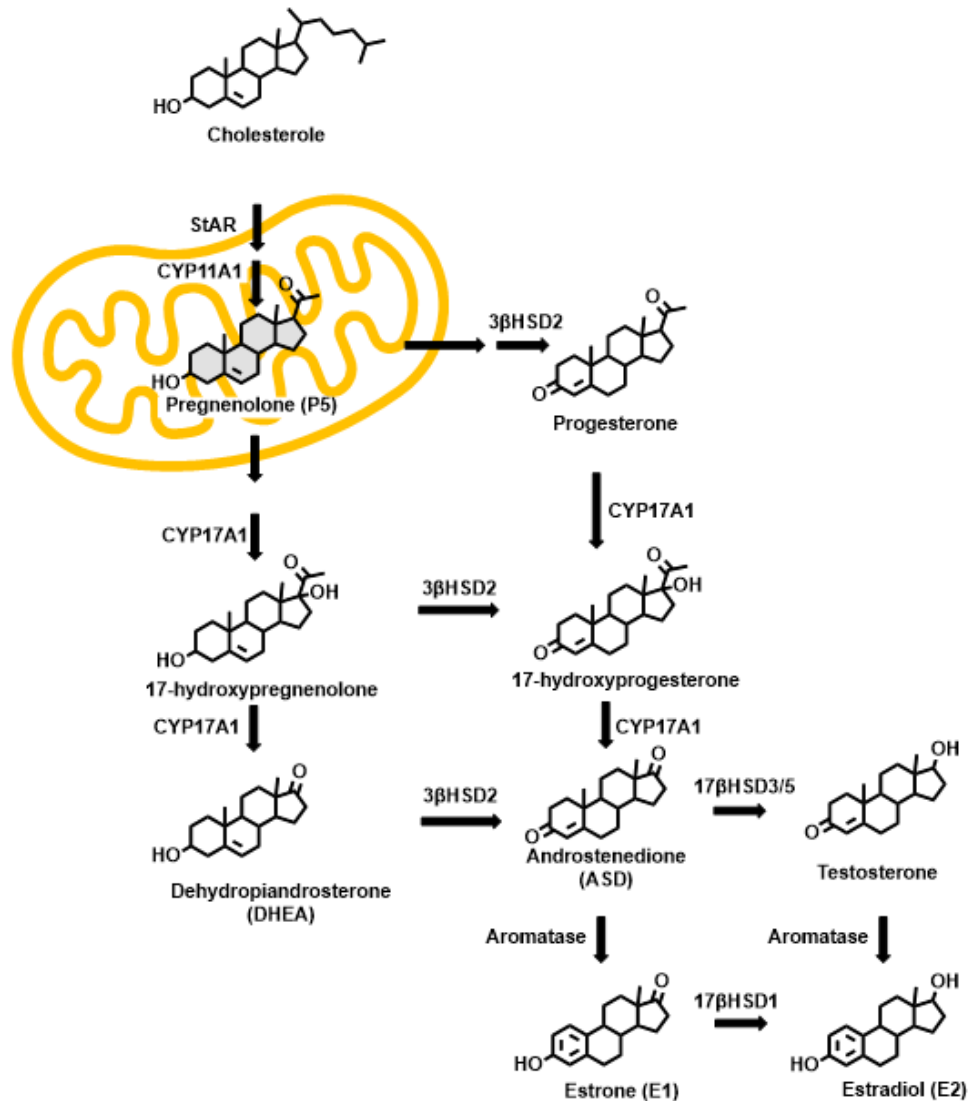


**Figure 2.** Estrogens biosynthetic pathway.

In premenopausal women, estrogens are mainly synthesized in the ovaries by theca and granulosa cells, and in minimal part in several other tissues, such as adipose tissue of the breast, osteoblast and chondrocytes, aortic smooth muscle cells,

vascular endothelium and several parts of the brain. In postmenopausal women, due to the drop in ovary function, and in men, the extragonadal tissues represent the main source of estrogen synthesis.

The main role of estrogens is their involvement in the proliferation and growth of tissues related to female development and reproduction. Moreover, they are responsible for the regulation of skeletal homeostasis, lipids and carbohydrates metabolism, electrolytes balance, skin physiology, and affect cardiovascular and central nervous systems (CNS).<sup>9</sup>

### 1.3 THE AROMATASE ENZYME

Human AR, belonging to the cytochrome P450 superfamily, is an integral membrane protein, anchored to the membrane of the endoplasmic reticulum by the amino terminal domain. It is responsible of the aromatization of ASD, TST, and 16 $\alpha$ -hydroxytestosterone to E1, E2, and E3, respectively. AR is the only enzyme able to catalyze the key step of estrogens endogenous biosynthesis and, for this reason, its activity is highly specific.<sup>10, 11</sup> In humans, the gene of CYP19A, cloned for the first time in the early 90s,<sup>12-14</sup> is located on chromosome 15q21.2 and is composed by 30 kb of coding region and 93 kb of regulatory region. The gene structure comprises 10 exons and, within the regulatory region, there are 10 different promoters distributed in a tissues-specific manner.<sup>15</sup> In humans, several tissues express AR and are thus able to synthesize estrogens; these comprise ovaries and testes, placenta, adipose tissue, bone (chondrocytes and osteoblasts), vascular smooth muscle and numerous sites in the brain (hypothalamus, limbic system, cerebral cortex).<sup>16</sup> AR is a multi-enzymatic complex, formed by the cytochrome P450 heme protein (CYP19A1), responsible for the aromatization process, and NADPH-cytochrome P450 reductase (CPR), which provides the electrons needed for the reaction (Figure 3). CPR is a transmembrane protein, composed by two flavin-containing domains linked to each other by a “connecting domain”: the flavin adenine dinucleotide (FAD) domain, also containing the NADPH binding site, and the flavin mononucleotide (FMN) domain. An additional hydrophobic loop connects the FMN domain to the membrane. The electronic transfer (ET), necessary

for the aromatization reaction, requires specific interdomain interactions, since it is considered to occur from the NADPH/FAD to the FMN domains and then to the hemeprotein, thus FMN plays the key role of recognizing both the FAD domain and CYP19A1. Through these interactions, CPR is in a dynamic equilibrium between an “open” and a “closed” conformation. In the “closed” form, the FMN is close to the FAD/NADPH domain, favoring the internal transfer of electrons, while in the “open” arrangement, the two subdomains are far away and FMN binds through electrostatic interactions a highly conserved portion of CYP19A1. The latter conformation enables the intermolecular ET from FMN to the P450 hemeprotein. Since both the FMN domain and CYP19A1 are connected to the membrane by their hydrophobic anchor, the movement of the FAD/NADPH domain, via the hinge, is responsible for the interconversion between the closed and the open form, and regulates the electronic activity of CPR (Figure 3).<sup>17, 18</sup>

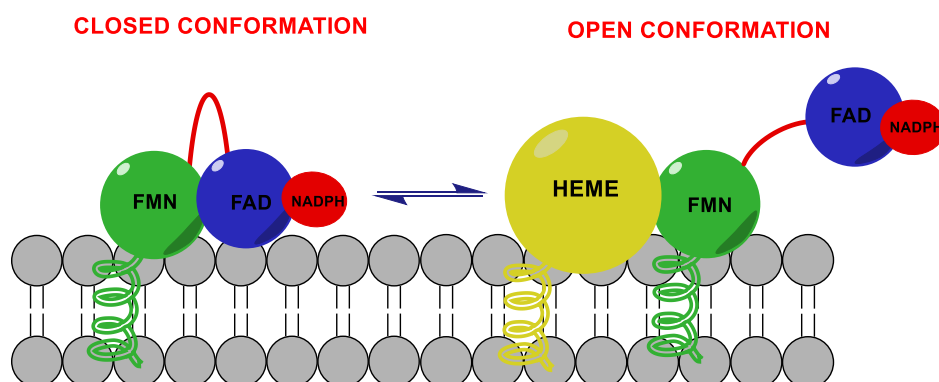


**Figure 3.** Aromatase complex. Flavin adenine dinucleotide (FAD) and flavin mononucleotide (FMN) domains of NADPH-cytochrome P450 reductase (CPR) can take a “closed” conformation, favoring the internal transfer of electrons, or an “open” conformation, where the two cofactor domains are far away, allowing the transfer of electrons from FMN to P450 hemeprotein.<sup>19</sup>

In 2009, Ghosh *et al.* reported for the first time the crystallographic structure of human placental AR with ASD, the natural substrate of the enzyme.<sup>20</sup> This work allowed to get new information about the structure of this enzyme, until then postulated on the basis of sequence homologies with other P450s.<sup>21, 22</sup> It was possible to establish the binding pose of androgens within the enzyme active site and to explain the peculiar substrate selectivity of AR compared with other

cytochromes. AR consists of a heme group and a single polypeptide of 503 amino acids that folds up in a tertiary structure composed by 12  $\alpha$ -helices (A-L) and 10  $\beta$ -strands (1-10) distributed into 3 major sheets and 1 minor.<sup>23</sup> From the crystal structure of the AR-ASD complex it was observed that Pro308, a specific residue of AR, causes a 3.5 Å dislocation of the central axes of I-helix, which results in the formation of the androgen specific binding pocket at the active site of the enzyme. ASD settles into this binding site by arranging its  $\beta$ -face towards the heme group and C19 4.0 Å from the iron atom. Moreover, the axes shift, allowing ASD to place its 3-keto group near the fifth turn of the helix, enabling the formation of a hydrogen bond between the side chain of Asp309 and the oxygen of this keto group. The Asp309 residue is also important for the stabilization of this displacement because it forms strong hydrogen bonds with Thr310 (2.8 Å) and with water (3.4 Å).<sup>20</sup> AR performs its function in a three-steps process that involves the consumption of 3 mol of O<sub>2</sub> and 3 mol of NADPH. The first two steps (Figure 4) are classical hydroxylation reactions, typical of most cytochromes P450, to give a C19-gem-diol (compound II, Figure 4) which undergoes a dehydration reaction leading to the formation of the corresponding C19-aldehyde (compound III, Figure 4).

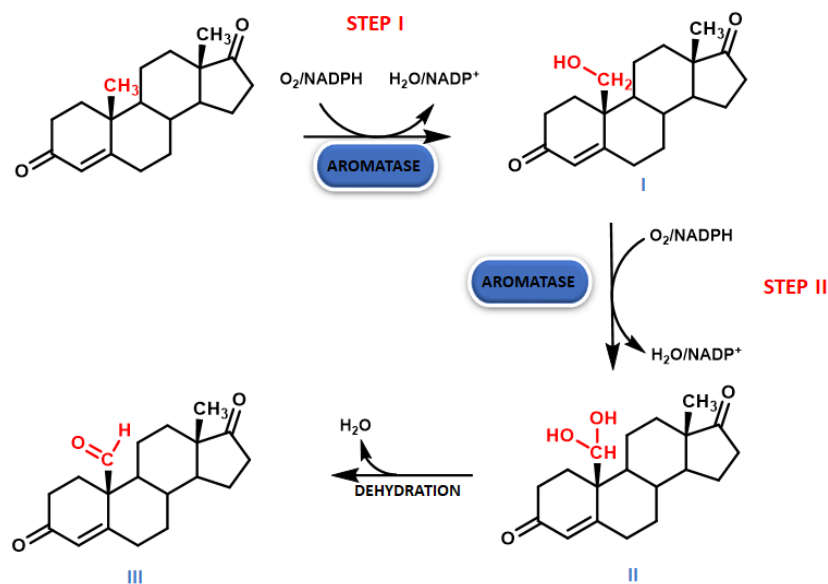


**Figure 4.** First two steps of AR aromatization process.

The third step represents the real aromatization reaction and involves the elimination of the aldehyde group of compound III (Figure 4) and the formation of the aromatic ring. Despite the numerous studies performed to understand the mechanism underlying this step of the AR-catalyzed aromatization process and the different hypothesis developed so far,<sup>24-26</sup> there is still considerable controversy regarding this issue.

#### 1.4 ESTROGEN RECEPTORS

Estrogens perform their physiological functions interacting with their receptors (ERs). There are two classes of receptors: nuclear estrogen receptors (ER $\alpha$  and ER $\beta$ ), which are nuclear transcription factors, and the lately identified membrane estrogen receptors (mERs) that belong to the G protein-coupled receptors superfamily.<sup>27</sup>

ER $\alpha$  was discovered by Jensen and Jacobson in the 1960s and the corresponding gene was cloned in 1986;<sup>28</sup> later, in 1996, Kuiper *et al.* discovered the existence of a new estrogen receptor, called ER $\beta$ , expressed in rat prostate and ovary.<sup>29</sup> ER $\alpha$  and ER $\beta$  are encoded by different genes, the gene for ER $\alpha$  is located on 6q25.1 chromosome, while ER $\beta$  gene is observed on 14q23.2 chromosome. The human ER $\alpha$  is formed by 595 amino acids with molecular size of 66 kDa, while ER $\beta$  has a length of 530 amino acids and a molecular size of 54 kDa. The two receptors show a high similarity in their amino acid sequences and are formed by six different functional regions (Figure 5). Among these, the three main domains are known as N-terminus domain (NTD, A/B domain), DNA binding domain (DBD, C domain) and ligand-binding domain (LBD, E domain).<sup>30</sup> The transcriptional activity of these receptors is mediated by two different activation functions: AF1, located within the NTD, that is an independent activation function and shows a small similarity between ER $\alpha$  and ER $\beta$ , and AF2, located within the LBD, that is a ligand-dependent activation domain.

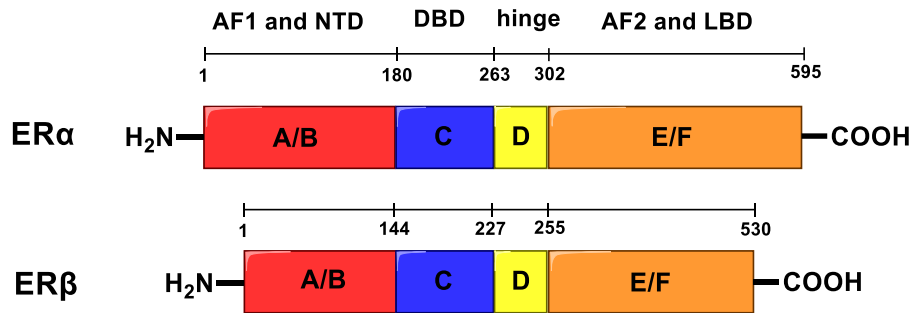


**Figure 5.** Structure of  $\alpha$  and  $\beta$  estrogen receptors (ERs). In red (A/B) the independent activation function 1 (AF1) and the N-terminus domain (NTD), in blue (C) the DNA binding domain (DBD), in yellow (D) the flexible hinge and in orange (E/F) the ligand-dependent activation function 2 (AF2) and the ligand binding domain (LBD).

The distribution of the two receptors varies depending on the tissue; ER $\alpha$  is mainly expressed in ovary (thecal cells), uterus, prostate (stroma), Leydig cells in testis, epididymis, breast and liver, while ER $\beta$  is mainly present in prostate (epithelium), testes, ovary (granulosa cells), bone marrow and brain. Moreover, ER $\alpha$  and ER $\beta$  are involved in cells proliferation and can have opposite effects, since ER $\alpha$  is able to stimulate cell growth, while ER $\beta$  has antiproliferative effects, counteracting the activity of ER $\alpha$ , and the final response is therefore given by a balance of the two effects.<sup>31, 32</sup>

Recently, a new type of estrogen receptor was discovered, the G Protein-Coupled Estrogen Receptor (GPER1) or mER, a member of the G protein-coupled receptors superfamily. It is widely expressed in the brain and at the level of synapse and, binding to G proteins and modulating second messenger signaling cascades, it seems to be the main responsible for the rapid non-genomic action of estrogens.<sup>33</sup> Based on the events that follow the activation of ERs (modulation of gene expression or activation of signaling cascades), estrogen-dependent signaling can be divided in genomic and non-genomic. Moreover, the binding of estrogen-ER complex to DNA can occur directly or indirectly. Thus, ER-mediated signaling can be divided based on four different mechanisms. *Direct genomic signaling:* considering the classical signaling mechanism, the binding between estrogens and ER $\alpha$  or ER $\beta$  leads to a conformational change that allows receptor dimerization. The dimer is then translocated into the cell nucleus, where the complex estrogen-ER interacts with chromatin in correspondence of specific DNA sequences called

estrogen response elements (ERE), located in proximity of genes promoters. In this way, estrogen-ER complex modulates genes transcription.<sup>9</sup> *Indirect genomic signaling*: there is no direct binding between estrogen-ER complex and DNA, but the modulation occurs through protein-protein interactions, with the involvement of other transcription factors and their response elements. In this way, estrogens can also regulate the expression of genes that do not have EREs near the promoters. Around one third of the genes modulated by estrogens lack ERE-like sequences. *Non-genomic signaling*: it was observed that some responses mediated by estrogens occurred too fast to be associated to gene transcription and to protein synthesis. Estrogens interact with membrane receptor GPER1, triggering changes such as stimulation of adenylate cyclase and cyclic adenosine monophosphate (cAMP) production, mobilization of intracellular calcium and activation of various protein-kinases cascades that can lead to an indirect modulation of gene expression through the phosphorylation of transcription factors. *Ligand independent signaling*: ERs can also be activated in the absence of estrogens or other appropriate ligands, for example through phosphorylation of serine and tyrosine residues. This mechanism is modulated by regulators of general cellular phosphorylation state (protein kinase A (PKA) or protein kinase C (PKC)), extracellular signals such as peptide growth factors, cytokines or neurotransmitters and cell cycle regulators.<sup>9, 27, 34</sup>

## 2. ENDOCRINE THERAPY FOR ER+ BREAST CANCER

Two main therapies are currently used in the treatment of the ER+ BC, acting on two different targets. The first is represented by molecules able to bind ERs and to selectively modulate their activity (SERMs or SERDs), while the second involves the inhibition of the key enzyme AR, blocking the endogenous biosynthesis of estrogens.

### 2.1 SERMs

SERMs (Selective Estrogen Receptor Modulators) represent the first class of compounds developed for the treatment of ER+ BC. They are nonsteroidal compounds able to bind estrogen receptors ER $\alpha$  and ER $\beta$  showing a tissue-selective pharmacology. They act as agonists in tissues such as bone, liver, and cardiovascular system, as antagonists in other tissues, such as breast and brain, and as mixed agonists/antagonists in the uterus.<sup>35</sup> The peculiar pharmacology of SERMs is due to three main mechanisms: the tissue-specific expression of ER $\alpha$  and ER $\beta$ , different conformational changes of the receptor generated by ligand binding, and different expression and binding of co-factors to the receptors. Primarily, the level of expression of homodimers of one or both receptors change in the different types of estrogen target cells. The two subtypes have opposite effects, since ER $\alpha$  mainly acts as an activator, while ER $\beta$  has antiproliferative effects, counteracting ER $\alpha$  activity. Thus, the different levels of expression of the two receptors influence the effect of estrogens and of compounds able to bind both receptor subtypes. Moreover, based on the different ligands binding, the receptor undergoes different conformational changes, and the binding with SERMs produces an intermediate shape between the two extreme conformations generated by an agonist and an antagonist. In addition, more than 20 coregulators, involved in the modulation of estrogenic activity, have been discovered. Depending on the type of conformation induced, the receptor interacts with different cofactors modulating its function.<sup>36</sup> The binding of estrogen to the hydrophobic pocket of the LBD allows helix 12 to cap and seal the ligand inside the ligand-binding pocket, leading to the opening of AF-2 fissure and allowing the binding of coregulators to the LXXLL motifs inside

the cleft. Conversely, when a SERM binds to the receptor, a conformational change occurs between helices 11 and 12, preventing helix 12 from sealing the LBD and pushing H12 to reach AF-2 surface. H12 interacts with the LXXLL motifs, mimicking and preventing the cofactors from binding to AF-2, thus blocking receptor activation.<sup>37</sup>

The prototype of this class of compounds is tamoxifen (TAM, Figure 6), a triphenylethylene derivative originally known as ICI 46,474, synthesized in 1962 in the pharmaceutical laboratories of the Imperial Chemical Industries (ICI) within a project to develop a contraceptive pill. Despite being designed as antiestrogen, this compound showed to stimulate ovulation in women, and for this reason at first it was not patented in the USA. The usefulness of this molecule was reconsidered when Arthur Walpole, the team's leader, included TAM in a project involved in the development of treatment for ER+ BC. In 1973, it was approved by the Committee on the Safety of Medicines in the United Kingdom for the treatment of BC and some years later, in 1977, it was approved in the USA by Food and Drug Administration (FDA).<sup>38</sup> TAM is administered as single *Z*-isomer (as the citrate salt), endowed with higher affinity for estrogen receptors with respect to its *E*-counterpart.

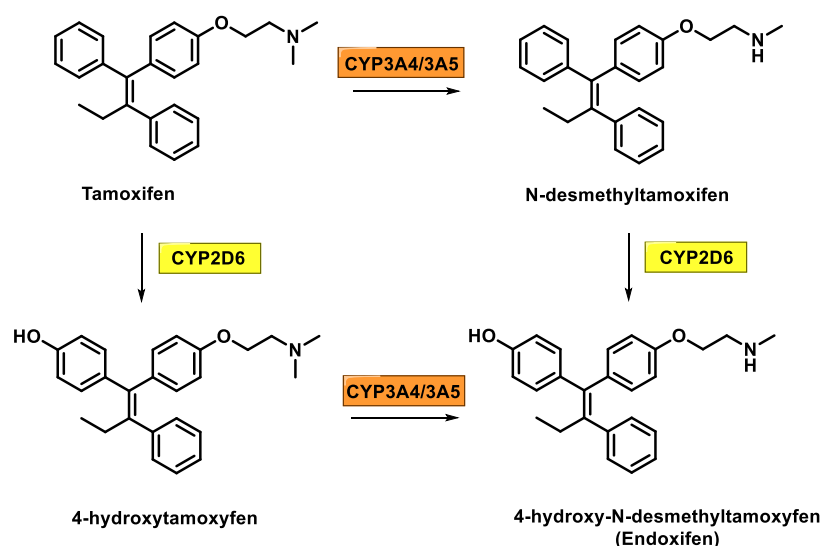


**Figure 6.** Tamoxifen (TAM) and its main metabolites.

Within the body, TAM is converted by different cytochromes P450 in three main active metabolites (Figure 6): 4-hydroxytamoxifen, *N*-des-methyltamoxifen, and 4-hydroxy-*N*-desmethyltamoxifen (endoxifen, END). Pharmacological studies of TAM metabolism indicate that the anticancer activity of this drug is mainly due to the action of its metabolites, in particular 4-hydroxytamoxifen and END, obtained by the action of hepatic CYP2D6 and CYP3A4/5 that catalyze hydroxylation and *N*-demethylation, respectively.<sup>39</sup> Despite its therapeutic benefits, prolonged use of TAM leads to the development of intrinsic and acquired resistance and notable side effects such as endometrial cancer, caused by its agonistic effect in the uterine tissues. Several studies demonstrated that women receiving TAM have two to three times greater risk of developing endometrial cancer than the rest of the population, and this risk is dose and time dependent.<sup>40</sup>

In addition to TAM, compounds belonging to the SERMs class can be classified based on their chemical structure as triphenylethylenes (TAM and TAM-like), benzothiophenes (raloxifene, arzoxifene), phenylindoles (bazedoxifene, pipendoxifene) and tetrahydronaphthalenes (lasofoxifene).

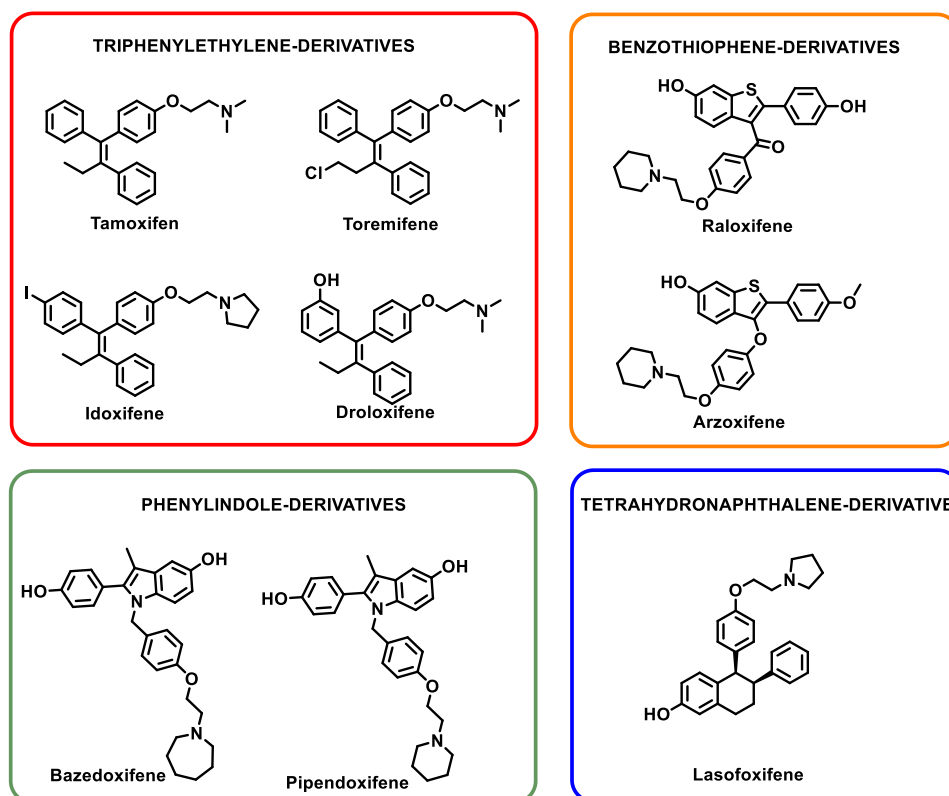


**Figure 7.** Structures of different classes of SERMs.

The side effects of TAM on the endometrium led to the development of TAM derivatives that could reduce negative events while maintaining high activity. Toremifene (Figure 7), a triphenylethylene antiestrogen synthesized for the first time in 1981, differs from TAM only for a chlorine atom on the ethyl chain. It presented a weaker estrogenic effect compared to TAM, but the two compounds exhibited similar safety and side effects profile.<sup>41</sup> Droloxifene (Figure 7), also known as 3-hydroxytamoxifen, carries a hydroxyl group on the phenyl moiety of TAM. Its preclinical profile was qualitatively similar to that of TAM, demonstrating clinical activity in the same range of that observed with TAM in phase II clinical trials. Nevertheless, its development for the treatment of BC was stopped in phase III clinical trials.<sup>42</sup> Idoxifene (Figure 7) is another TAM derivative with an iodine atom in position 4, developed to improve the potency and reduce the side effects of TAM. This compound was active and well tolerated in postmenopausal women with metastatic BC and exhibited efficacy and safety similar to TAM. The lack of benefits with respect to TAM led to the interruption of idoxifene development.<sup>43</sup> Raloxifene (Figure 7), also known as keoxifene, is a benzothiophene derivative that acts as an estrogen agonist in some tissues, such as skeleton and lipids, but exerts an antagonist effect on breast and uterus, being able to inhibit the endometrial carcinoma stimulated by TAM. Raloxifene was approved for medical use in the United States by the FDA in 1997.<sup>44, 45</sup> Arzoxifene (Figure 7) is a benzothiophene structurally related to raloxifene, in which the carbonyl moiety was replaced with an ether linker and the hydroxyl group was methylated improving the pharmacokinetics properties of the molecule. Arzoxifene is a potent antagonist in the breast and acts as agonist to maintain bone density and to lower serum cholesterol. Unlike TAM, this compound did not show uterotrophic effect, suggesting a lower risk of developing endometrial cancer. However, arzoxifene was never marketed because its clinical development was terminated.<sup>46</sup>

Over the years, other SERMs with an indolic structure (bazedoxifene and pibendoxifene) were developed. Bazedoxifene (WAY 142404, Figure 7) is an indole-based SERM developed by Wyeth pharmaceutical and currently approved in Europe and in the USA for prevention and treatment of osteoporosis. This

compound presents antagonistic activity on the breast with no agonistic effects on the endometrium, while preserving estrogenic activity on the skeleton. Given its peculiar profile, bazedoxifene could represent a new therapeutic tool for the treatment of osteoporosis and BC.<sup>47</sup> Pipendoxifene (ERA-923, Figure 7), is an indole-derivative with a piperidine ring on the side chain. It inhibits BC growth mediated by estrogens, while not showing uterotrophic effects. It was developed for the treatment of TAM-resistant BC, but it was never marketed.<sup>48, 49</sup>

The search for compounds with SERM activity and with a good oral bioavailability led to the development of lasofoxifene (Figure 7), a naphthalene-derivative that shows high affinity for both ERs, good safety profile and high efficacy in preventing bone loss. It was observed that, in post-menopausal women with osteoporosis, lasofoxifene treatment caused a decrease in the development of ER+ BC.<sup>50</sup>

#### 2.1.1 Development of SERMs: state of the art

Given the great therapeutic efficacy of TAM, over the years many research groups have focused on the design and synthesis of new potential SERMs by modifying its structure. However, most of the triphenylethylene derivatives reported in literature also showed cytotoxic activity against MDA-MB-231 (ER-) cells, suggesting an ER-independent activity.

Starting from the structure of TAM derivative ospemifene, Kaur *et al.*<sup>51</sup> synthesized some analogs by replacing Cl with an amine, azide or amide group and/or the hydroxy group with an amine or azide group (Figure 8). Compounds carrying an amine or amide group proved to be more effective than ospemifene against both MCF-7 (ER+) and MDA-MB-231 (ER-) cell lines. Among these, compound **1** (Figure 8) was slightly more selective for MFC-7 cells (MCF-7 and MDA-MB-231, IC<sub>50</sub> = 76 and > 100 μM, respectively) while compound **2** (Figure 8) resulted to be the best compound of the series on both cell lines (MCF-7 and MDA-MB-231, IC<sub>50</sub> = 11.2 and 13.4 μM, respectively).

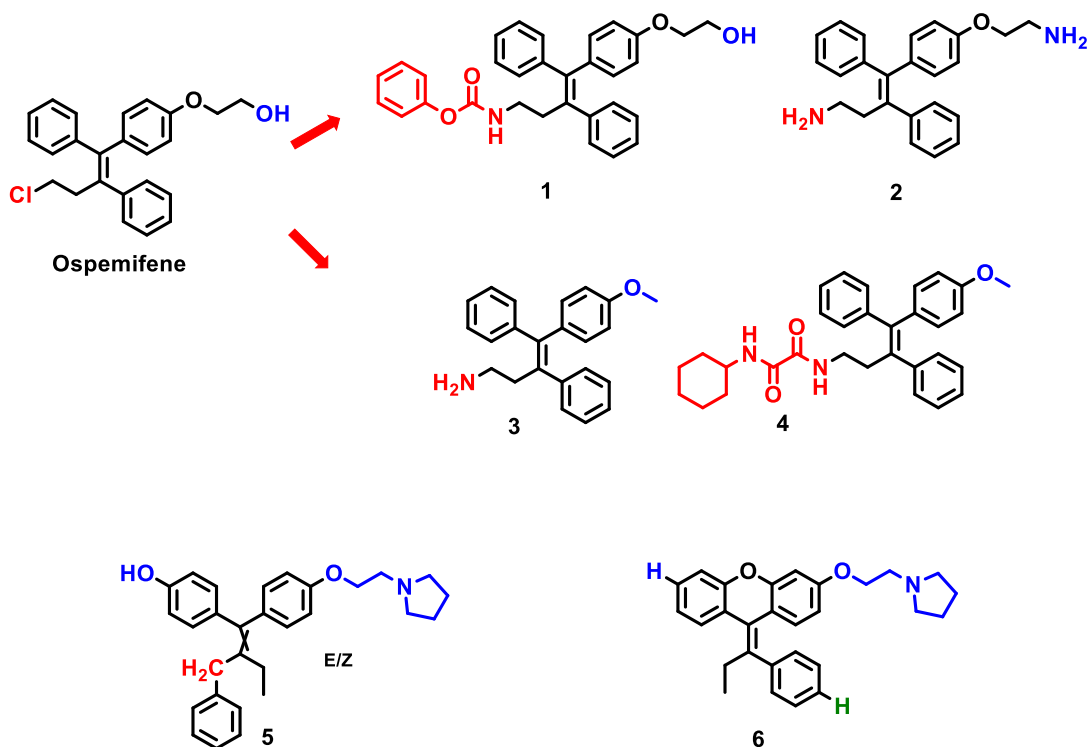


**Figure 8.** Structures of different recently developed TAM derivatives.

In 2016, the same research group developed a new series of triarylethylene derivatives by replacing the Cl group of ospemifene with an amino-/amidoethyl moiety and the TAM dimethylaminoethoxy chain with a short methoxy chain.<sup>52</sup> Compounds **3** (MCF-7 and MDA-MB-231,  $IC_{50} = 16.9$  and  $11.4 \mu M$ , respectively) and **4** (MCF-7 and MDA-MB-231,  $IC_{50} = 12.1$  and  $12.2 \mu M$ , respectively) (Figure 8) proved to have potent activity against both MCF-7 and MDA-MB-231 cell lines. These results suggested that the presence of an amino or oxalamido group on the O-methyl derivatives caused an increase in potency, while the shortening of the O-hydroxy ethyl chain to the O-methyl chain did not affect the activity.

Some flexible TAM derivatives were synthesized by Elghazawy *et al.*<sup>53</sup> A hydroxy or an ester group were inserted in *para* position on one of the phenyl rings, blocking the hydroxylation catalyzed by CYP2D6, and a methylene spacer between the other phenyl ring and the central double bond was added, providing flexibility to the structure. Furthermore, dimethylaminoethoxy, pyrrolidinyloxy, or piperidinyloxy side chains were introduced to investigate the effect of cyclization, size of the ring and nitrogen basicity. The antiproliferative activity of

the new derivatives was evaluated against the MCF-7 cell line and all compounds exhibited higher activities than TAM. The best compound (**5**, Figure 8), carrying a pyrrolidinylethyloxy side chain, showed an  $IC_{50}$  value  $< 0.25 \mu\text{M}$  and 80-times higher binding affinity and 900 times higher selectivity towards  $ER\alpha$  than TAM. In 2019, Catanzaro and coworkers developed new TAM derivatives, in which some structural modifications provided greater rigidity to the molecule; in particular, the dimethylaminoethyloxy side chain was replaced by pyrrolidinylethyloxy or different aminobutyloxy tails.<sup>54</sup> Other structural changes affected the triphenylethylene central core that was merged with a xanthene structure giving compound **6** (Figure 8), that proved to be the best compound of the series, with  $IC_{50}$  values of 12.4 and 25.4  $\mu\text{M}$  against MCF-7 and MDA-MB-231, respectively. New naphthalene derivatives were synthesized by Jha *et al.*<sup>55</sup> In these new series of compounds, a 4-hydroxypiperidine and different dialkylaminoethoxybenzyl groups were added in different positions of the molecule (Figure 9). The cytotoxicity against MFC-7 cell line of the new derivatives was evaluated and two compounds, **7** and **8** showed higher cytotoxicity than TAM ( $IC_{50}$  values of 3.41 and 2.46  $\mu\text{M}$ , respectively). Moreover, compound **8** exhibited high binding and antagonistic effect against  $ER\alpha$ .

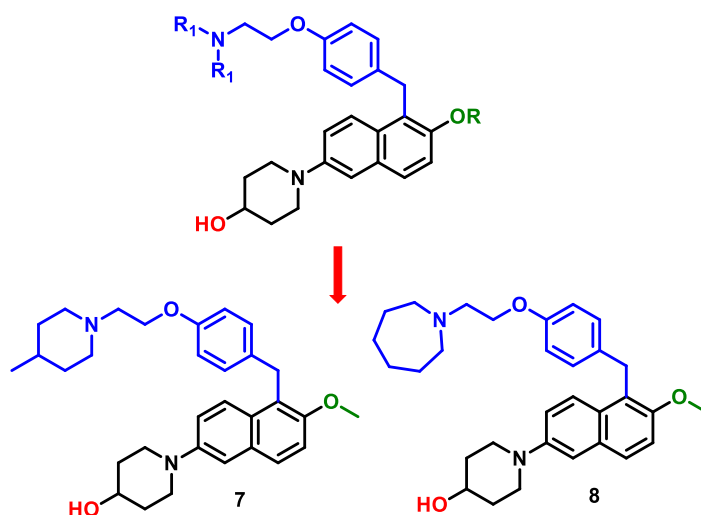


**Figure 9.** New naphthalene-based SERMs.

Starting from structural modifications on the coumarin and the side chain of two lead compounds (**9** and **10**, Figure 10), new 3-aryl-4-anilino-2H-chromen-2-one

derivatives were synthesized.<sup>56</sup> The ER $\alpha$  binding and antiproliferative activities against MCF-7 were determined and most of the new compounds showed moderate to potent affinity for ER $\alpha$  and higher antiproliferative activity than TAM. Considering ER $\alpha$  binding affinity, the most potent compound resulted to be **11** (Figure 10), while compound **12** (Figure 10) exhibited the best antiproliferative activity against MCF-7 with IC<sub>50</sub> value of 4.52  $\mu$ M.

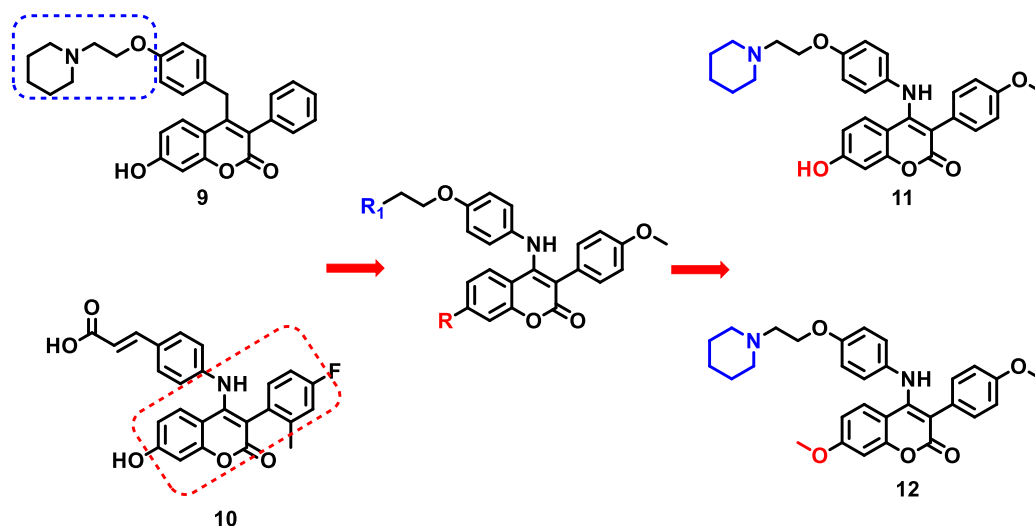


**Figure 10.** Coumarin-based SERMs.

## 2.2 SERDs

A more recent class of ER modulating drugs is represented by SERDs (Selective Estrogen Receptor Degraders). These compounds are mechanistically different from SERMs since, binding to the receptor, they are able to trigger its ubiquitination and degradation. The first ER ligand that showed a pure antiestrogenic activity was ICI 164,384 (Figure 11), discovered during the development of estrogen derivatives with a side chain in position 7 $\alpha$ . This compound was devoid of uterotrophic activity and was able to block the partial agonism of TAM on uterus of immature rats.<sup>57</sup> Starting from this compound, other steroidal pure antiestrogens were developed, including ICI 182,780 (fulvestrant, Figure 11), the only approved SERD to date. Binding to the receptor, fulvestrant caused the block of estrogen action impairing the dimerization, increasing the turnover and disrupting the nuclear localization of the receptor. This compound exhibited a 100-fold higher binding affinity for ER

than TAM and, unlike SERMs, it lacked estrogenic activity in tissues such as uterus, overcoming the risk of developing endometrial cancer.<sup>58</sup> The pure antagonistic profile of the drug seemed to be due to a distortion of helix 12 of ER, causing the exposure of a hydrophobic region and making the receptor a target for ubiquitination, triggering degradation.<sup>59</sup> However, fulvestrant is characterized by poor oral bioavailability and the need of intramuscular injections. Further investigations for the development of alternative orally available compounds have thus been performed to overcome these drawbacks.

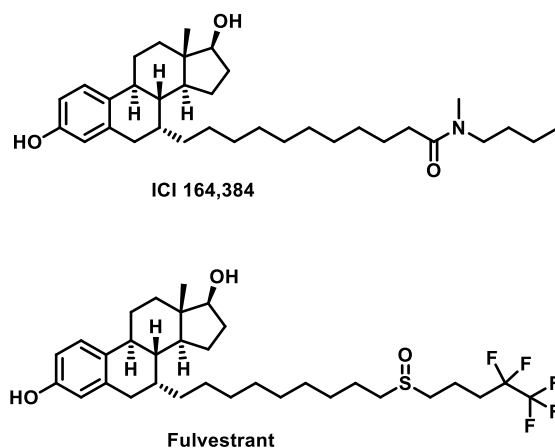


**Figure 11.** Structures of ICI 164.384 and fulvestrant.

### 2.2.1 Development of oral SERDs: state of the art

Several industries focused their interest on the development of new compounds endowed with SERD activity and oral bioavailability. Many of these candidates, widely reviewed by Lu *et al.*,<sup>60</sup> are currently evaluated in clinical trials and can be classified into different families, based on the chain inserted on the central core of the structure, containing either an acrylic acid or a basic moiety.

#### *Derivatives with an acrylic acid side chain*

GW 5638 (Figure 12) is a TAM derivative in which the dimethylaminoethoxy side chain was replaced by an acrylic acid moiety.<sup>61</sup> This compound did not show

uterotropic activity in the rat and exhibited efficacy in TAM-resistant BC cells. Like TAM, GW-5638 could be considered a prodrug, since it was metabolized producing the active metabolite GW-7604 (Figure 12). The interaction between the carboxylic acid and Asp351 and other aminoacids in H12 caused the exposure of the hydrophobic residues of the helix triggering receptor destabilization and degradation.<sup>62</sup>

SAR studies on the triphenylalkene scaffold led to the development of a series of indazole derivatives that showed to be potent ERs antagonists and degraders. The best candidate of this series was GDC-0810 (Figure 12),<sup>63</sup> also known as ARN-810, that proved to have good activity in TAM-sensitive and TAM-resistant BC cells. This compound exhibited affinity for ER $\alpha$  in the nanomolar range and good oral bioavailability. Despite sharing some characteristics with fulvestrant, it was observed that the interactions in the GDC-0810-ER complex were different from those of fulvestrant-ER complex, suggesting different conformational changes and therefore distinct mechanisms underlying ER turnover.<sup>64</sup> GDC-0810 reached phase II clinical trial and then its development was interrupted for intolerable side effects.

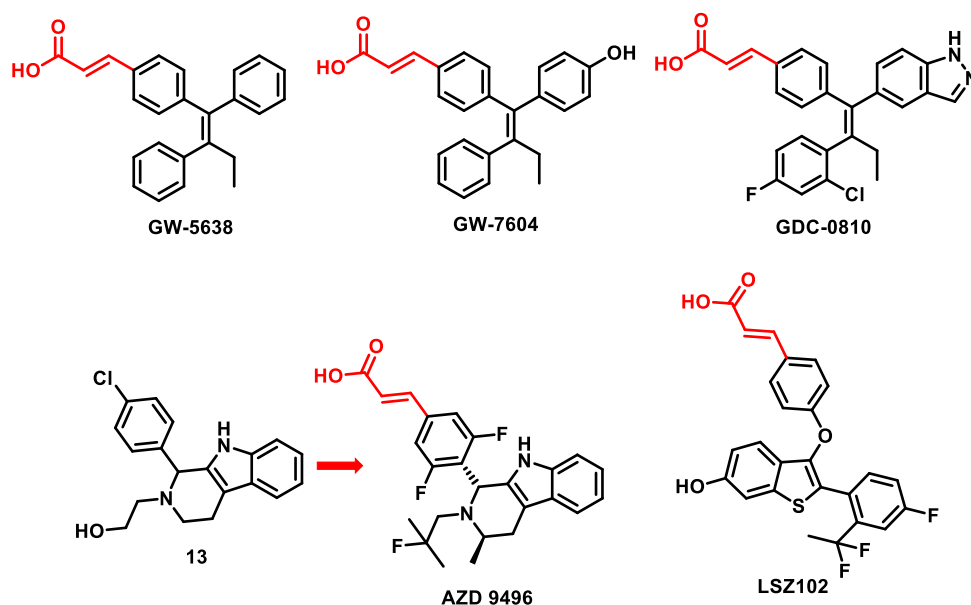


**Figure 12.** Structures of representative SERDs bearing an acrylic side chain.

In 2015, in order to identify new SERDs endowed with improved potency and oral bioavailability, AstraZeneca performed a screening assay that led to the

identification of novel hit compounds (e.g. compound **13**, Figure 12)<sup>65</sup> characterized with a new motif that was optimized in a following study allowing the development of AZD-9496 (Figure 12).<sup>66</sup> AZD-9496 showed selectivity over other tested nuclear receptors, high oral bioavailability and it was able to inhibit tumor growth in *in vivo* models of both ER $\alpha$  sensitive and ESR1 mutant BC cells.<sup>67</sup><sup>68</sup> To date, AZD-9496 has completed phase I clinical trials (NCT03236974).

Tria *et al.* from Novartis reported a series of benzothiophene derivatives that showed activity as SERDs and high oral bioavailability.<sup>69</sup> Among the new compounds, LSZ102 (Figure 12) exhibited potent receptor degradation and antagonistic activities, together with good tolerability and safety profiles. Therefore, it was selected for further investigations and is currently being evaluated in a phase I/Ib trial in advanced or metastatic ER+ BC (NCT02734615).

#### *Derivatives with a basic side chain*

In 2015, Radius reported compound RAD1901, in which the acrylic acid side chain typical of SERDs was replaced by an amino side tail (Figure 13). This compound selectively bound to ERs triggering their degradation, moreover it exhibited potent antiproliferative activity on the MFC-7 ER+ BC cell line, inducing a robust inhibition of tumor growth.<sup>70, 71</sup> RAD1901 is currently evaluated in phase III clinical trials (NCT03778931).

Recently, Astrazeneca reported the optimization of a series of tricyclic indazoles that led to the identification of a compound carrying a basic amino side chain, AZD-9833 (Figure 13).<sup>72</sup> This compound proved to be a potent SERD, with a pharmacological profile similar to that of fulvestrant and endowed with promising physicochemical and preclinical pharmacokinetic properties for oral administration. To date, AZD-9833 is being evaluated in phase I/II studies for the treatment of ER+ BC alone or in combination (NCT04541433, NCT04588298, NCT04214288, NCT03616587).

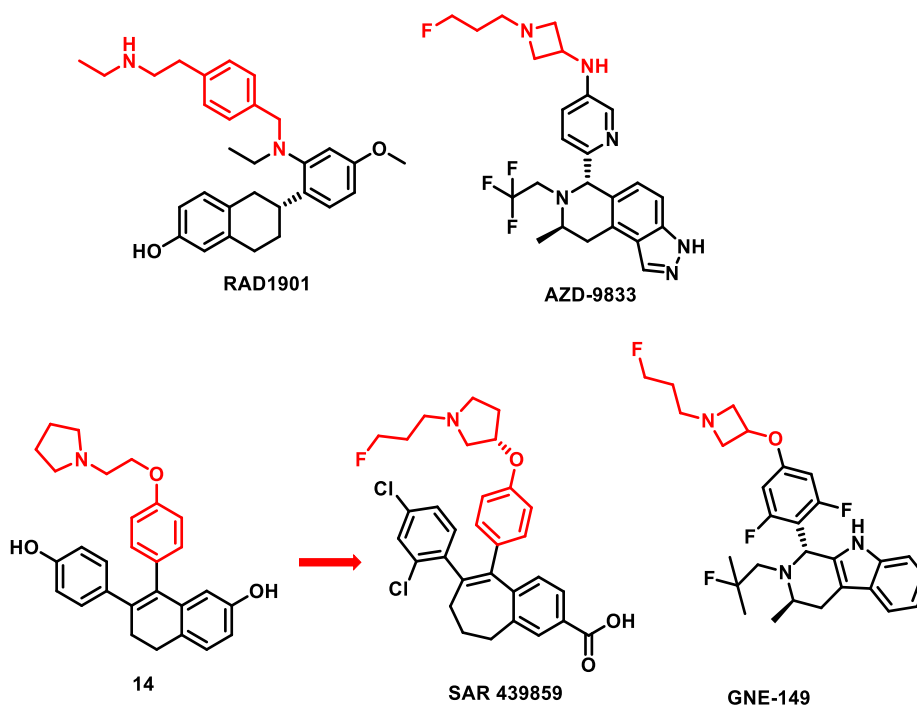


**Figure 13.** Structures of representative SERDs with a basic side chain.

In 2020 Sanofi, through a medium throughput screening (MTS), identified the lead compound **14** (Figure 13) endowed with interesting *in vitro* biological properties.<sup>73</sup> This molecule was the starting point for the development of new derivatives carrying various side chains, together with different open or cyclic amines (Figure 13). Among these compounds, SAR439859 resulted a potent ER $\alpha$  degrader, with IC<sub>50</sub> value of 0.2 nM, and showed good oral bioavailability among different species. Given these promising results, this compound is currently evaluated in phase I/II trials in patients with advanced ER+ BC (NCT04191382, NCT03816839, NCT04059484).

Liang *et al.* from Genentech investigated the tetrahydrocarbinone scaffold in combination with different basic side chains.<sup>74</sup> This study allowed the identification of GNE-149 (Figure 13), which exhibited potency similar to fulvestrant and improved antiproliferative effects. The central core of this compound lacked the phenolic group, present in some SERDs structure, leading to improved metabolic stability.

## 2.3 AROMATASE INHIBITORS

Since AR plays a crucial role in the biosynthesis of estrogens, this enzyme is one of the most important targets investigated in the search for an endocrine therapy to fight ER+ BC. Aromatase inhibitors (AIs) are compounds able to bind AR and block its activity; they cause the inhibition of the endogenous synthesis of estrogens, with consequent radical decrease in the circulating levels of these hormones through the body. Based on their chemical structure and their mechanism of interaction and inhibition of the enzyme, AIs can be classified into two main groups, i.e. steroidal (type I) and non-steroidal (type II) inhibitors. Steroidal AIs are derivatives of ASD, the natural substrate of AR, that interact with the binding site of the enzyme with a competitive mechanism in the same manner of the ASD. Some of them are also called “suicide inhibitors”, since they act as false substrates and are converted into irreversible inhibitors at the active site of the enzyme, causing its inhibition. Non-steroidal AIs block AR with a reversible mode; key structural feature of these molecules is the presence of a nitrogen-containing heterocycle that interacts with the enzyme by coordinating the iron atom of the heme group.<sup>75-78</sup>

AIs can also be chronologically classified as first, second and third generation agents (Figure 14). Aminoglutethimide (AG) and testolactone (Figure 14), that represent first generation AIs, were both marketed drugs that were later shown to inhibit AR. AG, the amino derivative of the hypnotic glutethimide, was introduced in the United States in 1960 as anticonvulsant, but already in 1966 it was withdrawn by the FDA due to the insurgence of adrenergic insufficiency.<sup>79</sup> Since then, numerous studies have focused on the identification of site and mechanism by which AG blocked steroidogenesis, and it was observed to inhibit the P450<sub>scc</sub> enzyme, blocking the conversion of cholesterol to pregnenolone. Some years later, Santen *et al.*<sup>80</sup> reported an inhibitory activity of AG against AR, resulting its main mechanism of action. AG has been recognized as a valuable endocrine therapy for the treatment of advanced BC, but as it lacked selectivity for AR and presented a number of side effects, its use as an anticancer has not been promoted. Testolactone, a structural derivative of TST, has been used as BC drug since the early 1960s, but its mechanism of action was discovered only a few years later. In 1975, Siiteri *et al.*<sup>81</sup> reported that this compound was able to block the synthesis of estrogens *in*

*vitro* by inhibiting AR, inducing BC regression. By the time its mechanism of action was discovered, testolactone was considered an agent with a weak clinical activity as compared to its “competitor” AG.<sup>82</sup>

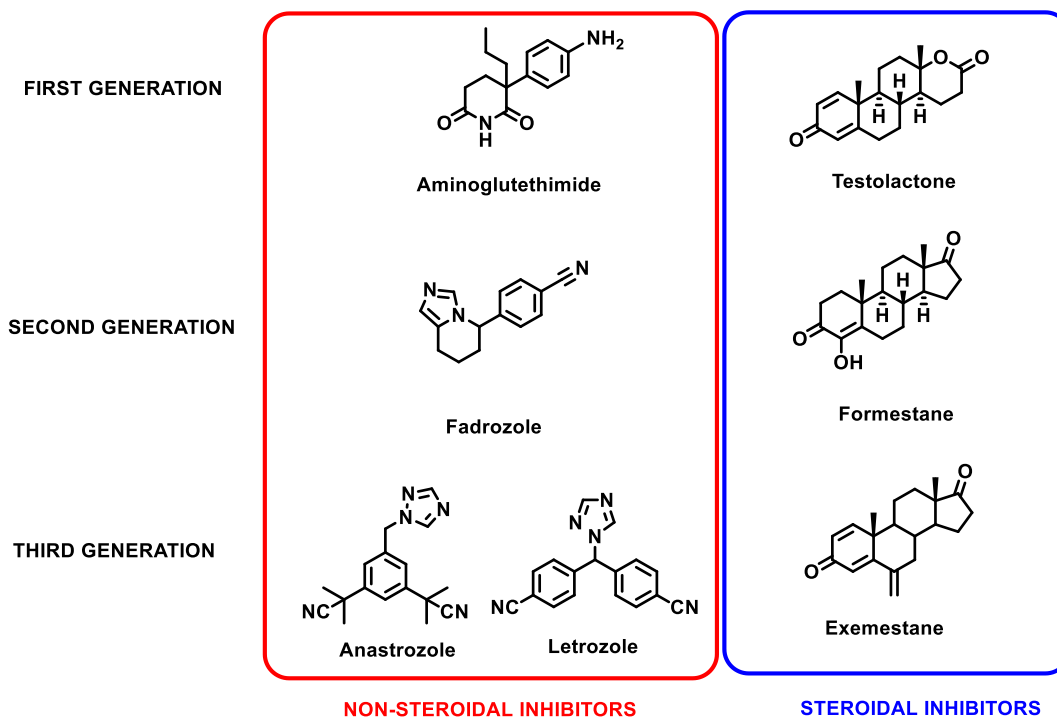


**Figure 14.** Structures of steroidal and non-steroidal aromatase inhibitors of I, II and III generation.

The promising clinical results obtained with first generation AIs focused the interest of researchers on the development of new inhibitors with improved selectivity for AR and second generation AIs, represented by fadrozole and formestane (Figure 14), has therefore been developed. Fadrozole is a non-steroidal inhibitor with similar effectiveness and fewer side effects as compared to TAM,<sup>83</sup> that was thus considered as a possible alternative to this drug as first line therapy for the treatment of advanced BC.<sup>76</sup> Formestane, or 4-hydroxyandrostenedione (4-OHA), is a compound whose design was based on the structure of androstenedione. As the other steroid inhibitors, it is able to bind the substrate-binding site of the enzyme causing its irreversible inhibition, so that a continuous administration of the drug was not required, resulting in an improved tolerability with respect to AG.<sup>84</sup> Despite the considerable improvement in selectivity and efficacy obtained with second

generation inhibitors, these compounds have not been deeply studied because third generation agents (anastrozole, letrozole (LTZ) and exemestane (EXE)) (Figure 14) were quickly developed. These compounds, now commercially available, have high selectivity for AR without interfering with the biosynthesis of other steroid hormones, and have been approved from FDA as first-line agents for the treatment of post-menopausal women with ER+ BC. Anastrozole and LTZ are non-steroidal compounds, characterized by a triazole ring needed for the coordination with the iron atom of the heme moiety of AR, while EXE is a steroidal irreversible blocker that mimics the natural substrate of the enzyme. To understand how a steroidal “suicide inhibitor” could block the aromatization process, Ghosh *et al.* compared the binding pose of ASD with that of EXE.<sup>20</sup> With the exception of ring A, the two molecules overlapped quite well. The methylidene group at C6-position of EXE was accommodated in a hydrophobic cleft, surrounded by Thr310, Val370 and Ser478, close to the active site access channel. The positioning of the C6 methylidene in this hydrophobic pocket reduced the mobility of Thr310 side chain, interfering with its capacity to interact with the catalytic water. In this way, EXE could not be hydroxylated at C19, remaining bound within the binding pocket.

Inhibition of AR causes the complete depletion of circulating estrogens, leading to the onset of side effects such as musculoskeletal pain, reduction of bone density, increase of fractures and cardiovascular events.<sup>85-87</sup> Several trials have focused on comparing the treatment with AIs to the use of SERMs, as monotherapies or in combination for the treatment of postmenopausal women with ER+ BC, but the different studies gave controversial results. While the International Group (BIG) 1-98 trial<sup>88, 89</sup> and the Arimidex, Tamoxifen, Alone or in Combination (ATAC) trial<sup>90, 91</sup> concluded that five years treatment with an AI alone (LTZ in BIG 1-98 and anastrozole in ATAC) led to benefits in terms of efficacy and tolerability compared to TAM alone or in combination, on the other hand, other combinations of compounds such as the pure antiestrogenic favestrant with LTZ<sup>92</sup> or EXE with TAM<sup>93</sup> resulted more effective than the various monotherapies. Several studies were also conducted to evaluate the effect of TAM on the pharmacokinetics, pharmacodynamics and safety of EXE and it was observed that the combination of

the two drugs was well tolerated and there were no relevant pharmacokinetic interactions between EXE and TAM or its metabolites.<sup>94-96</sup>

Despite the clinical efficacy demonstrated by the currently used AIs anastrozole, LTZ and EXE, the side effects and the development of resistance associated with their use suggest that the search for improved AIs is still needed. Indeed, in recent years many research groups have been involved in the design and synthesis of new molecules that could overcome the limits of current inhibitors.

### 2.3.1 Development of non-steroidal AIs: state of the art

In the past decades researchers have engaged in the development of new potent and selective non-steroidal AIs, mainly focusing on compounds containing nitrogen scaffolds such as triazole or imidazole rings, present also in currently used AIs.<sup>78</sup>

One of the most investigated scaffold that proved to be able to inhibit AR expression in MCF-7 BC cells is the indole moiety. Indeed, many indole derivatives have been demonstrated to have a potent inhibitory activity against AR.<sup>97-99</sup> In the last few years, other groups have engaged in the search for new molecules based on this scaffold. Kang *et al.*<sup>100</sup> synthesized a series of new non-steroidal AIs containing the 2-phenyl indole moiety with an azole group (imidazole or triazole) in position 3 (Figure 15).

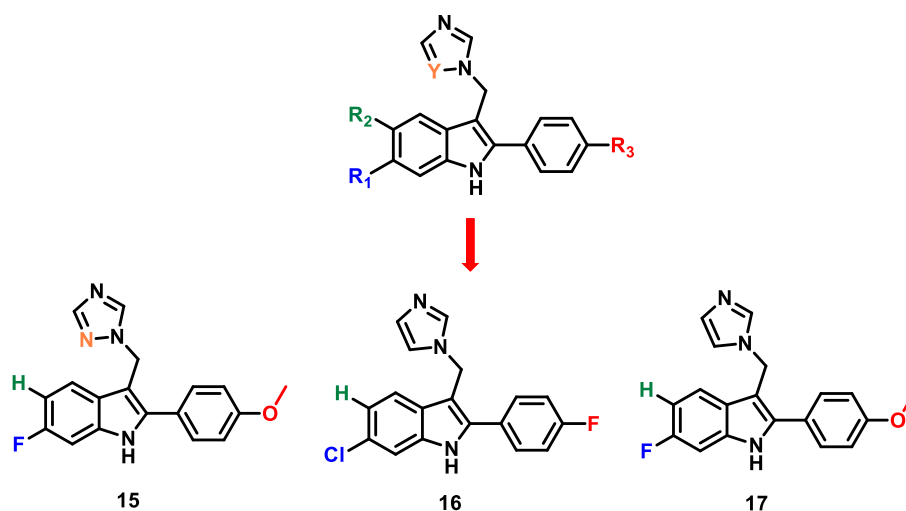


**Figure 15.** New indole derivatives as non-steroidal AIs.

Twenty new compounds were tested to investigate their inhibitory activity against AR and the binding mode of the most potent compound was then analyzed, by applying an integrated computational protocol. The most potent compounds, **15**, **16** and **17** (Figure 15), with IC<sub>50</sub> values of 14.1, 32.3 and 36.1 nM, respectively, proved to be more potent than LTZ, which showed an IC<sub>50</sub> of 49.5 nM. The results obtained suggested that a small group is necessary in R<sub>1</sub> position and that the introduction of a methoxy group on the 2-phenyl moiety (R<sub>3</sub>) led to potent AIs. Moreover, the triazole structure seemed to grant a stronger inhibitory activity than imidazole. The toxicity in MCF-7 cells was also tested and the new derivatives resulted less toxic than LTZ. Compound **15**, that showed the best inhibitory activity (14.1 nM), was subjected to an integrated computational study, that combined quantum mechanics (QM), molecular docking and atomistic molecular dynamics (MD) simulations, in order to analyze its binding pose with the enzyme. It was found that the triazole was beneficial for the interaction with the heme group, the F atom did not give a strong contribution but its substitution with a larger atom such as Cl led to atomic overlaps with the enzyme, causing a reduction in activity. Finally, the flexibility of the methoxy group allowed compound **15** to interact with several hydrophobic residues in the binding pocket. Replacing this group with rigid spherical atoms such as F or Cl led to a reduction of flexibility with a consequent decrease in activity.

Starting from the lead compound SYN20028567 (Figure 16), that proved to be a potent AI with an *in vitro* IC<sub>50</sub> of 9.4 nM, Di Matteo and coworkers synthesized a library of 26 sulfonamide-containing compounds (Figure 16A).<sup>101</sup> The new derivatives carried different substituents on the aromatic ring while the imidazole, necessary for heme coordination, the piperidine moiety and the sulfonyl portion were maintained. The aromatase inhibitory activity of the new compounds was tested and many of them showed IC<sub>50</sub> values in the nanomolar range. The most potent compounds, in term of AR inhibition, were **18**, **19** and **20**, with IC<sub>50</sub> values of 9, 7 and 6 nM, respectively.

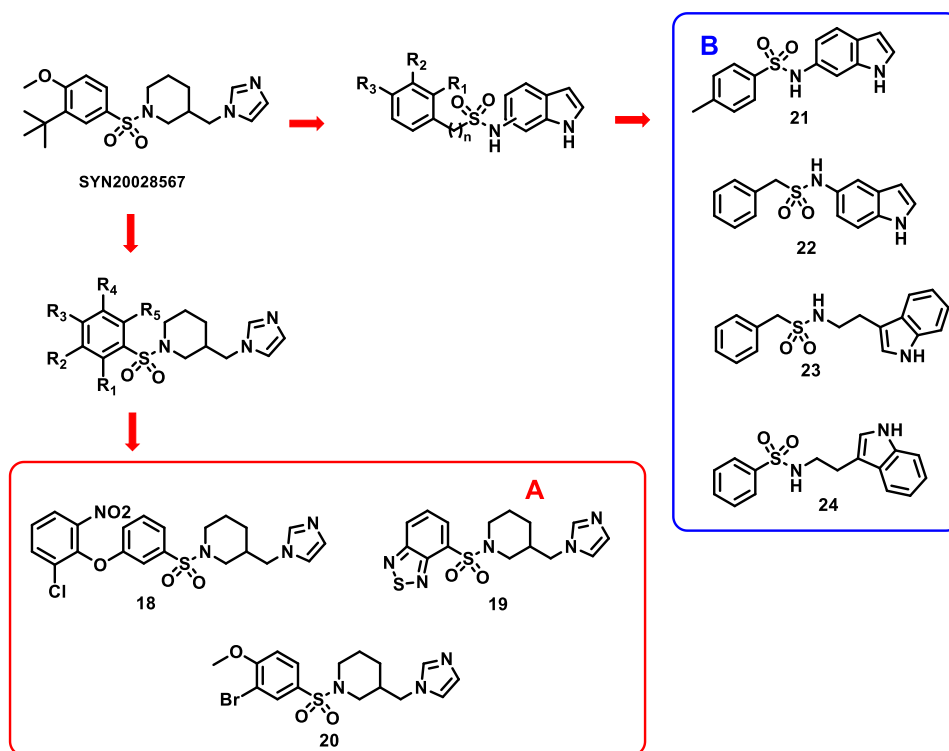


**Figure 16.** Structures of SYN20028567 and derivatives.

Later, the same research group<sup>102</sup> synthesized another library of 30 non-steroidal compounds containing a sulfonamide moiety linked to an indole group (Figure 16B). Docking studies conducted on SYN20028567 showed that the imidazole group was able to coordinate the heme iron atom, the oxygen of sulfonamide interacted with Ser478 via H-bond and the piperidyl group interacted with the hydrophobic pocket of the enzyme. In the new compounds, the sulfonamide was preserved while the nitrogen was not included in a ring, the aryl group was unsubstituted or substituted with different groups and the imidazole moiety was replaced by an indole. The new compounds were tested to evaluate their ability to inhibit the AR enzyme and four compounds (**21**, **22**, **23** and **24**, Figure 16B) showed an IC<sub>50</sub> value in the sub-micromolar range (0.49, 0.16, 0.75 and 0.20  $\mu$ M respectively). The best compounds were subjected to docking analysis proving to interact with the key binding residues present in the binding pocket. It was also observed that the presence of the indole group, for the interaction with the heme of the enzyme, the sulfonamide linker, able to establish H-bonds, and the unsubstituted

or *para*-methyl substituted benzene for hydrophobic interactions were required for good inhibitory activity.

Pingaew *et al.*<sup>103</sup> designed and synthesized three series of compounds characterized by a 1,2,3-triazole moiety linked *via* a phenyl ring to a sulfonamide as open-chain (Type I) or to a sulfonamide carrying a tetrahydroisoquinoline (THIQ) moiety (Type II and III). These new derivatives presented different aryl substituents in position 4 of the triazole and some of them also carried two methoxy groups on the THIQ structure. The 7-coumaril derivative **25** (Figure 17), resulted to be the most potent AIs with an IC<sub>50</sub> of 0.2 μM. Docking analysis of **25** suggested that this compound formed hydrophobic interactions with some residues of the enzyme and hydrogen bonds with Met374 and Ser478 via the sulfonyl oxygen and the oxycoumarinyl group, respectively, which seemed to be essential for good inhibitory activity. The lower potency of **25** compared to LTZ (0.2 μM and 3.3 nM, respectively) seemed to be due to the lack of coordination with the iron atom of the heme group.

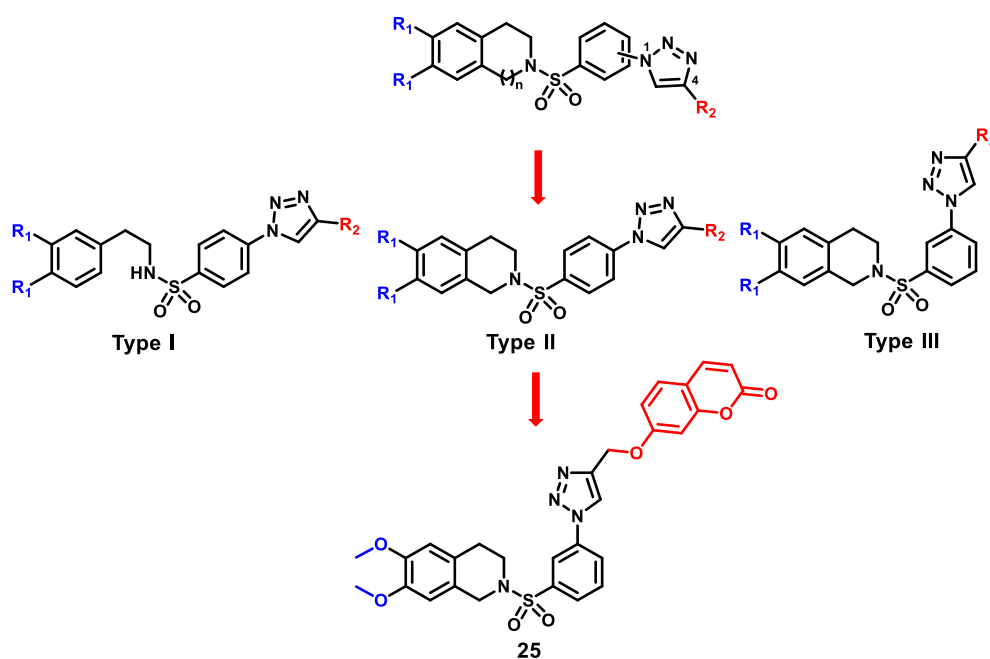


**Figure 17.** New sulfonamide-1,2,3-triazole derivatives.

Several molecules containing a coumarin scaffold were reported in literature to have good inhibitory activity against AR. In 2011 Stefanachi *et al.*,<sup>104</sup> starting from

the lead compounds **26** and **27** (Figure 18), which previously proved to be potent AIs<sup>105</sup>, designed and synthesized two new series of coumarin derivatives introducing substituents on 7-benzyloxy (Series I, Figure 18) or on 7-phenoxy aromatic rings (Series II, Figure 18). In addition, some derivatives of compound **27** substituted at the methylene bridge were also synthesized to explore the effect of these changes on activity.

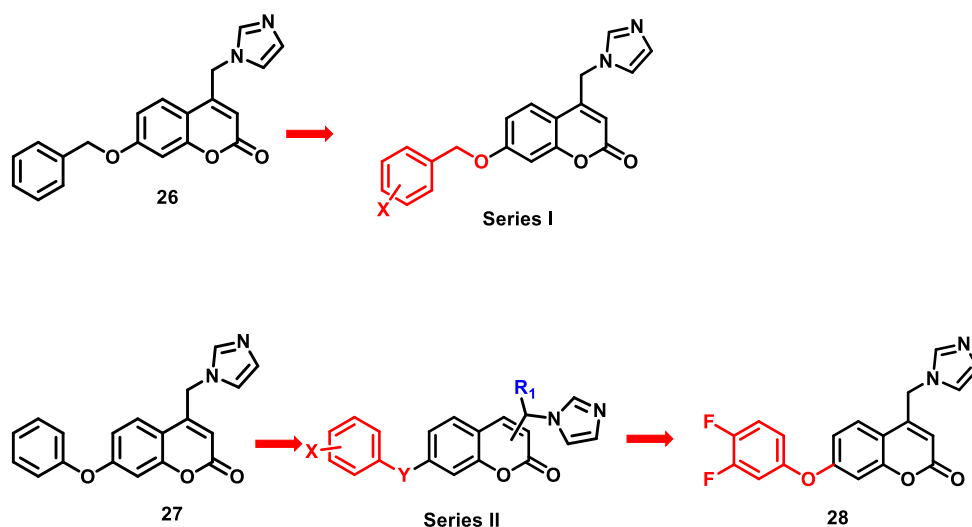


**Figure 18.** New 7-benzyloxy- or phenoxy coumarin derivatives.

The new molecules were tested for their inhibitory activity against AR and against 17 $\alpha$ -hydroxylase and all compounds proved highly selective for AR, some of them showing activity in the nanomolar range. As regard derivatives of compound **26**, many *meta* or *para*-substituted analogues showed an improvement in activity while, among derivatives of **27**, only one compound (**28**, Figure 18) showed slightly improved activity, resulting the most active compound of these two series. In both series, the *meta*-substitution gave a higher inhibitory effect than the corresponding *para*-substitution. Some compounds, including **26** and **27**, were subjected to docking analysis, allowing to underline the interactions required to obtain good inhibitory activity. The results suggested that the imidazole group coordinated the heme iron atom and the coumarin scaffold lay almost perpendicular to the plane of the imidazole ring. This binding pose seemed to be stabilized by a hydrogen bond

between the lactone carbonyl and Ser478. Moreover, the phenoxy and benzyloxy groups were located in an accessory pocket constituted by hydrophobic residues. More recently, Yamaguchi *et al.*<sup>106</sup> reported a series of coumarin derivatives carrying different substituents in positions 3 and 7 as potential AIs. Compounds **29** and **30** (Figure 19) resulted the most potent inhibitors, with an IC<sub>50</sub> of 30.3 and 28.7 nM, respectively. Docking studies of the new compounds were performed and compound **29**, containing an azole ring (pyridine), seemed to interact with the enzyme similarly to non-steroidal third-generation AIs. Compound **30**, on the other hand, seemed not to fit in the active site pocket and it was supposed to bind to a different site. However, clear structure-activity correlations were not found.

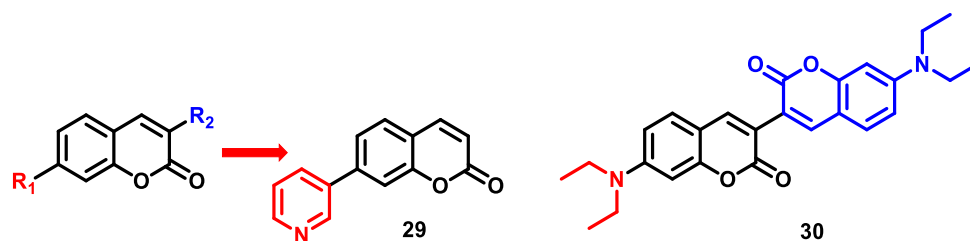


**Figure 19.** 3- and 7-substituted coumarin derivatives.

In the past years, my research group has developed potent AIs based on a xanthone scaffold. Starting from a previously reported xanthone derivative (compound **31**, Figure 20),<sup>107</sup> some structural modifications were introduced, varying the position of the imidazolymethyl chain and replacing the xanthone nucleus with some bioisosteric structures or “open” analogs, such as aza- and thioxanthenes, phenoxy- and phenylsulfanylbenzylimidazole (Figure 20). The aim of this work was to evaluate the appropriate position of the methylimidazole group and to define the role of the potential H-bond acceptor group (nitro or carbonyl) on the different scaffolds.<sup>108</sup> The new molecules were tested for their inhibition against CYP19 and CYP17 and all compounds proved to be selective for AR. The best compound resulted to be **32** and **33** (Figure 20), with IC<sub>50</sub> values of 3.98 and 5.59 nM, respectively. In general, it was observed that replacing the oxygen with sulfur increased potency, while substituting with a nitrogen atom led to a drop in activity on both rigid and flexible derivatives. As regard the role of the nitro group, when

the carbonyl group was in the right position with respect to the imidazolylmethylene chain and was able to establish H-bond with the enzyme, the nitro group was not essential for inhibitory activity. On the other hand, when the ketone group was removed, the presence of the NO<sub>2</sub> was essential because it established H-bonds with the enzyme, stabilizing the open diphenylether derivatives and increasing their potency.

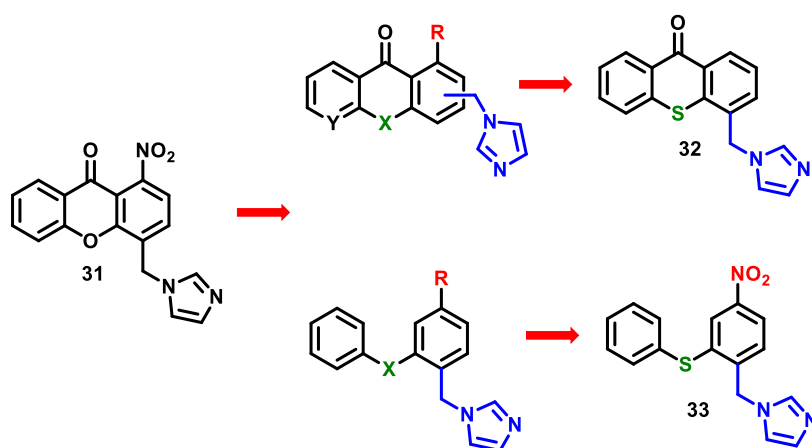


**Figure 20.** Xanthone bioisosters or open-derivatives.

Other studies focused their attention on derivatives of benzimidazole-triazolothiadiazine. In a first study, Acar-Çevic *et al.*<sup>109</sup> synthesized seven new compounds carrying different substituents on the phenyl ring **A** (Figure 21). The MTT assay was used for evaluating the cytotoxicity of the new compounds against MCF-7 BC cells and healthy NIH3T3 cells, to calculate their selectivity towards carcinogenic cells. Compounds **34-37** (Figure 21) resulted the most active and selective, with IC<sub>50</sub> values of 0.036, 0.024, 0.022 and 0.012 μM against MCF-7 cells, respectively. The ability of these four compounds to inhibit AR was also determined, and the most potent **37** showed an IC<sub>50</sub> of 0.037 μM. Docking analyses were performed on **37** and it proved to adopt a similar binding pose with respect to LTZ, interacting with the heme and Cys437 through the nitrogen of the central triazolethiadiazine moiety by salt bridge. The 2,4-difluorophenyl group was also able to interact with the heme group via π-π interactions, while the phenyl group near the benzimidazole moiety formed π-π interactions with the phenyl of Phe430.

Finally, the NH of the benzimidazole interacted with Ser314 through an H-bond with the carbonyl group of this residue.

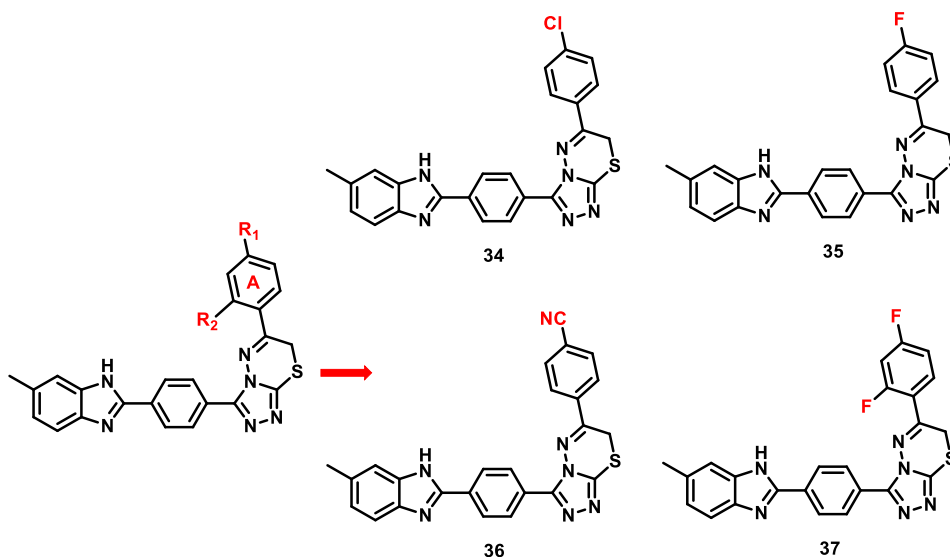


**Figure 21.** Benzimidazole-triazolothiadiazine derivatives carrying substituents on ring A.

In a second study,<sup>110</sup> the same research group synthesized sixteen new benzimidazole-triazolothiadiazine derivatives, in which the methyl group of the benzimidazole ring was eliminated or substituted by a chlorine atom. Moreover, the new compounds carried different substituents on the phenyl ring A. The MTT cytotoxic assay performed on MCF-7 BC cells and healthy NIH3T3 cells identified compounds **38-41** (Figure 22) as the most active derivatives with IC<sub>50</sub> values of 0.119, 0.016, 0.110 and 0.018  $\mu$ M against MCF-7 cells, respectively. Again, the *in vitro* inhibitory activity on AR of the most active compounds was evaluated and **39** was identified as the best compound of the series. Finally, docking studies revealed that **39** perfectly fitted into the binding pocket of the enzyme forming  $\pi$ - $\pi$  interactions between its benzimidazole group and Arg115 and Phe134, and interacting with heme and Cys437 via nitrogen atoms of the triazolothiadiazine structure by salt bridge. Moreover, the 4-cyanophenyl moiety formed  $\pi$ - $\pi$  interactions with the heme molecule and the nitrogen of the cyano group interacted with Ser314 via a hydrogen bond that appeared to be important for inhibitory activity.

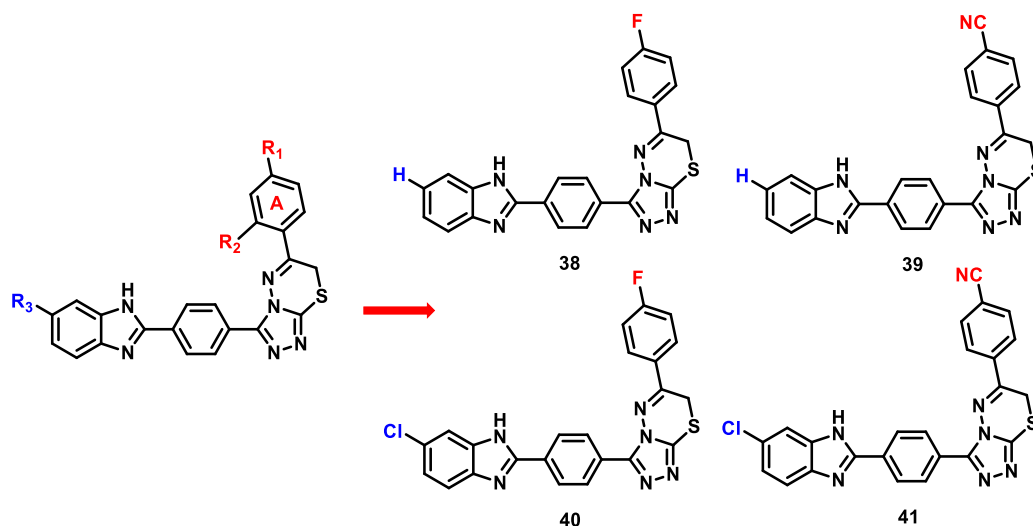


**Figure 22.** R<sub>3</sub>-modified benzimidazole-triazolothiadiazine derivatives.

El-Naggar *et al.*,<sup>111</sup> starting from compound **42**, in which a 1,2,3-triazole ring and a pyrazole moiety were combined in the same structure, developed new series of molecules with potent AR inhibitory activity. Compound **43** (Figure 23), with an IC<sub>50</sub> value of 0.2 nM, proved to be the best derivative, probably due to the presence on the structure of ester and pyridine groups.

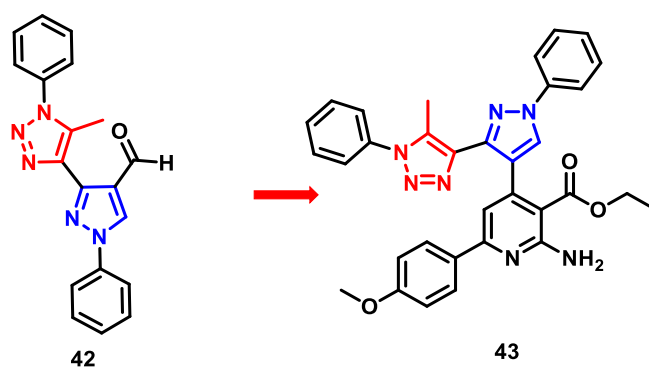


**Figure 23.** 1,2,3-triazole-pyrazole derivatives.

### 2.3.2 Development of steroidal AIs: state of the art

Most of the research groups involved in the development of new potential steroidal AIs designed the structure of these molecules by modifying the structure of ASD, the natural substrate of AR enzyme. Initial SAR investigation on steroidal AIs suggested that an effective inhibition required appropriate structural features, such

as an A/B trans ring junction, a ketone group at position 3, the presence of unsaturation in the steroid core, and either a ketone or a hydroxyl group at C-17 position.<sup>112</sup>

#### *Derivatives substituted on the A-ring*

Numazawa *et al.*<sup>113</sup> developed 2 $\alpha$ - and 2 $\beta$ -methyl and 2,2-dimethyl ASD derivatives in order to investigate the effect of C<sub>2</sub> substitution on AR inhibitory activity. The obtained results showed for the disubstituted compound (**44**, K<sub>i</sub>= 8.8 nM and IC<sub>50</sub> = 0.089  $\mu$ M, Figure 24) a higher inhibitory activity with respect to the monosubstituted derivatives (**45**, K<sub>i</sub>= 22 nM, IC<sub>50</sub>= 0.25  $\mu$ M, and **46**, K<sub>i</sub>= 55 nM, IC<sub>50</sub>= 0.69  $\mu$ M, Figure 24) and the 2-methylene derivative **47** (K<sub>i</sub>= 68 nM, IC<sub>50</sub>= 0.55  $\mu$ M, Figure 24). Considering these results, a combination of 2 $\beta$ - and 2 $\alpha$ -methyl substitution seemed to be crucial for a favorable interaction between **44** and the active site of the enzyme.

Namazawa *et al* developed two series of 4-substitued 4-ene- or 5-ene-3-deoxyandrogen derivatives.<sup>114</sup> They introduced a non-polar alkoxy, alkyl, or phenylalkyl group in 4 $\beta$ -position of androst-5-en-17-ones and acyloxy groups in 4-position of androst-4-en-17-ones. The 4-acyloxyandrost-4-ene derivatives **48** and **49** (Figure 24), carrying a 4-benzoyloxy and 4-acetoxy group, respectively, proved to have the highest AR inhibitory activity, with K<sub>i</sub> values of 70 and 60 nM, respectively. It was also observed that the extension of the acetoxy moiety of 4-acyloxy derivatives, or the methyl group of 4 $\beta$ -alkyl compounds, led to a decrease in activity.

Several series of 2-alkyl-, alkoxy- or bromo-substitued 1,4-diene derivatives were also developed, and the capacity to inhibit AR activity of the new compounds was evaluated.<sup>115</sup> All the 2-alkyl and 2-bromo derivatives proved to be good AR inhibitors, while the 2-alkoxy compounds, with the exception of the methoxy derivative (**50**, Figure 24), showed poor potency. The hexyl compound (**51**, Figure 24) showed the best affinity for the enzyme, with a K<sub>i</sub> value of 31 nM.

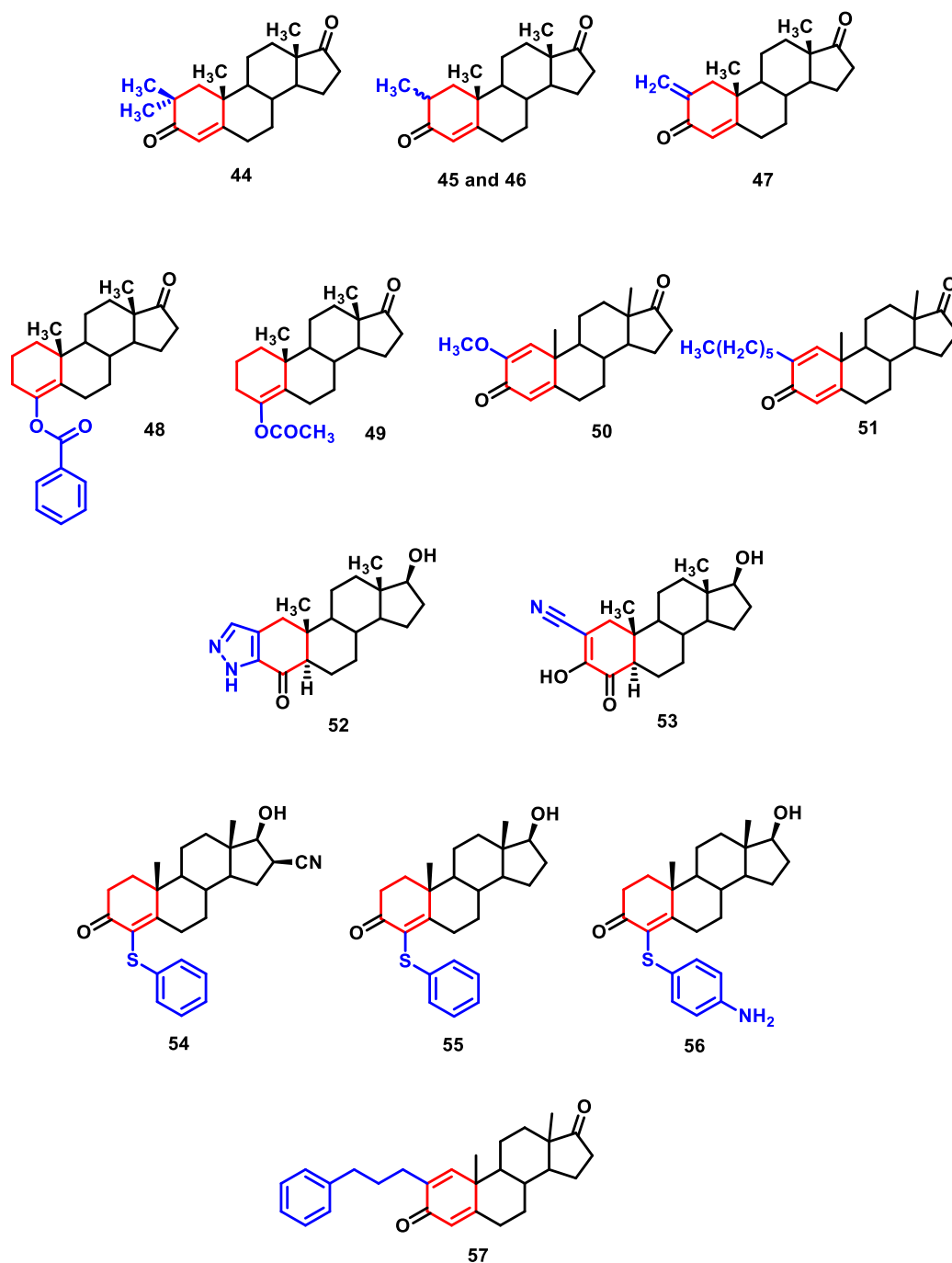


**Figure 24.** Derivatives substituted on the A-ring.

Novel steroidal derivatives, in which a five-membered heterocycle (isoxazole or pyrazole) was fused on positions 2,3 of ring A, or a nitrile group was introduced, were synthesized by Yadav *et al.*<sup>116</sup> Among these compounds, the pyrazole derivative (compound **52**, Figure 24) showed the highest inhibitory activity, followed by the nitrile derivative (compound **53**, Figure 24). It was observed that

the best compounds carried a H-bond donating group in position 3, and this feature could stabilize the enzyme-inhibitor complex leading to an improvement in activity. The same research group developed some 4-phenylthiaderivatives (compounds **54-56**, Figure 24).<sup>117</sup> Among the synthesized compounds, the 16 $\beta$ -carbonitrile derivative (**54**, Figure 24) proved to be the best compound with an IC<sub>50</sub> value of 169.3 nM. The phenylthio group at C4 and the 16-nitrile group demonstrated to establish favorable interactions with the enzyme leading to a potent AI.

To further investigate the effect of substituents on position 2 of the  $\Delta^1$ -ASD structure, some derivatives carrying different phenylaliphatic, *p*-methylphenyl or *p*-trifluoromethylphenylethyl groups were synthesized.<sup>118</sup> The phenylpropyl derivative (**57**, K<sub>i</sub> = 16 nM, Figure 24) was the most potent compound. Docking analyses on this compound suggested that **57** interacted with the active site forming two hydrogen bonds through 3- and 17-carbonyl groups and establishing hydrophobic interactions with the phenylpropyl moiety. All these interactions stabilized the enzyme-inhibitor complex leading to high inhibitory activity.

#### *Derivatives substituted on the B-ring*

Some 6 $\beta$ ,19-bridged steroids, epoxy-, cyclo-, epithio-, and methanoandrostenedione derivatives, were synthesized (**58-61**, Figure 25) by Komatsu *et al.* and their AR inhibitory activity was evaluated.<sup>119</sup> These compounds showed extremely low affinities (K<sub>i</sub> values > 2.2  $\mu$ M), probably because 19 substituents could not freely rotate around the C<sub>10 $\beta$</sub> -C<sub>19</sub> bond.

A series of 6-bromoandrostenediones with a 2,2-dimethyl or 2-methyl substituent was reported by Numazawa *et al.*<sup>120</sup> The new compounds showed apparent K<sub>i</sub> values between 10 and 87 nM and two of the most potent derivatives, 6 $\alpha$ - (**62**, Figure 25) and 6 $\beta$ -bromosteroids (**63**), carrying a 2,2-dimethyl group, presented IC<sub>50</sub> values of 0.11 and 0.10  $\mu$ M, respectively.

Starting from the 7 $\alpha$ -allylandrostenedione derivative (compound **64**, Figure 25), that proved to be a potent AR inhibitor (IC<sub>50</sub> = 0.59  $\mu$ M, K<sub>i</sub> = 80 nM), Varela *et al.* developed several compounds performing two main chemical modifications: C3 decarboxylation and introduction of a double bond at C1 position (**65-67**, Figure 25)<sup>121</sup>. The obtained results suggested that the 3-deoxo derivative **65** (Figure 25)

was less potent with respect to **64**; conversely, the introduction of the double bond at C1 position was beneficial, leading to compounds **66** and **67** with  $IC_{50} = 0.45$  and  $0.47 \mu\text{M}$  and  $K_i = 65$  and  $45 \text{ nM}$ , respectively. The presence of the double bond at C1 increased the planarity of ring A, improving AR inhibitory activity. The anti-aromatase activity and *in vitro* effects in sensitive and resistant BC cells of the new  $7\alpha$ -substituted compounds were further investigated.<sup>122</sup> It was seen that all compounds are potent inhibitors of AR in BC cells, in particular **66** and **67** proved to be the best compounds ( $IC_{50}$  values of  $0.5$  and  $0.3 \mu\text{M}$ , respectively), confirming the results obtained with placental microsomes. Moreover, it was seen that these derivatives were able to sensitize resistant cancer cells.

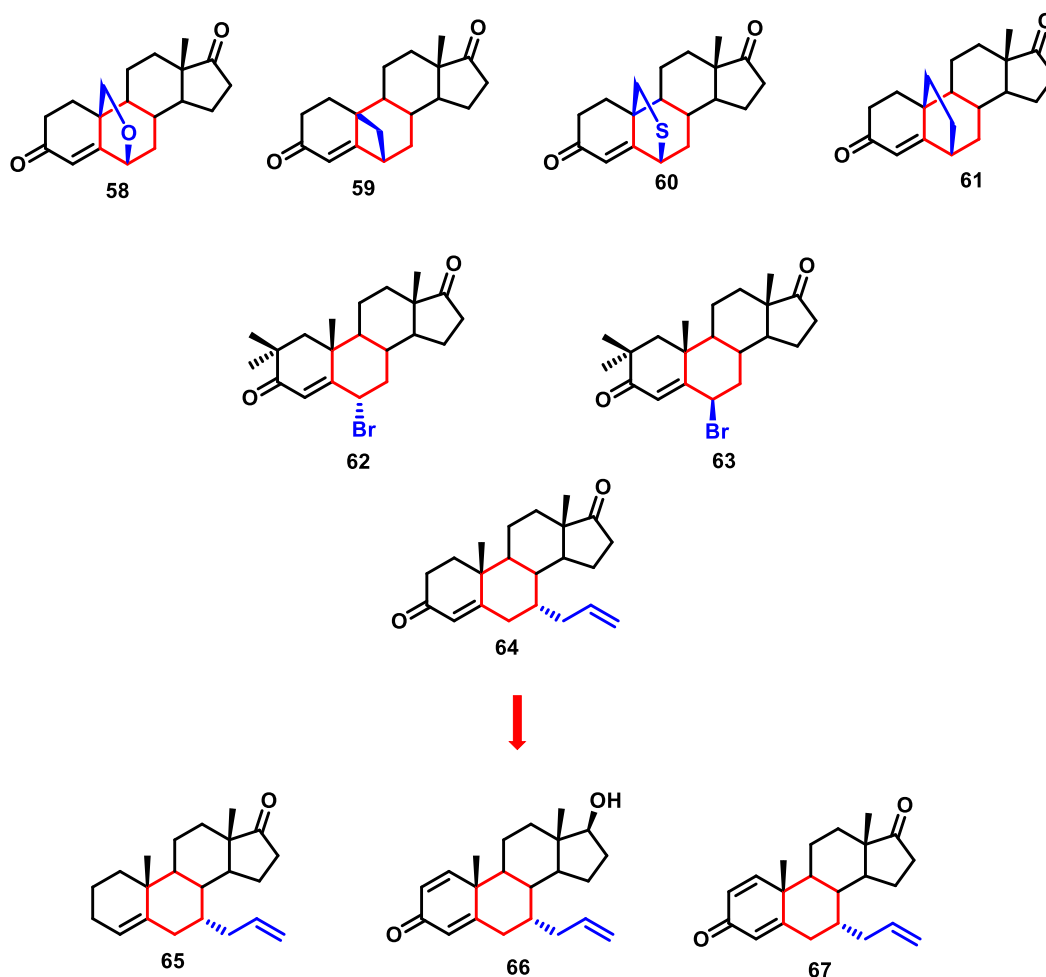


**Figure 25.** Derivatives substituted on the B-ring

New series of C-6 $\alpha$  or C-7 $\alpha$  substituted compounds were synthesized and analyzed in order to evaluate which of the two positions was more convenient for substitution to increase AR inhibitory activity.<sup>123</sup> The hit compounds, identified in previous work, carried a double bond or an epoxide group in various position of ring A (Figure 26). In the new derivatives, methyl, hydroxyl or allyl groups were inserted at C-6 $\alpha$  or C-7 $\alpha$  and their anti-AR activity was evaluated. Almost all C6-compounds proved to have higher inhibitory activity with respect to the corresponding C7-derivatives. In addition, the methyl substituent showed the best results, followed by allyl and hydroxyl groups. Among all compounds, **68** and **69** (Figure 26) showed the best activity, with IC<sub>50</sub> values of 0.06 and 0.055  $\mu$ M, respectively.

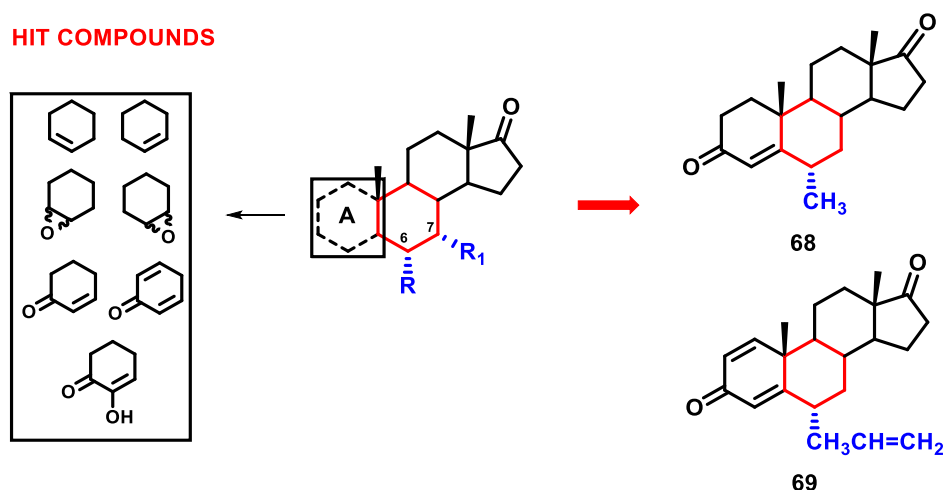


**Figure 26.** C6 $\alpha$ - or C7 $\alpha$ -substituted derivatives.

A series of 7-oximino-5-androstene and its O-alkylated derivatives was developed and screened for cytotoxic and AR inhibitory activity by Bansal *et al.*<sup>124</sup>. The cytotoxic activity was tested against three different cancer cell lines, MCF-7 (breast), NC1-H460 (lung) and SF-268 (CSN), and no compound proved to be toxic at 100  $\mu$ M. The imidazolyl derivatives (compounds **70** and **71**, Figure 27), with moderate AR inhibitory activity (IC<sub>50</sub> values of 3.1 and 12  $\mu$ M, respectively), proved to be the most potent derivatives of the series, probably due to the coordination of one of the two imidazole nitrogens with the iron of the heme group of AR.

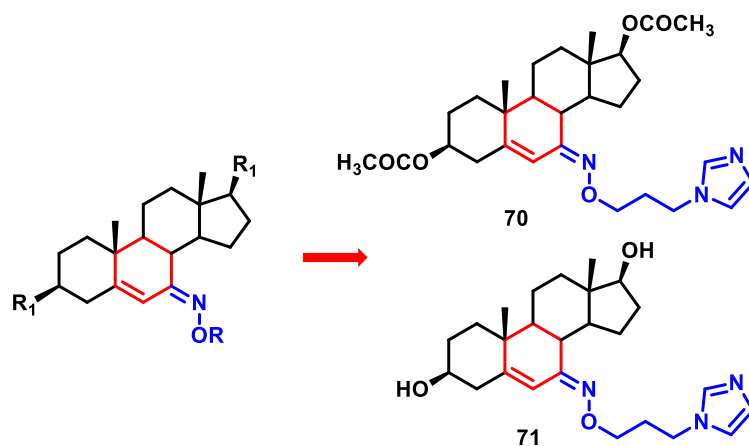


**Figure 27.** 7-oximino-5-androstene derivatives.

Some metabolites of EXE were synthesized by Valera *et al.* modifying one of the double bonds of A- or B-ring to an epoxide group (compounds **72** and **73**, Figure 28), or reducing the 17-carbonyl group to a hydroxyl group (compound **74**, Figure 28).<sup>125</sup> The anti-AR activity of the new compounds and of the reference EXE was investigated in human placental microsomes and in MCF-7 (ER+) cell line. The replacement of the double bond with an epoxide group led to a decrease in activity in microsomes but, for compound **72**, a more potent activity in MCF-7 cells than EXE was observed. The reduction of the 17-carbonyl to a hydroxyl group (**74**) resulted in an improvement of inhibitory activity in MCF-7 cells. Conversely, the replacement of the 6-methylene group of EXE with a hydroxymethyl (**75**) induced a decrease in activity. **74** was the best compound of the series, with IC<sub>50</sub> values of 0.10 μM in human placental microsomal and of 0.25 μM in MCF-7 cells.

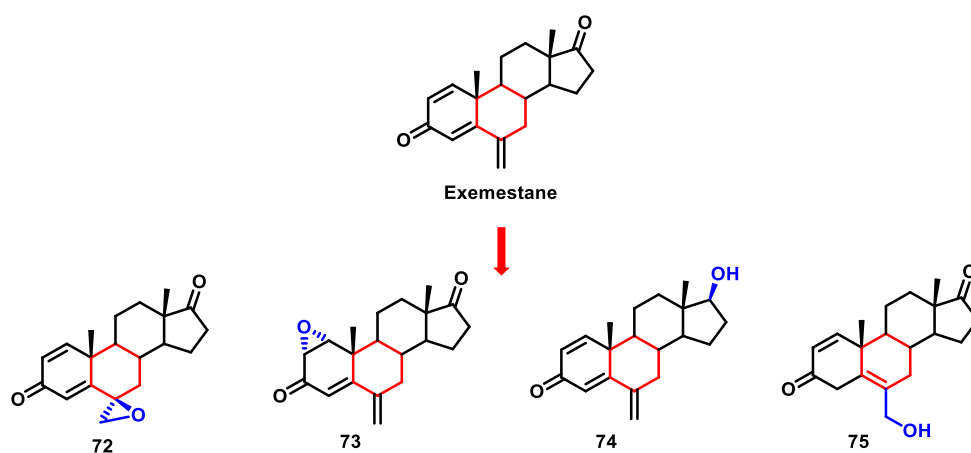


**Figure 28.** New EXE metabolites.

### Derivatives substituted on the D-ring

In order to enhance the AR inhibitory activity, the research group of Bansal produced different series of hybrid compounds, combining the classical structure of steroidal AIs with an imidazole ring typical of nonsteroidal AIs. In a first series, they synthesized some 16*E*-aryldienosteroids and evaluated cytotoxicity and AR inhibition of the new compounds. Derivatives **76** and **77** (Figure 29) showed the best inhibitory activity, with IC<sub>50</sub> values of 4.4 and 2.4 μM, respectively.<sup>126</sup>

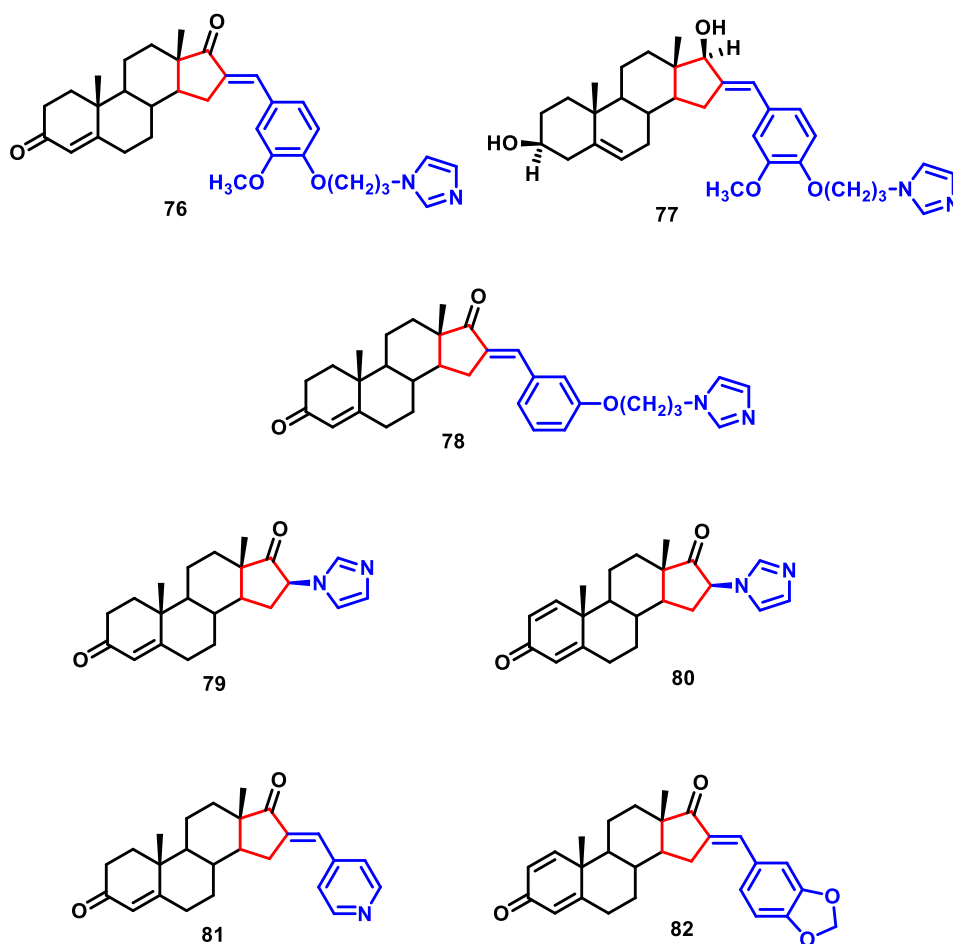


**Figure 29.** Derivatives substituted on the D-ring.

In a second work, the same research group reported other 16*E*-aryldienosteroids carrying an imidazolyl side chain, investigating the effect of this substituent in *meta* and *para* position of the phenyl ring (Figure 29).<sup>127</sup> The obtained results suggested

that the compounds with a side chain containing the imidazole group in *meta* position presented  $\approx 2.5$ -times higher AR affinity than the *para* substituted analogues. Compound **78** showed the best anti-AR activity, with IC<sub>50</sub> value of 4.4  $\mu$ M.

Later, some hybrids with the imidazole ring directly connected at 16 position of the steroidal structure were developed.<sup>128</sup> Biological analyses of new compounds showed that the imidazolyl derivatives **79** and **80** (Figure 29), carrying a carbonyl group at C3 position, were the best AIs, with IC<sub>50</sub> values of 0.16 and 0.18  $\mu$ M, respectively.

The same research group also developed a series of 16*E*-arylidensteroids with different aromatic rings on the double bond at position 16 of the steroidal core and evaluated the AR inhibitory activity of the new derivatives.<sup>129</sup> Derivatives **81** and **82** (Figure 29) were the best compounds of the series, with moderate activity against AR (IC<sub>50</sub> values of 5.2 and 6.4  $\mu$ M, respectively).

#### 2.4 NEW APPROACHES FOR ER+ BREAST CANCER TREATMENT

Despite the effectiveness of current therapies for the treatment of ER+ BC, both the available treatments, third generation AIs and SERMs, present some serious drawbacks. The use of AIs, with the consequent complete depletion of estrogens levels in the whole body, leads to the development of severe side effects, such as reduction of bone density and increase of cardiovascular events; on the other side, the treatment with SERMs, especially in long term therapies, increases the risk of developing endometrial cancer. Moreover, for both classes of drugs the development of intrinsic or acquired resistance is common. For these reasons, numerous research groups have focused their studies on the development of new compounds and new strategies to overcome these issues. In particular, in recent years the role of AR enzyme was reconsidered, opening the way for the development of molecules with a new mechanism of action with respect to the classic one. Moreover, a crosstalk between AR enzyme and ERs was also recently observed, which could lead to the design of novel anticancer agents.

#### 2.4.1 Potential allosteric modulation of aromatase

The modulation of a target protein can sometimes be obtained by the interaction of ligands with a binding site located out of the area of the active site, named allosteric site. Upon binding, the three-dimensional structure of the receptor/enzyme undergoes conformational changes that can lead to modifications in the catalytic or orthosteric binding site of the target. Depending on whether the modifications induced by allosteric modulators increase or decrease the affinity and/or the efficacy of the natural ligand, these molecules can be classified as positive or negative modulators, respectively.

In the field of breast cancer, it is widely known that TAM metabolites maintain great affinity for estrogen receptors and potent antiestrogenic activity, taking part in the ERs modulation due to TAM administration. Attempts to correlate metabolites concentrations with the clinical effects of TAM gave mixed results, so that the involvement of other mechanisms of action together with ER antagonism was suggested. In 2012, Lu et al. carried out an *in vitro* study documenting that some TAM metabolites were able to inhibit AR.<sup>130</sup> In detail, END and N-desmethyltamoxifen (Figure 30) showed  $K_i$  values of 4 and 15.9  $\mu\text{M}$ , respectively, while TAM or Z-4-hydroxytamoxifen did not exhibit appreciable inhibition at similar concentrations. For the two active inhibitors, a non-competitive mechanism of action was observed, that led to the hypothesis of an allosteric interaction between the compounds and AR. The same research group tested the ability of ten TAM metabolites to inhibit the enzyme, and the most potent compound resulted to be norendoxifen (Figure 30), with a competitive mechanism of action and a  $K_i$  value of 35 nM.<sup>131</sup>

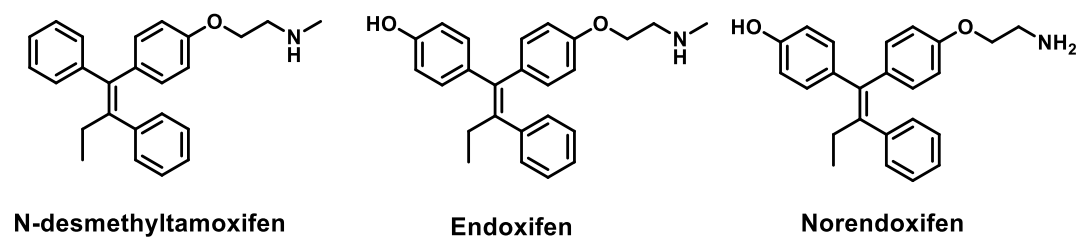


**Figure 30.** Structures of *N*-desmethyltamoxifen, endoxifen (END) and norendoxifen.

Based on the non-competitive inhibition observed for TAM metabolites, the research group of Magistrato and coworkers studied the mechanism of AR non-competitive inhibition.<sup>132</sup> In order to detect the presence of hypothetical allosteric binding pockets, different computational methods were used, identifying three putative binding sites in different regions of AR structure (Site 1, Site 2 and Site 3, Figure 31), two of which (Site1 and Site 2) were able to bind different TAM metabolites forming stable complexes. Visual examination revealed that Site 1 (red, Figure 31) was located close to the most favorable access channel for the catalytic site, while Site 2 (blue, Figure 31), being situated in the proximity of Lys108 and Lys420, was involved in the transfer of electrons from CPR to AR. MD studies were performed with END, that showed the strongest non-competitive inhibitory activity, and it was observed that this compound, binding to one of the hypothetical sites, increased the rigidity of the enzyme and altered its functional collective motion, critical for the breathing of the channel for substrate release/uptake, interfering with the catalytic activity.

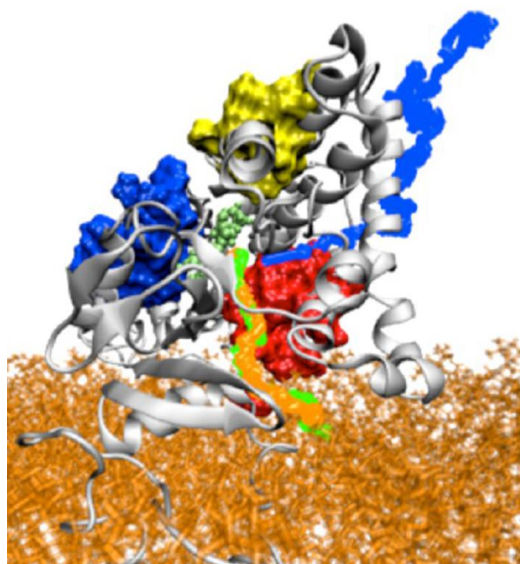


**Figure 31.** Positions of site\_1 (red), site\_2 (blue), and site\_3 (yellow) relative to the three ASD entrance/exit routes (blue, orange, and green lines).<sup>132</sup>

The same research group, using an integrated computational protocol, analyzed the putative entry/exit channels accessible to the natural substrate of the enzyme ASD

and the non-steroidal inhibitor LTZ.<sup>133</sup> It was observed that these two compounds, characterized by different size, shape and lipophilicity, could enter the binding site via different routes, as they exited using preferentially only one channel. Comparing the location of these channels to the putative allosteric sites identified in their previous work, it was shown that they were located in the same region of the enzyme.

Simultaneously, studying some azole fungicides, together with the AI LTZ, Ghosh *et al.* observed that these compounds presented a non-competitive or mixed mechanism of inhibition.<sup>134</sup> These results suggested that the biological effects caused by these compounds could be due to alternative mechanisms of interaction with the enzyme. In particular, in addition to the active site distal to the heme moiety, that represented the site of interaction with ASD, two more cavities were revealed. One pocket was found close to the access channel of AR active site, where the binding of a ligand could hinder the entry of the substrate, while another site was discovered at the heme proximal region, and the binding of molecules at this site could impair the coupling between CPR and AR, interrupting the flow of electrons necessary for the catalytic activity. Moreover, the binding of an inhibitor to these regions could also allosterically trigger conformational changes in the active site. The location of the putative additional binding sites found in this study seemed to be in accordance with that presented by Magistrato.

Given these discoveries concerning the presence of putative allosteric sites within AR structure, one of the possible strategies to overcome the drawbacks of the currently used therapies in BC treatment could be the development of compounds able to interact with these sites or with both the active site and an allosteric pocket. Allosteric modulation could indeed lead to some advantages over classical competitive inhibition: i) the maximal inhibitory activity of allosteric drugs could be reached without completely blocking estrogen synthesis, ii) their activity could not be conditioned by high concentration of the natural ligand and finally, iii) molecules binding to an allosteric site, a part of the structure less conserved than the active site within a family of protein, may be characterized by higher selectivity. At the same time, dual acting inhibitors, able to interact with both the active site and the allosteric pocket may bind the enzyme with higher stability, leading to an

increase in inhibitory potency, and maybe delay or reduce the insurgence of resistance due to the additional interaction.

Thus, the search of new AR ligands that could modulate activity via possible allosteric mechanisms for therapeutic benefits was of great of interest. In 2012, Ghosh *et al.* designed and synthesized a series of EXE derivatives, based on the binding environment observed in the crystallographic structure of the enzyme complexed with the inhibitor EXE and the natural substrate ASD.<sup>135</sup> Within the binding site, the steroid skeleton was surrounded by hydrophobic residues and by H-bond donor groups that interacted with 3- and 17-keto oxygens through H-bonds. The only two exposed positions in the structure were C4 and C6, located close to the active site access channel. Modeling analysis suggested that substituents on these two positions could occupy the available space and that a linear carbon chain was the best substituent to penetrate the “hydrophobic clamp”, an entry point positioned into the access channel between Ser478 and Thr310. In this study, new steroidal compounds with different alkynyloxy chains inserted in position 6 were synthesized (Figure 32) and the inhibitory and antiproliferative activities were evaluated to confirm the assumptions resulted from the molecular modeling analysis. The 6-substituted andro-1,4-diene-3,17-diones carrying a six atoms side chain (compounds **83** and **84** Figure 32) resulted to be the best compounds, with IC<sub>50</sub> values of 12 and 20 nM, respectively, in the same range of the non-steroidal inhibitor LTZ (10 nM).

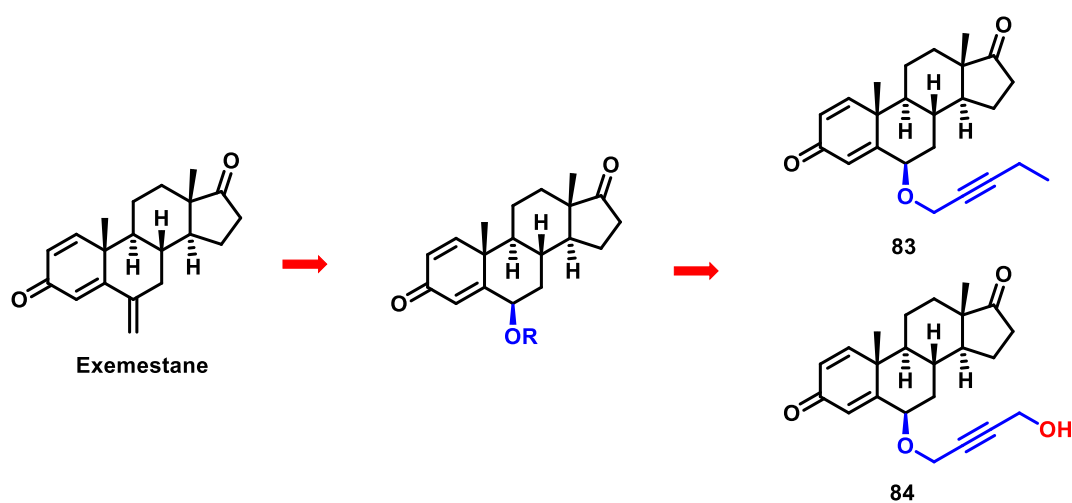


**Figure 32.** New 6-alkynyloxy EXE derivatives shown to occupy AR active site access channel.

It was observed that the progressive elongation of the side chain led to an increase of the IC<sub>50</sub> values, suggesting that the six atoms side chain had the optimal size to establish favorable interactions with the active site cleft. The antiproliferative activity of the new compounds was also tested; most of the derivatives were able to inhibit TST-stimulated proliferation of MCF-7 cells, and the best compound resulted once again to be **83**, followed by **84** with EC<sub>50</sub> values of 0.03 and 0.3 nM, respectively. Moreover, the X-ray structure of the AR-**83** complex was compared with those of ASD and EXE. It was observed that, like in the EXE-complex, the backbone ring-A shifted away from the access channel, while the backbone ring-D was positioned similarly to that of ASD. Superposition of the EXE and **83** complexes showed that the orientation of the unsaturated C6-methylidene of EXE was different from that of the C6 $\beta$ -pentynyloxy chain of **83**; indeed, the side chain of the new inhibitor could protrude into the “hydrophobic clamp” of the access channel, interacting with the putative allosteric site and also conditioning the catalytic residues of the enzyme. Furthermore, the terminal C-24 methyl group of the side chain of **83** interfered with some water molecules confined in the access channel between the polar residues Ser478, Arg192 and Asp309, that were considered crucial for the aromatization activity of the enzyme.

The inhibition of AR via allosteric modulation could be a new therapeutic strategy characterized by fewer side effects and a delay in the onset of resistance compared to currently used therapies. In 2019, in order to explore this new inhibition mechanism, Spinello *et al.* identified new commercial molecules able to inhibit the enzyme with a non-competitive or mixed mechanism, developing an integrated computational and experimental protocol.<sup>136</sup> As it was found that LTZ acted via a non-competitive or mixed mechanism, at first they performed docking analysis of this inhibitor into the two putative allosteric sites identified in a previous work. LTZ was able to penetrate inside Site 1, displacing the network of water molecules from the cavity. The same mechanism was also observed for *E*-END which, once inside Site 1, hampered the proton delivery to the substrate. Considering the second putative allosteric pocket, located close to the CPR binding site, both molecules were able to bind to Site 2, lying between Lys440 and Tyr361. The binding of a

drug into this cavity hindered the formation of the AR-CPR complex, affecting the flow of electrons required for the catalytic process. Subsequently, in order to identify different molecules able to bind both allosteric sites, virtual screening (VS) simulations of different libraries of compounds, followed by MD simulations and free energy calculation ( $\Delta G_b$ ), were performed. The compounds that showed the best results from these analyses were tested to determine their inhibitory activity and  $IC_{50}$  values were calculated for each compound. Five molecules (Figure 33) exhibited the best inhibitory activity, with  $IC_{50}$  values in the  $\mu M$  range; compounds **85-87** were identified by performing VS on Site 1, while compounds **88** and **89** on Site 2. The antiproliferative activities of the new compounds and LTZ against MCF-7 (ER+) and MDA-MB-231 (ER-) cell lines were also tested, and compounds **85**, **86**, **88** and **89** were seen to reduce the MCF-7 cellular growth with  $GI_{50}$  values in the micromolar range. Considering the MDA-MB-231 cell line, only compounds **85** and **88** showed antiproliferative activity, while the best compounds for each site, **86** and **89**, did not show any activity against these ER- cells, confirming that the two compounds acted on AR. Moreover, enzymatic kinetics assays supported the hypothesis of a non-competitive or mixed mechanism of inhibition for the new compounds.

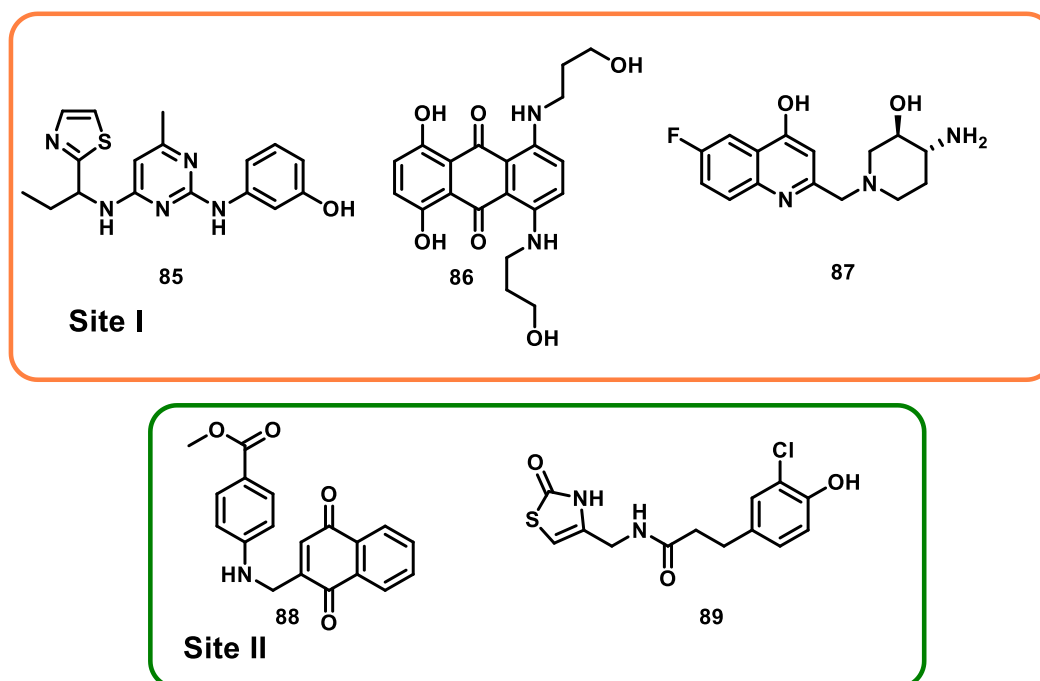


**Figure 33.** Allosteric modulators of AR identified by virtual screening.

#### 2.4.2 Multipotent agents targeting both aromatase and ERs

In the field of ER+ BC treatment, numerous research groups have investigated the potential synergistic activity of a combination of drugs that modulate different targets involved in crucial pathways of the pathology. Indeed, the two main current therapeutic strategies, aromatase inhibition and ER modulation, have been extensively combined and compared to evaluate the final effect. However, conflicting results appeared from different clinical studies. As mentioned above, the ATAC study, where five years' treatment with anastrozole or TAM alone were compared with the combination of the two drugs, revealed that anastrozole alone was more effective<sup>90, 91</sup>. In another study conducted by Brodie *et al.*,<sup>92</sup> the therapy with the AILTZ was compared with the SERD fulvestrant alone or in combination. From this study, in contrast to ATAC, the antitumor activity of the combination of the two drugs resulted to be more effective than when the two compounds were administered alone. As a result, it appears that unambiguous conclusions concerning potential efficacy cannot be assumed for any SERM/SERD and AI combination.

In the last decades the multitarget approach, that is the development of a single molecule able to interact with multiple targets involved in the same disease, has become one of the most investigated therapeutic strategies for the treatment of complex multifactorial pathologies. This approach has largely been exploited in different medicinal chemistry fields for the development of potent and effective agents, but only in recent years has been applied to ER+ BC research.

In this scenario, the work of Lu *et al.*<sup>130, 131</sup> reported the first evidence of the existence of a single compound capable of interacting with significant activities on two targets, AR and ER, involved in the progression of this tumor. As mentioned above, in this work the aromatase inhibitory activities of several TAM metabolites were tested, and most of them resulted to be competitive AIs with a wide range of activities, norendoxifen proving to be the most active compound (IC<sub>50</sub> = 90 nM). These results allowed to establish some structure-activity relationships between the different compounds. Indeed, the data suggested that the progressive hydroxylation and demethylation of TAM led to an improvement in the inhibitory activity. A

rationale for these results could be that within the ligand binding site, in the region where the amino group was positioned, the available space was limited and the decrease in activity when one or more methyl groups were present was caused by steric hindrance. Moreover, the amino moiety was involved in a H-bond interaction with Ala306, and the presence of methyl groups could decrease its capacity to act as H-bond donor, resulting in loss of activity. Subsequently, the same research group synthesized (*E*)-norendoxifen, (*Z*)-norendoxifen and (*E,Z*)-norendoxifen isomers and evaluated their activity on both targets. The mixed norendoxifen showed potent aromatase inhibitory activity ( $IC_{50} = 102$  nM) and good affinity for both ERs, the *E* isomer exhibited at least 10 times higher aromatase inhibitory activity than *Z*-norendoxifen, while the latter had slightly more affinity toward the receptors. These findings increased the interest in the development of new small molecules that could act as AR inhibitors while maintaining SERMs activity. Furthermore, the structure of the central core of TAM, completely different from that of current AIs, could be characterized by better efficacy and fewer side effects. Lv *et al.* synthesized the first series of norendoxifen analogues with the aim of optimizing the activity on both targets.<sup>137</sup> Based on the previously obtained binding mode of *E*- and *Z*-norendoxifen in the active site of AR, some structural modifications were performed leading to the design of the new derivatives (Figure 34). These changes concerned the introduction of a hydroxyl group in the *para* position of ring **A**, the elimination or the substitution with an amino group of the hydroxyl on ring **B**, the introduction on the ethyl side chain of a group able to coordinate the iron or various alkyl groups, the replacement of the side chain amino terminal moiety with different groups and of the ether oxygen with a methylene group. The biological results suggested that the presence of the hydroxyl group on ring **A** was favorable for both activities; the introduction of an iron coordinating group on the ethyl moiety, as well as the replacement of the hydroxyl group on the B ring with an amino group, led to an increase in AR inhibitory activity but greatly decreased the binding with ERs. Finally, the substitution of the amino terminal group and the ether oxygen generally decreased activities. Among these derivatives, 4'-hydroxynorendoxifen (Figure 34), carrying a hydroxyl group on the **A** ring, was the most potent, with increased activities toward AR, ER $\alpha$  and ER $\beta$  with respect to

the parent norendoxifen, exhibiting IC<sub>50</sub> values of 45 nM, 15 nM and 9.5 nM, respectively.

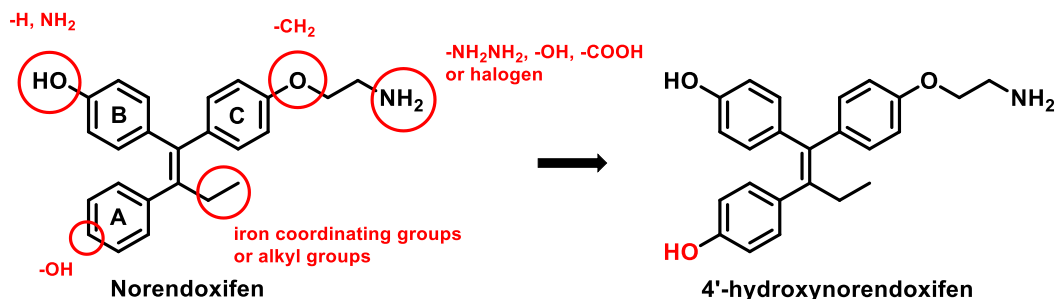


**Figure 34.** Norendoxifen SAR and development of 4'-hydroxynorendoxifen as dual AI/SERM.

The same research group developed another series of norendoxifen analogues, in which the aminoethoxy side chain was replaced by a hydroxyl group, in order to overcome the problem of *E/Z* isomerization, typical of triphenylethylene derivatives.<sup>138</sup> TAM bisphenol, another known metabolite of this drug (Figure 35) had also been previously shown to possess significant affinity for ERs,<sup>139</sup> supporting the hypothesis that the removal of the side chain did not affect the antiestrogenic activity of this class of compounds.

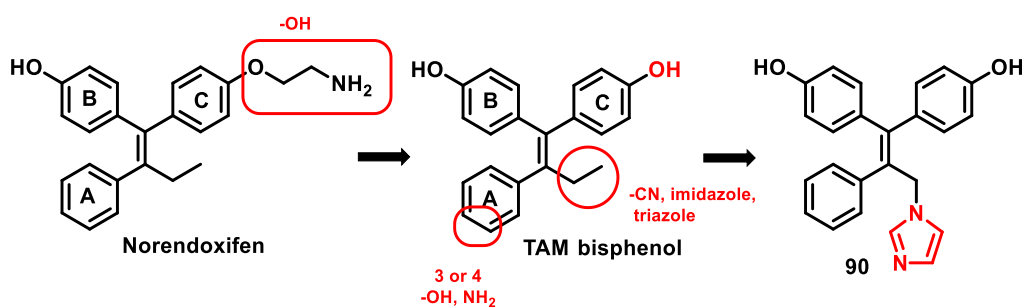


**Figure 35.** Development of compound **90** as dual AI/SERM.

In this new series, different iron-coordinating groups (nitrile, imidazole, or triazole) were introduced on the ethyl moiety, while hydrogen bond donors (hydroxyl or amino) were inserted on the *meta* or *para* positions of ring **A** (Figure 35). The biological evaluation showed that the introduction of an imidazole group in the ethyl moiety was optimal for both AR inhibitory activity and ER binding affinities, while the introduction of a substituent on ring **A** was less significant. Compound **90**

resulted the best one, with high inhibitory activity against AR ( $IC_{50} = 4.77$  nM) and good affinity for ER $\alpha$  and ER $\beta$  ( $EC_{50}$  values of 27.3 nM and 40.9 nM, respectively). Further modifications of the structure of norendoxifen led to the development of new derivatives, in which an amino or a nitro group were inserted on the *para* position of ring **A**, the aminoethoxy chain was replaced by either hydroxyl, to give a bisphenol moiety as in the previous series, or an amino group, that together with the amino/hydroxy group replacement on ring **B** led to a series of bis-anilino derivatives. Moreover, the ethyl group was shortened to a methyl moiety (Figure 36)<sup>140</sup>. SAR studies on these compounds confirmed that the aminoethoxy chain was not essential for favorable interactions with AR and ERs and the insertion of an amino group on ring **A** led to an increased AR inhibitory activity, while the corresponding nitro derivative showed low activities. Moreover, the shortening of the ethyl group was detrimental for both activities. Among these derivatives, the bis-aniline **91** showed potent AR inhibitory activity ( $IC_{50} = 62.2$  nM) and high binding affinity toward ER $\alpha$  and ER $\beta$ , with  $EC_{50}$  values of 70.1 nM and 70.8 nM, respectively. Moreover, compound **92** carrying an amino group on ring **A** showed the best AR inhibitory activity ( $IC_{50} = 8.8$  nM), but low affinity for the receptors.

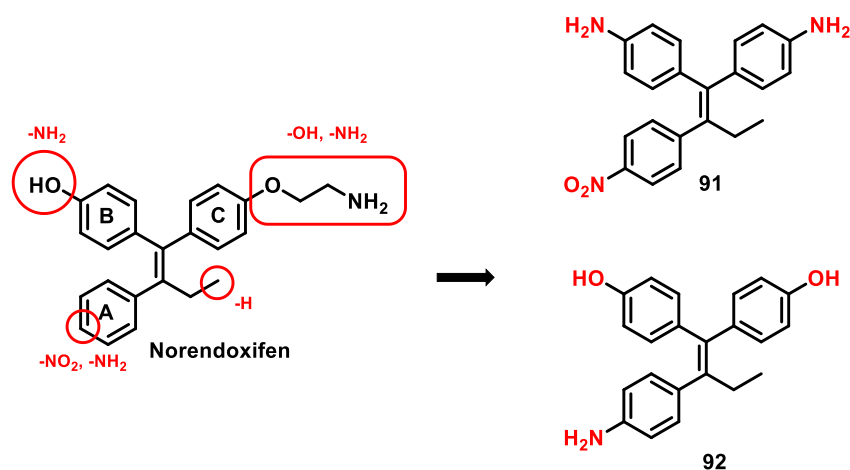


**Figure 36.** Development of compounds **91** and **92** as dual AI/SERM.

### 3. DESIGN AND SYNTHESIS OF NEW POTENTIAL AGENTS FOR THE TREATMENT OF ER+ BREAST CANCER

#### 3.1 POTENTIAL ALLOSTERIC OR DUAL-ACTING AROMATASE MODULATORS

As mentioned above, currently used therapies in BC treatment have some drawbacks, such as development of side effects and resistance. Therefore, it is necessary to develop new molecules that act with different mechanisms in order to overcome these issues. Given the latest discoveries concerning the presence of putative allosteric sites within AR structure<sup>132</sup>, one of the possible strategies could be the development of compounds able to interact with these sites or with both the active site and an allosteric pockets. Thus, a part of my project was focused on the development of new potential non-steroidal allosteric or dual acting AIs.

##### 3.1.1 Design and synthesis of alkoxyated imidazolymethylxanthenes<sup>141</sup>

Starting from some imidazolymethylxanthenes (**93-95**, Figure 37), previously synthesized by my research group,<sup>108</sup> and exhibiting competitive inhibitory activity against AR, new molecules with potential dual mode were envisaged.

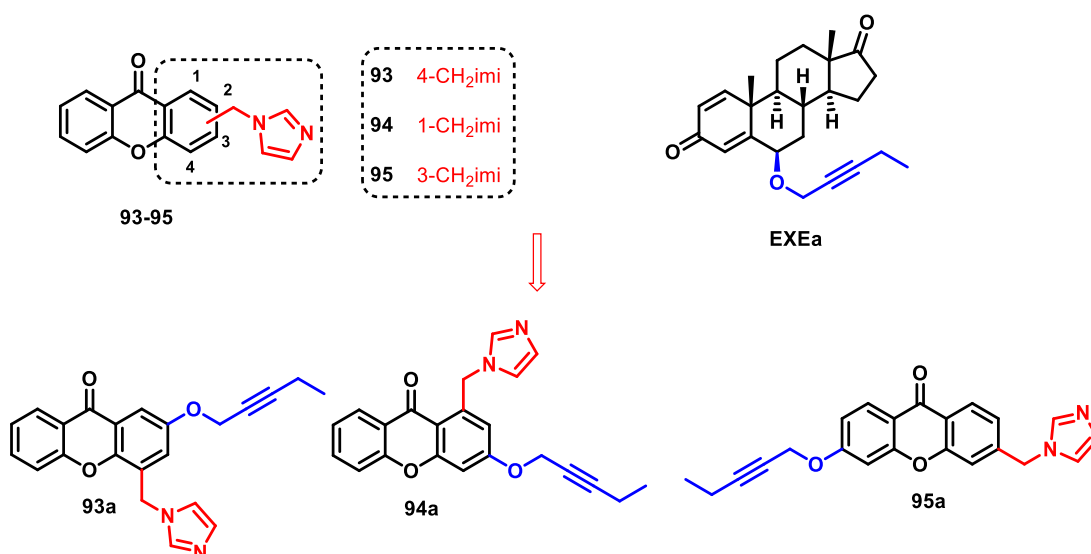


**Figure 37.** Design of new alkoxyated imidazolymethylxanthenes.

The new compounds were designed by inserting on the xanthone core a pentynyloxy chain, which resulted the most suitable group to establish favorable interactions with the putative allosteric site close to the access channel, when inserted on the steroidal structure of EXE to give compound EXEa<sup>135</sup> (**83**, Figure 32 and Figure 37).

Docking calculations were performed on the previously reported imidazolylmethylxanthenes **93-95** and on LTZ (Figure 38, left column). It was observed that the high activity of non-steroidal AIs such as LTZ was due to the coordination of the iron atom of the heme group with the nitrogen of theazole ring, and the same mechanism was supposed for the imidazolylmethylxanthenes derivatives. As the docking calculations do not take into account the coordination bond involving the transition metal, these analyzes were performed by imposing a constraint between Fe@heme and N@azole atoms, generating binding poses in which the imidazole ring was in proximity of the iron atom. In particular, compounds **93** and **94** adopted a suitable binding geometry with theazole ring almost perpendicular to the heme plane, with the nitrogen atom at a distance of 2.7 and 3 Å, respectively. Moreover, the xanthone moiety established  $\pi$ -stacking interactions with Trp224. Considering compound **95**, in the best binding pose theazole ring was tilted with respect to the heme plane, probably resulting in a lack of coordination, even if the xanthone established  $\pi$ -stacking interactions with Phe134. Notably, when this compound was analyzed without the Fe-N constraint, it was observed that the carbonyl group of the xanthone structure was located close to the iron.

Considering the excellent results given by the functionalization of EXE in the abovementioned steroidal structures and the binding pose obtained for compounds **93-95**, new derivatives were designed (**93a** and **94a**, Figure 37) by inserting the pentynyloxy chain on the imidazolylmethylxanthone core in *meta* position, postulated to be the best positions in order to fill the entrance of the access channel. Indeed, via docking calculations with a constraint on the Fe-N bond (Figure 38, right column), it was possible to identify binding poses only for compounds **93a** and **94a** with the side chain in *meta* position.

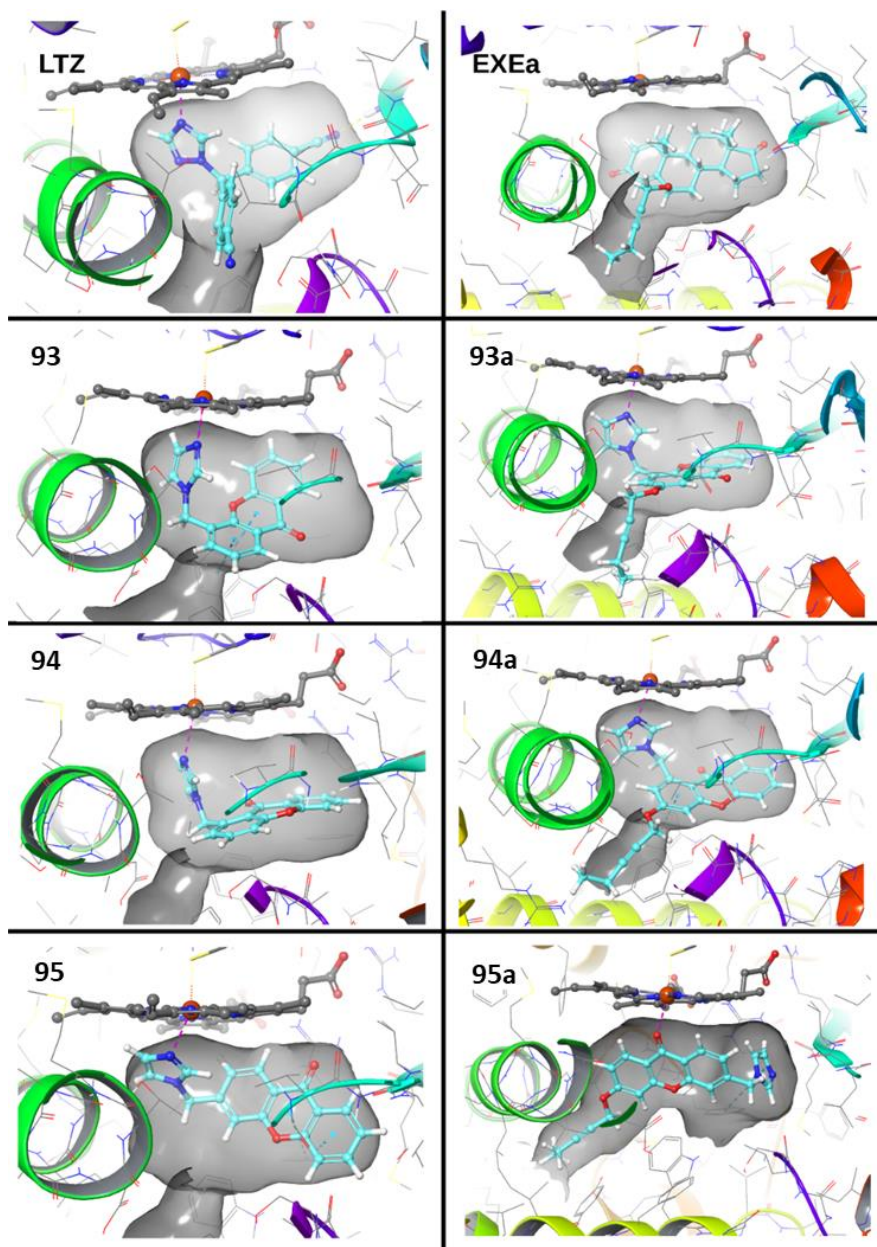


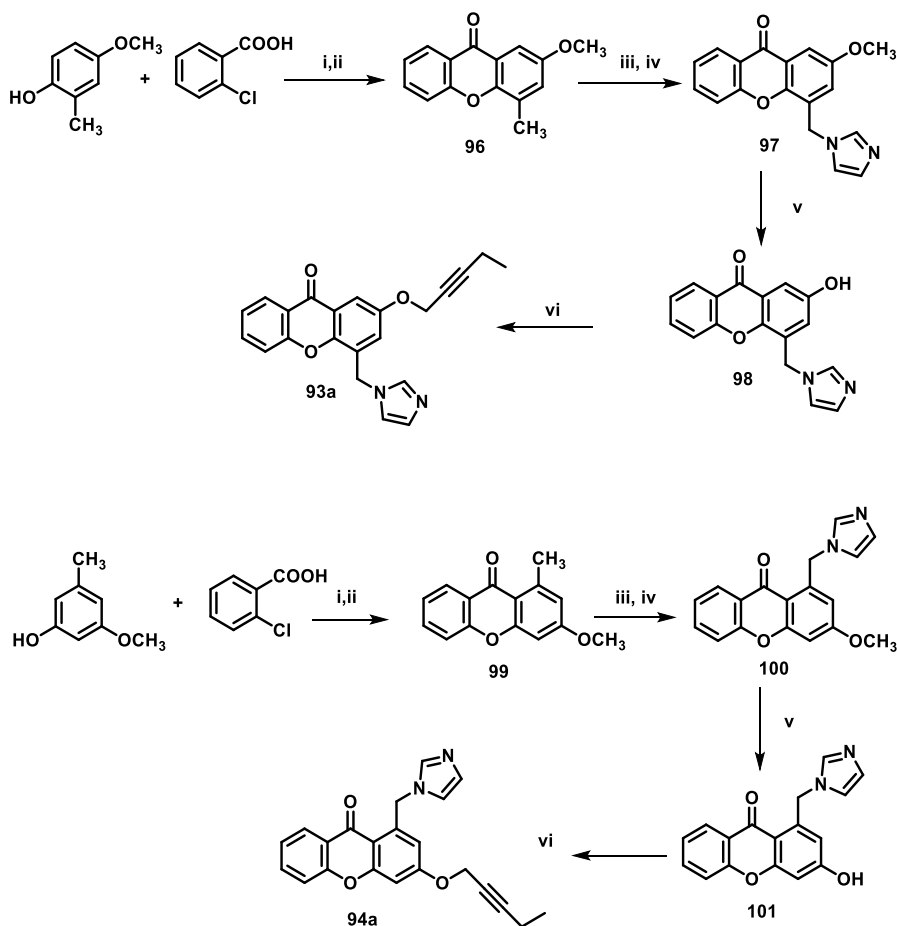
**Figure 38.** Best-ranked binding poses obtained for the AIs LTZ, EXEa and for compounds **93-95**, **93a-95a**. The protein is shown in ribbons, the binding site is highlighted with a transparent gray surface, while the inhibitors and the heme are shown in a ball and stick representation.<sup>141</sup>

Theazole ring of these new compounds was at a distance of 2.82 and 2.52 Å from the heme group, respectively, while the side chain was oriented into the access channel similarly to EXEa. Furthermore, the xanthone of **94a** exhibited  $\pi$ -stacking

interactions with Trp224. Docking calculation with a constraint on the Fe-N bond for compound **95** generated a binding pose in which the entrance of the access channel was not easily reached by the side chain. Thus, considering the additional peculiar binding pose identified for compound **95** (without the Fe-N constraint), **95a** was also designed (Figure 37). In this derivative, the carbonyl oxygen was at 2.57 Å from the iron while the side chain, located on the other aromatic ring with respect to the imidazolylmethyl group, was able to fit inside a hydrophobic cavity lined by residues Leu301, Leu305, Leu25, Tyr220, Ile125, and Met127.

### Chemistry

**Scheme 1.** Synthesis of compounds **93a** and **94a**.

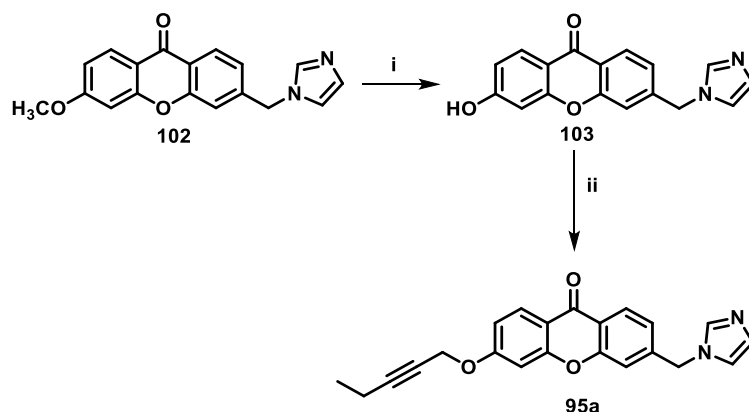


**Reagents and conditions:** i)  $K_2CO_3$ , Cu/CuI, pyridine,  $H_2O$ , reflux, 2 h; ii)  $H_3PO_4$ ,  $P_2O_5$ ,  $120\text{ }^\circ\text{C}$ , 7 h; iii) NBS, BPO,  $CCl_4$ , reflux, hv, 6 h; iv) imidazole,  $CH_3CN$ , reflux,  $N_2$ , 6 h; v)  $AlCl_3$ , toluene, reflux, 3 h; vi) 1-bromo-2-pentyne,  $K_2CO_3$ , acetone, reflux, 18-26 h.

For the synthesis of the new compounds **93a** and **94a** (Scheme 1) 4-methoxy-2-methylphenol, obtained from the reduction of 2-hydroxy-5-methoxybenzaldehyde with methyl formate, triethylamine, NaBH<sub>4</sub> and HCl,<sup>142</sup> or the commercially available 3-methoxy-5-methylphenol were reacted with 2-chlorobenzoic acid under Ullmann reaction conditions to give the corresponding diarylethers, which were then cyclized, without purification, by treatment with polyphosphoric acid to obtain the xanthone cores (**96** and **99**). Bromination of the methyl group with NBS (N-bromosuccinimide) in presence of benzoyl peroxide (BPO) and subsequent reaction with imidazole allowed obtaining intermediates **97** and **100**, which were then demethylated with AlCl<sub>3</sub> to give the corresponding hydroxyl derivatives **98** and **101**, subsequently alkylated with 1-bromo-2-pentyne to get the final compounds.

For the synthesis of xanthone **95a**, 6-methoxy-3-imidazolylmethylxanthone **102**<sup>143</sup> was subjected to a demethylation step followed by alkylation with 1-bromo-2-pentyne, as previously reported for xanthenes **97** and **100**, to obtain the desired compound (Scheme 2).

**Scheme 2.** Synthesis of compound **95a**.



**Reagents and conditions:** i) AlCl<sub>3</sub>, toluene, reflux, 3 h; ii) 1-bromo-2-pentyne, K<sub>2</sub>CO<sub>3</sub>, acetone, reflux, 21 h.

## Results and discussion

The inhibitory activity of the new compounds was quantified by the Aromatase Inhibitor Screening Kit (BioVision Inc., San Francisco, USA), monitoring the conversion of a fluorogenic substrate into a highly fluorescent metabolite as catalyzed by AR. The newly synthesized derivatives were tested at different concentrations (from 0.1 to 100  $\mu\text{M}$ ) and exhibited  $\text{IC}_{50}$  values in the low  $\mu\text{M}$  range (from 0.77 to 5.55  $\mu\text{M}$ , Table 1).

**Table 1.** AR inhibition and growth inhibition of ER+ (MCF-7) and ER- (MDA-MB-231) cell lines, distances between the nitrogen of the ligands and the iron of the heme, and angle between the planes of the imidazole ring and the heme moieties.

<b>Cmp</b>	<b>AR inhibition <math>\text{IC}_{50}</math> (<math>\mu\text{M}</math>)<sup>a</sup></b>	<b>MCF-7 <math>\text{GI}_{50}</math> (<math>\mu\text{M}</math>)<sup>a</sup></b>	<b>MB-MDA-231 <math>\text{GI}_{50}</math> (<math>\mu\text{M}</math>)<sup>a</sup></b>	<b>Distance (<math>\text{\AA}</math>)</b>	<b>Angle (deg)</b>
<b>LTZ</b>	0.01 <sup>b</sup>	4.1 $\pm$ 1.1 <sup>c</sup>	34.0 $\pm$ 7.8	2.33 $\pm$ 0.15	91.8 $\pm$ 2.7
<b>93</b>	0.017 <sup>d</sup>	69.1 $\pm$ 0.8	58.3 $\pm$ 11.7	2.30 $\pm$ 0.13	88.8 $\pm$ 2.0
<b>94</b>	0.150 <sup>d</sup>	59.0 $\pm$ 2.6	44.3 $\pm$ 6.5	2.31 $\pm$ 0.15	89.0 $\pm$ 2.6
<b>95</b>	0.390 <sup>d</sup>	19.9 $\pm$ 5.9	30.4 $\pm$ 4.6	2.23 $\pm$ 0.12	91.3 $\pm$ 2.1
<b>93a</b>	5.55 $\pm$ 2.3	52.3 $\pm$ 16.3	21.1 $\pm$ 9.3	2.18 $\pm$ 0.10	92.3 $\pm$ 2.2
<b>94a</b>	2.85 $\pm$ 0.1	6.3 $\pm$ 1.1	17.5 $\pm$ 7.9	2.15 $\pm$ 0.08	91.8 $\pm$ 2.4
<b>95a</b>	0.77 $\pm$ 0.3	>100	>100		

<sup>a</sup>Data represent the mean  $\pm$  standard deviation of three independent experiments;

<sup>b</sup>ref<sup>134</sup>; <sup>c</sup>ref<sup>136</sup>; <sup>d</sup>ref<sup>108</sup>.

Compounds **93a** and **94a** showed a drastic decline of the inhibitory activity compared to their parent compounds **93** and **94**, while compound **95a** displayed an  $IC_{50}$  value in the same range of compound **95**. These results suggested that the introduction of a long and rigid alkoxy side chain in proximity of the imidazole group (**93a** and **94a**) could hinder the proper placement of the compounds in the active site of the enzyme; on the contrary, the interactions between the compound and the target were not hampered when the chain and the imidazole moiety were symmetrically located on the two different aromatic rings of the scaffold (**95a**).

The antiproliferative activities of **93-95** and **93a-95a** against the MCF-7 (ER+) and MDA-MB-231 (ER-) BC cell lines were also investigated (Table 1).

The previously synthesized compounds **93-95** moderately inhibited the growth of both cell lines with  $GI_{50}$  superior to 10  $\mu$ M. Regarding the new derivatives, compound **93a** showed higher antiproliferative activity with respect to compound **93** only in MDA-MB-231 cells, while **94a** exhibited better activity than **94** on both cell lines, with  $GI_{50}$  lower than 10  $\mu$ M against MCF-7, similar to that of LTZ. These results suggested that, generally, the introduction of the alkoxy chain led to either increase (**93a** on MDA-MB-231 and **94a** on both cell lines) or maintenance (**93a** on MCF-7) of the antiproliferative effect compared to the parent compounds **93** and **94**. Contrariwise, compound **95a** did not show antiproliferative activity on either cell line at any tested concentration; again, this contrasting behavior may be due to the different relative positioning of the two substituents, namely the alkoxy chain and the imidazole heterocycle. From these results, the antiproliferative activity did not seem to be directly related to AR inhibition.

### *Computational studies*

To rationalize the experimental results observed, sophisticated computational analyses were performed, in order to describe the coordination bond between the imidazole nitrogen of the inhibitor and the iron of the heme group.

Classical MD simulations with constraint Fe-N bond followed by quantum mechanics/molecular mechanics (QM/MM) MD simulations were carried out.

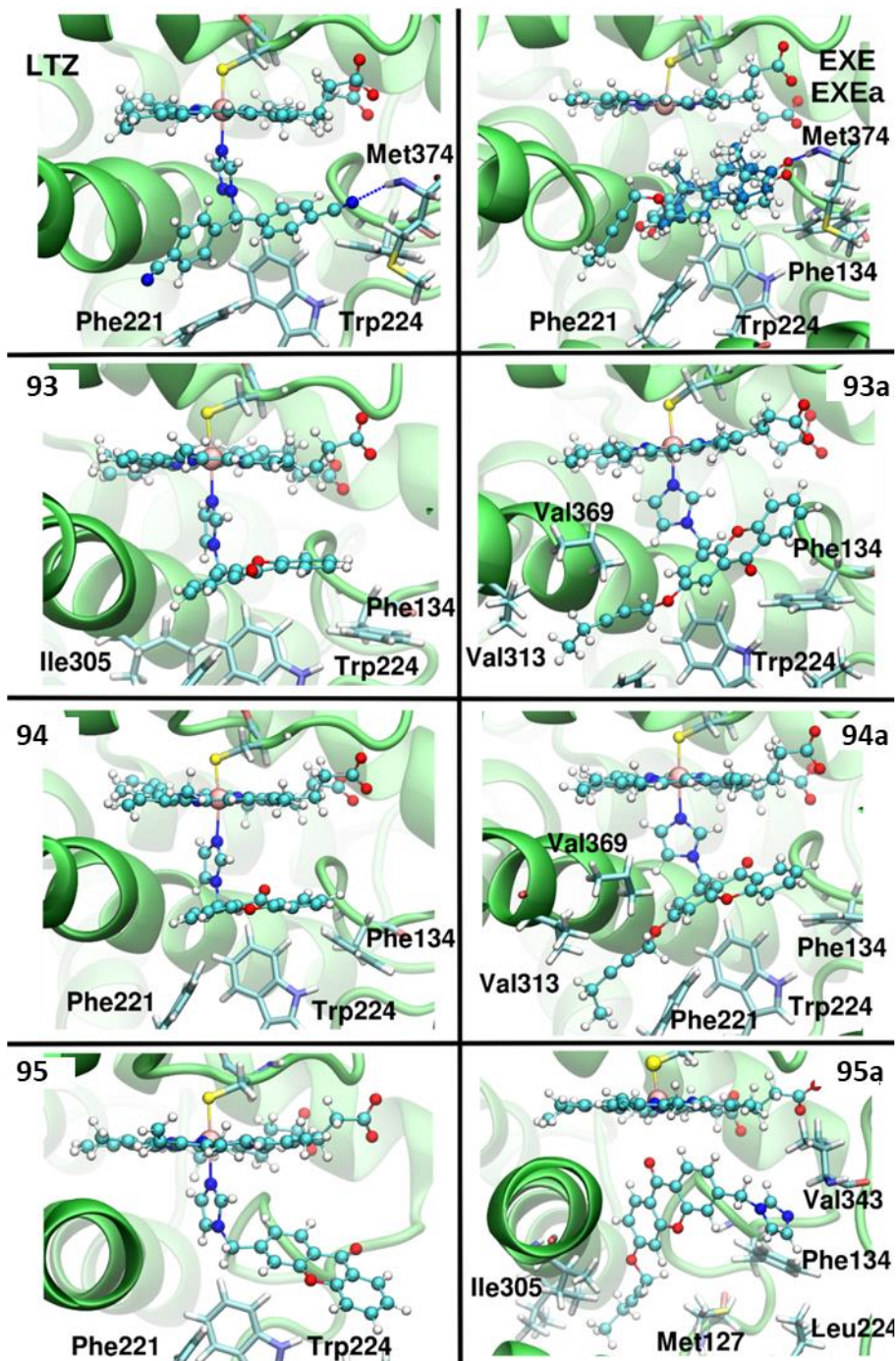


**Figure 39.** Representative structures obtained from quantum-classical molecular dynamics simulations of LTZ, EXE and its derivative (EXEa), **93-95** and **93a-95a**. For comparison, EXEa is reported superimposed to EXE. The inhibitors and the heme moiety are shown in ball and stick representation, while hydrophobic residues involved in stacking and hydrophobic interactions are highlighted as sticks. When present, hydrogen bonds are shown as dashed red and blue lines.<sup>141</sup>

From these studies (Figure 39), **93a** and **94a** exhibited a stable coordination bond between imidazole and AR, while the putative coordination bond of **95a**, observed in the docking pose, was lost during the QM/MM MD simulation. Moreover, the structural parameters obtained with the QM/MM MD simulation were compared with that of the clinically used LTZ. All compounds showed similar Fe-N bond lengths and a similar trend was also observed for the angle formed between the imidazole ring and the heme group, which resulted to be almost perpendicular (Table 1). Despite all these structural similarities, the potency of the new compounds was much lower than that of LTZ, and these results suggested that the coordination bond length and the orientation of the imidazole were not crucial for the inhibitory activity. It was observed that LTZ, besides coordinating the heme iron, formed a stable H-bond with Met374 and hydrophobic interactions with several residues positioned into the catalytic pocket (Phe221, Trp224, Phe132, Leu477, Val370, Leu372, and Ile133), and all these interactions could also account for the high activity of this molecule. Analyzing the binding pose of the steroidal inhibitor EXE, it was observed that this drug interacted with the enzyme similarly to the natural substrate ASD. It formed H-bonds with Asp309 and Met374 like LTZ and, in this case, the pentynyloxy side chain inserted in the structure was able to properly fit into the allosteric pocket, triggering the closure of the access channel without altering the binding mode of the compound.

Investigating the effects of **93a** on the entry channel, it was thus suggested that the hydrophobic tail could not perfectly fit into the channel, causing its rearrangement but leaving it partially open. The energetic cost necessary for the active site rearrangement upon the binding of the different drugs was also monitored. While EXE and its derivative with the pentynyloxy chain exhibited similar energy costs, compounds **93** and **95** showed lower deformation with respect to their derivatives **93a** and **95a**, suggesting that the insertion of the chain caused a strain in the orthosteric and allosteric sites. Finally, docking calculations followed by classical MD simulations on the two previously exploited <sup>132</sup> allosteric sites alone were also performed. Only compound **95a** was able to interact with the site close to the access channel (Site 1), while considering Site 2, located near the binding site of the CPR, all compounds (**93a-95a**) spontaneously dissociated after 50 ns of MD simulation.

In conclusion, it seemed that the presence of the side chain on the xanthone core could in fact partially hinder the interaction of the molecule with the active site of AR. Moreover, the selected tail proved not to be able to appropriately fit in the allosteric pocket when inserted on the rigid, planar xanthone scaffold.

### 3.1.2 Design and synthesis of alkoxyated imidazolymethylbenzophenones

The unexpected low AR inhibition potency of the substituted xanthenes **93a-95a** prompted us to design new derivatives that could better reach the enzyme access channel. The structure of the planar and conformationally constraint xanthone was modified with the aim of improving its flexibility, in order to allow the molecule to appropriately fit into the active site of the target, and the side chain to suitably occupy the allosteric pocket causing the closure of the access channel without hampering the correct binding mode of the whole molecule.

The benzophenone scaffold can be considered as an “open model” of the xanthone core. In previous studies, my research group developed a series of unsubstituted or 4'-substituted imidazolymethylbenzophenones, in which the position of the methyl imidazole on the benzophenone core was varied.<sup>144</sup> Among them, compounds **104g** and **104h** (Figure 40), both carrying the methyl imidazole moiety in position 3, resulted potent AIs with IC<sub>50</sub> values of 5.3 and 7.3 nM, respectively. Moreover, as part of a following project aimed at the development of steroidogenic CYP450 inhibitors, a series of 4'-substituted 4-imidazolymethylbenzophenones endowed with moderate activity as AIs was recently reported (**105e-h**, Figure 40).<sup>145</sup>

Based on the results obtained with our previously reported compounds, during my PhD new series of alkoxyated imidazolymethylbenzophenones were thus designed and synthesized. Considering the abovementioned structures, along with that of the most interesting alkoxyated imidazolymethylxanthone (**95a**), two series of flexible 3- or 4-imidazolymethylbenzophenones derivatives were designed (**104a-f**, **105a-d** Figure 40), in which side chains of different length and rigidity were inserted in position 4' of the scaffold. The insertion of different alkoxy tails could allow further investigation of the chemical space within the additional

binding site close to the access channel of AR and the determination of the optimal size and geometry of the chain for an appropriate interaction with the enzyme. In particular, the moderate activity of 4-imidazolylmethylbenzophenones **105e-h** could be improved by this potential additional interaction.

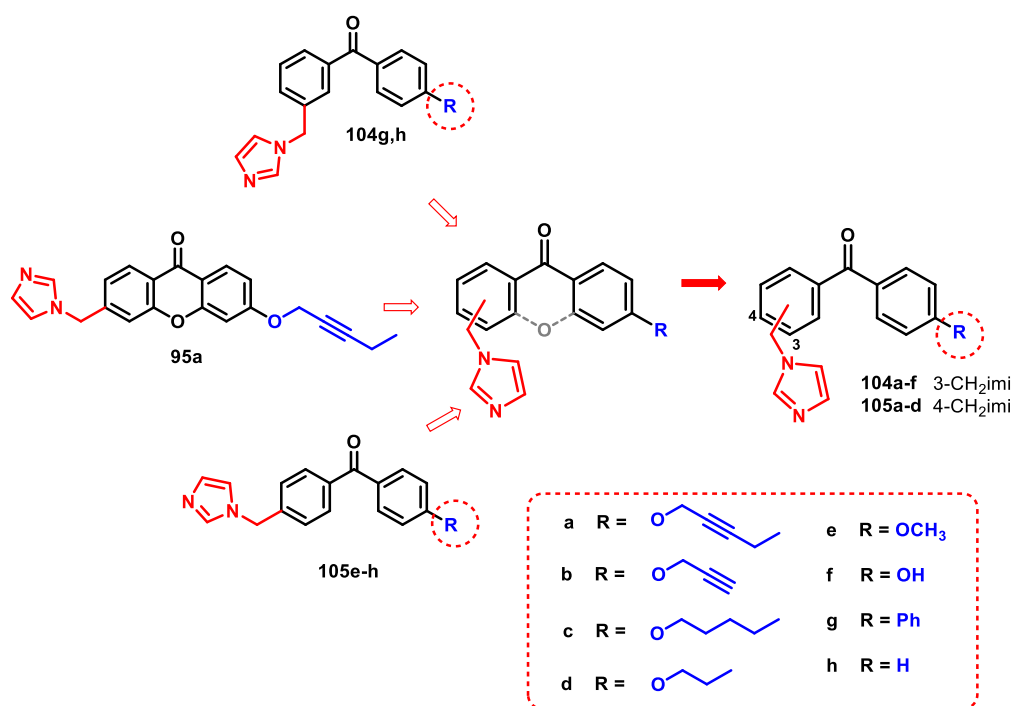
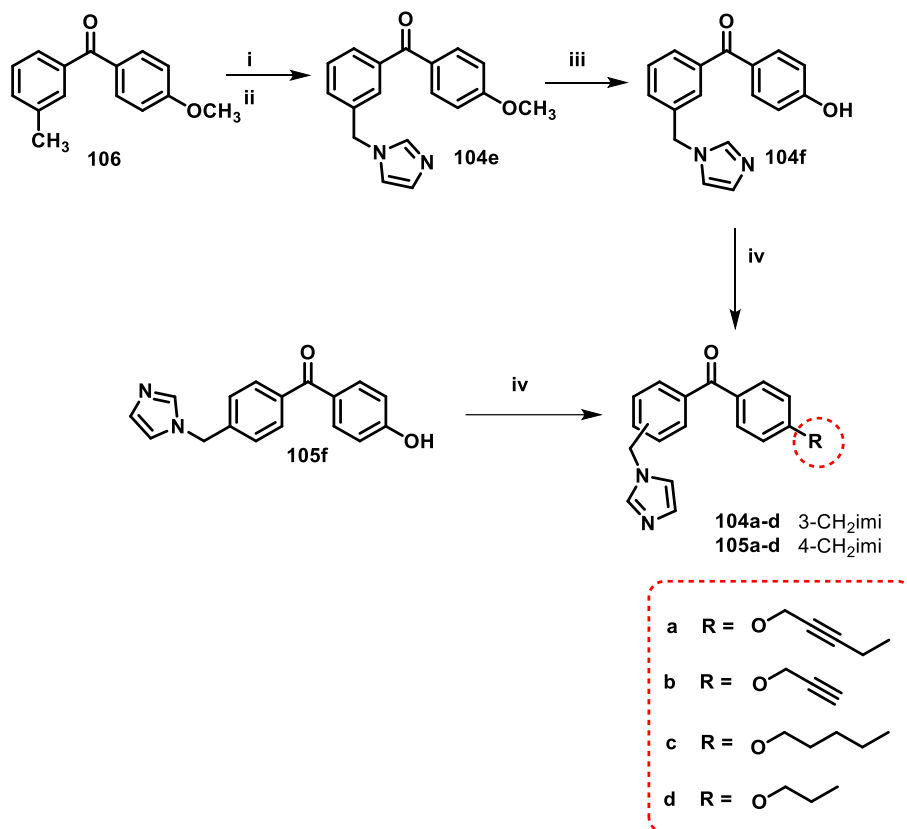


**Figure 40.** Structures of previously reported compounds (**95a**, **104g,h**, **105e-h**) and design of new alkoxyated imidazolylmethylbenzophenones (**104a-f** and **105a-d**).

### Chemistry

For the synthesis of compounds **104a-f** (Scheme 3), bromination of the methyl group of **106**<sup>146</sup> with NBS followed by reaction with imidazole led to compound **104e**, which was then demethylated with 48 % HBr. The obtained hydroxyl derivative **104f** was then alkylated by reaction with the suitable alkyl bromide, in the presence of K<sub>2</sub>CO<sub>3</sub> as base, to give **104a-d**. Similarly, **105f**<sup>145</sup> was alkylated in the same conditions to give **105a-d**.

**Scheme 3.** Synthesis of compounds **104a-f** and **105a-d**.



**Reagents and conditions:** i) NBS, BPO, hv, reflux 6-7 h; ii) imidazole, CH<sub>3</sub>CN, N<sub>2</sub>, reflux, 6 h; iii) 48 % HBr, reflux, 9 h; iv) K<sub>2</sub>CO<sub>3</sub>, acetone, reflux, 24 h.

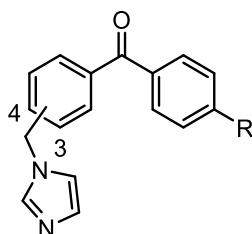
#### *Preliminary biological results*

The biological profile of the new compounds will be assessed by evaluating their AR inhibiting activities (Aromatase Inhibitor Screening Kit, BioVision Inc., San Francisco, USA) and cytotoxic potential on ER+, ER- BC and healthy cell lines but, up to now, only data for AR inhibition of 3-imidazolymethyl derivatives are available. The preliminary results are collected in Table 2 together with data for previously reported 3- or 4-imidazolymethyl derivatives **104g-h** and **105e-h** for a broader SAR study of this class of compounds.

AR inhibition data for tested 3-imidazolymethyl derivatives (**104a,c-h**) indicated for this subset of compounds a remarkable high potency, but only limited SAR

comments can be made. The introduction of properly selected alkoxy chains on **104h** proved to elicit different effects.

**Table 2.** AR inhibition of imidazolymethylbenzophenones compounds.



Cmp	CH <sub>2</sub> -imi position	R	AR inhibition IC <sub>50</sub> nM
<b>104a</b>	3		10
<b>104b</b>	3		n.t <sup>a</sup>
<b>104c</b>	3		40
<b>104d</b>	3		0.5
<b>104e</b>	3	OCH <sub>3</sub>	0.4
<b>104f</b>	3	OH	0.2
<b>104g<sup>b</sup></b>	3	Ph	5.3
<b>104h<sup>b</sup></b>	3	H	7.3
<b>105a</b>	4		n.t <sup>a</sup>
<b>105b</b>	4		n.t <sup>a</sup>
<b>105c</b>	4		n.t <sup>a</sup>
<b>105d</b>	4		n.t <sup>a</sup>
<b>105e<sup>c</sup></b>	4	OCH <sub>3</sub>	237.8
<b>105f<sup>c</sup></b>	4	OH	1100
<b>105g<sup>c</sup></b>	4	Ph	2531
<b>105h<sup>c</sup></b>	4	H	252.4

<sup>a</sup>n.t (not tested); <sup>b</sup> ref <sup>144</sup>; <sup>c</sup> ref <sup>145</sup>.

In detail, the rigid pentynyloxy moiety (**104a**) seemed to be well tolerated, but the more flexible saturated five methylene chain (**104c**) led to a slight decrease in potency. Notably, the introduction of a shorter alkoxy group or a hydroxyl proved to have beneficial effects, since compounds **104d**, **104e** and **104f** showed activity in the subnanomolar range. These results seem to suggest that a long alkoxy function does not have the appropriate features for a favorable interaction of the 3-imidazolymethyl derivatives with the accessory site close to the access channel, while a shorter substituent could probably form additional interactions, improving the binding mode of the whole molecule. Computational studies will be performed to define the binding poses of the new compounds and their potential ability to reach the abovementioned accessory site.

Remarkably, a significant boost in potency could be seen for compounds **104e-h** with respect to their corresponding 4-imidazolymethyl derivatives **105e-h**. This evidence clearly suggests that the correct positioning of the imidazole-containing chain on the benzophenone core is a crucial element for optimal inhibitory activity, since the unsubstituted **104h** showed a 35-fold higher potency with respect to **105h**. This trend was further emphasized by the functionalization of **104h** with a methoxy or hydroxyl group to obtain **104e** and **104f**, respectively (IC<sub>50</sub>s values of 0.4 and 0.2 nM, respectively) compared to **105e** and **105f** (IC<sub>50</sub>s values of 237.8 and 1100 nM, respectively).

Further information on the biological activities of the remaining synthesized molecules will allow for a more complete SAR discussion and for a deeper understanding of the potential binding to AR allosteric site for this class of compounds.

### 3.1.3 Experimental procedures

#### *General Methods*

All chemicals were purchased from Aldrich Chemistry, Milan (Italy), or from Alfa Aesar, Milan (Italy), and were of the highest purity grade. Melting points were determined in open glass capillaries using a Büchi apparatus and are uncorrected.

$^1\text{H}$  NMR and  $^{13}\text{C}$  NMR spectra were recorded in  $\text{CDCl}_3$ , unless otherwise indicated, on a Varian VXR Gemini spectrometer working at 400 MHz and 101 MHz, respectively. Chemical shifts are reported in parts per million (ppm) relative to tetramethylsilane (TMS) as internal standard and spin multiplicities are given as s (singlet), d (doublet), t (triplet), m (multiplet) or br (broad). Direct infusion ES-MS spectra were recorded on a Waters Micromass ZQ 4000 apparatus. Chromatographic separations were performed by flash column chromatography on silica gel columns (Kieselgel 40, 0.040-0.063 mm; Merck). Organic solutions were dried over anhydrous sodium sulfate. The purity of the tested compounds was determined by HPLC analysis, performed on a Jasco LC 1500 PU-1587; column: Phenomenex Luna C18(2) 5  $\mu\text{m}$  4.60 mm  $\times$  150 mm; elution conditions: mobile phase  $\text{CH}_3\text{CN}/\text{H}_2\text{O} + \text{KH}_2\text{PO}_4$  0.2 % 50/50; flow-rate: 1 ml/min; injection volume: 20  $\mu\text{l}$ ; peaks were detected at 220 nm and results were > 95% purity. Compounds were named relying on the naming algorithm developed by CambridgeSoft Corporation and used in ChemDraw Professional 19.1.

#### **General method for the synthesis of xanthenes 96 and 99.**

A mixture of 2-chlorobenzoic acid (1.0 eq), catalytic amounts of Cu and CuI,  $\text{K}_2\text{CO}_3$  (2.0 eq), pyridine (0.5 eq) and the selected phenol (1.0 eq) in  $\text{H}_2\text{O}$  (10 mL) was refluxed for 2 h. The basic reaction mixture was then washed with diethylether (3 x 15 mL) and acidified with 37 % HCl to give a precipitate that was filtered. The obtained dried solid was used without further purification and added portionwise, without further purification, to polyphosphoric acid (PPA, 10:1 w/w) obtained from orthophosphoric acid and  $\text{P}_2\text{O}_5$ . The mixture was heated at 120  $^\circ\text{C}$  for 7 h, then poured in to ice, the precipitated solid was filtered, suspended in  $\text{NaHCO}_3$  saturated solution and then filtered again to obtain a crude product that was purified by flash chromatography when needed.

**2-methoxy-4-methyl-9H-xanthen-9-one (96).** Starting from 2-chlorobenzoic acid (1.32 g, 8.44 mmol) and 4-methoxy-2-methylphenol (2.32 g, 16.88 mmol), **96** as grey solid was obtained (0.80 g, yield 20 %), mp 164-167  $^\circ\text{C}$ .  $^1\text{H}$  NMR:  $\delta$  2.57 (s, 3H,  $\text{CH}_3$ ), 3.92 (s, 3H,  $\text{OCH}_3$ ), 7.21 (s, 1H, arom), 7.37-7.41 (m, 1H, arom), 7.53-7.59 (m, 2H, arom), 7.72-7.75 (m, 1H, arom), 8.37 (d,  $J = 7.2$  Hz, 1H, arom).

**3-methoxy-1-methyl-9H-xanthen-9-one (99).** Starting from 2-chlorobenzoic acid (2.64 g, 17.00 mmol) and 3-methoxy-5-methylphenol (4.69 g, 34.00 mmol), a crude was obtained that was purified by flash column chromatography (petroleum ether/ethyl acetate 4:1) to give **99** as light-yellow solid (0.45 g, yield 12 %), mp 120-124 °C. <sup>1</sup>H NMR: δ 2.91 (s, 3H, CH<sub>3</sub>), 3.92 (s, 3H, OCH<sub>3</sub>), 6.71 (s, 1H, arom), 6.78 (s, 1H, arom), 7.33-7.37 (m, 1H, arom), 7.41 (d, *J* = 8.4 Hz, 1H, arom), 7.64-7.68 (m, 1H, arom), 8.29 (d, *J* = 9.2 Hz, 1H, arom).

**General method for the synthesis of imidazole derivatives 97, 100, 104e.**

A mixture of methylxanthone **96** or **99** or 3-methyl-4'-methoxybezophenone **106** (1.0 eq), *N*-bromosuccinimide (NBS, 1.0 eq) and a catalytic amount of benzoyl peroxide (BPO) in CCl<sub>4</sub> (15-30 mL) was refluxed for 6 h. The mixture was hot filtered and the solvent was evaporated under reduced pressure. The obtained residue, without further purification, was dissolved in acetonitrile (20-30 mL) and imidazole (3.0 eq) was added. The mixture was refluxed for 6 h under N<sub>2</sub> atmosphere, the solvent was evaporated under reduced pressure and the residue was purified by flash column chromatography with a suitable eluent.

**4-((1H-imidazol-1-yl)methyl)-2-methoxy-9H-xanthen-9-one (97).** Starting from **96** (0.40 g, 1.70 mmol), a crude was obtained that was purified by flash column chromatography (gradient elution starting from petroleum ether/ethyl acetate 4:1, then ethyl acetate) to give **97** as light-yellow solid (0.20 g, yield 40 %), mp 186-188 °C. <sup>1</sup>H NMR: δ 3.90 (s, 3H, OCH<sub>3</sub>), 5.51 (s, 2H, CH<sub>2</sub>imi), 7.05 (s, 1H, arom), 7.09 (d, *J* = 3.2 Hz, 1H, arom), 7.16 (s, 1H, arom), 7.40-7.44 (m, 1H, arom), 7.51 (d, *J* = 8.0 Hz, 1H, arom), 7.72 (d, *J* = 3.2 Hz, 1H, arom), 7.74-7.78 (m, 1H, arom), 7.95 (s, 1H, arom), 8.35 (dd, *J* = 7.8 and 1.4 Hz, 1H, arom).

**1-((1H-imidazol-1-yl)methyl)-3-methoxy-9H-xanthen-9-one (100).** Starting from **99** (0.54 g, 2.25 mmol), a crude was obtained that was purified by flash chromatography (gradient elution starting from toluene/ethyl acetate 9.75:0.25, then ethyl acetate) to give **100** as light-yellow solid (0.59 g, yield 84 %), mp 209-210 °C. <sup>1</sup>H NMR: δ 3.85 (s, 3H, OCH<sub>3</sub>), 5.94 (s, 2H, CH<sub>2</sub>imi), 6.20 (s, 1H, arom), 6.85 (s, 1H, arom), 7.02 (s, 1H, arom), 7.15 (s, 1H, arom), 7.37-7.40 (m, 1H, arom),

7.44 (d,  $J = 8.4$  Hz, 1H, arom), 7.64-7.73 (m, 2H, arom), 8.28 (d,  $J = 8.4$  Hz, 1H, arom).

**(3-((1H-imidazol-1-yl)methyl)phenyl)(4-methoxyphenyl)methanone (104e).**

Starting from **106** (1.09 g, 4.80 mmol) a crude compound was obtained that was purified by flash column chromatography (gradient elution starting from toluene, then toluene/acetone 1:1, then 1:4) to give **104e** as an oil (0.41 g, yield 38 %).  $^1\text{H}$  NMR:  $\delta$  3.89 (s, 3H, OCH<sub>3</sub>), 5.18 (s, 2H, CH<sub>2</sub>imi), 6.95-6.97 (m, 3H, arom), 7.10 (s, 1H, imi), 7.32 (d,  $J = 7.7$  Hz, 1H, arom), 7.44-7.48 (m, 1H, arom), 7.57 (s, 1H, imi), 7.61 (s, 1H, imi), 7.68 (d,  $J = 8.0$  Hz, 1H, arom) 7.77-7.80 (m, 2H, arom).  $^{13}\text{C}$  NMR:  $\delta$  50.6, 55.6, 113.8 (2C), 119.3, 128.5, 129.0, 129.7, 129.8, 130.2, 130.6, 132.6 (2C), 136.7, 137.5, 139.2, 163.6, 194.9.

**General method for the synthesis of hydroxyl derivatives 98, 101, 103 and 104f.**

**Method A.** A mixture of methoxyxanthone **97**, **100**, or **102** (1.0 eq) and AlCl<sub>3</sub> (4.5 eq) in toluene (10-25 mL) was refluxed for 3 h, cooled and evaporated under reduced pressure. Ice was added to the residue and the mixture was allowed to reach room temperature, the formed precipitate was collected by filtration and purified by flash column chromatography when needed.

**4-((1H-imidazol-1-yl)methyl)-2-hydroxy-9H-xanthen-9-one (98).** Starting from **97** (0.23 g, 0.75 mmol) a crude was obtained that was purified by flash chromatography (dichlorometane/methanol 9.5:0.5) to give **98** as grey solid (0.15 g, yield 69 %), mp 240-242 °C.  $^1\text{H}$  NMR (methanol- $d_4$ ):  $\delta$  5.75 (s, 2H, CH<sub>2</sub>imi), 7.02 (s, 1H, arom), 7.04 (s, 1H, arom), 7.31 (s, 1H, arom), 7.44 (s, 1H, arom), 7.50-7.52 (m, 1H, arom), 7.64-7.65 (m, 1H, arom), 7.87-7.88 (m, 1H, arom), 8.25 (d,  $J = 8.0$  Hz, 1H, arom), 8.89 (s, 1H, arom), 9.41 (s, 1H, OH).

**1-((1H-imidazol-1-yl)methyl)-3-hydroxy-9H-xanthen-9-one (101).** Starting from **100** (0.59 g, 1.90 mmol) **101** was obtained as beige solid (0.23 g, yield 42 %), mp 195-198 °C.  $^1\text{H}$  NMR (methanol- $d_4$ ):  $\delta$  6.00 (s, 2H, CH<sub>2</sub>imi), 6.60 (s, 1H, arom), 6.92 (d,  $J = 2.4$  Hz, 1H, arom), 7.30 (s, 1H, arom), 7.39-7.43 (m, 2H, arom), 7.52

(d,  $J = 8$  Hz, 1H, arom), 7.76-7.80 (m, 1H, arom), 8.20 (dd,  $J = 7.8$  and 2.0 Hz, 1H, arom), 8.49 (s, 1H, arom).

**3-((1*H*-imidazol-1-yl)methyl)-6-hydroxy-9*H*-xanthen-9-one (103).** Starting from **102**<sup>143</sup> (0.57 g, 1.90 mmol) **103** was obtained as grey solid (0.38 g, yield 68 %), mp 234-236 °C. <sup>1</sup>H NMR (methanol-*d*<sub>4</sub>):  $\delta$  5.56 (s, 2H, CH<sub>2</sub>imi), 6.87 (s, 1H, arom), 6.92 (dd,  $J = 8.6$  and 2.0 Hz, 1H, arom), 7.35 (d,  $J = 8.4$  Hz, 1H, arom), 7.40 (s, 1H, arom), 7.48-7.51 (m, 2H, arom), 8.12 (d,  $J = 8.4$  Hz, 1H, arom), 8.27 (d,  $J = 8.0$  Hz, 1H, arom), 8.60 (s, 1H, arom).

**Method B.** A solution of methoxybenzophenone (1eq) in 48 % HBr (20 mL) was heated to reflux for 9 h. The reaction mixture was basified with 6N NaOH solution and washed with dichloromethane (3 x 30 mL). The aqueous phase was acidified dropwise with 6N HCl until a precipitate was formed (pH  $\approx$  7). The solid obtained was filtered and dried to give the hydroxy derivative.

**(3-((1*H*-imidazol-1-yl)methyl)phenyl)(4-hydroxyphenyl)methanone (104f).** Starting from **104e** (1.00 g, 3.40 mmol) **104f** was obtained as white solid (500 mg, yield 52 %), mp 199-201 °C. <sup>1</sup>H NMR (methanol-*d*<sub>4</sub>):  $\delta$  5.34 (s, 2H, CH<sub>2</sub>imi), 6.87 (d,  $J = 2.0$  Hz, 2H, arom), 7.04 (s, 1H, imi), 7.19 (s, 1H, imi), 7.49-7.57 (m, 3H, arom), 7.64-7.69 (m, 3H, arom), 7.85 (s, 1H, imi). <sup>13</sup>C NMR (methanol-*d*<sub>4</sub>):  $\delta$  51.2, 116.2 (2C), 120.9, 129.4, 129.5, 129.5, 129.9, 130.2, 131.9, 134.0 (2C), 138.7, 138.8, 140.2, 163.9, 197.0.

**General method for the synthesis of alkoxyated compounds 93a-95a, 104a-d and 105a-d.**

A mixture of **98**, **101**, **103**, **104f** or **105f** (1.0 eq), K<sub>2</sub>CO<sub>3</sub> (1.0 eq) and the suitable alkyl bromide (1.0 eq) in acetone (20 mL) was refluxed for 18-26 h (monitored by TLC). The mixture was hot filtered and evaporated to dryness to obtain a residue that was purified by flash chromatography.

**4-((1*H*-imidazol-1-yl)methyl)-2-(pent-2-yn-1-yloxy)-9*H*-xanthen-9-one (93a).** Starting from **98** (0.10 g, 0.34 mmol) a crude compound was obtained that was

purified by flash column chromatography (ethyl acetate/methanol 9.5:0.5) to give **93a** as beige solid (0.02 g, yield 18 %), mp 138-140 °C. <sup>1</sup>H NMR (acetone-*d*<sub>6</sub>): δ 1.08 (t, *J* = 7.4 Hz, 3H, CH<sub>3</sub>), 2.22 (q, *J* = 7.4 Hz, 2H, CH<sub>2</sub>), 4.86 (s, 2H, OCH<sub>2</sub>), 5.65 (s, 2H, CH<sub>2</sub>imi), 6.96 (s, 1H, arom), 7.28 (s, 1H, arom), 7.29 (s, 1H, arom), 7.47-7.51 (m, 1H, arom), 7.73-7.75 (m, 1H, arom), 7.77 (s, 1H, arom), 7.87-7.91 (m, 2H, arom), 8.26 (dd, *J* = 7.8 and 1.4 Hz, 1H, arom). <sup>13</sup>C NMR: δ 12.7, 13.9, 45.4, 57.5, 74.8, 90.4, 108.5, 119.1 (2C), 121.9, 123.2, 124.9, 125.1 (2C), 127.0, 129.8, 135.9 (2C), 149.3, 154.8, 156.5, 176.5.

**1-((1*H*-imidazol-1-yl)methyl)-3-(pent-2-yn-1-yloxy)-9*H*-xanthen-9-one (94a).** Starting from **101** (0.23 g, 0.79 mmol) a crude compound was obtained that was purified by flash column chromatography (ethyl acetate/methanol 9.5:0.5) to give **94a** as grey solid (0.02 g, yield 8 %), mp 129-130 °C. <sup>1</sup>H NMR: δ 1.15 (t, *J* = 7.6 Hz, 3H, CH<sub>3</sub>), 2.25 (q, *J* = 7.6 Hz, 2H, CH<sub>2</sub>), 4.71 (s, 2H, OCH<sub>2</sub>), 5.94 (s, 2H, CH<sub>2</sub>imi), 6.29 (s, 1H, arom), 6.96 (s, 1H, arom), 7.01 (s, 1H, arom), 7.14 (s, 1H, arom), 7.37-7.41 (m, 1H, arom), 7.46 (d, *J* = 8.0 Hz, 1H, arom), 7.64 (s, 1H, arom), 7.69-7.73 (m, 1H, arom), 8.28 (dd, *J* = 7.6 and 1.6 Hz, 1H, arom). <sup>13</sup>C NMR: δ 12.5, 13.5, 49.9, 57.1, 72.8, 91.1, 101.4, 112.7, 113.2, 117.4, 119.9, 122.5, 124.2, 126.7, 129.8, 134.6, 138.2, 142.2, 155.4, 159.5, 162.5, 177.7.

**3-((1*H*-imidazol-1-yl)methyl)-6-(pent-2-yn-1-yloxy)-9*H*-xanthen-9-one (95a).** Starting from **103** (0.38 g, 1.30 mmol) a crude compound was obtained that was purified by flash column chromatography (ethyl acetate/methanol 9.5:0.5) to give **95a** light-yellow solid (0.06 g, yield 13 %), mp 118-120 °C. <sup>1</sup>H NMR: δ 1.16 (t, *J* = 7.6 Hz, 3H, CH<sub>3</sub>), 2.27 (q, *J* = 7.6 Hz, 2H, CH<sub>2</sub>), 4.80 (s, 2H, OCH<sub>2</sub>), 5.30 (s, 2H, CH<sub>2</sub>imi), 6.97-7.03 (m, 3H, arom), 7.13 (s, 1H, arom), 7.17-7.19 (m, 2H, arom), 7.64 (s, 1H, arom), 8.26 (d, *J* = 9.2 Hz, 1H, arom), 8.32 (d, *J* = 8.0 Hz, 1H, arom). <sup>13</sup>C NMR: δ 12.6, 13.6, 50.3, 57.2, 73.1, 90.9, 101.7, 114.0, 116.0, 116.2, 119.5, 121.8, 122.4, 127.7, 128.4, 130.5, 137.8, 143.4, 156.6, 157.9, 163.5, 175.8.

**(3-((1*H*-imidazol-1-yl)methyl)phenyl)(4-(pent-2-yn-1-yloxy)phenyl) methanone (104a).** Starting from **104f** (0.20 g, 0.72 mmol) and 1-bromopent-2-yne (0.08 mL, 0.72 mmol) a crude compound was obtained that was purified by flash column chromatography (ethyl acetate/methanol 4.75:0.25) to give **104a** as

beige solid (0.06 g, yield 24 %), mp 58-60 °C. <sup>1</sup>H NMR: δ 1.14 (t, *J* = 7.2 Hz, 3H, CH<sub>3</sub>), 2.24 (tq, *J* = 7.5 Hz, *J* = 2.1 Hz, 2H, CH<sub>2</sub>), 4.75 (t, *J* = 2.1 Hz, 2H, OCH<sub>2</sub>), 5.19 (s, 2H, CH<sub>2</sub>imi), 6.93 (s, 1H, aro), 7.02-7.05 (m, 2H, aro), 7.11 (s, 1H, imi), 7.31 (d, *J* = 7.7 Hz 1H, aro), 7.44-7.48 (m, 1H, aro), 7.57 (s, 1H, imi), 7.62 (s, 1H, imi), 7.69 (d, *J* = 7.7 Hz, 1H, aro), 7.79 (m, 2H, aro). <sup>13</sup>C NMR: δ 12.6, 13.6, 50.6, 56.8, 73.5, 90.4, 114.7 (2C), 119.3, 128.5, 129.0, 129.8, 130.1, 130.2, 130.6, 132.5 (2C), 136.7, 137.5, 139.1, 161.8, 194.9.

**(3-((1H-imidazol-1-yl)methyl)phenyl)(4-(prop-2-yn-1-yloxy)phenyl)**

**methanone (104b).** Starting from **104f** (0.20 g, 0.72 mmol) and 80 % 3-bromoprop-1-yne (0.11 mL, 0.72 mmol) a crude compound was obtained that was purified by flash column chromatography (dichloromethane/methanol 9.5:0.5) to give **104b** as with solid (0.04 g, 18 %), mp 119-121 °C. <sup>1</sup>H NMR: δ 2.57 (t, *J* = 2.4 Hz, 1H, CH), 4.79 (d, *J* = 2.4 Hz, 2H, OCH<sub>2</sub>), 5.19 (s, 2H, CH<sub>2</sub>-imi), 6.93 (s, 1H, aro), 7.07-7.02 (m, 2H, aro), 7.11 (s, 1H, imi), 7.33 (d, *J* = 7.7 Hz, 1H, aro), 7.47-7.44 (m, 1H, aro), 7.58 (s, 1H, imi), 7.62 (s, 1H, imi), 7.68 (d, *J* = 7.7 Hz, 1H, aro), 7.79-7.81 (m, 2H, aro). <sup>13</sup>C NMR: δ 50.6, 56.0, 76.3, 77.8, 114.6 (2C), 119.3, 128.5, 129.0, 129.7, 130.1, 130.5, 130.7, 132.5 (2C), 136.7, 137.5, 138.9, 161.3, 194.8.

**(3-((1H-imidazol-1-yl)methyl)phenyl)(4-(pentylloxy)phenyl)methanone (104c).**

Starting from **104f** (0.20 g, 0.72 mmol) and 1-bromopentane (0.09 mL, 0.72 mmol) a crude compound was obtained that was purified by flash column chromatography (ethyl acetate/methanol 4.75:0.25) to give **104c** as an oil (0.11 g, yield 44 %). <sup>1</sup>H NMR: δ 0.95 (t, *J* = 5.6 Hz, 3H, CH<sub>3</sub>), 1.39-1.48 (m, 4H, 2CH<sub>2</sub>), 1.73-1.84 (m, 2H, CH<sub>2</sub>), 4.04 (t, *J* = 6.6 Hz, 2H, OCH<sub>2</sub>), 5.18 (s, 2H, CH<sub>2</sub>imi), 6.93-6.95 (m, 3H, aro), 7.11 (s, 1H, imi), 7.31 (d, *J* = 7.6 Hz, 1H, aro), 7.44-7.46 (m, 1H, aro), 7.57 (s, 1H, imi), 7.61 (s, 1H, imi), 7.68 (d, *J* = 8.0 Hz, 1H, aro), 7.80-7.74 (m, 2H, aro). <sup>13</sup>C NMR: δ 14.1, 22.5, 28.2, 28.9, 50.7, 68.4, 114.2 (2C), 119.3, 128.5, 129.0, 129.5, 129.7, 130.1, 130.5, 132.6 (2C), 136.6, 137.5, 139.3, 163.2, 194.9.

**(3-((1H-imidazol-1-yl)methyl)phenyl)(4-propoxyphenyl)methanone (104d).**

Starting from **104f** (0.18 g, 0.65 mmol) and 1-bromopropane (0.07 mL, 0.65 mmol) a crude compound was obtained that was purified by flash column chromatography (dichloromethane/acetone 3:2) to give **104d** as an oil (0.09 g, yield 43 %). <sup>1</sup>H NMR:

$\delta$  1.06 (t,  $J = 7.6$  Hz, 3H, CH<sub>3</sub>), 1.82-1.88 (m, 2H, CH<sub>2</sub>), 4.00 (t,  $J = 6.6$  Hz, 2H, OCH<sub>2</sub>), 5.18 (s, 2H, CH<sub>2</sub>imi), 6.94-6.96 (m, 3H, arom), 7.11 (s, 1H, imi), 7.30 (d,  $J = 7.6$  Hz, 1H, arom), 7.44-7.46 (m, 1H arom), 7.58 (s, 1H, imi), 7.61 (s, 1H, imi), 7.68 (d,  $J = 7.7$  Hz, 1H, arom), 7.76-7.78 (m, 2H, arom). <sup>13</sup>C NMR:  $\delta$  10.6, 22.5, 50.6, 69.9, 114.2 (2C), 119.3, 128.5, 129.0, 129.5, 129.7, 130.2, 130.5, 132.6 (2C), 136.6, 137.5, 139.2, 163.2, 194.9.

**(4-((1H-imidazol-1-yl)methyl)phenyl)(4-(pent-2-yn-1-yloxy)phenyl)**

**methanone (105a).** Starting from **105f** (0.20 g, 0.72 mmol) and 1-bromopent-2-yne (0.08 mL, 0.72 mmol) a crude compound was obtained that was purified by flash column chromatography (ethyl acetate/methanol 4.75:0.25) to give compound **105a** as grey solid (0.04 g, yield 17 %), mp 92-96 °C. <sup>1</sup>H NMR:  $\delta$  1.14 (t,  $J = 7.2$  Hz, 3H, CH<sub>3</sub>), 2.21-2.27 (m, 2H, CH<sub>2</sub>), 4.75 (t,  $J = 1.8$  Hz, 2H, CH<sub>2</sub>), 5.22 (s, 2H, CH<sub>2</sub>imi), 6.94 (s, 1H, imi), 7.04 (d,  $J = 8.0$  Hz, 2H, arom), 7.14 (s, 1H, imi), 7.24 (d,  $J = 8.1$  Hz 2H, arom), 7.60 (s, 1H, imi), 7.75 (d,  $J = 8.0$  Hz, 2H, arom), 7.80 (d,  $J = 8.4$  Hz, 2H, arom). <sup>13</sup>C NMR:  $\delta$  12.6, 13.6, 50.6, 56.8, 73.5, 90.4, 114.7 (2C), 119.4, 127.0 (2C), 130.2, 130.3, 130.5 (2C), 132.5 (2C), 137.6, 138.3, 140.2, 161.7, 194.8.

**(4-((1H-imidazol-1-yl)methyl)phenyl)(4-(prop-2-yn-1-yloxy)phenyl)**

**methanone (105b).** Starting from **105f** (0.20 g, 0.72 mmol) and 3-bromoprop-1-yne (80 % in toluene, 0.11 mL, 0.72 mmol) a crude compound was obtained that was purified by flash column chromatography (dichloromethane/acetone 2:3) to give **105b** as white solid (0.03 g, yield 13 %), mp 140-143 °C. <sup>1</sup>H NMR:  $\delta$  2.57 (t,  $J = 2.4$  Hz, 1H, CH), 4.78 (d,  $J = 2.4$  Hz, 2H, OCH<sub>2</sub>), 5.22 (s, 2H, CH<sub>2</sub>imi), 6.94 (s, 1H, imi), 7.05 (d,  $J = 8.8$  Hz, 2H arom), 7.14 (s, 1H, imi), 7.24 (d,  $J = 8.4$  Hz, 2H, arom), 7.59 (s, 1H, imi), 7.75 (d,  $J = 8.4$  Hz, 2H, arom), 7.81 (d,  $J = 8.8$  Hz, 2H, arom). <sup>13</sup>C NMR:  $\delta$  50.6, 56.0, 76.3, 77.8, 114.6 (2C), 119.4, 127.0 (2C), 130.2, 130.5 (2C), 130.7, 132.5 (2C), 137.5, 138.2, 140.3, 161.3, 192.8.

**(4-((1H-imidazol-1-yl)methyl)phenyl)(4-(pentyloxy)phenyl)methanone (105c).**

Starting from **105f** (0.20 g, 0.72 mmol) and 1-bromopentane (0.09 mL, 0.72 mmol) a crude compound was obtained that was purified by flash column chromatography (ethyl acetate/methanol 4.75:0.25) to give **105c** as a yellow oil (0.15 g, yield 60 %).

<sup>1</sup>H NMR: δ 0.93 (t, *J* = 7 Hz, 3H, CH<sub>3</sub>), 1.36-1.47 (m, 4H, 2 x CH<sub>2</sub>), 1.78-1.83 (m, 2H, CH<sub>2</sub>), 4.03 (t, *J* = 6.4 Hz, 2H, CH<sub>2</sub>), 5.20 (s, 2H, CH<sub>2</sub>), 6.92-6.95 (m, 3H arom), 7.13 (s, 1H, imi), 7.22-7.24 (m, 2H, arom), 7.59 (s, 1H, imi), 7.72-7.79 (m, 4H, arom). <sup>13</sup>C NMR: δ 14.1, 22.5, 28.2, 28.9, 50.6, 68.4, 114.2 (2C), 119.5, 127.0 (2C), 129.6, 130.1, 130.5 (2C), 132.6 (2C), 137.6, 138.4, 140.0, 163.1, 194.8.

**(4-((1H-imidazol-1-yl)methyl)phenyl)(4-propoxyphenyl)methanone (105d).**

Starting from **105f** (0.18 g, 0.65 mmol) and 1-bromopropane (0.07 mL, 0.65 mmol) a crude compound was obtained that was purified by flash column chromatography (dichloromethane/acetone 3:2) to give **105d** as an oil (0.15 g, yield 65 %). <sup>1</sup>H NMR: δ 1.06 (t, *J* = 7.4 Hz, 3H, CH<sub>3</sub>), 1.84-1.86 (m, 2H, CH<sub>2</sub>), 4.00 (t, *J* = 6.4 Hz, 2H OCH<sub>2</sub>), 5.21 (s, 2H, CH<sub>2</sub>imi), 6.93-6.96 (m, 3H, arom), 7.12 (s, 1H, imi), 7.23 (d, *J* = 8.0 Hz, 2H, arom), 7.59 (s, 1H, imi), 7.73 (d, *J* = 8.1 Hz, 2H, arom), 7.78 (d, *J* = 8.8 Hz, 2H, arom). <sup>13</sup>C NMR: δ 10.6, 22.5, 50.5, 69.9, 114.2 (2C), 119.4, 127.0 (2C), 129.6, 130.1, 130.5 (2C), 132.6 (2C), 137.6, 138.4, 140.0, 163.1, 194.8.

### 3.2 DESIGN AND SYNTHESIS OF POTENTIAL MULTITARGET AGENTS.

As mentioned above, in recent years the AI/SERM dual action of TAM metabolites was discovered, paving the way for the search of new compounds endowed with multitarget activity and with improved pharmacokinetic profiles, able to overcome the typical issues derived from the administration of multiple drugs and to enhance patient's compliance. Moreover, a single compound that could block estrogen activity interfering with two different pathways could also decrease the incidence of side effects typical of either AIs or SERMs therapies. Part of my PhD project was thus devoted to the development of multitarget compounds.

#### 3.2.1 Design and synthesis of potential AIs/SERMs: bisphenols derivatives <sup>147</sup>

Structural modifications of TAM metabolite norendoxifen led to the development of symmetric bisphenol compounds, among which compound **90** <sup>138</sup> (Figure 35 and Figure 41) carrying an imidazole moiety able to coordinate the heme group of AR,

that proved to be a potent AI while maintaining good affinity for both ERs. With the aim to get new insight on the potential development of bioactive molecules based on the structure of TAM metabolites the design and synthesis of different series of potential multitarget agents, structurally inspired by TAM bisphenol<sup>139</sup> and **90**, was performed.

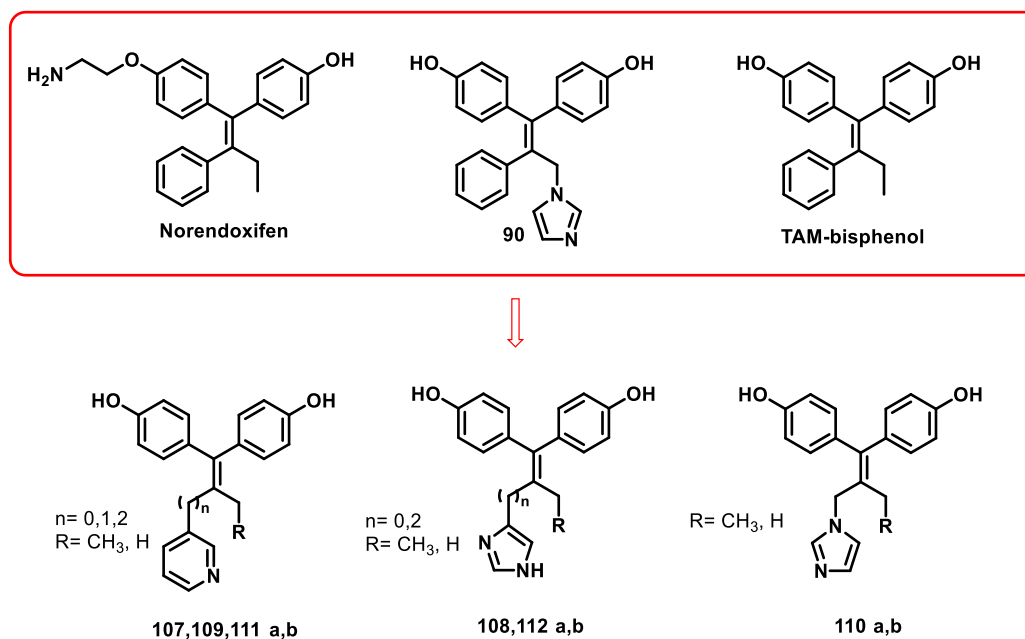


**Figure 41.** Design of new bisphenol derivatives.

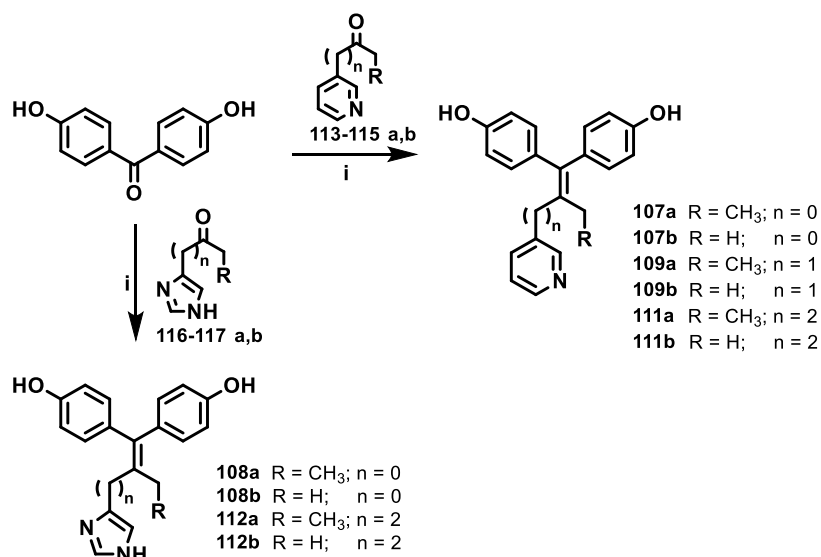
In the design of a first series (**107-112a,b**, Figure 41), in particular, the ethyl moiety of TAM metabolites was maintained (or shortened to a methyl group), together with the bisphenol structure, while the nitrogen atom necessary for the coordination of the heme group was introduced in the existing aromatic ring, by replacing the benzene with a pyridine or imidazole. Moreover, a spacer of one or two methylenes was inserted between the azole ring and the central double bond, in order to evaluate the effect of its length on both activities. The compounds were then docked into the active site of AR, imposing a constraint on the distance of the N-Fe bond, but it was not clear whether some compounds (**107a**, **107b**, **108a** and **108b**) were able to coordinate the heme group. Moreover, docking analyses were also performed on a representative structure of the ER $\alpha$  LBD obtained from previous classical MD simulations.<sup>148</sup> All compounds exhibited good docking scores (ranging from -8 to -

11 Kcal/mol), similarly to those predicted for END. Based on these analyses, the synthesis and the biological evaluation of the new compounds were performed.

### Chemistry

For the synthesis of compounds **107-109a,b** and **111-112a,b**, 4,4'-dihydroxybenzophenone and the appropriate ketone (**113-117a,b**) were reacted under McMurry reaction conditions, in the presence of titanium chloride and zinc powder (Scheme 4), to form a carbon-carbon double bond. Not commercially available ketones were synthesized with different procedures (see Schemes 6, 7 and 8).

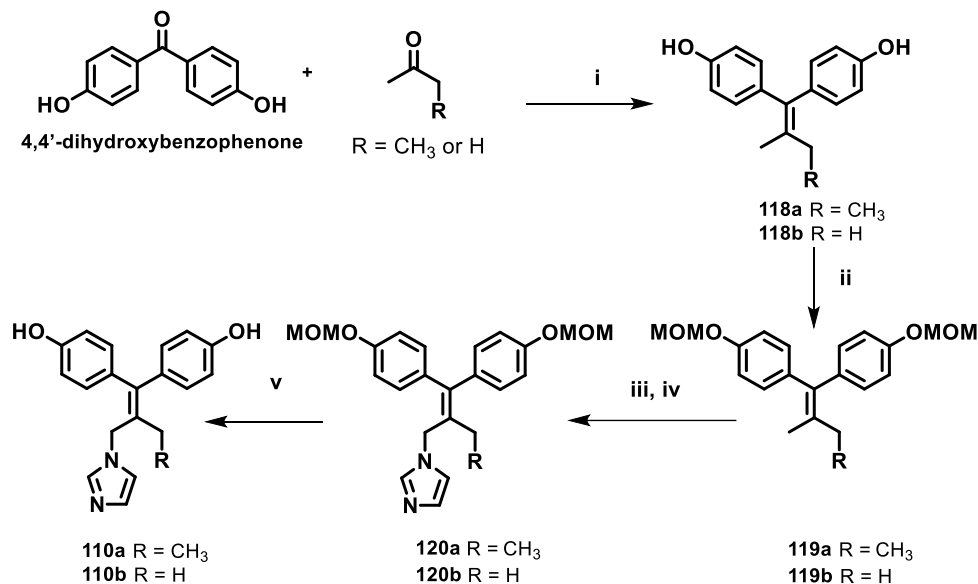
**Scheme 4.** Synthesis of compound **107-109a,b**, **111-112a,b**.<sup>a</sup>



<sup>a</sup>**Reagents and conditions:** i) Zn, TiCl<sub>4</sub>, THF, N<sub>2</sub>, reflux.

For the synthesis of compounds **110a,b**, 4,4'-dihydroxybenzophenone and acetone or methylethylketone were reacted under McMurry reaction conditions to give **118a,b**. The hydroxyl groups were protected with chloromethylmethylether (MOM) and the obtained intermediates **119a,b** were first brominated with NBS and then reacted with imidazole to give **120a,b**. Cleavage of MOM ethereal functions, to obtain the free hydroxyl groups, by acid hydrolysis afforded compounds **110a** and **110b** (Scheme 5).

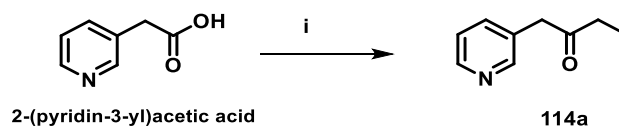
**Scheme 5.** Synthesis of compounds **110a,b**.<sup>a</sup>



<sup>a</sup>**Reagents and conditions:** i) Zn,  $\text{TiCl}_4$ , THF,  $\text{N}_2$  reflux; ii) NaH 60 %, THF, MOM-Cl,  $\text{N}_2$ , rt, 3 h; iii) NBS,  $\text{CCl}_4$ , BPO, hv, reflux 4 h; iv) imidazole,  $\text{CH}_3\text{CN}$ ,  $\text{N}_2$ , reflux, 5 h; v) methanol, HCl, rt, 12 h.

While the ketone intermediates **113a,b** and **114b**, for the synthesis of compounds **107a,b** and **109b** respectively, were commercially available, the other intermediates were synthesized following different strategies. In particular, **114a** was prepared starting from 2-(pyridine-3-yl)acetic acid and propionic anhydride in the presence of pyridine (Scheme 6).

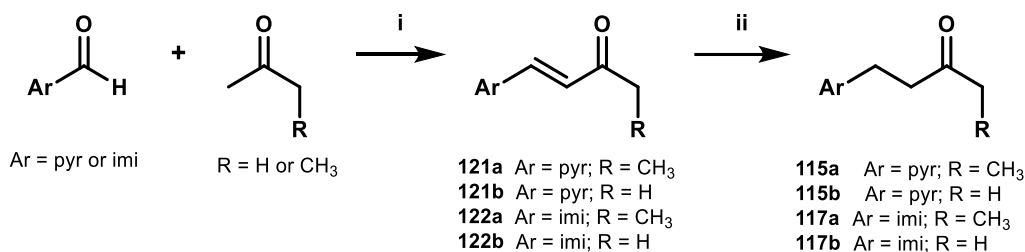
**Scheme 6.** Synthesis of intermediate **114a**.<sup>a</sup>



<sup>a</sup>**Reagent and conditions:** i) Pyridine, propionic anhydride,  $\text{N}_2$ , reflux, 6 h.

For the synthesis of ketones **115a,b** and **117a,b**, 3-pyridinecarboxyaldehyde or imidazole-4-carboxyaldehyde were reacted with acetone or methylethylketone in the presence of piperidine and acetic acid to give the corresponding  $\alpha,\beta$ -unsaturated ketones (**121-122a,b**), some of which are described in literature by employing different synthetic procedures (**121a**,<sup>149</sup> **121b**,<sup>150</sup> **122b**<sup>151</sup>). The double bond was then reduced with zinc in acetic acid and water to give **115a,b** (described in literature with a different synthetic procedure<sup>152</sup>) and **117a,b** (Scheme 7).

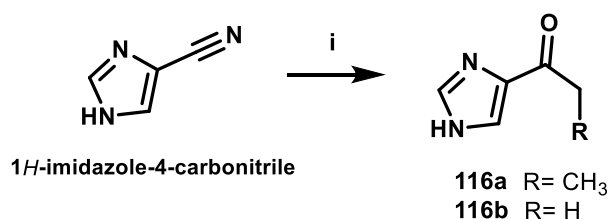
**Scheme 7.** Synthesis of intermediates **115a,b**, **117a,b**, **121a,b** and **122a,b**.<sup>a</sup>



<sup>a</sup>**Reagents and conditions:** i) Piperidine, AcOH, rt, 4 h; ii) Zn, AcOH, H<sub>2</sub>O, rt, 3 h.

For intermediates **116a,b**, 4(5)-cyanoimidazole<sup>153</sup> underwent Grignard reaction with ethyl- or methyl-Mg bromide to obtain **116a**<sup>153</sup> and **116b**, respectively (Scheme 8).

**Scheme 8.** Synthesis of intermediates **116a,b**.<sup>a</sup>



<sup>a</sup>**Reagents and conditions:** i) THF, RCH<sub>2</sub>MgBr, N<sub>2</sub>, rt, 3 h.

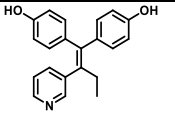
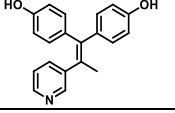
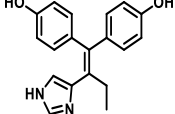
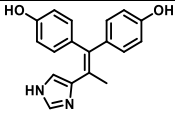
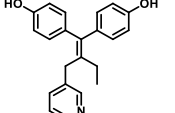
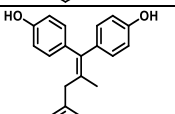
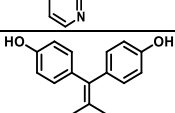
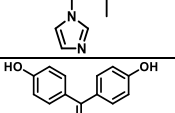
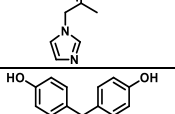
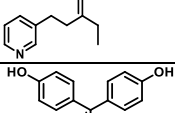
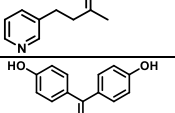
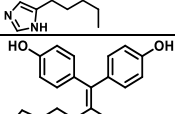
### *Biological evaluation*

The AR inhibitory activity of the new compounds was evaluated by the Aromatase Inhibitor Screening Kit (BioVision Inc., San Francisco, USA), monitoring the conversion of a fluorogenic substrate into a highly fluorescent metabolite as catalyzed by the AR enzyme, and results are reported in Table 3. Except for **107b**, all the compounds showed to be potent AIs, and several ligands exhibited IC<sub>50</sub> values in the nanomolar range. These results suggested that the presence of the ethyl chain typical of TAM derivatives was preferred to the shorter methyl group, and that both the imidazole and pyridine moieties were able to appropriately interact with AR leading to potent derivatives.

In detail, the contribution of the azole ring seemed to be dependent on the length of the spacer between the heterocycle and the central double bond. Apart from compounds with no linker, (**107-108a,b** n = 0) that exhibited weak activity and dissimilar results, in the presence of a single-carbon spacer both heterocycles led to compounds showing similar results (**109-110a,b** n = 1) while, when two methylene units were inserted between the azole ring and the vinyl group, imidazole derivatives exhibited higher activity than the corresponding pyridine compounds (**111-112a,b** n = 2).

Taking into account the pyridine series, the introduction of a methylene spacer between the heterocycle and the vinyl group significantly improved the activity of the ligands (**109a,b**) with respect to compounds with no linker **107a,b**, while its elongation to two methylenes caused a decrease in potency (**111a,b**). Considering the imidazole derivatives, the insertion of a methylene spacer on the structure of compound **108a** (n = 0, IC<sub>50</sub> = 0.95 μM), carrying the TAM-like ethyl group, led to an increase in activity (**110a**, n = 1, IC<sub>50</sub> = 35 nM) that was not further improved by the elongation of the linker to two units (**112a** n = 2, IC<sub>50</sub> = 52 nM). Contrariwise, the activity of the methyl derivative **108b** (IC<sub>50</sub> = 0.59 μM), reduced by the insertion of a methylene spacer (**110b** n = 1, IC<sub>50</sub> = 1.00 μM), was boosted by the elongation of the linker to two units (**112b** n = 2, IC<sub>50</sub> = 63 nM). The most potent AIs of this series resulted to be **109a**, **110a**, **112a** and **112b**, with IC<sub>50</sub> values of 23, 35, 52 and 63 nM, respectively.

**Table 3.** Biological profiles of **107-112a,b**: AR inhibition, ER $\alpha$  binding and proliferation of MCF7 (ER+) BC, MDA-MB-231 (ER-) BC, and MCF10A healthy breast cells.

Cmp	Code	AR inhibition IC <sub>50</sub> $\mu$ M <sup>a</sup>	ER $\alpha$ binding IC <sub>50</sub> $\mu$ M <sup>a</sup>	MCF-7 cells IC <sub>50</sub> $\mu$ M <sup>a</sup>	MDA-MB-231 cells IC <sub>50</sub> $\mu$ M <sup>a</sup>	MCF-10A cells IC <sub>50</sub> $\mu$ M <sup>a</sup>
	<b>107a</b>	1.253 $\pm$ 0.129	> 100	10.0 $\pm$ 2.1	6.2 $\pm$ 1.5	17.0 $\pm$ 0.5
	<b>107b</b>	> 100	0.076 $\pm$ 0.036	5.3 $\pm$ 1.1	5.3 $\pm$ 0.3	41.7 $\pm$ 0.3
	<b>108a</b>	0.952 $\pm$ 0.078	1.073 $\pm$ 1.010	60.0 $\pm$ 0.9	45.0 $\pm$ 1.2	>100
	<b>108b</b>	0.596 $\pm$ 0.045	0.223 $\pm$ 0.071	58.0 $\pm$ 8.5	23.4 $\pm$ 0.1	>100
	<b>109a</b>	0.023 $\pm$ 0.018	0.019 $\pm$ 0.001	27.6 $\pm$ 0.4	24.7 $\pm$ 1.0	>100
	<b>109b</b>	0.861 $\pm$ 0.062	1.770 $\pm$ 0.368	41.2 $\pm$ 1.6	19.0 $\pm$ 0.1	58.7 $\pm$ 0.9
	<b>110a</b>	0.035 $\pm$ 0.001	1.803 $\pm$ 0.221	24.3 $\pm$ 0.9	3.4 $\pm$ 0.2	34.7 $\pm$ 0.5
	<b>110b</b>	1.002 $\pm$ 0.171	4.950 $\pm$ 0.613	37.0 $\pm$ 1.0	1.6 $\pm$ 0.5	52.5 $\pm$ 0.5
	<b>111a</b>	0.900 $\pm$ 0.339	0.033 $\pm$ 0.003	42.1 $\pm$ 1.1	19.5 $\pm$ 0.6	20.0 $\pm$ 1.6
	<b>111b</b>	3.240 $\pm$ 0.438	0.313 $\pm$ 0.006	>100	>100	>100
	<b>112a</b>	0.052 $\pm$ 0.004	0.197 $\pm$ 0.031	37.1 $\pm$ 1.1	14.0 $\pm$ 0.5	>100
	<b>112b</b>	0.063 $\pm$ 0.003	1.737 $\pm$ 0.318	39.8 $\pm$ 4.7	5.8 $\pm$ 0.2	50.4 $\pm$ 0.7

<sup>a</sup>Data represent the mean  $\pm$  standard deviation of three independent experiments

The Invitrogen PolarScreen ER $\alpha$  Competitor Assay Kit Green was used to determine the relative affinity of the tested compounds towards ER $\alpha$ , by measuring their capacity to prevent estrogen binding to the receptor. All the new compounds, except for **107a**, were able to interact with the receptor causing the displacement of the natural ligand, exhibiting IC<sub>50</sub> values in the  $\mu$ M or sub-  $\mu$ M range (Table 3). These results suggested that, generally, the introduction of a pyridine led to a higher affinity than imidazole, and the presence of the TAM-like ethyl moiety was favored with respect to the shorter methyl group. Considering compounds carrying the ethyl and the pyridine groups, the introduction of a methylene spacer on **107a** led to the achievement of considerable affinity for the receptor (**109a**, IC<sub>50</sub> = 19 nM) that did not seem to be further affected by the extension of the spacer to two methylenes (**111a**, IC<sub>50</sub> = 33 nM). As regards the corresponding imidazole derivatives, the low activity of **108a** (n = 0) was maintained also in the presence of a methylene spacer (**110a** n = 1), while it significantly increased when the linker was extended (**112a** n = 2). Surprisingly, in compounds with no spacer (**107-108a,b**), the presence of the methyl group on the double bond resulted in IC<sub>50</sub> values in the sub- $\mu$ M range in both pyridine/imidazole series. Among the compounds of the series, **109a** and **111a** carrying the pyridine ring, the ethyl group and a spacer of one and two methylene units, respectively, proved to be the best derivatives.

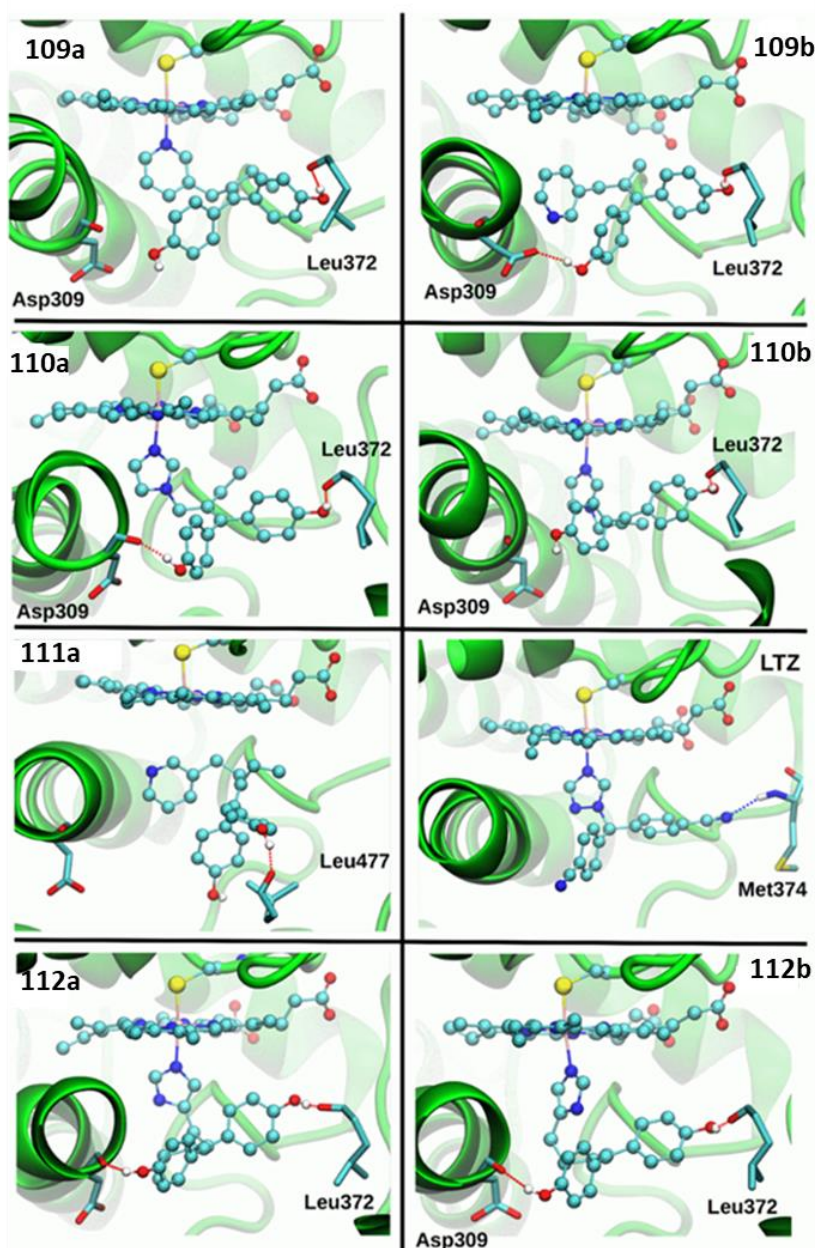
Moreover, the antiproliferative activity of the new compounds on ER<sup>+</sup> (MCF-7), ER<sup>-</sup> (MB-MDA-231) and on healthy breast cells (MCF10A) was evaluated (Table 3). Several compounds exhibited modest antiproliferative activity against MCF-7 and MB-MDA-231, with IC<sub>50</sub> values < 10  $\mu$ M. Compounds **110a**, **110b** and **112b**, with activities in the low  $\mu$ M range, were the best derivatives. Notably, compounds **108a**, **108b**, **109a** and **112a** had no cytotoxic effect on healthy breast cells.

### *Computational studies*

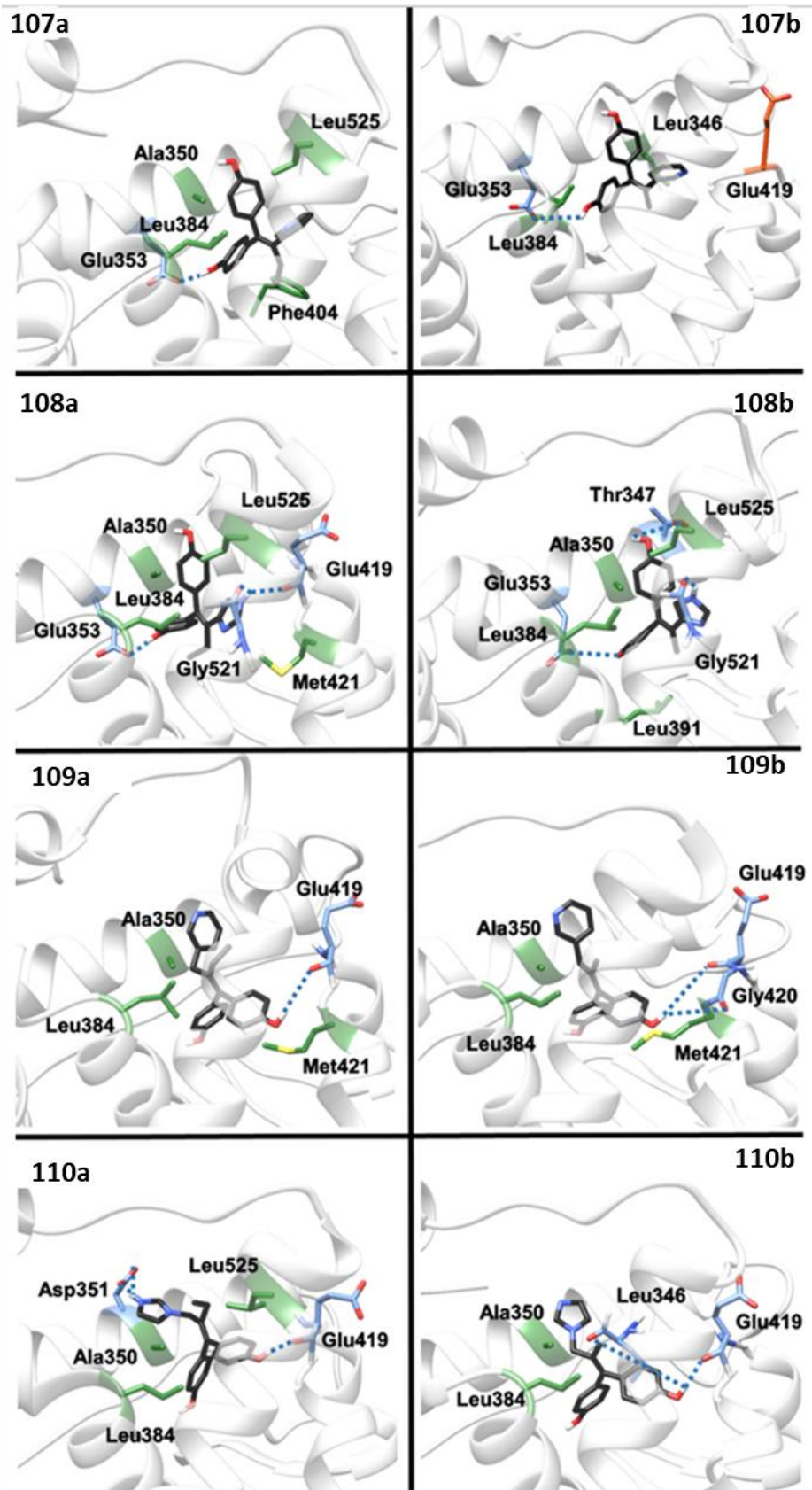
With the aim of defining the structural features underlying the experimental activities of the new compounds, extensive QM/MM MD simulations were

performed. Due to the high cost of these computational simulations, a subset of compounds was selected (**109a**, **109b**, **110a**, **110b**, **111a**, **112a**, **112b**, Figure 42). Structural analysis of the AR/drug adducts revealed that the coordination geometry (*i.e.* bond lengths and angles) of the inhibitors was not closely related with the experimental activity, since the binding geometry of the most potent compounds **109a**, **110a**, **112a** and **112b** was similar to that of the weak inhibitor **110b**. Remarkably, compounds **109b** and **111a** in QM/MM MD trajectories did not form any coordination bond with the heme iron. The behaviour of **111a** could be due to its bulky structure, characterized by a two methylene-units spacer and by the TAM-like ethyl group. On the other hand, the docking poses of **108a** and **108b** showed that the absence of a linker between the central double bond and theazole ring led to an increased structural rigidity, affecting the compound ability to rotate and to coordinate the metal centre.

The role of the hydroxyl groups in forming H-bonds with residues of AR active site was also evaluated. Considering compounds able to coordinate the heme group, **110a**, **112a** and **112b** showed two persistent H-bonds between their hydroxyl groups and the backbone of Leu372 and Asp309, while **109a**, despite having similar geometry, exhibited only one H-bond with the backbone of Leu372. The marketed AIs LTZ and EXE could also establish persistent H-bonds to the backbone of Met374, suggesting that they were essential for potent inhibitory activity. Generally, ligands that, due to geometric constraints, were unable to coordinate the heme group, such as **110b**, could also interact via persistent H-bond with the backbone of Leu372, providing a rationale for their activities in the low  $\mu\text{M}$  range. Moreover, the non-bonded interactions (hydrophobic or electrostatic interactions) between inhibitors and the enzyme were analysed by calculating their binding free energy ( $\Delta G_b$ ) with the Molecular Mechanics Generalized Born Surface Area (MM-GBSA) method followed by a decomposition analysis. The most potent compounds **109a**, **110a**, **112a** and **112b** exhibited hydrophobic interactions between their ethyl moiety and Ile133 and Trp244, and between their phenol rings and Val370 and Leu372.



**Figure 42.** Binding pose of LTZ and the selected newly synthesized inhibitors **109a**, **109b**, **110a**, **110b**, **111a**, **112a** and **112b** to the AR active site as obtained from representative frames of QM/MM MD trajectories. AR structure is displayed in green new cartons, the heme moiety, the cysteine and the inhibitors are shown in balls and sticks, the residues forming hydrogen bonds to the ligands are shown in licorice. All atoms are coloured by atom name (H white, O red, S yellow and N blue, C cyan).



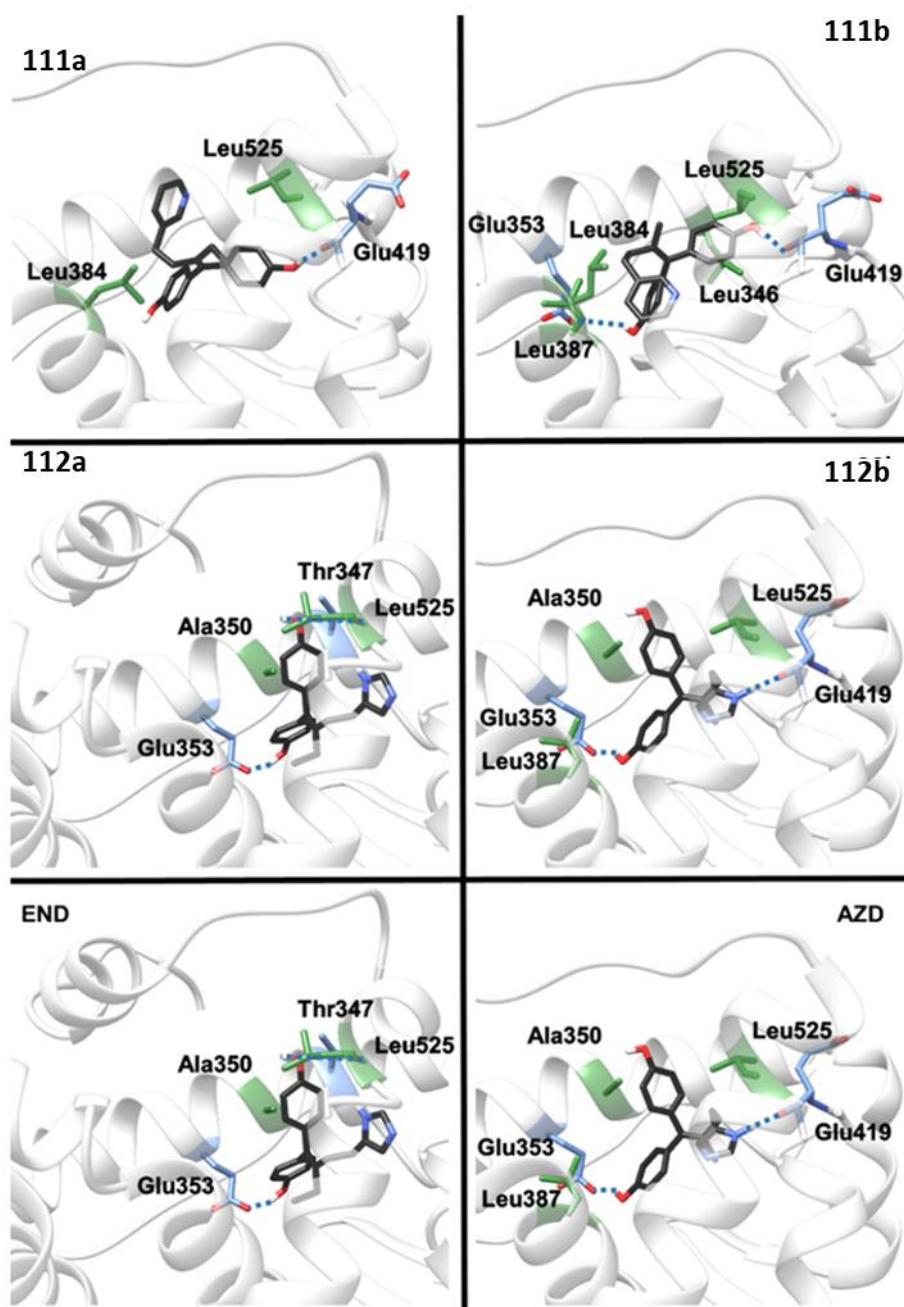


**Figure 43.** Binding pose of the synthesized inhibitors to the ligand-binding cavity of ER $\alpha$  as obtained from a representative cluster of classical MD trajectory. The binding mode of END and AZD-9496 (AZD), are also reported for comparison. ER $\alpha$  is shown as white new cartoons, the drug is displayed with back carbon atoms, the residues forming hydrophobic interactions are shown in green, those forming hydrogen-bonds are shown in blue, residues disfavoring the binding are displayed in orange. The rest of the atoms are coloured by atom name (H white, O red, S yellow and N blue).

Extensive classical MD simulations on the docking pose of each inhibitor/ER $\alpha$  adduct were also performed (Figure 43). The most potent compounds, **109a** and **111a**, showed among the highest  $\Delta G_b$  to ER $\alpha$ . Decomposition analysis revealed that their binding was stabilized by hydrophobic interactions. Indeed, **109a** formed hydrophobic interactions with Ala350, Leu384 and Met421 and H-bonds between the hydroxyl of one phenol ring to the backbone of Glu419 and His424. Similarly, **111a** was stabilized by hydrophobic interactions with Leu346, Ala350, Leu384, Leu387, and Leu525. Moreover, both ligands presented the same persistent H-bond with the backbone of Glu419. Apparently, most of the compounds often H-bonded to Glu419 and/or Glu353 and were stabilized by hydrophobic interactions similar to the most potent derivatives, regardless of their IC<sub>50</sub> values. These results suggested that the  $\Delta G_b$  *per se* did not fully account for their measured IC<sub>50</sub>.

### *Discussion*

In summary, as regards AR inhibitory activity, the presence of the ethyl group typical of SERMs and a spacer between the azole ring and the central double bond seemed to be crucial for gaining high potency. In particular, in the pyridine series only compounds carrying a methylene spacer resulted potent AIs, suggesting that this was the optimal length to properly fit into the active site of the enzyme. In contrast, for imidazole derivatives, the extensions of the linker to two units did not decrease the affinity for the enzyme, leading to potent compounds (IC<sub>50</sub> values in the low nanomolar range) regardless of the presence of a methyl (**112b**) or ethyl (**112a**) group on the central double bond. Despite most of compounds showing high activity were imidazole derivatives (**110a**, **112a** and **112b**), the most interesting compound resulted to be **109a** carrying a pyridine moiety. From these results it seemed that, in the presence of a suitable structure of the molecule, both heterocycles were able to form appropriate interactions with the target, leading to the development of potent AIs.

Concerning the binding affinity toward ER $\alpha$  receptor, again, the presence of the spacer and the ethyl group on the double bond seemed to grant high affinity to the molecules. Indeed, compounds **109a** and **111a**, both carrying the TAM-like ethyl

moiety, a one/two methylene spacer, respectively, and a pyridine ring were the derivatives with the best affinities ( $IC_{50}$ s of 19 nM and 33 nM, respectively). Since other derivatives all exhibited similar potency in the submicromolar range, except for the potent **107b**, it was not possible to highlight other SARs for these compounds. This behavior could be due to the greater flexibility of ER $\alpha$  LBD domain, that allowed the receptor to better adapt to the binding of different ligands, with respect to AR.

Furthermore, comparing the activities of the new compounds with those of the literature compound **90**, it seemed that by replacing its benzene ring with the TAM-like ethyl moiety (**110a**) the affinity toward ER $\alpha$  was reduced ( $IC_{50}$  values of 27.3 nM and 1.80  $\mu$ M, respectively), while the substitution of the imidazolyl group of **110a** with a pyridine (**109a**) caused a restoration of the activity in the low nanomolar range (19 nM). On the contrary, taking into account AR inhibitory activity, going from **90** to **110a** and **109a** the potency was maintained in the low nanomolar range, although with a slight increase of  $IC_{50}$  values (4.77, 35 and 23 nM, respectively).

As for the development of new multitarget ligands, the most promising result was the identification of derivatives able to interact with both AR and ER $\alpha$  with potent and balanced activities. Indeed, compounds **108b** and **112a**, despite their potency were not perfectly balanced, exhibited submicromolar activities on both targets. Remarkably, compound **109a** proved to be a potent AI and ER $\alpha$  ligand, with balanced activities in the low nanomolar range ( $IC_{50}$ s of 23 and 19 nM, respectively), and resulted the most interesting multitarget candidate of this series. Computational studies allowed to outline the structural features of a potent and balanced dual AR/ER $\alpha$  multitarget agent as **109a**. In particular, key elements seemed to be: i) the presence of a hydroxyl group able to H-bond to Leu372 of AR, and to Glu419 of ER $\alpha$ ; ii) the ethyl group that filled the active sites of both targets, allowing the coordination of the molecule with the heme group in AR and favourable hydrophobic interactions with both targets; iii) the presence of a methylene linker between the pyridine ring and the central double bond that allowed an internal  $\pi$ -stacking between the pyridine and the phenol ring in cis position on the double bond, while the remaining ethyl and phenol groups were connected by

hydrophobic interactions. This particular arrangement allowed for the inhibitor to pack and snugly fit in the binding cavity of both targets.

In conclusion, this study led to the development of new potential selective, potent, and balanced dual-targeting AR/ER $\alpha$  modulators as drug candidates. Surprisingly, the best derivative carried a pyridine moiety that was not previously investigated as potential moiety to be used in the development of multitarget anti BC agents.

### 3.2.2 Design and synthesis of potential AIs/SERMs: tricyclic derivatives

In a second series (Figure 44), the bisphenol moiety of compounds of series 1 was included in a tricyclic structure, increasing the rigidity of the molecules, to evaluate the effect of this modification on the affinity for both AR and ERs.

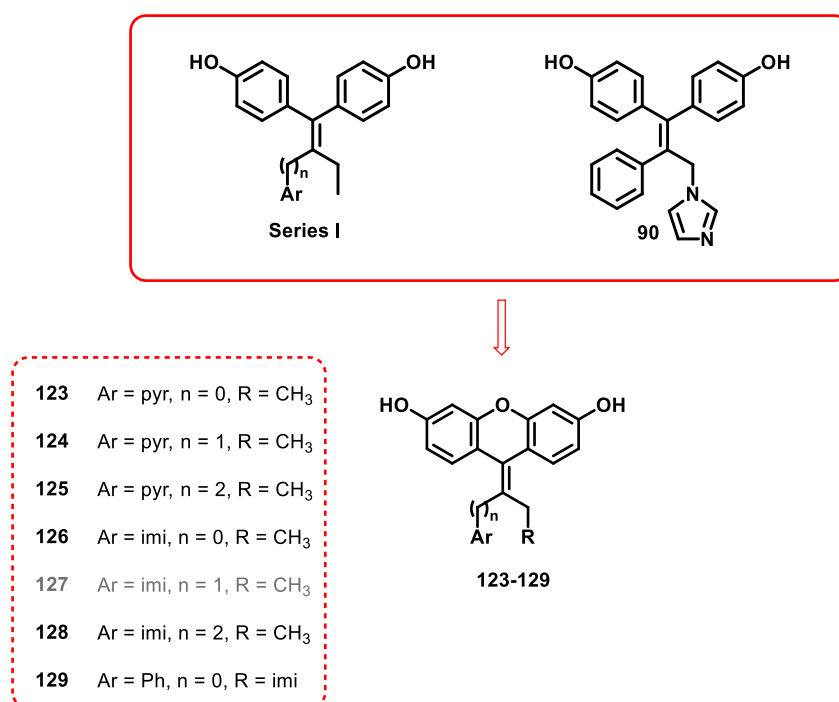


**Figure 44.** Design of new tricyclic derivatives. (In grey compound not yet synthesized)

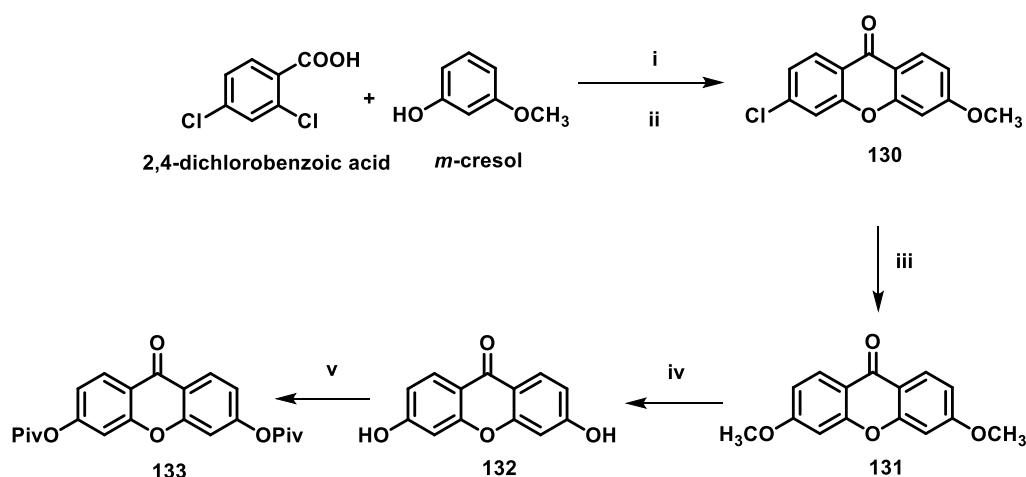
This scaffold was also reported in a previous study on TAM derivatives as anticancer agents, and the introduction of this rigid core allowed obtaining an interesting antiproliferative and proapoptotic compound.<sup>54</sup> Since the compounds

carrying the ethyl group typical of TAM gave the best results, we now focused our interest only on ethyl derivatives, carrying either imidazole or pyridine as heterocycles, synthesizing tricyclic compounds **123-128**; in addition, the previously mentioned compound **90** (Figure 35 and Figure 44) was also modified by introducing a tricyclic core to give **129** (Figure 44). For the new compounds, biological evaluation is ongoing to assess their anticancer profile.

### Chemistry

The synthesis of 9-oxo-9H-xanthen-3,6-diyl bis(2,2-dimethylpropanoate) **133**, key intermediate for the synthesis of compounds **123-129**, is shown in Scheme 9.

**Scheme 9.** Synthesis of intermediate **133**.<sup>a</sup>



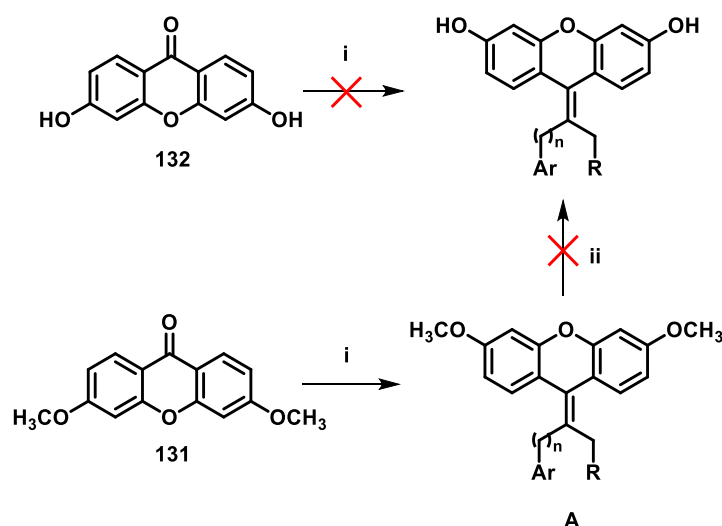
<sup>a</sup>**Reagents and conditions:** i)  $K_2CO_3$ , Cu/CuI, pyridine,  $H_2O$ , reflux 2 h; ii)  $H_3PO_4$ ,  $P_2O_5$ ,  $120\text{ }^\circ\text{C}$ , 7 h; iii) MeONa, MeOH, reflux 41 h; iv)  $AlCl_3$ , toluene, reflux 3 h; v) 60 % NaH, dry THF, pivaloyl chloride, rt, 5 h.

2,4-dichlorobenzoic acid was reacted with *m*-cresol in the presence of  $K_2CO_3$ , Cu/CuI and pyridine (Ullmann reaction) to give the corresponding diarylether, that was then cyclized by treatment with polyphosphoric acid to obtain the xanthenone **130**, isolated by flash column chromatography. **130** was then treated with sodium methoxide in methanol obtaining **131**, which was demethylated with  $AlCl_3$  in

toluene to give the dihydroxy derivative **132**. The final step involved the protection of the hydroxyl groups with pivaloyl chloride in the presence of 60 % NaH to give the key intermediate **133**.

Several attempts were initially made for the synthesis of compounds **123-129**. At first, the unprotected dihydroxyxanthone **132** was reacted under McMurry reaction conditions (Scheme 10), as seen for bisphenol derivatives, but the formation of the desired compound was not observed. Later, the dimethoxyxanthone **131** was reacted in the coupling reaction obtaining the intermediates **A**. However, the subsequent demethylation reaction, performed under different conditions, did not lead to any of the desired compounds.

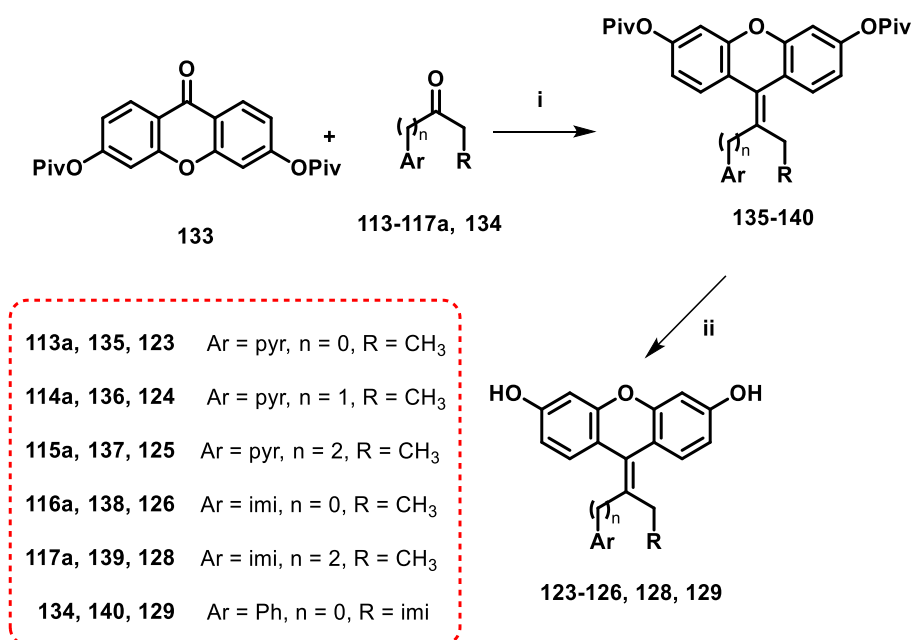
**Scheme 10.** First attempts for the synthesis of **123-129**.<sup>a</sup>



**Reagents and conditions:** i) selected ketone, THF, Zn, TiCl<sub>4</sub>, N<sub>2</sub>, reflux; ii) AlCl<sub>3</sub>, toluene, reflux 3 h; or BBr<sub>3</sub>, dichloromethane, overnight, rt or -78 °C.

Finally, **123-126**, **128** and **129** were obtained by protecting the hydroxyl groups with pivaloyl chloride to give **133**, which was reacted with the suitable ketone (**113a-117a**, **134**) under McMurry reaction conditions to give intermediates **135-140**, which were deprotected with 10 % LiOH to give the desired compounds (Scheme 11).

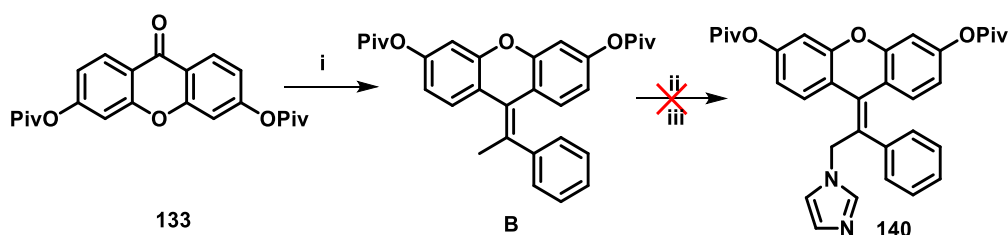
**Scheme 11.** Synthesis of the final compounds **123-126**, **128**, **129**.<sup>a</sup>



<sup>a</sup>**Reagents and conditions:** i) THF, Zn, TiCl<sub>4</sub>, N<sub>2</sub>, reflux; ii) 10 % LiOH, methanol, rt, 2 h.

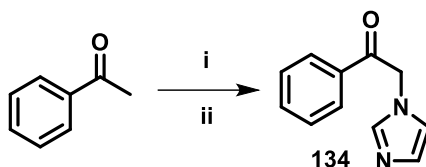
For the synthesis of compound **129**, a different strategy had first been attempted (Scheme 12) by reacting **133** and acetophenone under McMurry conditions obtaining intermediate **B**, following the same route employed for the synthesis of compounds **110a,b** (Series I, Scheme 5). However, the subsequent bromination with NBS followed by reaction with imidazole did not lead to the desired **140**. Thus, ketone **134** had to be synthesized by bromination of acetophenone with NBS in the presence of montmorillonite K10, and reaction with imidazole in CH<sub>3</sub>CN (Scheme 13). Compound **129** was thus obtained by reacting the intermediates **133** and **134** according to Scheme 11.

**Scheme 12.** First attempt for the synthesis of compound **129**.<sup>a</sup>



**Reagents and conditions:** i) acetophenone, THF, Zn, TiCl<sub>4</sub>, N<sub>2</sub>, reflux; ii) NBS, CCl<sub>4</sub>, BPO, hv, reflux 4 h; iii) imidazole, CH<sub>3</sub>CN, N<sub>2</sub>, reflux, 5 h.

**Scheme 13.** Synthesis of intermediate **134**.<sup>a</sup>



**Reagents and conditions:** i) NBS, montmorillonite K-10, MeOH, 60-65 °C, 30 min; ii) imidazole, CH<sub>3</sub>CN, reflux 1 h.

Except for the commercially available **113a**, the other ketone intermediates **114a-117a** were synthesized with the procedures reported above for compounds of series 1 (see Schemes 6-8).

Up to now, derivative carrying the imidazole and a single methylene spacer has not been synthesized (compound **127**, Figure 44). In a first attempt, the procedure described in Scheme 12 was used, but the imidazolyl derivative could not be obtained. Then, the reaction described in Scheme 13 was performed, starting from methylethylketone to obtain the ketone intermediate, but the subsequent McMurry reaction was not successful. A different approach is thus necessary for the synthesis of this compound.

### 3.2.3 Design and synthesis of potential AIs/SERDs

As mentioned above, in recent years the search for new derivatives with SERD activity led to promising compounds with clinical effectiveness. A novel therapeutic strategy for the treatment of ER+ BC could therefore be represented by the development of a single molecule with dual AI and SERD activity.

Taking into account the structure of the known degrader GW5638 and its metabolite GW7604 (Figure 12 and Figure 45), with the aim of obtaining hybrid molecules endowed with both AR inhibiting and SERD activities, some modifications were designed on the structure of our previously synthesized series of bisphenols, together with the literature compound **90**.

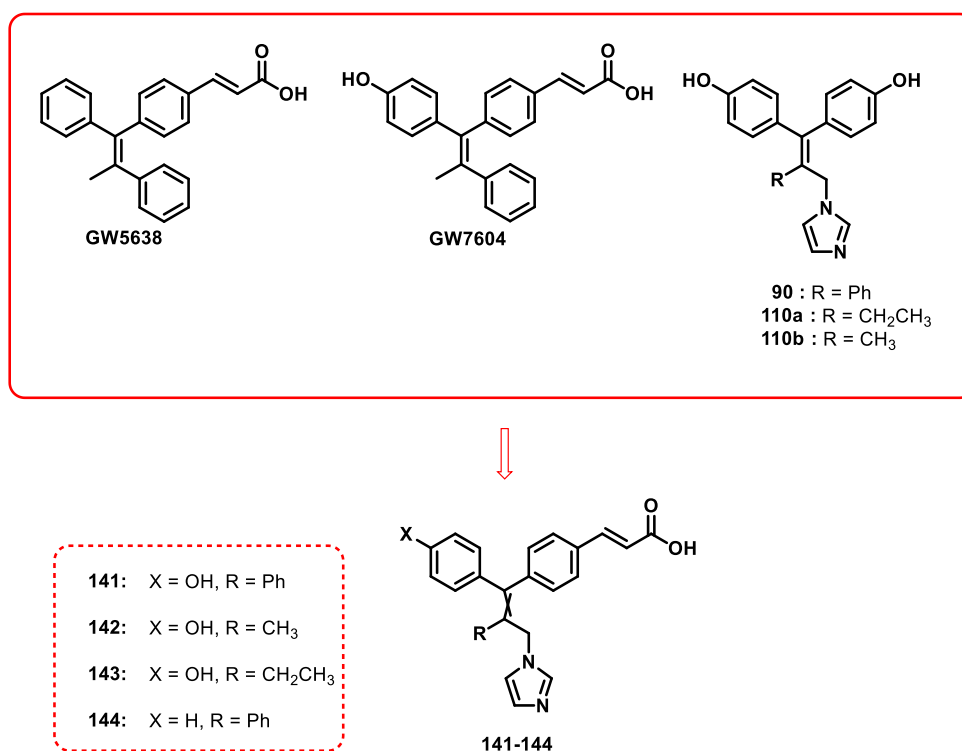


**Figure 45.** Design of potential AIs/SERDs with an acrylic acid side chain.

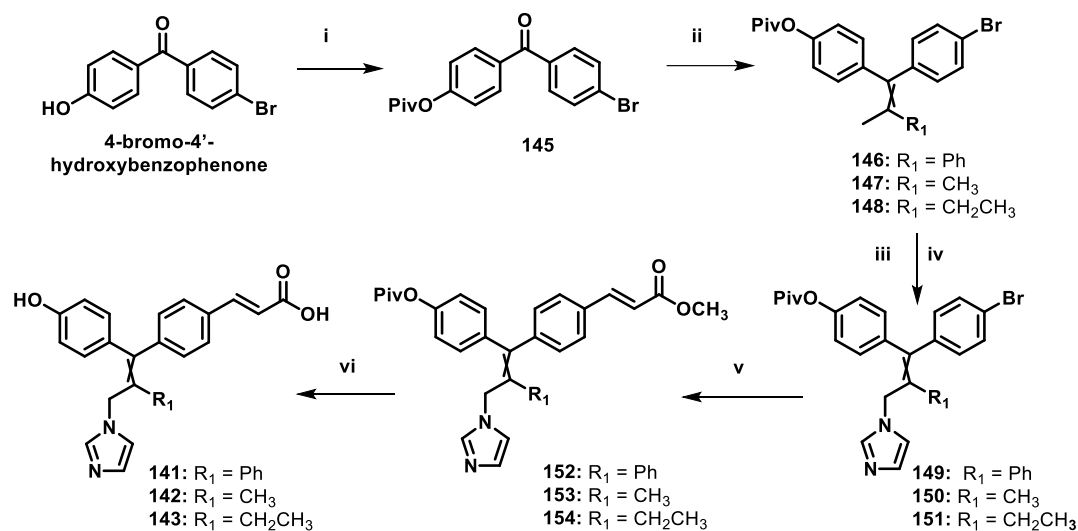
In detail, the introduction of the acrylic acid side chain on one of the phenyl rings was envisaged to achieve ER degradation potential for the new molecules. In a first attempt, our attention was focused on modifications of imidazole derivatives

carrying a single methylene spacer (**110a-b**), as in **90**, and compounds **141-143** were synthesized. In order to evaluate the role of the phenol moiety, the hydroxyl group was also removed to give the prototype compound **144**. The newly synthesized compounds are now undergoing biological evaluation to assess their relative affinity towards ER $\alpha$  and to determine their ability to degrade the receptor.

### Chemistry

Compounds **141-143** were synthesized following Scheme 14.

**Scheme 14.** Synthesis of compounds **141-143**.<sup>a</sup>



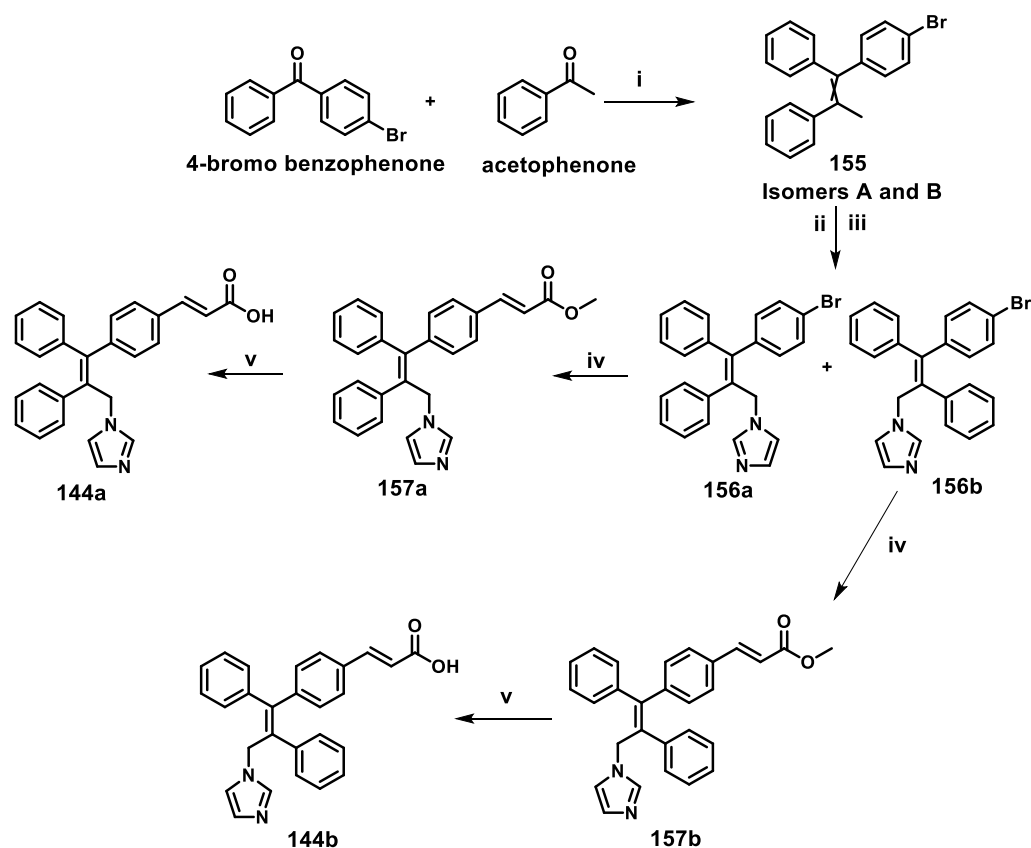
**Reagents and conditions:** i) 60 % NaH, dry THF, pivaloyl chloride, rt, 5 h; ii) Zn, TiCl<sub>4</sub>, THF, N<sub>2</sub> reflux; iii) NBS, CCl<sub>4</sub>, BPO, hv, reflux 4 h; iv) imidazole, CH<sub>3</sub>CN, N<sub>2</sub>, reflux, 5 h; v) triethylamine, methyl acrylate, Pd(PPh<sub>3</sub>)<sub>2</sub>Cl<sub>2</sub>, DMF, 1 h, 120 °C, mw; vi) 10 % LiOH, methanol, rt, 2 h.

The hydroxy group of 4-bromo-4'-hydroxybenzophenone<sup>137</sup> was protected with pivaloyl chloride in the presence of 10 % NaH to give compound **145**, that was reacted with the appropriate ketone (acetone, methylethylketone or acetophenone) under McMurry conditions to obtain both isomers of intermediates **146-148**. Bromination with NBS and subsequent reaction with imidazole led to derivatives

**149-151** that were reacted with methyl acrylate in the presence of  $\text{Pd}(\text{PPh}_3)_2\text{Cl}_2$  under microwave irradiation to give **152-154**. One-pot deprotection of phenolic hydroxyl and carboxylic acid with 10 %  $\text{LiOH}$  in methanol allowed obtaining the final compounds **141-143**. Several attempts to separate the two isomers by flash column chromatography have been made at different stages of the synthetic route, without satisfactory results. Different strategies will thus be exploited in order to obtain the two isomers with suitable purity.

Compounds **144a** and **144b** were synthesized according to Scheme 15.

**Scheme 15.** Synthesis of compounds **144a** and **144b**.<sup>a</sup>



<sup>a</sup>**Reagents and conditions:** i)  $\text{Zn}$ ,  $\text{TiCl}_4$ , THF,  $\text{N}_2$  reflux; ii)  $\text{NBS}$ ,  $\text{CCl}_4$ ,  $\text{BPO}$ ,  $h\nu$ , reflux 4 h; iii) imidazole,  $\text{CH}_3\text{CN}$ ,  $\text{N}_2$ , reflux, 5 h; iv) triethylamine, methyl acrylate,  $\text{Pd}(\text{PPh}_3)_2\text{Cl}_2$ , DMF, 1 h,  $120^\circ\text{C}$ , mw; v) 10 %  $\text{LiOH}$ , methanol, rt, 2 h.

4-bromobenzophenone and acetophenone were reacted under McMurry conditions to obtain both isomers of compound **155** (**A** and **B**) that were isolated by flash column chromatography. The methyl group of both **A** and **B** was brominated with NBS, and then reacted with imidazole without further purification. In both cases, a mixture (*E/Z*) of compounds **156a** and **156b** was obtained, suggesting that isomerization took place during the bromination reaction. **156a** and **156b** were thus isolated by flash column chromatography and then reacted with methyl acrylate in the presence of Pd(PPh<sub>3</sub>)<sub>2</sub>Cl<sub>2</sub> under microwave irradiation to give **157a** and **157b**, respectively. In the last step of this synthetic route, the carboxylic acid was deprotected with 10 % LiOH in methanol to give compounds **144a** and **144b**.

The *Z* and *E* geometries of **144a** and **144b** were assigned by <sup>1</sup>H-<sup>1</sup>H COSY and NOE NMR spectroscopy. Considering **144a**, H<sub>a</sub> protons (Figure 46, red) were first assigned by NOE correlation with H<sub>b</sub> (yellow), and H<sub>c</sub> (blue) was assigned by COSY and NOE correlation with H<sub>a</sub>. Subsequently, irradiation of H<sub>d</sub> methylene protons (Figure 46, green) showed a clear NOE correlation with H<sub>c</sub>. This evidence suggested that compound **144a** corresponded to *Z* isomer. Similarly, for compound **144b**, H<sub>a</sub> protons (red) were first assigned by NOE correlation with H<sub>b</sub> (yellow) and H<sub>c</sub> (blue) were assigned by COSY and NOE correlation with H<sub>a</sub>. The irradiation of aromatic H<sub>c</sub> protons of **144b** produced a NOE correlation with protons of the aromatic ring in orange (Figure 46) and no correlation with H<sub>d</sub> protons, confirming the *E* configuration for compound **144b**.

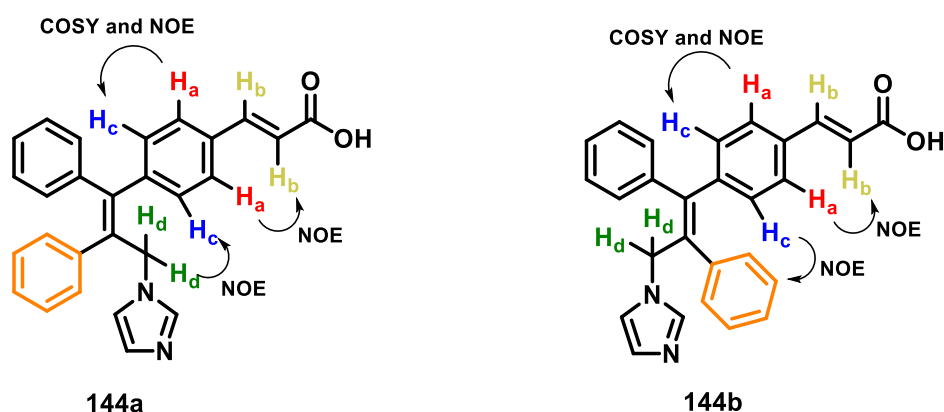


**Figure 46.** Stereochemistry determination of **144a** and **144b**.

### 3.2.4 Experimental procedures

#### *General Methods*

Starting materials, unless otherwise specified, were used as high grade purity commercial products. Solvents were of analytical grade. Reaction progress was followed by thin layer chromatography (TLC) on precoated silica gel plates (Merck Silica Gel 60 F254) and then visualized with a UV254 lamplight. Chromatographic separations were performed on silica gel columns by flash method (Kieselgel 40, 0.040-0.063 mm, Merck). Melting points were determined in open glass capillaries, using a Büchi apparatus and are uncorrected.  $^1\text{H}$  NMR and  $^{13}\text{C}$  NMR spectra were recorded on a Varian Gemini spectrometer 400 MHz and 101 MHz, respectively, in  $\text{CDCl}_3$  solutions unless otherwise indicated, and chemical shifts ( $\delta$ ) were reported as parts per million (ppm) values relative to tetramethylsilane (TMS) as internal standard; coupling constants ( $J$ ) are reported in Hertz (Hz). Standard abbreviations indicating spin multiplicities are given as follow: s (singlet), d (doublet), t (triplet), br (broad), q (quartet), dd (doublet of doublets) or m (multiplet). Mass spectra were recorded on Waters Xevo G2-XS QToF apparatus operating in electrospray mode (ES). All tested compounds were found to have >95% purity, as determined by HPLC analysis, performed on a chromatograph PU-1587 UV model equipped with a 20  $\mu\text{L}$  loop valve (Jasco Europe, Italy) by using a Phenomenex Luna 5  $\mu\text{m}$  C18 column (150  $\times$  4.60 mm) as stationary phase and a mixture of  $\text{H}_2\text{O}/\text{MeCN}$  (60:40, v/v) as mobile phase, or a Waters Spherisorb 5  $\mu\text{m}$  C18 column (250  $\times$  4.60 mm) as stationary phase and a mixture of  $\text{H}_2\text{O}/\text{MeCN}$  (70:30, v/v) as mobile phase; for all compounds, detection at  $\lambda = 254$  nm, flow rate of 1.0 mL/min. Compounds were named relying on the naming algorithm developed by CambridgeSoft Corporation and used in ChemDraw Professional 19.1.

#### **General procedure of McMurry reaction.**

**Method A.** Zinc powder (10 eq) was suspended in anhydrous THF, the mixture was cooled to 0  $^\circ\text{C}$  and  $\text{TiCl}_4$  (5 eq) was added dropwise under nitrogen atmosphere. At

the end of the addition, the mixture was brought to room temperature and then warmed to reflux for 2 hours. After cooling, a solution of benzophenone (1 eq) and the corresponding ketone (3 eq) in dry THF was added and the mixture was heated to reflux in the dark for 3 hours. After cooling, the mixture was poured into a 10 % K<sub>2</sub>CO<sub>3</sub> solution and extracted with diethylether (3 x 25 mL). The combined organic layers were washed with brine, dried over anhydrous Na<sub>2</sub>SO<sub>4</sub> and concentrated to dryness. The crude compound was then purified by flash column chromatography with a suitable eluent to provide the desired McMurry product.

**Method B.** Zinc powder (6 eq) was suspended in anhydrous THF (3-20 mL), the mixture was cooled to 0 °C and TiCl<sub>4</sub> (3 eq) was added dropwise under nitrogen atmosphere. At the end of the addition, the mixture was brought to room temperature and then warmed to reflux for 1 hour. After cooling, a solution of benzophenone (1 eq) and the corresponding ketone (1 eq) in dry THF (3-20 mL) was added and the mixture was heated to reflux for 2 hours. After cooling, the mixture was poured into a 10 % K<sub>2</sub>CO<sub>3</sub> solution and extracted with diethyl ether (3 x 5-25 mL). The combined organic layers were washed with brine, dried over anhydrous Na<sub>2</sub>SO<sub>4</sub> and concentrated to dryness. The crude compound was then purified by flash column chromatography with a suitable eluent to provide the desired McMurry product.

**4,4'-(2-(pyridine-3-yl)but-1-ene-1,1-diyl)diphenol (107a).** Bis(4-hydroxyphenyl)methanone (0.50 g, 2.30 mmol) and 1-(pyridin-3-yl)propan-1-one (**113a**) (0.29 mL, 2.30 mmol) in dry THF were reacted according to **Method B**. The crude was purified by flash column chromatography (petroleum ether/ethyl acetate 1:1) to give **107a** as grey solid (0.18 g, yield 24 %), mp 240-241 °C. <sup>1</sup>H NMR (methanol-*d*<sub>4</sub>): δ 0.95 (t, *J* = 7.4 Hz, 3H, CH<sub>3</sub>), 2.55 (q, *J* = 7.4 Hz, 2H, CH<sub>2</sub>), 6.46 (d, *J* = 8.8 Hz, 2H, arom), 6.67 (d, *J* = 8.4 Hz, 2H, arom), 6.78 (d, *J* = 8.8 Hz, 2H, arom), 7.05 (d, *J* = 8.4 Hz, 2H, arom), 7.29 (dd, *J* = 4.8 and 7.6 Hz, 1H, arom), 7.67 (dd, *J* = 2.0 and 7.6 Hz, 1H, arom), 8.16 (d, *J* = 1.6 Hz, 1H, arom), 8.22 (dd, *J* = 1.6 and 4.8 Hz, 1H, arom). <sup>13</sup>C NMR (methanol-*d*<sub>4</sub>): δ 13.8, 29.2, 115.4 (2C), 115.9 (2C), 124.6, 131.4 (2C), 133.2 (2C), 135.2, 135.5, 137.3, 139.0, 140.8, 142.8, 146.8, 151.4, 156.9, 157.6. HRMS C<sub>21</sub>H<sub>19</sub>NO<sub>2</sub> [M+H] calcd: 318.14886, found: 318.14897.

**4,4'-(2-(pyridine-3-yl)prop-1-ene-1,1-diyl)diphenol (107b).** Bis(4-hydroxyphenyl)methanone (0.50 g, 2.30 mmol) and 1-(pyridin-3-yl)ethan-1-one (**113b**) (0.78 mL, 7.00 mmol) in dry THF were reacted according to **Method A**. The crude was purified by flash column chromatography (gradient elution starting from petroleum ether/ethyl acetate 3:2, then 1:1, then 2:3) and crystallized from ethyl acetate to give **107b** as beige solid (0.17 g, yield 24 %), mp > 230 °C. <sup>1</sup>H NMR (methanol-*d*<sub>4</sub>): δ 2.18 (s, 3H, CH<sub>3</sub>), 6.50 (d, *J* = 8.4 Hz, 2H, arom), 6.71 (d, *J* = 8.4 Hz, 2H, arom), 6.80 (d, *J* = 8.8 Hz, 2H, arom), 7.08 (d, *J* = 8.0 Hz, 2H, arom), 7.29 (dd, *J* = 5.0 and 7.8 Hz, 1H, arom), 7.71 (d, *J* = 8.0 Hz, 1H, arom), 8.19–8.23 (m, 2H, arom). <sup>13</sup>C NMR (methanol-*d*<sub>4</sub>): δ 23.7, 116.3 (2C), 116.7 (2C), 125.5, 131.5, 132.9 (2C), 134.1 (2C), 136.2, 136.4, 139.6, 143.5, 144.0, 147.6, 151.8, 157.9, 158.4. HRMS C<sub>20</sub>H<sub>17</sub>NO<sub>2</sub> [M+H] calcd: 304.13321, found: 304.13319.

**4,4'-(2-(1H-imidazol-4-yl)but-1-ene-1,1-diyl)diphenol (108a).** Bis(4-hydroxyphenyl)methanone (0.50 g, 2.30 mmol) and **116a** (0.29 g, 2.30 mmol) in dry THF were reacted according to **Method B**. The crude was purified by flash column chromatography (gradient elution starting from petroleum ether/ethyl acetate 1:1, then 3:7, then 2:8) to give **108a** as grey solid (0.06 g, yield 9 %), mp 147–150 °C. <sup>1</sup>H NMR (methanol-*d*<sub>4</sub>): δ 0.99 (t, *J* = 7.4 Hz, 3H, CH<sub>3</sub>), 2.47 (q, *J* = 7.4 Hz, 2H, CH<sub>2</sub>), 6.42 (s, 1H, arom), 6.57 (d, *J* = 8.8 Hz, 2H, arom), 6.74 (d, *J* = 8.4 Hz, 2H, arom), 6.80 (d, *J* = 8.4 Hz, 2H, arom), 6.99 (d, *J* = 8.8 Hz, 2H, arom), 7.48 (s, 1H, arom). <sup>13</sup>C NMR (methanol-*d*<sub>4</sub>): δ 14.4, 28.0, 115.6 (2C), 115.8 (2C), 123.6, 131.3 (3C), 132.1 (2C), 135.3, 136.0, 136.4 (2C), 141.1, 157.0, 157.3. HRMS C<sub>19</sub>H<sub>18</sub>N<sub>2</sub>O<sub>2</sub> [M+H] calcd: 307.14410, found: 307.14422.

**4,4'-(2-(1H-imidazol-4-yl)prop-1-ene-1,1-diyl)diphenol (108b).** Bis(4-hydroxyphenyl)methanone (0.34 g, 1.60 mmol) and **116b** (0.18 g, 1.60 mmol) in dry THF were reacted according to **Method B**. The crude was purified by flash column chromatography (gradient elution starting from petroleum ether/ethyl acetate 2:3, then 0.5:9.5) to give **108b** as white solid (0.07 g, yield 15 %) mp 161–162 °C. <sup>1</sup>H NMR (methanol-*d*<sub>4</sub>): δ 2.10 (s, 3H, CH<sub>3</sub>), 6.37 (s, 1H, arom), 6.63 (d, *J* = 8.0 Hz, 2H, arom), 6.74 (d, *J* = 8.8 Hz, 2H, arom), 6.84 (d, *J* = 8.8 Hz, 2H, arom), 6.99 (d, *J* = 8.4 Hz, 2H, arom), 7.45 (s, 1H, arom). <sup>13</sup>C NMR (methanol-*d*<sub>4</sub>): δ 21.0, 115.7 (2C), 115.9 (2C), 125.0, 131.9 (3C), 132.1 (2C), 135.1, 135.9, 136.4 (2C),

140.8, 157.2, 157.3 HRMS C<sub>18</sub>H<sub>16</sub>N<sub>2</sub>O<sub>2</sub> [M+H] calcd: 293.12845, found: 293.12837.

**4,4'-(2-(pyridine-3-ylmethyl)but-1-ene-1,1-diyl)diphenol (109a).** Bis(4-hydroxyphenyl)methanone (0.20 g, 0.90 mmol) and **114a** (0.14 g, 0.90 mmol) in dry THF were reacted according to **Method B**. The crude was purified by flash column chromatography (ethyl acetate) to give **109a** as white solid (0.03 g, yield 10 %), mp 202-204 °C. <sup>1</sup>H NMR (methanol-*d*<sub>4</sub>): δ 0.97 (t, *J* = 7.2 Hz, 3H, CH<sub>3</sub>), 2.05 (q, *J* = 7.2 Hz, 2H, CH<sub>2</sub>), 3.57 (s, 2H, CH<sub>2</sub>Py), 6.69-6.72 (m, 4H, arom), 6.97-6.99 (m, 4H, arom), 7.35 (dd, *J* = 4.7 and 7.8 Hz, 1H, arom), 7.66 (d, *J* = 7.6 Hz, 1H, arom), 8.32-8.34 (m, 2H, arom). <sup>13</sup>C NMR (methanol-*d*<sub>4</sub>): δ 13.49, 25.99, 35.46, 115.83 (2C), 115.9 (2C), 125.0, 130.5, 131.2 (2C), 131.2 (2C), 135.7, 135.8, 137.4, 138.3, 141.9, 147.4, 150.0, 156.9, 157.0. HRMS C<sub>22</sub>H<sub>21</sub>NO<sub>2</sub> [M+H] calcd: 332.16451, found: 332.16485.

**4,4'-(2-methyl-3-(pyridin-3-yl)prop-1-ene-1,1-diyl)diphenol (109b).** Bis(4-hydroxyphenyl)methanone (0.32 g, 1.50 mmol) and 1-(pyridin-3-yl)propan-2-one (**114b**) (0.20 g, 1.50 mmol) in dry THF were reacted according to **Method B**. The crude was purified by flash column chromatography (petroleum ether/ethyl acetate 1:1) to give **109b** as beige solid (0.13 g, yield 28 %), mp 205-207 °C. <sup>1</sup>H NMR (acetone-*d*<sub>6</sub>): δ 1.67 (s, 3H, CH<sub>3</sub>), 3.52 (s, 2H, CH<sub>2</sub>Py), 6.77-6.80 (m, 4H, arom), 7.02 (d, *J* = 8.8 Hz, 2H, arom), 7.06 (d, *J* = 8.4 Hz, 2H, arom), 7.28 (dd, *J* = 4.8 and 7.7 Hz, 1H, arom), 7.58 (d, *J* = 8.0 Hz, 1H, arom), 8.23 (d, *J* = 8.8 Hz, 1H, arom), 8.39-8.41 (m, 1H, arom). <sup>13</sup>C NMR (acetone-*d*<sub>6</sub>): δ 19.7, 38.9, 115.3 (2C), 115.6 (2C), 124.1, 130.8, 131.0 (2C), 131.2 (2C), 135.0, 135.2, 136.4, 136.9, 140.4, 147.9, 150.5, 156.6, 156.7. HRMS C<sub>21</sub>H<sub>19</sub>NO<sub>2</sub> [M+H] calcd: 318.14886, found: 318.14866.

**4,4'-(2-ethyl-4-(pyridin-3-yl)but-1-ene-1,1-diyl)diphenol (111a).** Bis(4-hydroxyphenyl)methanone (0.07 g, 0.30 mmol) and **115a** (0.05 g, 0.30 mmol) in dry THF were reacted according to **Method B**. The crude was purified by flash column chromatography (dichloromethane/acetone 9:1) to give **111a** as beige solid (0.02 g, yield 19 %), mp 210-212 °C. <sup>1</sup>H NMR (methanol-*d*<sub>4</sub>): δ 1.02 (t, *J* = 7.4 Hz, 3H, CH<sub>3</sub>), 2.21 (q, *J* = 7.6 Hz, 2H, CH<sub>2</sub>), 2.46 (t, *J* = 7.6 Hz, 2H, CH<sub>2</sub>), 2.73 (t, *J* =

7.8 Hz, 2H, CH<sub>2</sub>), 6.64-6.69 (m, 4H, arom), 6.72-6.75 (m, 2H, arom), 6.84-6.86 (m, 2H, arom), 7.29 (dd, *J* = 4.9 and 7.8 Hz, 1H, arom), 7.46-7.48 (m, 1H, arom), 8.21 (d, *J* = 1.2 Hz, 1H, arom), 8.32 (dd, *J* = 5.2 and 1.6 Hz, 1H, arom). <sup>13</sup>C NMR (methanol-*d*<sub>4</sub>): δ 13.6, 25.9, 32.5, 33.9, 115.7 (2C), 115.7 (2C), 125.0, 131.1 (2C), 131.2 (2C), 136.1, 136.1, 138.3, 138.6, 139.7, 140.6, 147.3, 150.0, 156.7, 156.7. HRMS C<sub>23</sub>H<sub>23</sub>NO<sub>2</sub> [M+H] calcd: 346.18016, found: 346.17999.

**4,4'-(2-methyl-4-(pyridin-3-yl)but-1-ene-1,1-diyl)diphenol (111b).** Bis(4-hydroxyphenyl)methanone (0.26 g, 1.20 mmol) and **115b** (0.18 g, 1.20 mmol) in dry THF were reacted according to **Method B**. The crude was purified by flash column chromatography (petroleum ether/ethyl acetate 2:3) to give **111b** as white solid (0.18 g, yield 45 %), mp 206-207 °C. <sup>1</sup>H NMR (methanol-*d*<sub>4</sub>): δ 1.81 (s, 3H, CH<sub>3</sub>), 2.45 (t, *J* = 7.6 Hz, 2H, CH<sub>2</sub>), 2.79 (t, *J* = 7.4 Hz, 2H, CH<sub>2</sub>), 6.63-6.70 (m, 6H, arom), 6.81-6.84 (m, 2H, arom), 7.29 (dd, *J* = 4.9 and 7.8 Hz, 1H, arom), 7.50 (d, *J* = 7.6 Hz, 1H, arom), 8.24 (d, *J* = 1.6 Hz, 1H, arom), 8.33 (dd, *J* = 4.8 and 1.6 Hz, 1H, arom). <sup>13</sup>C NMR (methanol-*d*<sub>4</sub>): δ 19.9, 32.3, 37.8, 115.5 (2C), 115.6 (2C), 125.0, 131.4 (2C), 131.5 (2C), 132.3, 136.0, 136.1, 138.3, 139.6, 140.6, 147.3, 150.0, 156.7, 156.7. HRMS C<sub>22</sub>H<sub>21</sub>NO<sub>2</sub> [M+H] calcd: 332.16451, found: 332.16434.

**4,4'-(2-ethyl-4-(1H-imidazol-4-yl)but-1-ene-1,1-diyl)diphenol (112a).** Bis(4-hydroxyphenyl)methanone (0.11 g, 0.50 mmol) and **117a** (0.08 g, 0.50 mmol) in dry THF were reacted according to **Method B**. The crude was purified by flash column chromatography (gradient elution starting from petroleum ether/ethyl acetate 0.5:9.5; then ethyl acetate; then ethyl acetate/methanol 8:2) to give **112a** as orange solid (0.02 g, yield 11 %), mp 139-141 °C. <sup>1</sup>H NMR (methanol-*d*<sub>4</sub>): δ 1.01 (t, *J* = 7.4 Hz, 3H, CH<sub>3</sub>), 2.18 (q, *J* = 7.6 Hz, 2H, CH<sub>2</sub>), 2.45 (t, *J* = 7.8 Hz, 2H, CH<sub>2</sub>), 2.68 (t, *J* = 7.8 Hz, 2H, CH<sub>2</sub>), 6.64-6.70 (m, 5H, arom), 6.82 (d, *J* = 8.8 Hz, 2H, arom), 6.89 (d, *J* = 8.4 Hz, 2H, arom), 7.51 (s, 1H, arom). <sup>13</sup>C NMR (methanol-*d*<sub>4</sub>): δ 13.8, 26.0, 26.2, 32.4, 115.9 (2C), 115.9 (3C), 131.4 (2C), 131.5 (2C), 133.7, 135.9, 136.5, 136.6, 139.3, 140.3, 156.8, 156.9. HRMS C<sub>21</sub>H<sub>22</sub>N<sub>2</sub>O<sub>2</sub> [M+H] calcd: 335.17540, found: 335.17552.

**4,4'-(4-(1H-imidazol-4-yl)-2-methylbut-1-ene-1,1-diyl)diphenol (112b).** Bis(4-hydroxyphenyl)methanone (0.13 g, 0.60 mmol) and **117b** (0.08 g, 0.60 mmol) in dry THF were reacted according to **Method B**. The crude was purified by flash column chromatography (gradient elution starting from ethyl acetate; then ethyl acetate/methanol 8:2) to give **112b** as orange solid (0.03 g, yield 16 %), mp 95-99 °C. <sup>1</sup>H NMR (methanol-*d*<sub>4</sub>): 1.78 (s, 3H, CH<sub>3</sub>), 2.44 (t, *J* = 7.6 Hz, 2H, CH<sub>2</sub>), 2.73 (t, *J* = 7.6 Hz, 2H, CH<sub>2</sub>), 6.65-6.68 (m, 5H, arom), 6.78 (d, *J* = 8.8 Hz, 2H, arom), 6.87 (d, *J* = 8.8 Hz, 2H, arom), 7.54 (s, 1H, arom). <sup>13</sup>C NMR (methanol-*d*<sub>4</sub>): δ 19.8, 26.1, 36.3, 115.4 (2C), 115.6 (2C), 118.7, 131.5 (2C), 131.6 (2C), 133.0, 135.2, 136.2, 136.4, 137.5, 139.9, 156.6, 156.8. HRMS C<sub>20</sub>H<sub>20</sub>N<sub>2</sub>O<sub>2</sub> [M+H] calcd: 321.15975, found: 321.15967.

**4,4'-(2-methylbut-1-ene-1,1-diyl)diphenol (118a).** 4,4'-dihydroxybenzophenone (0.60 g, 2.80 mmol) and methylethylketone (0.25 mL, 0.20 g, 2.80 mmol) in dry THF were reacted according to **Method B**. The crude was purified by flash column chromatography (petroleum ether/ethyl acetate 3,5:1,5) to give **118a** as yellow solid (0.53 g, yield 73 %) mp 175-176 °C (lit.<sup>154</sup> mp 179-180 °C). <sup>1</sup>H NMR: δ 1.03 (t, *J* = 7.4 Hz, 3H, CH<sub>3</sub>), 1.76 (s, 3H, CH<sub>3</sub>), 2.11 (q, *J* = 7.4 Hz, 2H, CH<sub>2</sub>), 4.68 (br, 2H, 2OH), 6.72-6.74 (m, 4H, arom), 6.97-7.00 (m, 4H, arom).

**4,4'-(2-methylprop-1-ene-1,1-diyl)diphenol (118b).** 4,4'-dihydroxybenzophenone (0.60 g, 2.80 mmol) and acetone (0.20 mL, 0.16 g, 2.80 mmol) in dry THF were reacted according to **Method B**. The crude was purified by flash column chromatography (petroleum ether/ethyl acetate 4:1) to give **118b** as yellow solid (0.56 g, yield 83 %) mp 180-182 °C (lit.<sup>154</sup> mp 188-189 °C). <sup>1</sup>H NMR: δ 1.79 (s, 6H, 2 x CH<sub>3</sub>), 4.60 (br, 2H, 2OH), 6.71-6.75 (m, 4H, arom), 6.97-7.00 (m, 4H, arom).

**9-(1-(pyridin-3-yl)propylidene)-9H-xanthene-3,6-diyl bis(2,2-dimethylpropanoate) (135).** Compound **133** (0.31 g, 0.78 mmol) and propionyl pyridine (**113a**) (0.08 mL, 0.78 mmol) in dry THF were reacted according to **Method B**. The crude was purified by flash column chromatography (petroleum ether/ethyl acetate 3:2) to give compound **135** as orange solid (0.13 g, yield 33%), mp 123-125 °C. <sup>1</sup>H NMR: δ 0.96 (t, *J* = 7.4 Hz, 3H, CH<sub>3</sub>) 1.30 (s, 9H, 3 x CH<sub>3</sub>) 1.37

(s, 9H, 3 x CH<sub>3</sub>) 2.79 (q, *J* = 7.4 Hz, 2H, CH<sub>2</sub>) 6.38 (dd, *J* = 9.0 and 2.2 Hz, 1H, arom) 6.43 (d, *J* = 8.4 Hz, 1H, arom) 6.87 (d, *J* = 2.4 Hz, 1H, arom) 6.93 (dd, *J* = 8.4 and 2.0 Hz, 1H, arom) 6.96 (d, *J* = 2.4 Hz, 1H, arom) 7.20-7.24 (m, 1H, arom) 7.36-7.38 (m, 1H, arom) 7.55 (d, *J* = 8.0 Hz, 1H, arom) 8.39 (d, *J* = 2.0 Hz, 1H, arom) 8.45 (dd, *J* = 4.8 and 1.6 Hz, 1H, arom).

**9-(1-(pyridin-3-yl)butan-2-ylidene)-9H-xanthene-3,6-diyl bis(2,2-dimethylpropanoate) (136).** Compound **133** (0.30 g, 0.76 mmol) and compound **114a** (115 mg) in dry THF were reacted according to **Method B**. The crude was purified by flash column chromatography (ethyl acetate) to give compound **136** as orange solid (0.10 g, yield 24 %), mp 92-95 °C. <sup>1</sup>H NMR: δ 1.10 (t, *J* = 7.6 Hz, 3H, CH<sub>3</sub>), 1.34 (s, 9H, 3 x CH<sub>3</sub>), 1.37 (s, 9H, 3 x CH<sub>3</sub>), 2.36 (q, *J* = 7.2 Hz, 2H, CH<sub>2</sub>), 3.87 (s, 2H, CH<sub>2</sub>Py), 6.77 (dd, *J* = 8.4 and 2.3 Hz, 1H, arom), 6.88 (dd, *J* = 8.4 and 2.3 Hz, 1H, arom), 6.93-6.95 (m, 2H, arom), 7.22 (dd, *J* = 7.8 and 4.2 Hz, 1H, arom), 7.29 (d, *J* = 8.8 Hz, 1H, arom), 7.41-7.48 (m, 2H, arom), 8.45-8.51 (m, 2H, arom).

**9-(1-(pyridin-3-yl)pentan-3-ylidene)-9H-xanthene-3,6-diyl bis(2,2-dimethylpropanoate) (137).** Compound **133** (0.30 g, 0.76 mmol) and compound **115a** (0.12 g, 0.76 mmol) in dry THF were reacted according to **Method B**. The crude was purified by flash column chromatography (gradient elution starting from petroleum ether, then petroleum ether/ethyl acetate 1:1) to give compound **137** as orange solid (0.09 g, yield 22 %), mp 119-123 °C. <sup>1</sup>H NMR: δ 1.26 (t, *J* = 7.5 Hz, 3H, CH<sub>3</sub>), 1.35 (s, 9H, 3 x CH<sub>3</sub>), 1.37 (s, 9H, 3 x CH<sub>3</sub>), 2.46 (q, *J* = 7.5 Hz, 2H, CH<sub>2</sub>), 2.71 (t, *J* = 7.6 Hz, 2H, CH<sub>2</sub>), 2.78 (t, *J* = 7.5 Hz, 2H, CH<sub>2</sub>), 6.83 (dd, *J* = 8.4 and 2.3 Hz, 1H, arom), 6.89 (dd, *J* = 8.4 and 2.3 Hz, 1H, arom), 7.09-7.11 (m, 2H, arom), 7.14-7.16 (m, 2H, arom), 7.30-7.33 (m, 2H, arom), 8.19 (s, 1H, arom), 8.36 (m, 1H, arom).

**9-(1-(1H-imidazol-4-yl)propylidene)-9H-xanthene-3,6-diyl bis(2,2-dimethylpropanoate) (138).** Compound **133** (0.38 g, 0.95 mmol) and compound **116a** (0.12 g, 0.95 mmol) in dry THF were reacted according to **Method B**. The crude was purified by flash column chromatography (gradient elution starting from dichloromethane, then dichloromethane/acetone 9:1, then 8:2) to give compound

**138** as orange solid (0.09 g, yield 18 %), mp 125-128 °C. <sup>1</sup>H NMR: δ 1.15 (t, *J* = 7.2 Hz, 3H, CH<sub>3</sub>), 1.33 (s, 9H, 3 x CH<sub>3</sub>), 1.36 (s, 9H, 3 x CH<sub>3</sub>), 2.73 (q, *J* = 7.1 Hz, 2H, CH<sub>2</sub>), 6.52-6.55 (m, 1H, arom), 6.82 (s, 1H, arom), 6.84 (s, 1H, arom), 6.86-6.88 (m, 1H, arom), 6.90-6.93 (m, 2H, arom), 6.94-6.96 (m, 1H, arom), 7.52-7.54 (m, 2H, arom).

**9-(1-(1H-imidazol-4-yl)pentan-3-ylidene)-9H-xanthene-3,6-diyl bis(2,2-dimethylpropanoate) (139)**. Compound **133** (0.35 g, 0.88 mmol) and compound **117a** (0.15 g, 0.88 mmol) in dry THF were reacted according to **Method B**. The crude was purified by flash column chromatography (gradient elution starting from dichloromethane, then dichloromethane/acetone 3:2) to give compound **139** as brown/orange solid (0.07 g, yield 15 %), mp 112-115 °C. <sup>1</sup>H NMR: δ 1.20 (t, *J* = 7.4 Hz, 3H, CH<sub>3</sub>), 1.36 (s, 18H, 6 x CH<sub>3</sub>), 2.41 (q, *J* = 7.4 Hz, 2H, CH<sub>2</sub>), 2.73 (d, *J* = 7.6 Hz, 2H, CH<sub>2</sub>), 2.79 (d, *J* = 7.6 Hz, 2H, CH<sub>2</sub>), 6.59 (s, 1H, arom), 6.76-6.89 (m, 4H, arom), 7.34-7.36 (m, 2H, arom), 7.48 (s, 1H, arom).

**9-(2-(1H-imidazol-1-yl)-1-phenylethylidene)-9H-xanthene-3,6-diyl bis(2,2-dimethylpropanoate) (140)**. Compound **133** (0.50 g, 1.26 mmol) and compound **134** (0.23 g, 1.26 mmol) in dry THF were reacted according to **Method B**. The crude was purified by flash column chromatography (dichloromethane, dichloromethane/acetone 8:2, 7:3) to give compound **140** as orange solid (0.13 g, yield 19 %), mp 196-198 °C. <sup>1</sup>H NMR: δ 1.31 (s, 9H, 3 x CH<sub>3</sub>) 1.39 (s, 9H, 3 x CH<sub>3</sub>) 5.20 (s, 2H, CH<sub>2</sub>imi) 6.41 (dd, *J* = 8.4 and 2.4 Hz, 1H, arom) 6.57 (d, *J* = 8.4 Hz, 1H, arom) 6.76 (s, 1H, arom) 6.87-6.94 (m, 4H, arom) 6.97 (dd, *J* = 8.4 and 2.4 Hz, 1H, arom) 7.07 (d, *J* = 2.4 Hz, 1H, arom) 7.17-7.20 (m, 3H, arom) 7.26-7.27 (m, 1H, arom) 7.51 (d, *J* = 8.4 Hz, 1H, arom).

**4-(1-(4-bromophenyl)-2-phenylprop-1-en-1-yl)phenyl pivalate (146)**. Compound **145** (0.50 g, 1.45 mmol) and acetophenone (0.55 mL, 4.35 mmol) in dry THF were reacted according to **Method A**. The crude was purified by flash column chromatography (petroleum ether/toluene 3:2) to give **146** as beige solid (0.27 g, yield 41 %). <sup>1</sup>H NMR: δ *E/Z* 1.29 (s, 9H, 3 x CH<sub>3</sub>), 1.37 (s, 9H, 3 x CH<sub>3</sub>), 2.12 (s, 3H, CH<sub>3</sub>), 2.13 (s, 3H, CH<sub>3</sub>), 6.72-6.75 (m, 4H, arom), 6.84-6.86 (m, 2H, arom), 7.05-7.07 (m, 2H, arom), 7.11-7.15 (m, 10H, arom), 7.16-7.21 (m, 4H, arom), 7.22-7.24 (m, 2H, arom), 7.45-7.48 (m, 2H, arom).

**4-(1-(4-bromophenyl)-2-methylprop-1-en-1-yl)phenyl pivalate (147).**

Compound **145** (520 mg, 1,51 mmol) and acetone (0.32 mL, 4.53 mmol) in dry THF were reacted according to **Method A**. The crude was purified by flash column chromatography (gradient elution starting from petroleum ether, then petroleum ether/ethyl acetate 9.5:0.5) to give **147** as orange oil (0.20 g, yield 34 %). <sup>1</sup>H NMR:  $\delta$  1.34 (s, 9H, 3 x CH<sub>3</sub>), 1.78 (s, 3H, CH<sub>3</sub>), 1.79 (s, 3H, CH<sub>3</sub>), 6.96-6.99 (m, 4H, arom), 7.09 (d,  $J = 8.8$  Hz, 2H, arom), 7.39 (d,  $J = 8.4$  Hz, 2H, arom).

**4-(1-(4-bromophenyl)-2-methylbut-1-en-1-yl)phenyl pivalate (148).** Compound **145** (0.52 g, 1,51 mmol) and methylethyl ketone (0.40 mL, 4.53 mmol) in dry THF were reacted according to **Method A**. The crude was purified by flash column chromatography (gradient elution starting from petroleum ether, then petroleum ether/ethyl acetate 9.5:0.5) to give **148** as brown/yellow oil (0.25 g, yield 41 %). <sup>1</sup>H NMR:  $\delta$  *E/Z* 1.02-1.07 (m, 6H, 2 x CH<sub>3</sub>), 1.34 (s, 9H, 3 x CH<sub>3</sub>), 1.35 (s, 9H, 3 x CH<sub>3</sub>), 2.09-2.14 (m, 4H, 2 x CH<sub>2</sub>), 6.98-7.02 (m, 8H, arom), 7.10-7.12 (m, 4H, arom), 7.39-7.41 (m, 4H, arom).

**(1-(4-bromophenyl)prop-1-ene-1,2-diyl)dibenzene (155).** (4-

bromophenyl)(phenyl)methanone (1 g, 3.82 mmol) and acetophenone (0.44 mL, 3.82 mmol) in dry THF were reacted according to **Method B**. The crude was purified by flash column chromatography (petroleum ether) to give isomer **A** and **B** both as white solids (0.36 and 0.22 g, respectively; yield 43 %), mp 159-162 and 111-113 °C, respectively. Configurations of two isomers were not determined. <sup>1</sup>H NMR:  $\delta$  (**A**) 2.13 (s, 3H, CH<sub>3</sub>), 6.85-6.87 (m, 2H, arom), 7.02-7.03 (m, 3H, arom), 7.11-7.17 (m, 7H, arom), 7.47 (d,  $J = 8.4$  Hz, 2H, arom). (**B**) 2.12 (s, 3H, CH<sub>3</sub>), 6.75 (d,  $J = 8.0$  Hz, 2H, arom), 7.11-7.15 (m, 5H, arom), 7.16-7.20 (m, 2H, arom), 7.21-7.26 (m, 3H, arom), 7.32-7.38 (m, 2H, arom).

**General procedure for MOM-protection (119a,b).**

A suspension of **118a** or **118b** (1 eq) and NaH (60 %, 4.1 eq) in dry THF (15-20 mL) was stirred at room temperature for 30 min under an inert N<sub>2</sub> atmosphere. Then, chloromethylmethyl ether (4 eq) was added and the resulting mixture was stirred at room temperature for 3 hours. The reaction was quenched with aq NaHCO<sub>3</sub> (10-15

mL), the organic solvent was removed under reduced pressure and the aqueous layer was extracted with ethyl acetate (3 x 10-15 mL). The organic phase was dried and concentrated in *vacuum* and the crude compound was then purified by flash column chromatography.

**4,4'-(2-methylbut-1-ene-1,1-diyl)bis((methoxymethoxy)benzene) (119a).**

Starting from **118a** (0.53 g, 2.10 mmol), a crude compound was obtained that was purified by flash column chromatography (petroleum ether/ethyl acetate 9.5:0.5) to give **119a** as orange oil (0.44 g, yield 62 %). <sup>1</sup>H NMR: δ 1.03 (t, *J* = 7.4 Hz, 3H, CH<sub>3</sub>), 1.76 (s, 3H, CH<sub>3</sub>), 2.11 (q, *J* = 7.4 Hz, 2H, CH<sub>2</sub>), 3.47 (s, 6H, 2 x OCH<sub>3</sub>), 5.14 (s, 4H, 2 x OCH<sub>2</sub>), 6.91-6.95 (m, 4H, arom), 7.01-7.04 (m, 4H, arom).

**4,4'-(2-methylprop-1-ene-1,1-diyl)bis((methoxymethoxy)benzene) (119b).**

Starting from **118b** (0.41 g, 1.70 mmol), a crude compound was obtained that was purified by flash column chromatography (petroleum ether/ethyl acetate 8:2) to give **119b** as an oil (0.35 g, yield 62 %). <sup>1</sup>H NMR: δ 1.79 (s, 6H, 2 x CH<sub>3</sub>), 3.48 (s, 6H, 2 x OCH<sub>3</sub>), 5.16 (s, 4H, 2 x OCH<sub>2</sub>), 6.92-6.95 (m, 4H, arom), 7.02-7.04 (m, 4H, arom).

**General procedure for imidazolyl derivatives 120a,b, 149-151, 156a,b.**

A mixture of **119a,b** or **146-148** or **155** (isomers **A** and **B**) (1 eq), NBS(1 eq) and a catalytic amount of BPO in CCl<sub>4</sub> (15 mL) was refluxed for 4h. The mixture was hot filtered and the solvent was evaporated under reduced pressure. The resulting residue, without further purification, was dissolved in acetonitrile (7-10 mL) and imidazole (3 eq) was added. The reaction mixture was refluxed for 6 h under N<sub>2</sub> atmosphere, the solvent was evaporated, and the crude compound was purified by flash column chromatography with a suitable eluent.

**1-(2-(bis(4-(methoxymethoxy)phenyl)methylene)butyl)-1H-imidazole (120a).**

Starting from **119a** (0.44 g, 1.30 mmol), a crude compound was obtained that was purified by flash column chromatography (gradient elution starting from toluene/ethyl acetate 7:3, then 1:1, then ethyl acetate) to give **120a** as brown oil (0.10 g, yield 19 % two steps). <sup>1</sup>H NMR: δ 0.95 (t, *J* = 7.6 Hz, 3H, CH<sub>3</sub>), 2.03 (q, *J*

= 7.4 Hz, 2H, CH<sub>2</sub>), 3.46 (s, 6H, 2 x OCH<sub>3</sub>), 4.63 (s, 2H, CH<sub>2</sub>imi), 5.14 (s, 4H, 2 x OCH<sub>2</sub>), 6.88 (s, 1H, imi), 6.95-6.99 (m, 4H, arom), 7.04-7.07 (m, 5H, arom), 7.45 (s, 1H, imi).

**1-(3,3-bis(4-(methoxymethoxy)phenyl)-2-methylallyl)-1H-imidazole (120b).** Starting from **119b** (0.35 g, 1.10 mmol), a crude compound was obtained that was purified by flash column chromatography (gradient elution starting from toluene/ethyl acetate 9:1, then 7:3, then 1:1, then ethyl acetate) to give **120b** as brown oil (0.08 g, yield 19 % two steps) mp 231-232 °C. <sup>1</sup>H NMR: δ 1.71 (s, 3H, CH<sub>3</sub>), 3.28 (s, 6H, 2 OCH<sub>3</sub>), 4.60 (s, 2H, CH<sub>2</sub>imi), 5.24 (s, 4H, 2 x OCH<sub>3</sub>), 6.89 (s, 1H, imi), 6.95-6.97 (m, 4H, arom), 7.03-7.05 (m, 5H, arom), 7.47 (s, 1H, imi).

**4-(1-(4-bromophenyl)-3-(1H-imidazol-1-yl)-2-phenylprop-1-en-1-yl)phenyl pivalate (149).** Starting from compound **146** (0.27 g, 0.60 mmol) a crude compound was obtained that was purified by flash column chromatography (gradient elution starting from petroleum ether/ethyl acetate 1:4, then ethyl acetate) to give **149** as grey solid (0.15 g, yield 48 %). <sup>1</sup>H NMR: δ *E/Z* 1.28 (s, 9H, 3 x CH<sub>3</sub>), 1.37 (s, 9H, 3 x CH<sub>3</sub>), 4.85 (s, 2H, CH<sub>2</sub>imi), 4.86 (s, 2H, CH<sub>2</sub>imi), 6.70 (s, 2H, arom), 6.75-6.78 (m, 4H, arom), 6.87-6.89 (m, 2H, arom), 6.94-6.99 (m, 6H, arom), 7.11-7.17 (m, 12H, arom), 7.22-7.27 (m, 4H, arom), 7.54 (d, *J* = 8.4 Hz, 2H, arom).

**4-(1-(4-bromophenyl)-3-(1H-imidazol-1-yl)-2-methylprop-1-en-1-yl)phenyl pivalate (150).** Starting from compound **147** (0.20 g, 0.52 mmol) a crude compound was obtained that was purified by flash column chromatography (petroleum ether/ethyl acetate 1:4) to give **150** as brown/yellow oil (0.09 g, yield 38 %). <sup>1</sup>H NMR: δ *E/Z* 1.33 (s, 9H, 3 x CH<sub>3</sub>), 1.34 (s, 9H, 3 x CH<sub>3</sub>), 1.67 (s, 3H, CH<sub>3</sub>), 1.69 (s, 3H, CH<sub>3</sub>), 4.57 (s, 2H, CH<sub>2</sub>imi), 4.58 (s, 2H, CH<sub>2</sub>imi), 6.85 (s, 2H, arom), 6.99-7.03 (m, 4H, arom), 7.04-7.06 (m, 2H, arom), 7.07-7.09 (m, 4H, arom), 7.10-7.13 (m, 2H, arom), 7.14-7.16 (m, 2H, arom), 7.43 (d, *J* = 8.4 Hz, 2H, arom), 7.46-7.48 (m, 4H, arom).

**4-(2-((1H-imidazol-1-yl)methyl)-1-(4-bromophenyl)but-1-en-1-yl)phenyl pivalate (151).** Starting from compound **148** (0.25 g, 0.62 mmol) a crude compound was obtained that was purified by flash column chromatography (gradient elution starting from petroleum ether/ethyl acetate 9.5:0.5, then 2:8) to give **151** as brown/yellow oil (0.09 g, yield 31 %). <sup>1</sup>H NMR: δ *E/Z* 0.92-0.97 (m, 6H, 2 x CH<sub>3</sub>),

1.98-2.04 (m, 4H, 2 x CH<sub>2</sub>), 4.60 (s, 2H, CH<sub>2</sub>imi), 4.62 (s, 2H, CH<sub>2</sub>imi), 6.85 (s, 2H, arom), 7.00-7.06 (m, 10H, arom), 7.11-7.15 (m, 4H, arom), 7.41-7.46 (m, 6H, arom).

**1-(3-(4-bromophenyl)-2,3-diphenylallyl)-1H-imidazole (156).** Starting from compound **155** (0.12 g, 0.35 mmol) a crude compound was obtained that was purified by flash column chromatography (petroleum ether/ethyl acetate 8:2) to give **156a** and **156b** both as white solids (0.04 and 0.04 g, respectively; yield 55 %), mp 140-144 and 86-89 °C, respectively. <sup>1</sup>H NMR: δ (**156a**) 4.87 (s, 2H, CH<sub>2</sub>imi), 6.72 (s, 1H, imi), 6.88-6.91 (m, 2H, arom), 6.97-7.00 (m, 3H, arom), 7.05-7.07 (m, 3H, arom), 7.13-7.16 (m, 5H, arom), 7.31 (s, 1H, imi), 7.54 (d, *J* = 8.4 Hz, 2H). (**156b**) 4.86 (s, 2H, CH<sub>2</sub>imi), 6.72 (s, 1H, imi), 6.78 (d, *J* = 8.4 Hz, 2H, aro), 6.94-7.00 (m, 3H, arom), 7.14-7.21 (m, 5H, arom), 7.23-7.25 (m, 2H, arom), 7.30 (s, 1H, imi), 7.36-7.45 (m, 3H, arom).

#### **General procedure for MOM deprotection (110a,b).**

To a solution of **120a** or **120b** in methanol (5 mL), 37 % HCl (0.05 mL) was added. The reaction mixture was stirred at room temperature for 12 h and then the solvent was evaporated to dryness. The residue was dissolved in H<sub>2</sub>O (10 mL) and neutralized with saturated solution of NaHCO<sub>3</sub>. The formed precipitate was collected by *vacuum* filtration to afford compound **110a** or **110b**.

**4,4'-(2-((1H-imidazol-1-yl)methyl)but-1-ene-1,1-diyl)diphenol (110a).** Starting from **120a** (0.10 g, 0.20 mmol), **110a** was obtained as light-yellow solid (0.06 g, yield 83 %), mp > 250 °C. <sup>1</sup>H NMR (acetone-*d*<sub>6</sub>): δ 0.95 (t, *J* = 7.4 Hz, 3H, CH<sub>3</sub>), 2.00 (q, *J* = 7.4 Hz, 2H, CH<sub>2</sub>), 4.76 (s, 2H, CH<sub>2</sub>imi), 6.79-6.84 (m, 4H, arom), 6.98 (s, 1H, imi), 7.03-7.09 (m, 5H, arom), 7.65 (s, 1H, imi). <sup>13</sup>C NMR (acetone-*d*<sub>6</sub>): δ 13.3, 24.0, 47.9, 115.8 (2C), 115.9 (2C), 129.2, 130.7 (2C), 131.0 (2C), 131.3, 132.5, 134.1, 134.4, 134.5, 143.6, 157.2, 157.4. HRMS C<sub>20</sub>H<sub>20</sub>N<sub>2</sub>O<sub>2</sub> [M+H] calcd: 321.15975, found: 321.15993.

**4,4'-(3-(1H-imidazol-1-yl)-2-methylprop-1-ene-1,1-diyl)diphenol (110b).** Starting from **120b**, (0.08 g, 0.20 mmol), **110b** was obtained as orange solid (0.03

g, yield 30 %), mp > 250 °C. <sup>1</sup>H NMR (acetone-*d*<sub>6</sub>): δ 1.64 (s, 3H, CH<sub>3</sub>), 4.69 (s, 2H, CH<sub>2</sub>imi), 6.79 (d, *J* = 8.6 Hz, 2H, arom), 6.83 (d, *J* = 8.5 Hz, 2H, arom), 6.93 (s, 1H, imi), 6.99-7.02 (m, 3H, arom), 7.06 (d, *J* = 8.5 Hz, 2H, arom), 7.51 (s, 1H, imi), 8.39 (br, 1H, OH), 8.45 (br, 1H, OH). <sup>13</sup>C NMR (acetone-*d*<sub>6</sub>): δ 17.8, 51.1, 115.6 (2C), 115.9 (2C), 119.3, 128.5, 129.8, 131.3 (2C), 131.3 (2C), 134.2, 134.5, 138.2, 142.7, 157.2, 157.4. HRMS C<sub>19</sub>H<sub>18</sub>N<sub>2</sub>O<sub>2</sub> [M+H] calcd: 307.14410, found: 307.14464.

### **General procedure for the synthesis of chalcones 121-122a,b.**

A solution of the selected aldehyde (1 eq), piperidine (1.8 eq) and acetic acid (1.6 eq) in acetone (10 mL) or methylethylketone (10-20 mL) was stirred at room temperature until TLC indicated complete conversion of the starting material. The solvent was evaporated to dryness and the obtained crude compound was purified by flash column chromatography with a suitable eluent.

**(E)-1-(pyridin-3-yl)pent-1-en-3-one (121a).** Starting from 3-pyridinecarboxyaldehyde (1.00 g, 0.88 mL, 9.30 mmol) in methylethylketone, a crude was obtained that was purified by flash column chromatography (toluene/acetone 6:4) to give **121a** as brown oil (0.48 g, yield 32 %). <sup>1</sup>H NMR: δ 1.18 (t, *J* = 7.2 Hz, 3H, CH<sub>3</sub>), 2.72 (q, *J* = 7.2 Hz, 2H, CH<sub>2</sub>), 6.81 (d, *J* = 16.4 Hz, 1H, CH=C), 7.34-7.37 (m, 1H, arom), 7.55 (d, *J* = 16.4 Hz, 1H, CH=C), 7.88 (d, *J* = 8.0 Hz, 1H, arom), 8.62-8.64 (m, 1H, arom), 8.78 (s, 1H, arom).

**(E)-4-(pyridin-3-yl)but-3-en-2-one (121b).** Starting from 3-pyridinecarboxyaldehyde (0.50 g, 0.44 mL, 4.70 mmol) in acetone, a crude was obtained that was purified by flash column chromatography (gradient elution starting from petroleum ether/ethyl acetate 1:9, then 0.5:9.5, then ethyl acetate) to give **121b** as brown oil (0.38 g, yield 55 %). <sup>1</sup>H NMR: δ 2.38 (s, 3H, CH<sub>3</sub>), 6.76 (d, *J* = 16.4 Hz, 1H, CH=C), 7.30-7.46 (m, 1H, arom), 7.48 (d, *J* = 16.4 Hz, 1H, CH=C), 7.84 (d, *J* = 8.0 Hz, 1H, arom), 8.59 (d, *J* = 4.4 Hz, 1H, arom), 8.74 (s, 1H, arom).

**(E)-1-(1H-imidazol-4-yl)pent-1-en-3-one (122a).** Starting from 1H-imidazole-4-carboxyaldehyde (0.50 g, 5.20 mmol) in methylethylketone, a crude compound was obtained that was purified by flash column chromatography

(dichloromethane/methanol 8:2) to give **122a** as brown oil (0.70 g, yield 89 %). <sup>1</sup>H NMR (methanol-*d*<sub>4</sub>): δ 1.14 (t, *J* = 7.2 Hz, 3H, CH<sub>3</sub>), 2.75 (q, *J* = 7.2 Hz, 2H, CH<sub>2</sub>), 6.88 (d, *J* = 16.8 Hz, 1H, CH=C), 7.53 (d, *J* = 16.0 Hz, 1H, CH=C), 7.92 (s, 1H, imi), 9.04 (s, 1H, imi).

**(E)-4-(1H-imidazol-4-yl)but-3-en-2-one (122b)**. Starting from 1H-imidazole-4-carboxyaldehyde (0.50 g, 5.20 mmol) in acetone, a crude compound was obtained that was purified by flash column chromatography (acetone + 0.5 % NH<sub>3</sub>) to give **122b** as brown oil (0.24 g, yield 34 %). <sup>1</sup>H NMR: δ 2.31 (s, 3H, CH<sub>3</sub>), 6.75 (d, *J* = 16.0 Hz, 1H, CH=C), 7.34 (s, 1H, imi), 7.47 (d, *J* = 16.0 Hz, 1H, CH=C), 7.72 (s, 1H, imi).

#### **General procedure for double bond reduction (115a,b and 117a,b).**

A mixture of **121a,b** or **122a,b** (1 eq) and Zn (5 eq) in acetic acid (10-15 mL) was heated to reflux for 3 h. The reaction mixture was poured in water (10-15 mL), basified with 2M NaOH solution and extracted with dichloromethane (3 x 10 mL). The organic phase was washed with NaHCO<sub>3</sub> saturated solution (3 x 10 mL), dried over anhydrous Na<sub>2</sub>SO<sub>4</sub> and concentrated *in vacuum*. The crude compound, when necessary, was purified by flash column chromatography with a suitable eluent.

**1-(pyridin-3-yl)pentan-3-one (115a)**. Starting from **121a** (0.48 g, 2.80 mmol), a crude compound was obtained and was purified by column chromatography (toluene/acetone 7:3) to give **115a** as brown oil (0.29 g, yield 62 %). <sup>1</sup>H NMR: δ 1.04 (t, *J* = 7.4 Hz, 3H, CH<sub>3</sub>), 2.41 (q, *J* = 7.4 Hz, 2H, CH<sub>2</sub>), 2.74 (t, *J* = 7.4 Hz, 2H, CH<sub>2</sub>), 2.90 (t, *J* = 7.4 Hz, 2H, CH<sub>2</sub>), 7.18-7.22 (m, 1H, arom), 7.51 (d, *J* = 8.0 Hz, 1H, arom), 8.44-8.46 (m, 2H, arom).

**4-(pyridin-3-yl)butan-2-one (115b)**. Starting from **121b** (0.41 g, 2.80 mmol), a crude compound was obtained that was used without further purification as brown oil (0.18 g, yield 43 %). <sup>1</sup>H NMR: δ 2.15 (s, 3H, CH<sub>3</sub>), 2.79 (t, *J* = 7.2 Hz, 2H, CH<sub>2</sub>), 2.92 (t, *J* = 7.4 Hz, 2H, CH<sub>2</sub>), 7.27-7.29 (m, 1H, arom), 7.61 (d, *J* = 7.6 Hz, 1H, arom), 8.46-8.48 (m, 2H, arom).

**1-(1H-imidazol-4-yl)pentan-3-one (117a).** Starting from **122a** (0.35 g, 2.30 mmol), a crude compound was obtained and was purified by column chromatography (dichlorometane/methanol 9:1) to give **117a** as brown oil (0.15 g, 43 %). <sup>1</sup>H NMR: 1.06 (t, *J* = 7.4 Hz, 3H, CH<sub>3</sub>), 2.45 (q, *J* = 7.4 Hz, 2H, CH<sub>2</sub>), 2.82 (t, *J* = 6.0 Hz, 2H, CH<sub>2</sub>), 2.89 (t, *J* = 6.0 Hz, 2H, CH<sub>2</sub>), 4.17 (br, 1H, NH), 6.82 (s, 1H, imi), 7.66 (s, 1H, imi).

**4-(1H-imidazol-4-yl)butan-2-one (117b).** Starting from **122b** (0.18 g, 1.30 mmol), a crude compound was obtained that was used without further purification as brown oil (0.12 g, 66 %). <sup>1</sup>H NMR: δ 2.16 (s, 3H, CH<sub>3</sub>), 2.78-2.86 (m, 4H, 2 x CH<sub>2</sub>), 6.80 (s, 1H, imi), 7.65 (s, 1H, imi).

#### **General procedure for pivaloyl protection (133 and 145).**

A suspension of compound **132** or 4-bromo-4'-hydroxybenzophenone (1 eq) and 60 % NaH (3.2 or 1.6eq, respectively) in dry THF (3-5 mL) was stirred at room temperature for 10 min under N<sub>2</sub> atmosphere. Pivaloyl chloride (3 or 1.5 eq, respectively) was added and the mixture was stirred at room temperature for 5h. The reaction was quenched with H<sub>2</sub>O (3-5 mL) and extracted with ethyl acetate (3 x 5 mL). The organic layer was evaporated to dryness, the residue was suspended in 2N NaOH and extracted with ethyl acetate. The organic phase was dried over Na<sub>2</sub>SO<sub>4</sub> and dried under *vacuum* to give the desired compounds.

**9-oxo-9H-xanthene-3,6-diyl bis(2,2-dimethylpropanoate) (133).** Starting from **132** (0.92 g, 4.03 mmol) **133** was obtained as grey solid (1.28 g, yield 80 %), mp 156-158 °C. <sup>1</sup>H NMR: δ 1.40 (s, 18H, 6 x CH<sub>3</sub>) 7.12 (dd, *J* = 8.4 and 2.0 Hz, 2H, arom) 7.26 (s, 2H, arom) 8.35 (d, *J* = 8.4 Hz, 2H, arom).

**4-(4-bromobenzoyl)phenyl pivalate (145).** Starting from 4-bromo-4'-hydroxybenzophenone (0.63 g, 2.28 mmol) compound **145** was obtained as grey solid (0.69 g, yield 84 %), mp > 250 °C. <sup>1</sup>H NMR: δ 1.38 (s, 9H, 3 x CH<sub>3</sub>), 7.19 (d, *J* = 8.4 Hz, 2H, arom), 7.62-7.66 (m, 4H, arom), 7.82 (d, *J* = 8.4 Hz, 2H).

**General procedure for hydrolysis (123-126, 128, 129, 141-144).**

To a solution of compound **135-140**, **152-154** and **157a,b** (1eq) in methanol (4-5 mL), 10 % LiOH (7-10 mL) was added and the reaction mixture was stirred at room temperature for 2h. The solvent was evaporated under reduced pressure and the residue was dissolved in NH<sub>4</sub>Cl saturated solution (5 mL) and extracted with ethyl acetate (3 x 5 mL). The organic phase was dried over Na<sub>2</sub>SO<sub>4</sub> and dried under *vacuum* to give a crude compound that was purified by flash column chromatography with a suitable eluent.

**9-(1-(pyridin-3-yl)propylidene)-9H-xanthene-3,6-diol (123).** Starting from **135** (0.13 g, 0.26 mmol), a crude compound was obtained that was purified by flash column chromatography (petroleum ether/ethyl acetate 3:2) to give **123** as orange solid (0.03 g, yield 35 %), mp 238-240 °C. <sup>1</sup>H NMR (acetone-*d*<sub>6</sub>): δ 0.96 (t, *J* = 7.4 Hz, 3H, CH<sub>3</sub>) 2.80 (q, *J* = 7.4 Hz, 2H, CH<sub>2</sub>) 6.17 (dd, *J* = 8.6 e 2.2 Hz, 1H, arom) 6.30 (d, *J* = 8.8 Hz, 1H, arom) 6.58 (d, *J* = 2.4 Hz, 1H, arom) 6.70 (d, *J* = 2.8 Hz, 1H, arom) 6.75 (dd, *J* = 8.6 e 2.2 Hz, 1H, arom) 7.31-7.34 (m, 1H, arom) 7.50 (d, *J* = 8.4 Hz, 1H, arom) 7.53-7.56 (m, 1H, arom) 8.28 (d, *J* = 1.6 Hz, 1H, arom) 8.45 (dd, *J* = 4.8 e 1.8 Hz, 1H, arom). <sup>13</sup>C NMR (acetone-*d*<sub>6</sub>): δ 13.73, 26.78, 103.43, 103.89, 111.23, 111.36, 118.98, 119.05, 124.95, 126.76, 129.00, 129.36, 134.03, 138.35, 138.73, 147.86, 150.34, 156.88, 156.97, 158.89, 158.06.

**9-(1-(pyridin-3-yl)butan-2-ylidene)-9H-xanthene-3,6-diol (124).** Starting from **136** (0.95 g, 0.18 mmol) a crude compound was obtained that was purified by flash column chromatography (gradient elution starting from dichloromethane, then dichloromethane/acetone 4:1, then 3:2) to give **124** as orange solid (0.04 g, yield 61 %), mp 220-223 °C. <sup>1</sup>H NMR (methanol-*d*<sub>4</sub>): δ 1.09 (t, *J* = 7.5 Hz, 3H, CH<sub>3</sub>), 2.33 (q, *J* = 7.5 Hz, 2H, CH<sub>2</sub>), 3.90 (s, 2H, CH<sub>2</sub>Py), 6.50 (dd, *J* = 8.4 and 2.5 Hz, 1H, arom), 6.58-6.61 (m, 3H, arom), 7.18 (d, *J* = 8.5 Hz, 1H, arom), 7.29-7.35 (m, 2H, arom), 7.62 (d, *J* = 7.8 Hz, 1H, arom), 8.32-8.38 (m, 2H, arom). <sup>13</sup>C NMR (methanol-*d*<sub>4</sub>): δ 14.2, 26.7, 36.0, 103.9, 104.1, 111.1, 111.2, 119.3, 119.5, 125.2, 126.8, 128.5, 128.9, 133.7, 138.2, 138.7, 147.7, 150.1, 156.5, 156.7, 158.5, 158.6.

**9-(1-(pyridin-3-yl)pentan-3-ylidene)-9H-xanthene-3,6-diol (125).** Starting from **137** (0.09 g, 0.16 mmol) a crude compound was obtained that was purified by flash

column chromatography (gradient elution starting from dichloromethane, then dichloromethane/acetone 4:1) to give **125** as orange solid (0.04 g, yield 69 %), mp 220-224 °C. <sup>1</sup>H NMR (methanol-*d*<sub>4</sub>): δ 1.25 (t, *J* = 7.5 Hz, 3H, CH<sub>3</sub>), 2.41 (q, *J* = 7.5 Hz, 2H, CH<sub>2</sub>), 2.74 (t, *J* = 7.5 Hz, 2H, CH<sub>2</sub>), 2.81 (d, *J* = 7.5 Hz, 2H, CH<sub>2</sub>), 6.43 (dd, *J* = 9.2 and 2.5 Hz, 2H, arom), 6.49-6.52 (m, 2H, arom), 7.00 (d, *J* = 8.3 Hz, 1H, arom), 7.09-7.11 (m, 1H, arom), 7.19-7.21 (m, 2H, arom), 8.02 (s, 1H, arom), 8.19-8.21 (m, 1H, arom). <sup>13</sup>C NMR (methanol-*d*<sub>4</sub>): δ 13.9, 26.2, 32.3, 33.6, 103.7, 104.0, 111.2, 111.3, 119.1, 119.2, 125.2, 126.9, 128.4, 129.0, 133.6, 138.2, 138.6, 147.5, 150.2, 156.4, 156.6, 158.6, 158.7.

**9-(1-(1H-imidazol-4-yl)propylidene)-9H-xanthene-3,6-diol (126)**. Starting from **138** (0.35 g, 0.17 mmol) a crude compound was obtained that was purified by flash column chromatography (gradient elution starting from dichloromethane, then dichloromethane/acetone 1:1) to give **126** as orange solid (0.03 g, yield 55 %), mp > 250 °C. <sup>1</sup>H NMR (methanol-*d*<sub>4</sub>): δ 1.03 (t, *J* = 7.4 Hz, 3H, CH<sub>3</sub>), 2.69 (q, *J* = 7.4 Hz, 2H, CH<sub>2</sub>), 6.19 (dd, *J* = 8.6 and 2.4 Hz, 1H, arom), 6.48-6.52 (m, 2H, arom), 6.59 (d, *J* = 2.4, 1H, arom), 6.63 (dd, *J* = 8.4 and 2.4 Hz, 1H, arom), 6.68 (s, 1H, arom), 7.40 (d, *J* = 8.5 Hz, 1H, arom), 7.62 (s, 1H, arom). <sup>13</sup>C NMR (methanol-*d*<sub>4</sub>): δ 13.8, 28.9, 103.3, 103.8, 111.1 (2C), 117.9, 118.8, 127.0, 128.1, 129.2, 129.6, 135.5, 155.9, 156.7, 158.31(2C), 159.0 (2C).

**9-(1-(1H-imidazol-4-yl)pentan-3-ylidene)-9H-xanthene-3,6-diol (128)**. Starting from **139** (0.10 g, 0.19 mmol) a crude compound was obtained that was purified by flash column chromatography (gradient elution starting from dichloromethane, then dichloromethane/acetone 1:9) to give **128** as orange solid (0.03 g, yield 45 %), mp 228-231 °C. <sup>1</sup>H NMR (methanol-*d*<sub>4</sub>): δ 1.16 (t, *J* = 7.4 Hz, 3H, CH<sub>3</sub>), 2.43 (q, *J* = 7.4 Hz, 2H, CH<sub>2</sub>), 2.66-2.84 (m, 4H, 2 x CH<sub>2</sub>), 6.47-6.60 (m, 4H, arom), 6.67 (s, 1H, arom), 7.16 (d, *J* = 8.6 Hz, 1H, arom), 7.21 (d, *J* = 8.4 Hz, 1H, arom), 7.57 (s, 1H, arom). <sup>13</sup>C NMR (methanol-*d*<sub>4</sub>): δ 14.3, 26.2, 29.5, 36.5, 103.8, 103.9, 110.9, 111.1, 119.7, 119.8, 122.7, 124.9, 128.9, 129.0, 135.8, 156.5, 156.5, 158.0, 158.1, 159.6, 159.7.

**9-(2-(1H-imidazol-1-yl)-1-phenylethylidene)-9H-xanthene-3,6-diol (129)**. Starting from **140** (0.08 g, 0.14 mmol), a crude compound was obtained that was purified by flash column chromatography (gradient elution starting from

dichloromethane, then dichloromethane/methanol 9.75:0.25) to give **129** as orange solid (0.03 g, yield 56 %), mp > 250 °C. <sup>1</sup>H NMR (acetone-*d*<sub>6</sub>): δ 5.36 (s, 2H, CH<sub>2</sub>imi) 6.16 (dd, *J* = 8.4 and 2.8 Hz, 1H, arom) 6.39 (d, *J* = 8.8 Hz, 1H, arom) 6.62 (d, *J* = 2.8 Hz, 1H, arom) 6.73 (s, 1H, arom) 6.76-6.79 (m, 2H, arom) 6.84 (s, 1H, arom) 6.97-7.00 (m, 2H, arom) 7.15-7.18 (m, 3H, arom) 7.25 (s, 1H, arom) 7.51 (d, *J* = 9.2 Hz, 1H, arom). <sup>13</sup>C NMR (acetone-*d*<sub>6</sub>): δ 51.2, 103.9, 104.0, 111.1, 111.2, 119.6, 119.8, 123.1, 124.7, 125.0, 126.7, 127.9, 128.6, 128.7, 128.8, 129.9, 130.0, 136.0, 154.3, 154.5, 158.6, 158.7.

**(2E)-3-(4-(1-(4-hydroxyphenyl)-3-(1H-imidazol-1-yl)-2-phenylprop-1-en-1-yl)phenyl)acrylic acid (141)**. Starting from **152** (0.10 g, 0.19 mmol), a crude compound was obtained that was purified by flash column chromatography (gradient elution starting from dichloromethane/methanol 9.5:0.5, then 8:2) to give **141** as light-yellow solid (0.04 g, yield 50 %). *E/Z* <sup>1</sup>H NMR (acetone-*d*<sub>6</sub>): δ 4.98 (s, 2H, CH<sub>2</sub>imi), 5.02 (s, 2H, CH<sub>2</sub>imi), 6.38 (d, *J* = 16.4 Hz, 1H, CH=C), 6.46 (d, *J* = 8.8 Hz, 2H, arom), 6.53-6.57 (m, 2H, arom), 6.76 (d, *J* = 8.4 Hz, 2H, arom), 6.84-6.86 (m, 3H, arom), 6.94 (d, *J* = 8.4 Hz, 2H, arom), 6.98-7.01 (m, 2H, arom), 7.07-7.15 (m, 10H, arom), 7.18-7.25 (m, 4H arom), 7.32 (d, *J* = 8.4 Hz, 2H, arom), 7.37-7.44 (m, 4H, arom), 7.60 (d, *J* = 8 Hz, 2H, arom). <sup>13</sup>C NMR (acetone-*d*<sub>6</sub>): δ 51.2, 51.3, 115.4, 116.3, 119.3, 119.4, 119.6, 119.7, 127.6, 127.8, 128.2, 128.8, 128.9, 129.2, 129.4, 130.5, 130.6, 131.3, 131.7, 132.5, 133.4, 133.5, 133.7, 134.7, 135.9, 138.0, 138.1, 140.5, 140.7, 144.5, 144.6, 144.7, 144.8, 144.9, 145.2, 145.4, 157.2, 158.0, 159.2, 159.7.

**(2E)-3-(4-(1-(4-hydroxyphenyl)-3-(1H-imidazol-1-yl)-2-methylprop-1-en-1-yl)phenyl)acrylic acid (142)**. Starting from **153** (0.06 g, 0.13 mmol), a crude compound was obtained that was purified by flash column chromatography (gradient elution starting from dichloromethane/methanol 9:1, then 8:2) to give **142** as white solid (0.03 g, yield 64 %). *E/Z* <sup>1</sup>H NMR (methanol-*d*<sub>4</sub>): δ 1.64 (s, 3H, CH<sub>3</sub>), 1.67 (s, 3H, CH<sub>3</sub>), 4.69 (s, 2H, CH<sub>2</sub>imi), 4.73 (s, 2H, CH<sub>2</sub>imi), 6.47-6.52 (m, 2H), 6.72-6.80 (m, 4H, arom), 6.97-7.06 (m, 8H, arom), 7.17 (d, *J* = 7.6 Hz, 2H, arom), 7.22 (d, *J* = 8.0 Hz, 2H, arom), 7.48-7.57 (m, 6H, arom), 7.63-7.65 (m, 2H, arom). <sup>13</sup>C NMR (methanol-*d*<sub>4</sub>): δ 13.8, 13.9, 51.1, 51.3, 116.0, 116.1, 116.5, 120.5, 120.7, 120.9, 127.5, 129.3, 129.4, 130.7, 130.8, 131.1, 131.3, 131.7, 131.8, 132.6, 133.0,

133.2, 133.5, 134.2, 134.7, 135.0, 135.5, 135.6, 144.5, 144.6, 144.7, 144.9, 145.0, 145.5, 157.8, 158.0.

**(2E)-3-(4-(2-((1H-imidazol-1-yl)methyl)-1-(4-hydroxyphenyl)but-1-en-1-yl)phenyl)acrylic acid (143).** Starting from **154** (0.06 g, 0.13 mmol), a crude compound was obtained that was purified by flash column chromatography (gradient elution starting from dichloromethane/methanol 9:1, then 8:2) to give **143** as white solid (0.04 g, yield 82 %). *E/Z* <sup>1</sup>H NMR (methanol-*d*<sub>4</sub>): δ 0.94-0.99 (m, 6H, 2 x CH<sub>3</sub>), 1.98-2.08 (m, 4H, 2 x CH<sub>2</sub>), 4.74 (s, 2H, CH<sub>2</sub>imi), 4.79 (s, 2H, CH<sub>2</sub>imi), 6.46-6.50 (m, 2H), 6.74-6.79 (m, 4H, arom), 7.00-7.05 (m, 6H, arom), 7.10-7.12 (m, 2H, arom), 7.22-7.26 (m, 4H, arom), 7.55-7.59 (m, 5H, arom), 7.63 (s, 1H, arom), 7.70-7.72 (m, 2H, arom). <sup>13</sup>C NMR (methanol-*d*<sub>4</sub>): 13.3, 24.5, 24.6, 51.2, 52.3, 116.0, 116.1, 116.2, 116.4, 120.5, 120.8, 120.9, 127.7, 129.0, 129.2, 130.4, 130.6, 131.0, 131.2, 131.7, 131.8, 132.6, 133.0, 133.3, 133.7, 134.2, 134.7, 135.0, 135.4, 135.5, 144.3, 144.4, 144.6, 144.9, 145.1, 145.4, 157.8, 158.0.

**(E)-3-(4-((Z)-3-(1H-imidazol-1-yl)-1,2-diphenylprop-1-en-1-yl)phenyl)acrylic acid (144a).** Starting from **157a** (0.06 g, 0.14 mmol), a crude compound was obtained that was purified by flash column chromatography (gradient elution starting from dichloromethane/methanol 9.75:0.25, then 8:2, then 5:5) to give **144a** as a white semisolid (0.04 g, yield 70 %). <sup>1</sup>H NMR (methanol-*d*<sub>4</sub>): δ 5.02 (s, 2H, CH<sub>2</sub>imi), 6.55 (d, *J* = 16.0 Hz, 1H, CH=C), 6.86 (s, 1H, imi), 6.95-7.00 (m, 2H, arom), 7.02 (s, 1H, imi), 7.04-7.12 (m, 8H, arom), 7.37 (d, *J* = 8.1 Hz, 2H, arom), 7.41 (s, 1H, imi), 7.51 (d, *J* = 16.0 Hz, 1H, CH=C), 7.62 (d, *J* = 8.1 Hz, 2H arom). <sup>13</sup>C NMR (methanol-*d*<sub>4</sub>): δ 51.7, 111.4, 120.5, 125.6, 125.9, 128.2 (2C), 128.7 (2C), 129.0 (2C), 129.1 (2C), 130.7 (2C), 130.8 (2C), 131.3 (2C), 136.0, 136.4, 138.4, 140.3, 141.4, 142.7, 144.0, 145.5.

**(E)-3-(4-((E)-3-(1H-imidazol-1-yl)-1,2-diphenylprop-1-en-1-yl)phenyl)acrylic acid (144b).** Starting from **157b** (0.08 g, 0.19 mmol), a crude compound was obtained that was purified by flash column chromatography (gradient elution starting from dichloromethane/methanol 9.75:0.25, then 8:2, then 5:5) to give **144b** as a white semisolid (0.05 g, yield 65 %). <sup>1</sup>H NMR (methanol-*d*<sub>4</sub>): δ 4.99 (s, 2H,

CH<sub>2</sub>imi), 6.36 (d, *J* = 16.0 Hz, 1H, CH=C), 6.85 (s, 1H, imi), 6.95 (d, *J* = 8.2 Hz, 2H, arom), 6.99 (s, 1H, imi), 7.04-7.15 (m, 5H, arom), 7.22 (d, *J* = 8.4 Hz, 2H, arom), 7.30 (s, 1H, imi), 7.34-7.38 (m, 4H, arom), 7.44-7.48 (m, 2H). <sup>13</sup>C NMR (methanol-*d*<sub>4</sub>): δ 51.8, 111.3, 120.6, 125.2, 127.9 (2C), 128.3, 128.5, 128.9, 129.3 (2C), 129.9 (2C), 130.2 (2C), 130.8 (2C), 131.7 (2C), 135.3, 136.2, 138.4, 140.2, 141.4, 142.6, 143.9, 145.4.

### **General procedure for the synthesis of acrylate derivatives 152-154 and 157a,b.**

To a solution of compound **149-152** (1eq) in DMF (dimethylformamide) (2-3 mL) triethylamine (5eq), methyl acrylate (2eq) and Pd(PPh<sub>3</sub>)<sub>2</sub>Cl<sub>2</sub> (10 mol %) were added and the mixture was reacted for 1 h at 120 °C under microwave irradiation. After cooling, the mixture was diluted with H<sub>2</sub>O (5 mL) and extracted with ethyl acetate (3 x 5mL). The organic layer was washed with brine (3 x 5 mL), dried over Na<sub>2</sub>SO<sub>4</sub> and the solvent was evaporated under *vacuum* to give a crude product purified by flash column chromatography with a suitable eluent.

**Methyl (2E)-3-(4-(3-(1H-imidazol-1-yl)-2-phenyl-1-(4-(pivaloyloxy)phenyl)prop-1-en-1-yl)phenyl)acrylate (152).** Starting from **149** (0.15 g, 0.29 mmol), a crude compound was obtained that was purified by flash column chromatography (dichloromethane/acetone 9:1) to give **152** as yellow semisolid (0.10 g, yield 66 %). <sup>1</sup>H NMR: δ *E/Z* 1.28 (s, 9H, 3 x CH<sub>3</sub>), 1.37 (s, 9H, 3 x CH<sub>3</sub>), 3.76 (s, 3H, OCH<sub>3</sub>), 3.82 (s, 3H, OCH<sub>3</sub>), 4.87 (s, 2H, CH<sub>2</sub>imi), 4.88 (s, 2H, CH<sub>2</sub>imi), 6.30 (d, *J* = 16.0 Hz, 1H, CH=C), 6.47 (d, *J* = 16.0 Hz, 1H, CH=C), 6.70-6.72 (m, 2H, arom), 6.75-6.78 (m, 2H, arom), 6.89-6.95 (m, 5H, arom), 6.99-7.00 (m, 4H, arom), 7.12-7.22 (m, 10H, arom), 7.24-7.29 (m, 5H, arom), 7.45-7.47 (m, 2H, arom), 7.50-7.56 (m, 2H, arom), 7.66-7.69 (m, 2H, arom).

**Methyl (2E)-3-(4-(3-(1H-imidazol-1-yl)-2-methyl-1-(4-(pivaloyloxy)phenyl)prop-1-en-1-yl)phenyl)acrylate (153).** Starting from **150** (0.09 g, 0.20 mmol), a crude compound was obtained that was purified by flash column chromatography (petroleum ether/ethyl acetate 0.5:9.5) to give **153** as yellow oil (0.06 g, yield 65

%). <sup>1</sup>H NMR: δ *E/Z* 1.33 (s, 9H, 3 x CH<sub>3</sub>), 1.34 (s, 9H, 3 x CH<sub>3</sub>), 1.70 (s, 3H, CH<sub>3</sub>), 1.71 (s, 3H, CH<sub>3</sub>), 3.79 (s, 3H, OCH<sub>3</sub>), 3.80 (s, 3H, OCH<sub>3</sub>), 4.59 (s, 4H, 2 x CH<sub>2</sub>imi), 6.39-6.45 (m, 2H), 6.86 (s, 2H), 7.01-7.07 (m, 6H, arom), 7.12-7.20 (m, 7H), 7.44-7.49 (m, 5H, arom), 7.51-7.54 (m, 2H, arom), 7.64-7.69 (m, 2H, arom).

**Methyl (2E)-3-(4-(2-((1H-imidazol-1-yl)methyl)-1-(4-(pivaloyloxy)phenyl)but-1-en-1-yl)phenyl)acrylate (154).** Starting from **151** (0.09 g, 0.19 mmol), a crude compound was obtained that was purified by flash column chromatography (petroleum ether/ethyl acetate 0.5:9.5) to give **154** as yellow oil (0.06 g, yield 67 %). <sup>1</sup>H NMR: δ *E/Z* 0.95-0.99 (m, 6H, 2 x CH<sub>3</sub>), 1.34 (s, 9H, 3 x CH<sub>3</sub>), 1.35 (s, 9H, 3 x CH<sub>3</sub>), 2.02-2.07 (m, 4H, 2 x CH<sub>2</sub>), 3.80 (s, 6H, 2 x OCH<sub>3</sub>), 4.64 (s, 4H, 2 x CH<sub>2</sub>-imi), 6.39-6.44 (m, 2H, 2 x CH=C), 6.88 (s, 2H, 2 x imi), 7.02-7.06 (m, 6H, arom), 7.14-7.20 (m, 7H, arom), 7.46-7.49 (m, 5H, arom), 7.53-7.56 (m, 2H, arom), 7.63-7.69 (m, 2H, arom).

**Methyl (E)-3-(4-((Z)-3-(1H-imidazol-1-yl)-1,2-diphenylprop-1-en-1-yl)phenyl)acrylate (157a).** Starting from **156a** (0.20 g, 0.48 mmol), a crude compound was obtained that was purified by flash column chromatography (petroleum ether/ethyl acetate 2:3) to give **157a** as brown/yellow oil (0.10 g, yield 49 %). <sup>1</sup>H NMR: δ 3.82 (s, 3H, OCH<sub>3</sub>), 4.88 (s, 2H, CH<sub>2</sub>imi), 6.46 (d, *J* = 16.0 Hz, 1H, CH=C), 6.74 (s, 1H, imi), 6.80-6.89 (m, 2H, arom), 6.96 (s, 1H, imi), 7.00-7.08 (m, 8H, arom), 7.20-7.24 (m, 3H, arom), 7.30 (d, *J* = 16.0 Hz, 1H, CH=C), 7.45 (d, *J* = 8.1 Hz, 2H, arom).

**Methyl (E)-3-(4-((E)-3-(1H-imidazol-1-yl)-1,2-diphenylprop-1-en-1-yl)phenyl)acrylate (157b).** Starting from **156b** (0.14 g, 0.33 mmol), a crude compound was obtained that was purified by flash column chromatography (petroleum ether/ethyl acetate 2:3) to give **157b** as brown/yellow oil (0.08 g, yield 57 %). <sup>1</sup>H NMR: δ 3.76 (s, 3H, OCH<sub>3</sub>), 4.88 (s, 2H, CH<sub>2</sub>imi), 6.30 (d, *J* = 16.0 Hz, 1H, CH=C), 6.73 (s, 1H, imi), 6.93 (d, *J* = 8.4 Hz, 2H, arom), 6.97 (s, 1H, imi), 7.16-7.25 (m, 5H, arom), 7.34 (s, 1H, imi), 7.37-7.44 (m, 3H, arom), 7.50-7.57 (m, 3H, arom), 7.64-7.68 (m, 2H, arom).

**1-(pyridine-3-yl)butan-2-one (114a).** A solution of 2-(pyridine-3-yl)acetic acid (0.58 g, 4.20 mmol), pyridine (2 mL) and propionic anhydride (2 mL) was refluxed under N<sub>2</sub> atmosphere for 6 h. Solvents were evaporated and the residue was dissolved in dichloromethane (5 mL) and washed with 2M NaOH solution (3 x 5mL). The organic layer was dried and concentrated *in vacuo* and the crude compound was purified by flash chromatography (ethyl acetate) to give **114a** as yellow oil (0.14 g, yield 22 %). <sup>1</sup>H NMR: δ 1.07 (t, *J* = 6.8 Hz, 3H, CH<sub>3</sub>), 2.53 (q, *J* = 6.8 Hz, 2H, CH<sub>2</sub>), 3.71 (s, 2H, CH<sub>2</sub>Py), 7.22-7.30 (m, 1H, arom), 7.55 (dd, *J* = 1.7 and 7.9 Hz, 1H, arom), 8.45 (d, *J* = 1.8 Hz, 1H, arom), 8.52 (d, *J* = 7.6 Hz, 1H, arom).

**1-(1H-imidazol-4-yl)ethan-1-one (116b).** 4(5)-cyanoimidazole<sup>153</sup> (0.48 g, 5.20 mmol) in THF (5 mL) was added to a 3M solution of methylmagnesium bromide (8.6 mL, 26 mmol) and the mixture was stirred at rt for 3h. Then, H<sub>2</sub>O (5 mL) and 10 % H<sub>2</sub>SO<sub>4</sub> solution (10 mL) were added dropwise and the mixture was stirred for 30 min and then brought to pH 8 with 30 % NaOH solution. After the organic layer was separated, the aqueous layer was extracted with ethyl acetate (3 x 25 mL). The organic layers were combined, washed with NaHCO<sub>3</sub> saturated solution and brine, and concentrated under reduced pressure. The crystals formed were collected by filtration to give **116b** as light yellow solid (0.30 g, yield 53 %) mp 179-180 °C (lit.<sup>155</sup> mp 172 °C). <sup>1</sup>H NMR: δ 2.52 (s, 3H, CH<sub>3</sub>), 7.76 (s, 1H, arom), 7.80 (s, 1H, arom).

**3-chloro-6-methoxy-9H-xanthen-9-one (130).** A mixture of 2,4-dichlorobenzoic acid (10.00 g, 52 mmol), catalytic amounts of Cu and CuI (0.25 g), K<sub>2</sub>CO<sub>3</sub> (14.40 g, 104 mmol), pyridine (2 mL, 26 mmol) and 3-methoxyphenol (11.40 mL, 104 mmol) in H<sub>2</sub>O (25 mL) was refluxed for 2 h. The basic reaction mixture was then washed with diethyl ether (3 x 30 mL) and acidified with HCl to give a precipitate (7.45 g) that was filtered, dried and added portion wise, without further purification, to a solution of phosphoric acid (74.50 mL) and phosphoric anhydride (74.45 g). When adding the precipitate, the temperature must be below 120°C. The mixture

was heated at 120 °C for 7 h, then poured in to ice. The formed precipitated was filtered, suspended in NaHCO<sub>3</sub> saturated solution (40 mL) and then filtered again to obtain a crude product that was purified by flash chromatography (petroleum ether/ethyl acetate 4:1) to give compound **130** as light-yellow solid (3.20 g, yield 24 %, over two steps), mp 164-166 °C (lit.<sup>156</sup> mp 166 °C). <sup>1</sup>H NMR: δ 3.96 (s, 3H, OCH<sub>3</sub>) 6.90 (d, *J* = 2.4 Hz, 1H, arom) 6.99 (dd, *J* = 9.2 and 2.4 Hz, 1H, arom) 7.35 (dd, *J* = 8.8 and 2.0 Hz, 1H, arom) 7.49 (d, *J* = 2.0 Hz, 1H, arom) 8.26 (t, *J* = 8.8 Hz, 2H, arom).

**3,6-dimethoxy-9H-xanthen-9-one (131)**. Na (2.18 g, 95.22 mmol) was dissolved in methanol (85 mL) at 0 °C. A solution of compound **130** (1.30 g, 5 mmol) in dioxane (40 mL) was added and the reaction mixture was refluxed for 40 h. After cooling, the solvent was evaporated under reduced pressure and the residue was suspended in 6N HCl (50 mL) and the mixture was stirred for ≈ 20 minutes. The precipitate was filtered to obtain a crude product that was purified by flash chromatography (dichloromethane/toluene 9:1) to give compound **131** as light-yellow solid (1.00 g, yield 78 %), mp 184-186 °C (lit.<sup>156</sup> 184-186°C). <sup>1</sup>H NMR: δ 3.94 (s, 6H, 2 x OCH<sub>3</sub>) 6.88 (d, *J* = 2.0 Hz, 2H, aro) 6.95 (dd, *J* = 8.8 e 2.2 Hz, 2H, aro) 8.25 (d, *J* = 8.8 Hz, 2H, aro).

**3,6-dihydroxy-9H-xanthen-9-one (132)**<sup>157</sup>. Compound **131** (1.32 g, 5.16 mmol) was added to a solution of AlCl<sub>3</sub> (5.28 g) in toluene (75 mL) and the reaction mixture was refluxed for 3 h. After cooling, the solvent was evaporated and the residue was dissolved in ice. The formed precipitate was filtered, dissolved in 2N NaOH aqueous solution (50 mL) and washed with ethyl acetate (3 x 59 mL). The aqueous layer was acidified with 6N HCl until a white precipitate was formed. The solid was filtered and dried to give compound **132** as white solid (0.97 g, yield 83 %), mp > 250°C. <sup>1</sup>H NMR (methanol-*d*<sub>4</sub>): δ 6.81 (d, *J* = 2.4 Hz, 2H, aro) 6.86 (dd, *J* = 8.8 and 2.4 Hz, 2H, aro) 8.07 (d, *J* = 8.8 Hz, 2H, aro).

**2-(1H-imidazol-1-yl)-1-phenylethan-1-one (134).** A mixture of acetophenone (0.50 mL, 4.17 mmol), NBS (0.89 g, 5 mmol) and montmorillonite K10 (50 mg, 10% p/p) in methanol (8 mL) was heated to 60-65 °C for 30 min. The reaction mixture was hot filtered, the solvent was evaporated and the residue was dissolved in H<sub>2</sub>O (10 mL) and extracted with dichloromethane (3 x 10 mL). The organic layer was dried over Na<sub>2</sub>SO<sub>4</sub> and evaporated under vacuum to give a crude compound that was reacted with imidazole (0.23 g, 3.53 mmol) in acetonitrile (15 mL) without further purification. The reaction mixture was refluxed for 1 h. After cooling. The solvent was evaporated to give a crude compound purified by flash column chromatography (dichloromethane/methanol 9:1) to give **134** as a light-yellow solid (0.18 g, yield 23%, over two steps), mp 134-136 °C. <sup>1</sup>HNMR: δ 5.48 (s, 2H, CH<sub>2</sub>imi) 6.99 (s, 1H, arom) 7.18 (s, 1H, arom) 7.55 (t, *J* = 7.4 Hz, 2H, arom) 7.67 (t, *J* = 7.6 Hz, 1H, arom) 7.76 (s, 1H, arom) 7.99 (d, *J* = 7.6 Hz, 2H, arom).

## 4. DESIGN AND SYNTHESIS OF HISTAMINE H<sub>4</sub> LIGANDS POTENTIALLY USEFUL IN THE MANAGEMENT OF TRIPLE NEGATIVE BREAST CANCER

### 4.1 HISTAMINE AND HISTAMINE RECEPTORS

Histamine (2-(1H-imidazol-4-yl)ethan-1-amine) (Figure 47) is a biogenic amine, ubiquitously present in the body, that mediates many physiological and pathological functions. It was isolated for the first time from the mould ergot by Sir Henry Dale and his colleagues and it was found to have effects on smooth muscle contraction, cause vasodepression and induce shock reaction when injected in animals.<sup>158</sup> Only in 1927, when Best *et al.* isolated it from the tissues of liver and lungs, it was discovered that it was a natural constituent of the body.<sup>159</sup> Based on the physiological effects triggered by histamine, it was assumed that this compound played an important role in allergy and anaphylaxis.

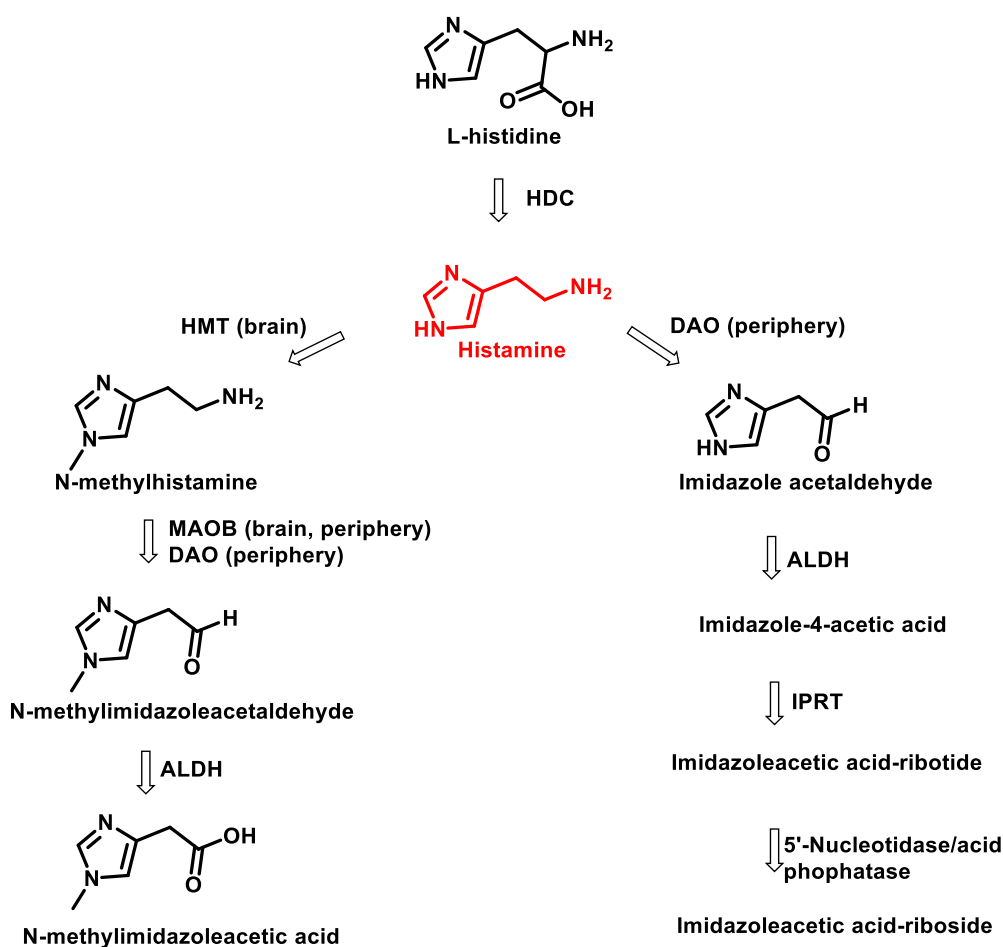


**Figure 47.** Synthesis and metabolism of histamine.

Histamine is synthesized from L-histidine by the action of L-decarboxylase enzyme. Once synthesized, histamine can be directly released or stored into specialized cells such as mast cells, basophils and enterochromaffin cells that, when stimulated, are able to release large amounts of this amine.<sup>160</sup> Histamine is mainly metabolized in two pathways, one catalyzed by the enzyme histamine N-methyltransferase (HMT) (50 to 80 %) and the other by diamine oxidase (DAO) (15 to 30 %), while only 2 to 3 % is excreted unchanged (Figure 47). The HMT enzyme, present in the CNS, intestinal smooth muscle, mucosa of the small intestine, liver and kidneys, catalyzes the methylation of histamine to give N-methylhistamine. The latter can be further metabolized by monoamine oxidase B (MAOB) or by DAO to give N-methylimidazoleacetaldehyde that is oxidized to N-methylimidazoleacetic acid, the main metabolic product, by the action of the enzyme aldehyde dehydrogenase (ALDH). The remaining part of histamine is inactivated in the second pathway, where is converted by DAO into imidazole acetaldehyde, which is then further metabolized by other enzymes such as ALDH and imidazoleacetic acid phosphoribosyltransferase.<sup>161</sup>

Histamine exerts its physiological functions interacting with four receptors: H<sub>1</sub>, H<sub>2</sub>, H<sub>3</sub> and H<sub>4</sub>. They belong to the G protein-coupled receptor (GPCR) superfamily and consist of seven  $\alpha$ -transmembrane helices (7-transmembrane domains, 7-TM domains), an N-terminal extracellular domain and a C-terminal intracellular domain. G proteins are heterotrimeric proteins that consist of three subunits ( $\alpha$ ,  $\beta$  and  $\gamma$ ) and are able to bind the guanine nucleotide. In the inactive state, the G protein is formed by the  $\alpha\beta\gamma$  trimer with GDP linked to the  $\alpha$  subunit. The binding of an agonist to the GPCR triggers a conformational change in the cytoplasmic domain, that increases the affinity of the receptor for the  $\alpha\beta\gamma$  trimer. This association leads to the release of GDP from the  $\alpha$  subunit and its replacement with GTP; this, in turn, causes the release of the  $\alpha$ -GTP and  $\beta\gamma$  subunits, that represent the activated forms of G proteins and are able to interact with enzymes and ion channels modulating their activities. Finally, the  $\alpha$  subunit, endowed with GPTase activity, hydrolyzes GTP to GDP, dissociates from the effector and combines with the  $\beta\gamma$  subunit, reconstituting the inactive form of the protein.<sup>162, 163</sup>

#### 4.1.1 $H_1$ Receptor ( $H_1R$ ) and ligands

The  $H_1R$  is widely expressed throughout the body, including smooth muscles from airways, cardiovascular system endothelial cells, lymphocytes, and several parts of the brain such as neocortex, nucleus accumbens, thalamus, and the posterior part of the hypothalamus. The activation of  $H_1R$  leads to increased vascular permeability, stimulation of the sensory nerves of the airways and promotion of chemotaxis of eosinophils, causing sneezing, nasal congestion and rhinorrhea, contributing to the symptoms of rhinitis. The first compound reported as  $H_1R$  antagonist was piperoxan (Figure 48), discovered in the early 1930s by Daniel Bovet at the Pasteur Institute in France. This finding led to the development of the “first generation” of antihistamines, including mepyramine, doxepine and hydroxyzine (Figure 48A).

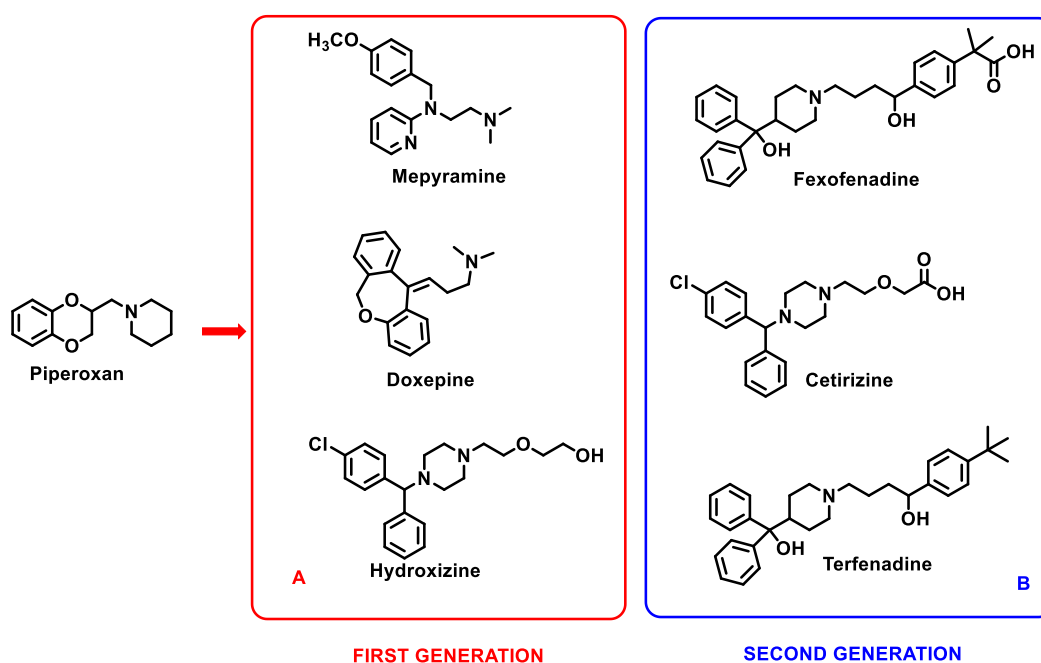


**Figure 48.** First (A) and second (B) generation  $H_1R$  antagonists.

Due to their high lipophilicity, first generation antihistamines were able to cross the blood-brain barrier and enter the CNS, causing side effects such as sedation and sleepiness; moreover, these compounds were often characterized by low  $H_1$  selectivity. Some structural modifications led to the development of new molecules

with reduced ability to enter the CNS, called “second generation” antihistamines, such as fexofenadine, cetirizine and terfenadine (Figure 48B).<sup>164</sup>

#### 4.1.2 $H_2$ Receptor ( $H_2R$ ) and ligands

The  $H_2R$  receptor is widely expressed in gastric parietal cells and in several peripheral tissues such as vascular smooth muscle, heart, uterus and in some parts of the CNS, including cerebral cortex and cerebellum. The existence of two different histamine receptors was postulated for the first time in 1966 by Ash and Schild,<sup>165</sup> concerned by the observation that the classical antihistamines did not block all histamine effects. Some years later, in 1972, the demonstration by Black *et al.*<sup>166</sup> of the existence of agonists that acted selectively on one of the two receptors and the development of the first  $H_2$ -antagonist, burimamide (Figure 49), allowed the classification of the receptors in the two distinct subtypes  $H_1$  and  $H_2$ .

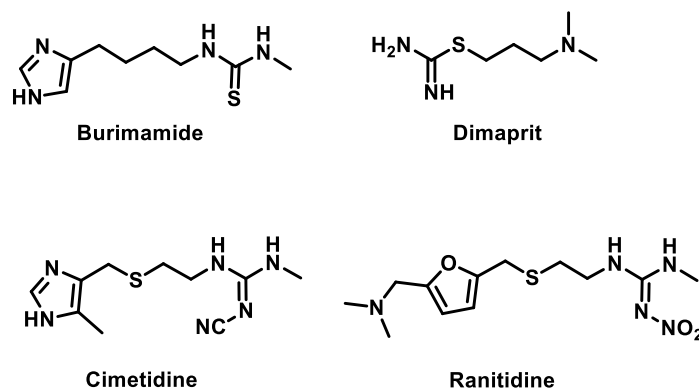


**Figure 49.** Representative  $H_2R$  ligands.

The first selective agonist of this receptor is dimaprit (Figure 49), a compound with two basic groups connected by a short alkyl chain similar to histamine.<sup>167</sup> Cimetidine and ranitidine (Figure 49) are representative compounds of the class of  $H_2$  antagonists. They can block gastric acid secretion and are used in the treatment of gastroduodenal ulcer and gastroesophageal reflux.<sup>168</sup>

#### 4.1.3 H<sub>3</sub> Receptor (H<sub>3</sub>R) and ligands

In 1983 histamine was discovered to inhibit its own release from neurons in rat cerebral cortex, and it was observed that this effect was not mediated by the previously discovered H<sub>1</sub> and H<sub>2</sub> receptors.<sup>169</sup> The existence of a new receptor was confirmed some years later, in 1987, when the H<sub>3</sub> agonist (R)- $\alpha$ -methylhistamine (Figure 50) and the inverse agonist thioperamide (Figure 50) were discovered.<sup>170</sup> The H<sub>3</sub> receptor was also found to be expressed in other types of neurons, such as catecholamine or serotonin neurons. Efforts by pharmaceutical chemists were then devoted to modify the histamine structure with the aim of developing ligands for H<sub>3</sub> receptor. This research yielded to the development of numerous H<sub>3</sub> potent ligands such as clobenpropit,<sup>171</sup> ciplralisant (GT-2331)<sup>172</sup> and GSK189254 (Figure 50) that were investigated as potential drugs for the treatment of various diseases such as attention deficit hyperactivity disorder, Alzheimer's disease, narcolepsy, and schizophrenia.<sup>173</sup> In particular, pitolisant (BF2.649, Figure 50), discovered by Schwartz and colleagues, was approved by FDA for excessive daytime sleepiness in patients with narcolepsy.<sup>174</sup>

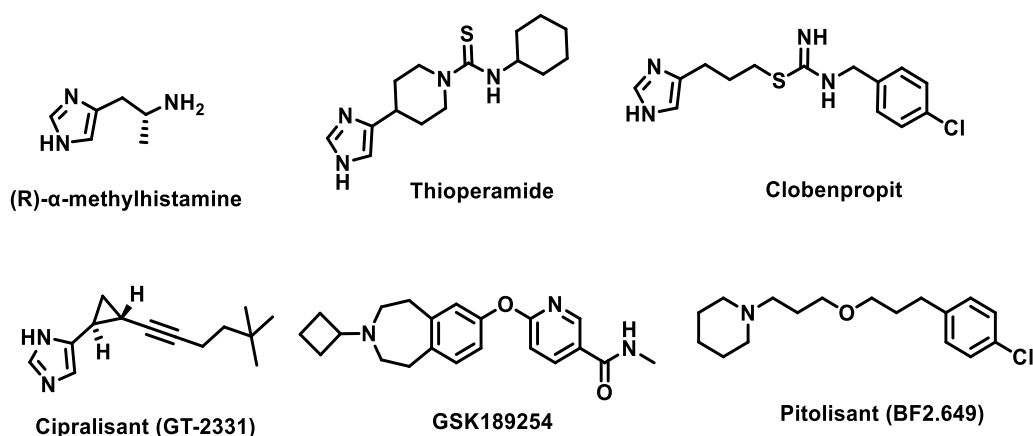


**Figure 50.** Representative H<sub>3</sub>R ligands.

#### 4.1.4 The H<sub>4</sub> Receptor (H<sub>4</sub>R)

Immediately after the identification of the H<sub>3</sub>R gene in 1999<sup>175</sup>, an orphan GPCR was identified that was 35 % identical to H<sub>3</sub>R and showed high affinity for

histamine. These observations led to the discovery of a new histamine receptor, now known as H<sub>4</sub>R. In those years, based on the homology between H<sub>3</sub>R and H<sub>4</sub>R, different research groups independently cloned the cDNA of this receptor.<sup>176-181</sup> In humans, the H<sub>4</sub>R gene is located as a single copy per haploid genome on chromosome 18q11.2 and is formed by three exons (amino acids 1-65, 66-119 and 120-139) and two introns (7867 and >17.500 pb) whose arrangement is similar to that of the introns observed in H<sub>3</sub> receptor. The structure of the H<sub>4</sub> gene differs from that of H<sub>1</sub> and H<sub>2</sub> receptors that do not have introns in their gene sequences. The promoter region of H<sub>4</sub> gene lacks TATA and CAAT sequences, but is rich in some binding sites for interferon, TNF $\alpha$  or IL-6, suggesting that gene expression can be modulated by these inflammatory factors.<sup>182</sup> Moreover, it was observed that the structure of H<sub>4</sub>R contains the conserved motif of class A (rhodopsin-like) GPCRs, including Asn<sup>1.50</sup>, Asp<sup>2.50</sup>, Arg<sup>3.50</sup>, Trp<sup>4.50</sup>, Pro<sup>5.50</sup>, Pro<sup>6.50</sup> and Pro<sup>7.50</sup> (using the Ballesteros-Weinstein numbering). Analyzing the binding pose of histamine inside the H<sub>4</sub> binding pocket (Figure 51), it was seen that the most involved residues in H<sub>4</sub>R-histamine bond were Asp<sup>3.32</sup>, located within TM3 and interacting with the amine group of histamine, and Glu<sup>5.46</sup> in TM5, that formed an H-bond with the protonated nitrogen of the imidazole ring. Asn<sup>4.57</sup> and Ser<sup>6.52</sup> seemed to be important residues for the activation of H<sub>4</sub>R, despite demonstrating no direct involvement in histamine binding.<sup>183</sup>

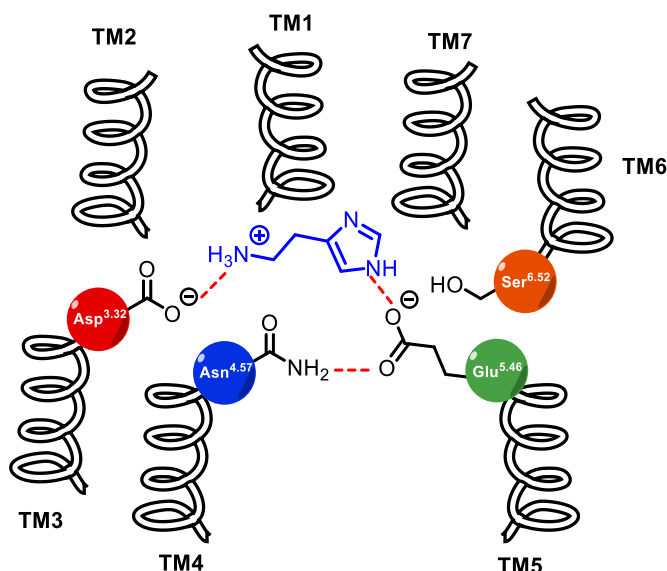


**Figure 51.** Simplified representation of histamine-H<sub>4</sub>R binding mode.

Unlike H<sub>3</sub>R, which is mainly located in the CNS, H<sub>4</sub>R is widely found in eosinophils, mast cells, lymphocytes T cells, dendritic cells, and basophils. It is also detected in small intestine, colon, lung, bone marrow, liver, and mammal glands. Like H<sub>3</sub>R, the activation of H<sub>4</sub>R results in the coupling of the receptor with the pertussis toxin (PTX) sensitive-G<sub>i</sub>/G<sub>o</sub> protein, causing the inhibition of adenylyate cyclase (AC) with reduction of cAMP, Ca<sup>2+</sup> mobilization, and activation of kinases such as extracellular signal-regulated kinase (ERK), phosphoinositide 3-kinase (PI3K) and p38, and the transcription factor activating protein-1.<sup>184</sup>

#### 4.2 H<sub>4</sub>R AND BREAST CANCER

The expression of H<sub>4</sub>R and the involvement of histamine in the modulation of proliferation was reported for different types of tumors, among which triple-negative BC, characterized by the absence of ER, PR, and HER2, which represents approximately 15 % of all BCs and is associated with poor prognosis and fast tumor progression.<sup>185, 186</sup> Several studies reported that histamine modulates many pathologic and physiologic effects of the mammary gland such as cell proliferation and differentiation, and plays a role in pregnancy and lactation. In MDA-MB-231 (ER-) BC cell line, histamine modulated cell proliferation in a dose-dependent manner, as it caused a significant decrease at a concentration of 10 μM while, at lower concentrations, it moderately increased proliferation through H<sub>3</sub>R.<sup>187</sup> Moreover, histamine showed an antiproliferative effect, mediated by H<sub>4</sub>R, in the two different BC cell lines MDA-MB-231 (ER-) and MCF-7 (ER+).<sup>188</sup> In *vitro* and in *vivo* treatments with H<sub>4</sub>R agonists such as histamine (the natural ligand), clozapine and JNJ28610244 on triple-negative BC suggested that H<sub>4</sub>R exhibited a crucial role in tumor progression. These agonists inhibited the proliferation in MDA-MB-231 cells, increased the exponential doubling time and the number of apoptotic and senescent cells, resulting in a decrease in tumor volume.<sup>189</sup> Therefore, targeting H<sub>4</sub>R could represent a novel adjuvant therapy for ER- BC treatment.

### 4.3 H<sub>4</sub>R LIGANDS

Due to the high homology between the two receptors, many compounds that proved to be active on H<sub>3</sub>R also showed considerable affinity for H<sub>4</sub>R as widely reviewed in the literature.<sup>184, 190</sup>

#### 4.3.1 H<sub>4</sub>R agonists

The first class of agonists showing some selectivity for H<sub>4</sub>R were 2,5-disubstituted tetrahydrofuranylimidazole analogs; in particular, 1-cyano-3-[[[(2R,5R)-5-(1H-imidazol-5-yl)oxolan-2-yl]methyl]-2-methylguanidine (OUP-16) (Figure 52) proved to be a potent H<sub>4</sub>R ligand, with a K<sub>i</sub> = 125 nM and 18-fold selectivity over H<sub>3</sub>R.<sup>191</sup>

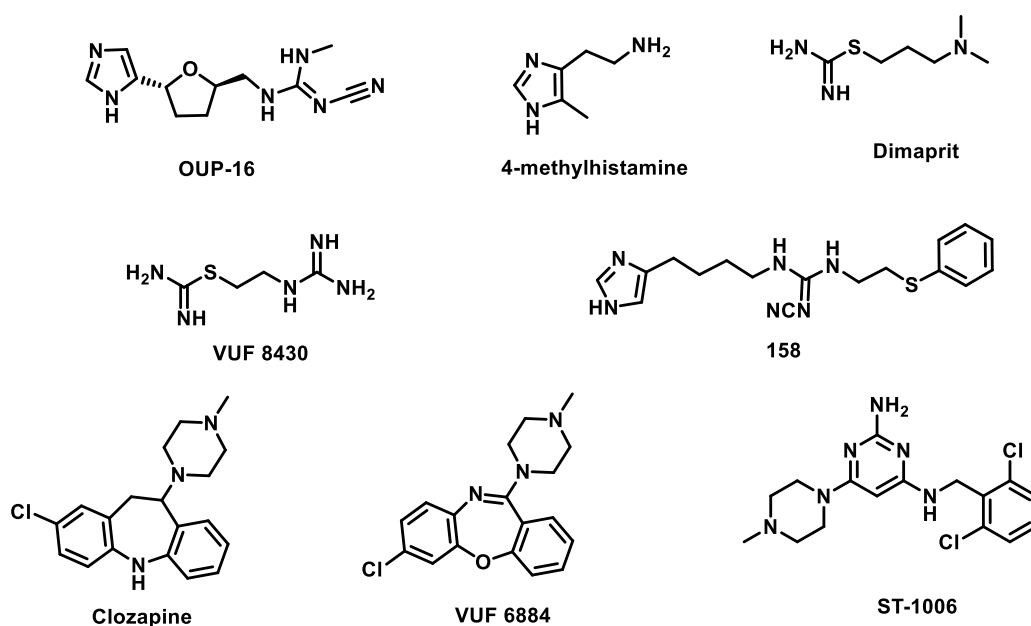


**Figure 52.** H<sub>4</sub>R agonists.

In 2005, Lim *et al.*<sup>192</sup> published the evaluation of the affinity for H<sub>4</sub>R of some known histaminergic compounds with different structural features. The most important finding of this study was that 4-methylhistamine (Figure 52), which was

previously investigated as H<sub>2</sub>R agonist, proved to be a high-affinity H<sub>4</sub>R agonist ( $K_i = 50$  nM), with a 100-fold selectivity over the other histaminergic receptors, including H<sub>2</sub>R. In the same work, many H<sub>3</sub>R ligands containing an imidazole moiety proved to act on H<sub>4</sub>R with high affinity, and the H<sub>2</sub>R agonist dimaprit (Figure 52) was identified as an H<sub>4</sub>R agonist with moderate affinity. Another study conducted by the same research group and focused on dimaprit derivatives led to the discovery of the potent H<sub>4</sub>R agonist VUF 8430 (Figure 52), with moderate selectivity over H<sub>3</sub>R but very selective over H<sub>1</sub>R and H<sub>2</sub>R. In this compound, the tertiary amine of dimaprit was substituted by a guanidine group, and the spacer was shortened from a propylene to an ethylene leading to an increase in affinity for H<sub>4</sub>R, with a  $pK_i$  almost as high as that of histamine.<sup>193</sup>

Igel *et al.*, with the aim of developing a potent and selective H<sub>4</sub>R agonist, replaced the acylguanidine of N<sup>G</sup>-acylated imidazolylpropylguanidine with different related groups. Within the series of derivatives carrying the cyanoguanidine group, compound **158** (Figure 52) proved to be the most potent H<sub>4</sub>R agonist, with significant selectivity over the other receptors.<sup>194</sup>

The antipsychotic clozapine (Figure 52), that acts as antagonist on most GPCRs, was also found to be able to establish favorable interactions with H<sub>4</sub>R, acting as full agonist. Structural modifications on this tricyclic dibenzodiazepine led to the development of VUF 6884 (Figure 52) that proved to have a 300-fold higher affinity for H<sub>4</sub>R over H<sub>3</sub>R, while showing high affinity also for H<sub>1</sub>R.<sup>195</sup>

In 2009, Sander *et al.*, starting from a ligand-based virtual screening, identified potential pyrimidine hit structures with affinities for H<sub>4</sub>R in the low micromolar range. Structural modifications on these hit compounds led to the development of a potent agonist (ST-1006, Figure 52) with 40-fold selectivity over H<sub>3</sub>R.<sup>196</sup>

#### 4.3.2 H<sub>4</sub>R antagonists

In 2003, Johnson and Johnson Pharmaceuticals (J&J) developed the first selective non-imidazole H<sub>4</sub>R antagonist JNJ7777120 (Figure 53) with  $K_i = 4.5$  nM versus the human receptor. This compound contained an indole group connected to a 4-

methylpiperazine through a carboxamide spacer and proved to be at least 1000 fold selective over H<sub>1</sub>, H<sub>2</sub> and H<sub>3</sub> receptors.<sup>197</sup>

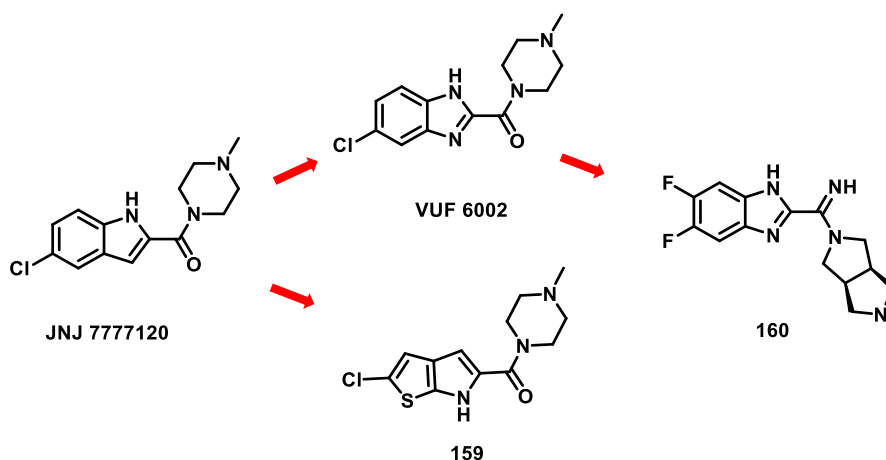


**Figure 53.** Development of H<sub>4</sub>R antagonists.

The bioisosteric replacement of the indole group with benzimidazole or thienopyrrole led to the development of VUF 6002<sup>198</sup> and thienopyrrole derivative **159** (Figure 53),<sup>199</sup> that showed potent H<sub>4</sub>R antagonist activity. Pfizer also focused its interest on similar scaffolds, replacing the N-methylpiperazine with the bicyclic octahydropyrrolo[3,4-c]pyrrole group and developing an amidine compound (**160**, Figure 53) with excellent H<sub>4</sub> potency and metabolic stability.<sup>200</sup>

Another structure identified as potential scaffold able to interact with H<sub>4</sub>R was 2-aminopyrimidine. The first two series of compounds with good H<sub>4</sub> potency were published by Bayer (**161** and **162**, Figure 54)<sup>201, 202</sup>. Other aminopyrimidine derivatives were disclosed in numerous patents by several companies. Palau Pharma proposed several 2-aminopyrimidine derivatives, in which the aromatic ring was connected to the pyrimidine heterocycle by an amino linker (**163**, Figure 54). In these series various aromatic moieties, such as thiophene, naphthalene and differently substituted phenyl groups were inserted in the amino linker.<sup>203</sup> In the same years, Pfizer disclosed other pyrimidine derivatives investigating the effect of aliphatic substituents linked to the pyrimidine moiety by an amino group. One of the best compounds resulted to be **164**, with a K<sub>i</sub> of 1.33 nM, (Figure 54).<sup>204</sup> Moreover, UCB Celltech developed several compounds with different saturated or

partially saturated heterocycles bound to the pyrimidine scaffold (**165**, Figure 54).<sup>205</sup> Abbot laboratories developed compounds with a rotationally constrained aminopyrimidine, A-943931<sup>206</sup> and A-987306 (Figure 54)<sup>207</sup>, that proved to be potent H<sub>4</sub>R antagonists with good selectivity over the other receptors. Further, other aminopyrimidine derivatives were presented by J&J, some of which showed affinities in the low nanomolar range (compounds **166** and **167**, Figure 54, with K<sub>i</sub> values of 3 and 4 nM, respectively).<sup>208</sup>

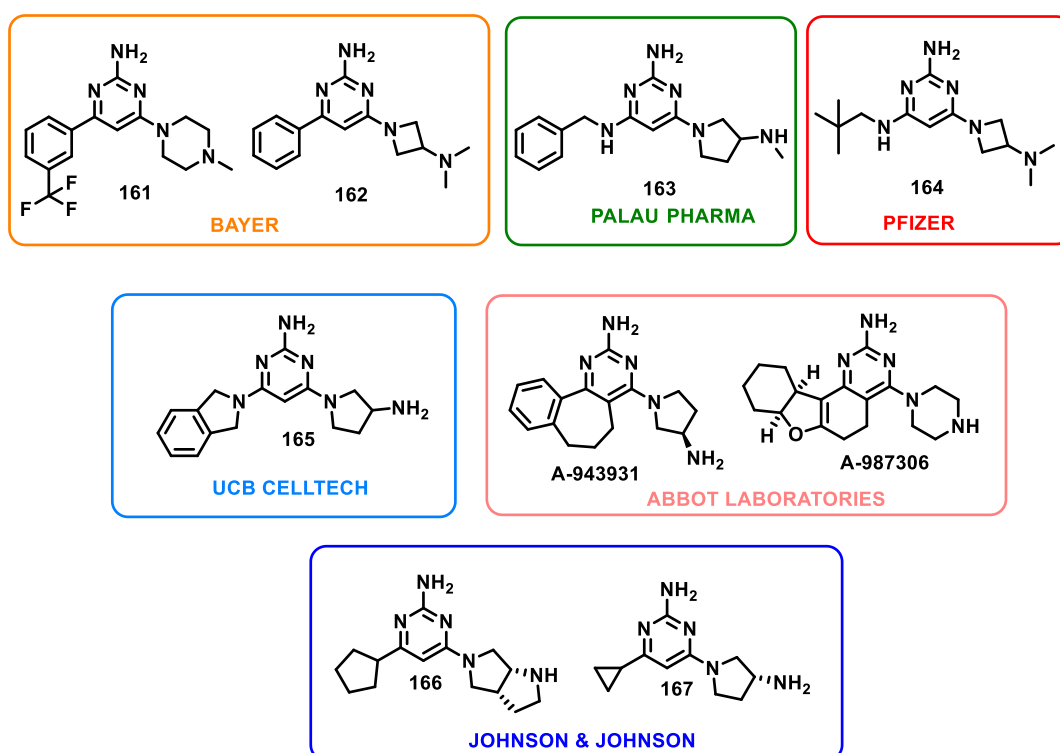


**Figure 54.** Pyrimidine derivatives as H<sub>4</sub>R antagonists.

Starting from a pharmacophore model built from the structures of the antipsychotic drug clozapine and the H<sub>4</sub>R antagonist JNJ 7777120, a research group of the VU University Amsterdam developed some quinoxaline derivatives, leading to the identification of VUF 10214 (Figure 55) and VUF 10148 (Figure 55), that proved to be the best compounds of the series with nanomolar affinity for H<sub>4</sub>R. The quinazoline scaffold was also able to interact with H<sub>4</sub>R with micromolar affinity and, given the high similarity between quinoxaline and quinazoline, it was assumed

that the two heterocycles interacted with the H<sub>4</sub>R binding site through a similar pose.<sup>209</sup> A series of quinazoline derivatives was synthesized, in which the N-methylpiperazine (crucial for activity) was left unchanged, a chlorine atom was added in position 6 and an amine group with different aromatic and aliphatic substituents was introduced in position 4. Compound **168** (Figure 55), carrying a thiophene group, was the most potent compound of the series.<sup>210</sup> The replacement of the thiophene group with a sulfonamide moiety led to the development of a series of derivatives carrying different functional groups on the sulfonamide moiety, as in compound **169** (Figure 55). The obtained results suggested that the introduction of various substituents on the sulfonamide was well tolerated, as the new compounds maintained a good affinity for H<sub>4</sub>R, acting as inverse agonists.<sup>211</sup>

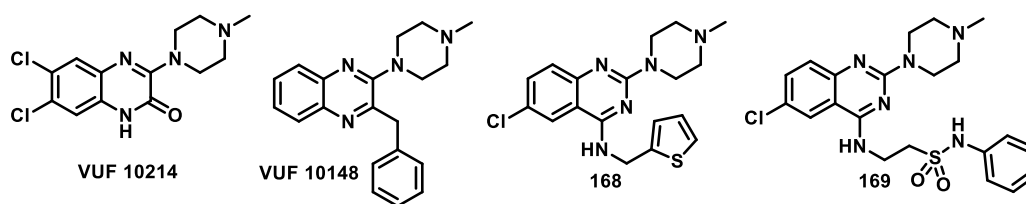


**Figure 55.** Quinazoline and quinoxaline H<sub>4</sub>R ligands.

#### 4.4 DESIGN AND SYNTHESIS OF POTENTIAL H<sub>4</sub>R LIGANDS

The project I was involved at the VU University in Amsterdam was aimed at the development of H<sub>4</sub>R ligands and had previously resulted in the identification of compound **168** (Figure 55 and Figure 56), showing high affinity for H<sub>4</sub> and H<sub>1</sub> receptors (pK<sub>i</sub> of 8.15 and 7.70, respectively) and considered as starting point for further optimization. QSAR investigations on **168** led to the development of compounds in which the thiophene group was replaced by a sulfonamide moiety (**170**, Figure 56). SAR study on scaffold **170** proved that the insertion of various N-ethylaminosulfonamides on the quinazoline nucleus led to potent H<sub>4</sub>R ligands. Moreover, it was observed that the substitution of the amino group in the sulfonamide moiety with different aromatic and aliphatic groups was quite tolerated, giving compounds with high affinity.

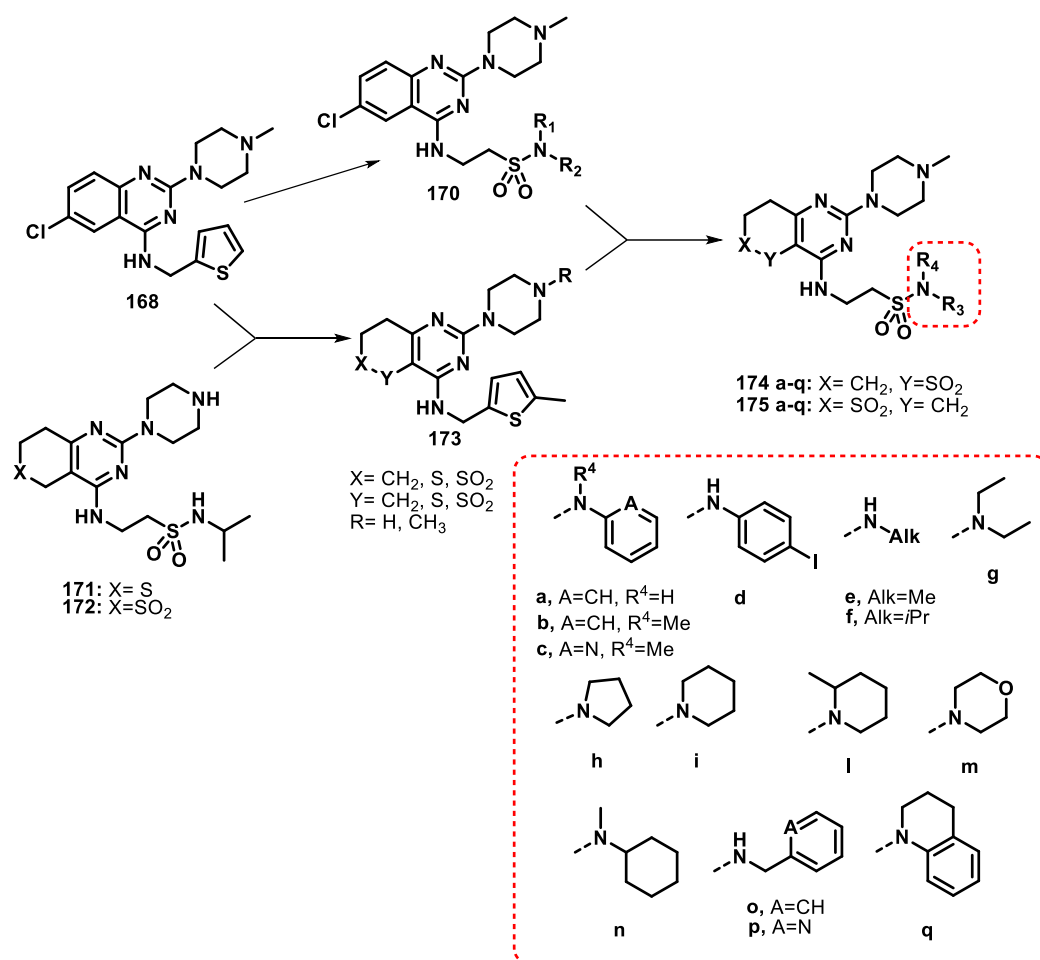


**Figure 56.** Design of new potential H<sub>4</sub>R ligands.

From an in-depth literature search for related molecules, two 7,8-dihydro-5*H*-thiopyrano[4,3-*d*]pyrimidine derivatives (**171** and **172**, Figure 56), with a partially saturated central core carrying a thioether or sulfone moiety, were also found to have affinity for H<sub>4</sub>R in the nanomolar range.<sup>212</sup> These compounds were then hybridized with **168** (to give **173**, Figure 56) by positioning a thioether or a sulfone group in positions 5 or 6 on the thiopyranopyrimidine central core, and a thiophene-2-ylmethylamine group in position 4; a methyl group was also inserted on the heterocycle, due to the potential metabolic lability of the thiophene moiety of the hit compound **168**.

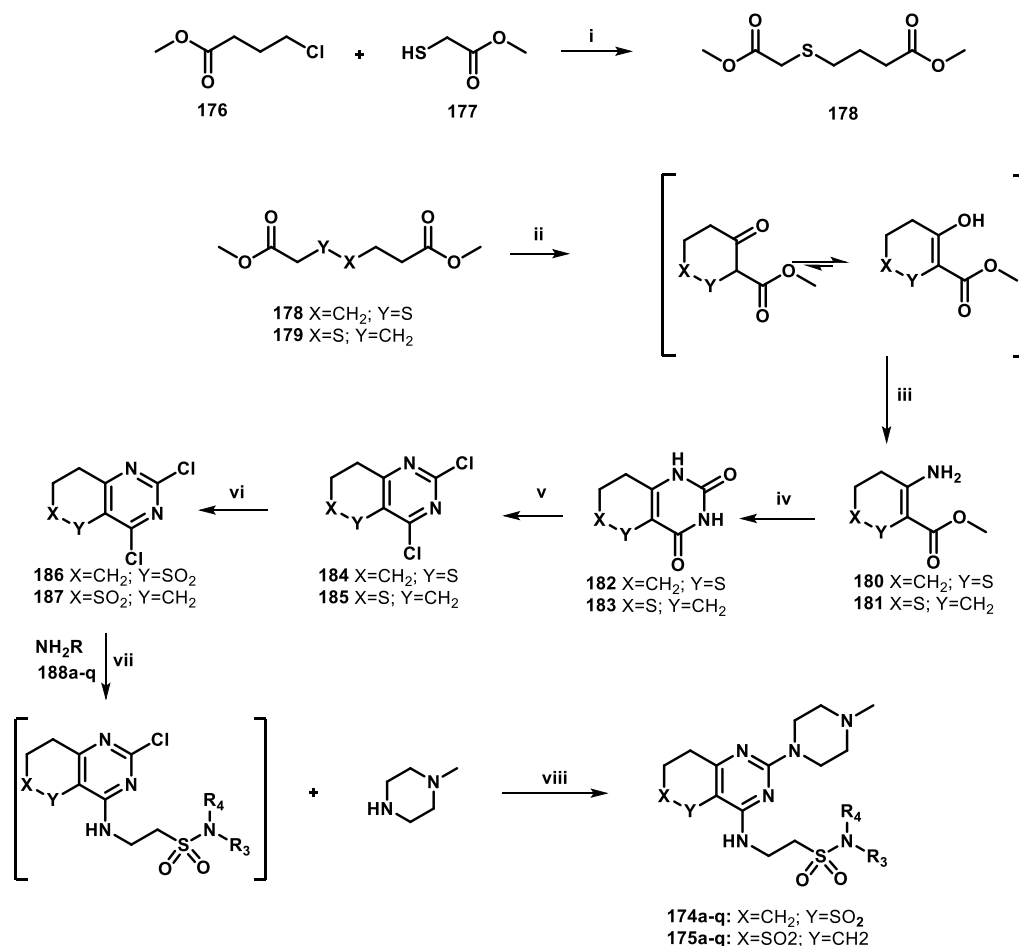
During my stay in the group, to further investigate the SAR of this class of compounds, a new series of derivatives was now designed and synthesized. Here, different ethylsulfonamide moieties were inserted in position 4 of the central core

(**174,175a-q** Figure 56), either based on the results obtained in a previous study,<sup>211</sup> indicating a favourable contribution to H<sub>4</sub> affinity, or suitable for the investigation of the chemical space of this area of the receptor binding site. These compounds are now undergoing radioligand displacement assay to determine their relative affinity towards H<sub>4</sub>R while functional data will be generated next for a selection of compounds.

### Chemistry

The designed compounds were synthesized as shown in Scheme 16.

**Scheme 16.** Synthesis of final compounds **174-175a-q**.<sup>a</sup>



<sup>a</sup>**Reagents and conditions:** i) NaOMe, EtOH, rt, overnight; ii) NaH, THF, rt, overnight; iii) CH<sub>3</sub>COONH<sub>4</sub>, MeOH, rt, 3 h; iv) **Method A:** COCl<sub>2</sub> in PhMe, pyridine, dichloroethane, 0 °C, 4 h, then aq. NH<sub>4</sub>OH, 50 °C, overnight; **Method B:** Urea, 160 °C, 6 h then 0.5 M NaOH,

5 min; v) POCl<sub>3</sub>, PhNMe<sub>2</sub>, reflux, 4 h; vi) Oxone<sup>TM</sup>, MeOH, H<sub>2</sub>O, rt, overnight; vii) NH<sub>2</sub>R (**188a-q**), DIPEA, EtOAc, rt; viii) *N*-methylpiperazine, μW, 120 °C, 30 min.

The thioglycolate **177** was alkylated with the alkyl chloride **176** to give compound **178**. Both **178** and the commercially available **179** were subjected to the Dieckmann condensation with NaH in THF, obtaining the thiane-derivatives that were reacted with ammonium acetate in methanol without further purification to give **180** and **181**, respectively. The condensation of **180** or **181** with phosgene led to the formation of the bicyclic derivatives **182** and **183**. This reaction was later optimized using a safer precursor (urea) instead of phosgene. Compounds **182** and **183** were reacted with POCl<sub>3</sub> to give the dichloro derivatives **184** and **185** that were oxidated with Oxone<sup>TM</sup> in H<sub>2</sub>O and MeOH obtaining the sulfone derivatives **186** and **187**. These key intermediates were then coupled on position 4 with suitable amines (**188a-q**) in the presence of DIPEA at room temperature, and then on position 2 with *N*-methylpiperazine via microwave heating to give the final compounds **174a-q** and **175a-q**.

In order to establish the regiochemistry of the final compounds **174-175a-q**, all protons and carbon atoms were assigned by performing <sup>1</sup>H-<sup>1</sup>H COSY, HMBC and HSQC spectroscopy experiments. Concerning derivatives **174a-q**, their identities were confirmed by HMBC correlations of C<sub>a</sub> (Figure 57, blue carbon) with protons H<sub>a</sub> (red), H<sub>b</sub> (orange) and H<sub>c</sub> (green), while structures of compounds **175a-q** were proved by HMBC correlations of C<sub>b</sub> (pink carbon) with protons H<sub>a</sub> (red), H<sub>d</sub> (light blue) and H<sub>e</sub> (yellow).

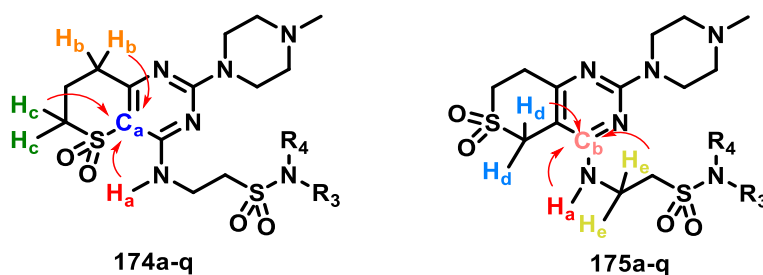
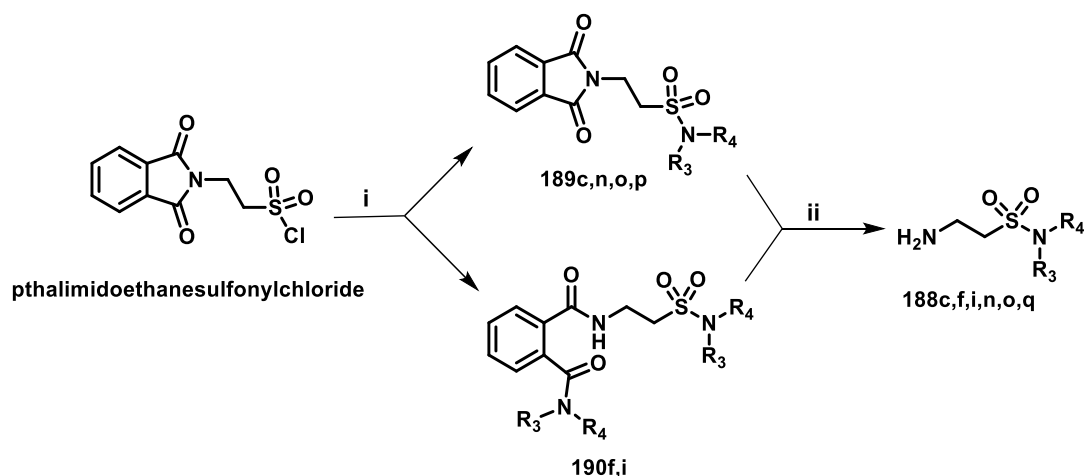


Figure 57. Regiochemistry of compounds **174-175a-q**.

Some of the amine intermediates were synthesized by reacting phthalimidoethanesulfonylchloride with the suitable amine in dichloromethane at room temperature to give the intermediates **189c,n,o,p** and **190f,i**. The nitrogen atom of the phthalimido core was then deprotected with hydrazine in ethanol to give the corresponding primary amines **188c,f,i,n,o,q** (Scheme 17). Other amines (**188a,b,d,h,e,g,l,m**) were prepared according to reported procedures.<sup>211</sup>

**Scheme 17.** Synthesis of the amine intermediates **188c,f,i,n,o,q**.



**Reagents and conditions:** i) NHR<sub>3</sub>R<sub>4</sub>, dichloromethane, rt, 16 h; ii) hydrazine, EtOH, rt, 3 h.

#### 4.4.1 Experimental procedures

##### *General Methods*

Chemicals and solvents were obtained from commercial suppliers and were used without further purification. Dry THF and dioxane were obtained from PureSolv solvent purification system by Inert<sup>®</sup>. All reactions were carried out under an inert N<sub>2</sub> atmosphere. Microwave reactions were performed with Biotage Initiator microwave system. TLC analyses were performed with Merck F254 alumina silica plates using UV visualization or staining. Column purifications were carried out

automatically using Biotage Isolera and Silicycle Ultra Pure silica gel. NMR spectra were recorded on a Bruker 300, 500 or 600 MHz spectrometer. Chemical shifts are reported in ppm ( $\delta$ ), and the residual solvent is used as internal standard ( $\delta$   $^1\text{H}$  NMR:  $\text{CDCl}_3$  7.26;  $\text{CD}_3\text{SOCD}_3$  2.50;  $^{13}\text{C}$  NMR:  $\text{CDCl}_3$  77.16;  $\text{CD}_3\text{SOCD}_3$  39.52). Data are reported as follows: chemical shift, multiplicity (s = singlet, d = doublet, t = triplet, p = pentet, br = broad signal, dd = doublet of doublets, m = multiplet, app = apparent), coupling constants (Hz) and integration. Heteronuclear NMR methods (HSQC, HMBC) were used for assignment of the regiochemistry of final products. HRMS spectra were recorded on Bruker microTOF mass spectrometer using ESI in positive ion mode. Analytical HPLC-MS analyses were conducted using a Shimadzu LC-20AD liquid chromatograph pump system connected to a Shimadzu SPD20A diode array detector with MS detection using a Shimadzu HPLC-MS 2010EV mass spectrometer. The column used is an Xbridge C18 5 mm column (50mm  $\times$  4.6 mm). Solvent B (MeCN / 0.1 % formic acid) and solvent A (water / 0.1 % formic acid), flow rate of 1.0 mL/min with a run time of 8 min. *Gradient settings*: start 5% B, linear gradient to 90% B in 4.5 min, then isocratic for 1.5 min at 90% B, then linear gradient to 5% B in 0.5 min, then isocratic for 1.5 min at 5% B. Unless specified otherwise, all compounds have a purity of  $\geq 95\%$ , calculated as the percentage peak area of the analysed compound by UV detection at 254 nm.

**Methyl 4-((2-methoxy-2-oxoethyl)thio)butanoate (178).** A fresh solution of MeONa was prepared by slowly adding Na (4.14 g, 180 mmol) to MeOH (75 mL) at 0°C. Keeping the temperature at 0°C, methyl thioglycolate (14.10 mL, 150 mmol) was slowly added and the resulting mixture was stirred for 30 min. Methyl 4-chlorobutanoate (20.60 mL, 150 mmol) and KI (0.167 g, 1.01 mmol) were added and the resulting mixture was heated at reflux for 20 h. The solvent was evaporated. The residue was diluted with water (300 mL) and extracted with ethylacetate (3  $\times$  225 mL). The combined organic phases were dried over  $\text{Na}_2\text{SO}_4$ , filtered and concentrated *in vacuum*. This yielded the title compound as a colorless oil (28.92 g, 94%).  $^1\text{H}$  NMR (500 MHz,  $\text{CDCl}_3$ )  $\delta$  3.74 (s, 3H), 3.68 (s, 3H), 3.22 (s, 2H), 2.68 (t,  $J = 7.2$  Hz, 2H), 2.44 (t,  $J = 7.3$  Hz, 2H), 1.93 (app p,  $J = 7.3$  Hz, 2H).

### **General procedure for the synthesis of compounds 180 and 181.**

A solution of ester **178** or **179** (1.0 eq) in THF (80-85 mL) was added dropwise at 0 °C to a suspension of NaH (60 %, 1.1 eq) in THF (80-85 mL). The resulting mixture was stirred overnight at room temperature. The reaction was neutralized with 1M aq. HCl and the organic solvent was evaporated under reduced pressure. The mixture was extracted with dichloromethane (3 x 50 mL). The organic phase was dried over Na<sub>2</sub>SO<sub>4</sub>, filtered and concentrated *in vacuo* to yield the thiane-derivatives (as mixture of enol/ketone tautomers) as a yellow oil used in the next step without further purification. A mixture of the crude intermediate and NH<sub>4</sub>OAc (1.8 eq) in methanol (100-120mL) was heated to reflux for 3 h. The reaction mixture was concentrated. The residue was diluted with ethylacetate and washed with H<sub>2</sub>O. The organic layer was dried over Na<sub>2</sub>SO<sub>4</sub>, filtered and concentrated under reduced pressure to give a crude product, which was purified by trituration with diethylether to give the title compound.

**Methyl 5-amino-3,4-dihydro-2H-thiopyran-6-carboxylate (180).** **178** (28.92 g, 140 mmol) in THF and NaH (3.84 g, 160 mmol) in THF were reacted according to the general procedure to yield the crude intermediate as yellow oil, that was reacted with NH<sub>4</sub>OAc (20.72 g, 269 mmol) in methanol to give crude product purified by trituration with diethylether to give **180** as light-yellow solid (8.43 g, 44 %). <sup>1</sup>H NMR (500 MHz, CDCl<sub>3</sub>): δ 3.73 (s, 3H), 2.80-2.75 (m, 2H), 2.35 (t, *J* = 6.5 Hz, 2H), 2.04 (app p, *J* = 6.5 Hz, 2H).

**Methyl 4-amino-5,6-dihydro-2H-thiopyran-3-carboxylate (181).** **179** (25.80 mL, 150 mmol) in THF and NaH (60 %, 4.10 g, 171 mmol) in THF was reacted according with the general procedure to yield the crude intermediate as yellow oil, that was reacted with NH<sub>4</sub>OAc (22.95 g, 298 mmol) in methanol to give crude product purified by column chromatography (c-Hex:ethylacetate 1:0 to 1:1) to give **23** as light-yellow solid (9.88 g, 46%). <sup>1</sup>H NMR (500 MHz, CDCl<sub>3</sub>) δ 3.68 (s, 3H), 3.39 (s, 2H), 2.73 (t, *J* = 6.5 Hz, 2H), 2.53 (t, *J* = 6.1 Hz, 2H).

### **General procedure for the synthesis of compounds 182 and 183.**

**Method A.** To a solution of compound **180** or **181** (1.0 eq) and pyridine (4.0 eq) in dichloroethane (65-105 mL), COCl<sub>2</sub> 15 % in toluene (1.0 eq) was added dropwise at 0 °C. The mixture was stirred for 4 h at 0 °C. Aq. NH<sub>4</sub>OH (28 %) was added dropwise and the mixture was stirred overnight at 50 °C (SAFETY NOTE: during the reagent addition and during the reaction, the outlet of the flask was connected to a scrubber filled with aq. NaOH (1M)). The solvent was evaporated. The residue was diluted with water, filtered, and dried to give the title compound.

**Method B.** A mixture of **180** or **181** (1.0 eq) and urea (10.0 eq) was stirred at 160 °C for 6 h. The reaction mixture was cooled to 100 °C. Water was added (20 mL) and stirring was continued at 100 °C for 5 min. The obtained precipitate was filtered, washed with water and suspended in an aqueous solution of 0.5 N NaOH. The suspension was heated to boiling for 5 min, cooled to room temperature and acidified (pH = 2) with aq. HCl. The precipitate was filtered and washed with H<sub>2</sub>O/MeOH 1:1 to give the title compound.

#### **7,8-dihydro-1H-thiopyrano[3,2-d]pyrimidine-2,4(3H,6H)-dione (182).**

Compound **180** (4.16 g, 24 mmol), pyridine (7.70 mL, 96 mmol) and COCl<sub>2</sub> (15.80 mL, 24 mmol) in dichloroethane were reacted according to **method A** to give the title compound **182** as yellow solid (2.63 g, 54%). <sup>1</sup>H NMR (500 MHz, DMSO-d<sub>6</sub>) δ 2.88-2.82 (m, 2H), 2.44 (t, *J* = 6.3 Hz, 2H), 2.00-1.91 (m, 2H).

#### **1,5,7,8-tetrahydro-2H-thiopyrano[4,3-d]pyrimidine-2,4(3H)-dione (183).**

Compound **181** (2.66 g, 15.30 mmol), pyridine (4.90 mL, 61.30 mmol) and COCl<sub>2</sub> (15% in toluene, 15.80 mL, 24 mmol) in dichloroethane were reacted according with **method A** to give the title compound **183** as yellow solid (2.63 g, 59%). <sup>1</sup>H NMR (500 MHz, DMSO-d<sub>6</sub>) δ 3.26 (d, *J* = 3.0 Hz, 2H), 2.79 (t, *J* = 5.9 Hz, 2H), 2.59-2.53 (m, 2H).

### **General procedure for the synthesis of compounds 184 and 185.**

A mixture of compound **182** or **183** (1.0 eq), POCl<sub>3</sub> (4.9 eq) and N,N-dimethylaniline (0.25 eq) was heated to reflux for 4 h. The reaction mixture was

carefully poured onto ice and stirred vigorously. The mixture was extracted with dichloromethane and the organic layer was dried over Na<sub>2</sub>SO<sub>4</sub> and concentrated *in vacuo*. The residue was dissolved in diethylether and the insoluble material was filtered off. The clear filtrate was evaporated to dryness to give the title compounds.

**2,4-dichloro-7,8-dihydro-6H-thiopyrano[3,2-d]pyrimidine (184).** Compound **182** (2.63 g, 14.28 mmol), POCl<sub>3</sub> (6.40 mL, 70 mmol) and N,N-dimethylaniline (0.44 mL, 3.50 mmol) were reacted according to the general procedure to give the title compound **184** as yellow solid (2.24 g, 71%). <sup>1</sup>H NMR (500 MHz, CDCl<sub>3</sub>) δ 3.14-3.07 (m, 2H), 3.03-2.92 (m, 2H), 2.28-2.19 (m, 2H).

**2,4-dichloro-7,8-dihydro-5H-thiopyrano[4,3-d]pyrimidine (185).** Compound **183** (0.95 g, 5.16 mmol), POCl<sub>3</sub> (2.30 mL, 25 mmol) and N,N-dimethylaniline (0.17 mL, 1.30 mmol) were reacted according to the general procedure to give the title compound **185** as yellow solid (0.95 g, 83%). <sup>1</sup>H NMR (500 MHz, CDCl<sub>3</sub>) δ 3.80 (s, 2H), 3.22 (t, *J* = 6.3 Hz, 2H), 2.95 (t, *J* = 6.0 Hz, 2H).

#### **General procedure for the synthesis of compounds 186 and 187.**

To a solution of compound **184** or **186** (1.0 eq) in methanol (15-40 mL) was added Oxone<sup>TM</sup> (3.0 eq) in H<sub>2</sub>O. The resulting mixture was stirred overnight at rt. The reaction mixture was diluted with H<sub>2</sub>O (15-40 mL) and extracted with dichloromethane. The organic phase was dried over Na<sub>2</sub>SO<sub>4</sub>, filtered and concentrated *in vacuo*. The crude compound was purified by flash chromatography to give the title compound.

**2,4-dichloro-7,8-dihydro-6H-thiopyrano[3,2-d]pyrimidine 5,5-dioxide (186).** A solution of compound **184** (2.21 g, 10 mmol) in methanol and Oxone<sup>TM</sup> (8.11 g, 30 mmol) in H<sub>2</sub>O were reacted according to the general procedure. The crude product was purified by flash chromatography (c-Hex:ethylacetate 1:0 to 1:1) to give the title compound as a white solid (1.97 g, 78%). <sup>1</sup>H NMR (500 MHz, DMSO-d<sub>6</sub>) δ 3.74-3.67 (m, 2H), 3.14 (t, *J* = 6.1 Hz, 2H), 2.36-2.23 (m, 2H).

**2,4-dichloro-7,8-dihydro-5H-thiopyrano[4,3-d]pyrimidine 6,6-dioxide (187).** To a solution of compound **185** (0.95 g, 4.28 mmol) in methanol was added

Oxone<sup>TM</sup> (3.51 g, 12.98 mmol) in H<sub>2</sub>O and the resulting mixture was reacted according with the general procedure obtaining a crude compound that was purified by flash chromatography (c-Hex: ethylacetate 1:0 to 1:1) to give the title compound as white solid (0.80 g, 74%). <sup>1</sup>H NMR (500 MHz, DMSO-d<sub>6</sub>) δ 4.56 (s, 2H), 3.63 (t, *J* = 6.6 Hz, 2H), 3.45 (t, *J* = 6.5 Hz, 2H).

**General procedure for the synthesis of phtalimido sulfonamides (compounds 189c,n,o,q) and compounds 190f,i.**

2-Phtalimidoethanesulfonylchloride (1.0 eq) was added in portions to a solution of the appropriate amine (3.3 eq) in dichloromethane (10-15 mL). The resulting mixture was stirred at rt for 16 h. The organic phase was washed with H<sub>2</sub>O (2 x 10 mL) and 1M HCl (2 10 mL), dried over Na<sub>2</sub>SO<sub>4</sub> and concentrated under *vacuum*. The crude compound was recrystallized from EtOH to give the title compound.

**2-(1,3-dioxoisindolin-2-yl)-N-methyl-N-(pyridin-2-yl)ethane-1-sulfonamide (189c).** Obtained according to the general procedure starting from 2-phtalimidoethanesulfonylchloride (2.00 g, 7.31 mmol), N-methylpyridin-2-amine (2.50 mL, 24.12 mmol) and dichloromethane. The title compound **189c** was obtained as light-yellow solid (2.16 g, 86 %). NMR (500 MHz, DMSO-d<sub>6</sub>) δ 8.36 (dd, *J* = 8.3, 4.8 Hz, 1H), 7.90- 7.78 (m, 5H), 7.32 (d, *J* = 8.3 Hz, 1H), 7.21 (dd, *J* = 7.4 and 4.8 Hz, 1H), 3.99 (t, *J* = 6.7 Hz, 2H), 3.88 (t, *J* = 6.7 Hz, 2H), 3.31 (s, 3H).

**N1-isopropyl-N2-(2-(N-isopropylsulfamoyl)ethyl)phthalamide (190f).** Obtained according to the general procedure starting from 2-phtalimidoethanesulfonylchloride (2.00 g, 7.31 mmol), isopropylamine (2.10 mL, 24.12 mmol) and dichloromethane. The title compound **190f** was obtained as light-yellow solid (1.60 g, 62 %). <sup>1</sup>H NMR (500 MHz, DMSO-d<sub>6</sub>) δ 8.32 (t, *J* = 5.8 Hz, 1H), 8.10 (d, *J* = 7.8 Hz, 1H), 7.49- 7.41 (m, 4H), 7.18 (d, *J* = 7.5 Hz, 1H), 3.99- 3.92 (m, 1H), 3.54- 3.51 (m, 2H), 3.48- 3.39 (m, 1H), 3.23- 3.16 (m, 2H), 1.14- 1.11 (m, 12H).

**N-(2-(piperidin-1-ylsulfonyl)ethyl)-2-(piperidine-1-carbonyl)benzamide**

**(190i).** Obtained according to the general procedure starting from 2-phtalimidoethanesulfonylchloride (2.00 g, 7.31 mmol), piperidine (2.05 g, 2.40 mL, 24.12 mmol) and dichloromethane. The title compound **190i** was obtained as light-yellow solid (2.30 g, 80 %). <sup>1</sup>H NMR (500 MHz, DMSO-d<sub>6</sub>) δ 8.57 (t, *J* = 5.6 Hz, 1H), 7.63 (dd, *J* = 7.6 and 1.4 Hz, 1H), 7.54- 7.49 (m, 1H), 7.48-7.44 (m, 1H), 7.25 (dd, *J* = 7.5 and 1.4 Hz, 1H), 3.58-3.52 (m, 4H), 3.20 (t, *J* = 7.1 Hz, 2H), 3.18- 3.15 (m, 4H), 3.08- 3.04 (m, 2H), 1.70- 1.42 (m, 12H).

**N-cyclohexyl-2-(1,3-dioxoisindolin-2-yl)-N-methylethane-1-sulfonamide**

**(189n).** Obtained according to the general procedure starting from 2-phtalimidoethanesulfonylchloride (2.00 g, 7.31 mmol), N-methylcyclohexanamine (2.40 mL, 24.12 mmol) and dichloromethane. The title compound **189n** was obtained as light-yellow solid (2.30 g, 90 %). NMR (500 MHz, DMSO-d<sub>6</sub>) δ 7.93-7.89 (m, 2H), 7.89- 7.85 (m, 2H), 3.92 (t, *J* = 6.5 Hz, 2H), 3.53-3.50 (m, 1H), 3.40 (t, *J* = 6.5 Hz, 2H), 2.73 (s, 3H), 1.79-1.73 (m, 2H), 1.69-1.64 (m, 2H), 1.62-1.54 (m, 1H), 1.54- 1.45 (m, 2H), 1.36- 1.26 (m, 2H), 1.10-1.00 (m, 1H).

**N-benzyl-2-(1,3-dioxoisindolin-2-yl)ethane-1-sulfonamide (189o).** Obtained according to the general procedure starting from 2-phtalimidoethanesulfonylchloride (1.50 g, 5.48 mmol), phenylmethanamine (1.80 mL, 18.09 mmol) and dichloromethane (11.30 mL). The title compound **189o** as light-yellow solid (1.51 g, 80 %). NMR (500 MHz, DMSO-d<sub>6</sub>) δ 8.53 (d, *J* = 4.9 Hz, 1H), 7.93-7.88 (m, 3H), 7.88-7.85 (m, 2H), 7.82-7.79 (m, 1H), 7.46 (d, *J* = 7.8 Hz, 1H), 7.31 (dd, *J* = 7.6 and 4.8 Hz, 1H), 4.30 (s, 2H), 4.05-3.90 (m, 2H), 3.50-3.40 (m, 2H).

**2-(2-((3,4-dihydroquinolin-1(2H)-yl)sulfonyl)ethyl)isoindoline-1,3-dione**

**(189q).** Obtained according to the general procedure starting from 2-phtalimidoethanesulfonylchloride (1.50 g, 5.48 mmol), 1,2,3,4-tetrahydroquinoline (2.30 mL, 18.09 mmol) and dichloromethane. The title compound **189q** was obtained as light-yellow solid (1.31 g, 64 %). NMR (500 MHz, DMSO-d<sub>6</sub>) δ 7.89-7.86 (m, 2H), 7.85-7.80 (m, 2H), 7.50 (dd, *J* = 8.6 and 1.2 Hz, 1H), 7.18-7.12 (m,

2H), 7.09-7.01 (m, 1H), 3.96-3.88 (m, 2H), 3.76-3.67 (m, 2H), 3.59-3.51 (m, 2H), 2.81 (t,  $J = 6.6$  Hz, 2H), 2.00-1.87 (m, 2H).

**General procedure for the deprotection of phthalimido sulfonamides to their corresponding primary amines (188c,f,i,n,o,q)**

A suspension of phthalimido sulfonamide (1.0 eq) in EtOH (20-30 mL) was heated to reflux after which  $\text{H}_2\text{NNH}_2$  (64 % in water) (1.1 eq) was added. After 3 h, the white suspension was cooled to room temperature. The solid was removed by filtration. The filtrate was evaporated to dryness and added to  $\text{H}_2\text{O}$  (15 mL). The aqueous suspension was acidified with conc. HCl and residual insoluble material was filtered. The clear filtrate was evaporated to dryness and the crude sulfonamide was recrystallized from EtOH to give the title compound.

**2-amino-N-methyl-N-(pyridin-2-yl)ethane-1-sulfonamide (188c).** Compound **189c** (2.16 g, 6.27 mmol),  $\text{H}_2\text{NNH}_2$  (64% in water, 0.33 mL) and EtOH were reacted according to the general procedure to give the title compound **188c** as light-yellow solid (0.98 g, 73 %). NMR (500 MHz,  $\text{DMSO-d}_6$ )  $\delta$  8.46 (dt,  $J = 4.9$  and 1.3 Hz, 1H), 8.24-8.19 (m, 2H), 7.94-7.88 (m, 1H), 7.44-7.38 (m, 1H), 7.44-7.38 (m, 1H), 7.32 (ddd,  $J = 7.4, 4.8$  and 0.9 Hz, 1H), 3.82 (dd,  $J = 8.5$  and 6.5 Hz, 2H), 3.36 (s, 3H), 3.23-3.14 (m, 2H).

**2-amino-N-isopropylethane-1-sulfonamide (188f).** Compound **190f** (1.60 g, 4.50 mmol),  $\text{H}_2\text{NNH}_2$  (64% in water, 0.24 mL) and EtOH were reacted according with the general procedure to give the title compound **188f** as light-yellow solid (0.58 g, 78 %).  $^1\text{H}$  NMR (500 MHz,  $\text{methanol-d}_4$ )  $\delta$  3.68-3.50 (m, 2H), 3.42-3.39 (m, 3H), 1.23 (d,  $J = 6.5$  Hz, 6H).

**2-(piperidin-1-ylsulfonyl)ethan-1-amine (188i).** Compound **190i** (2.30 g, 5.84 mmol),  $\text{H}_2\text{NNH}_2$  (64% in water, 0.31 mL) and EtOH were reacted according with the general procedure to give the title compound **188i** as light-yellow solid (0.60 g, 53 %).  $^1\text{H}$  NMR (500 MHz,  $\text{DMSO-d}_6$ )  $\delta$  3.15- 3.09 (m, 4H), 3.08-3.05 (m, 2H), 2.90-2.86 (m, 2H), 1.63-1.41 (m, 6H).

**2-amino-N-cyclohexyl-N-methylethane-1-sulfonamide (188n).** Compound **189n** (2.30 g, 6.56 mmol), H<sub>2</sub>NNH<sub>2</sub> (64% in water, 0.35 mL) and EtOH were reacted according with the general procedure to give the title compound **188n** as light-yellow solid (1.13 g, 78 %). NMR (500 MHz, DMSO-d<sub>6</sub>)  $\delta$  8.26 (br, 2H), 3.55-3.52 (m, 1H), 3.48-3.38 (m, 2H), 3.16-3.04 (m, 2H), 2.74 (s, 3H), 1.77-1.74 (m, 2H), 1.70-1.61 (m, 2H), 1.63-1.56 (m, 1H), 1.56-1.45 (m, 2H), 1.36-1.26 (m, 2H), 1.14-1.02 (m, 1H).

**2-amino-N-benzylethane-1-sulfonamide (188o).** Compound **189o** (1.51 g, 4.37 mmol), H<sub>2</sub>NNH<sub>2</sub> (64% in water, 0.23 mL) and EtOH were reacted according with the general procedure to give the title compound **188o** as light-yellow solid (0.69 g, 73 %). NMR (500 MHz, DMSO-d<sub>6</sub>)  $\delta$  8.63 (d,  $J = 4.7$  Hz, 1H), 8.32-8.29 (m, 1H), 8.15 (br, 2H), 8.08-7.99 (m, 1H), 7.62 (d,  $J = 7.8$  Hz, 1H), 7.55-7.47 (m, 1H), 4.40 (d,  $J = 5.8$  Hz, 2H), 3.46 (t,  $J = 7.0$  Hz, 2H), 3.23-3.13 (m, 2H).

**2-((3,4-dihydroquinolin-1(2H)-yl)sulfonyl)ethan-1-amine (188q).** Compound **189q** (1.31 g, 3.53 mmol), H<sub>2</sub>NNH<sub>2</sub> (64% in water, 0.12 mL) and EtOH were reacted according with the general procedure to give the title compound **188q** as light-yellow solid (0.65 g, 77 %). NMR (500 MHz, DMSO-d<sub>6</sub>)  $\delta$  8.15 (br, 2H), 7.43-7.45 (m, 1H), 7.23-7.15 (m, 2H), 7.14-7.09 (m, 1H), 3.76-3.68 (m, 2H), 3.60-3.53 (m, 2H), 3.16-3.05 (m, 2H), 2.82 (t,  $J = 6.7$  Hz, 2H), 1.99-1.89 (m, 2H).

**General procedure for the synthesis of 2,4-disubstituted quinazoline derivatives from their 2,4-dichloro precursor (174a-q and 175a-q).**

Dichloride precursor (1.0 eq) was added to a microwave tube containing dioxane and DIPEA (3.0 eq). The appropriate sulfonamide (1.0 eq) was added. The resulting mixture was stirred at rt overnight. *N*-methylpiperazine (10.5 eq) was added and the reaction mixture was heated at 150°C for 30 min under microwave irradiation. The obtained suspension was diluted with ethylacetate (15 mL) and washed with H<sub>2</sub>O (3 x 10 mL) and brine (3 x 10 mL). The organic phase was dried over Na<sub>2</sub>SO<sub>4</sub>, filtered and the solvent was evaporated. The crude product was purified by normal phase column chromatography to yield the title compound.

**2-((2-(4-methylpiperazin-1-yl)-5,5-dioxido-7,8-dihydro-6H-thiopyrano[3,2-d]pyrimidin-4-yl)amino)-N-phenylethane-1-sulfonamide (174a).** Dichloride **186** (0.25 g, 0.99 mmol) in dioxane (2.30 mL), DIPEA (0.52 mL, 2.96 mmol) and 2-amino-N-phenylethane-1-sulfonamide (**188a**) (198 mg, 0.99 mmol) were reacted according to the general procedure. The crude product was purified by normal phase column chromatography (ethylacetate:methanol 95:5 to 80:20) and subsequent trituration with methanol to yield the title compound as a white solid (0.12 g, 40 %). <sup>1</sup>H NMR (500 MHz, DMSO-d<sub>6</sub>) δ 9.91 (s, 1H), 7.35-7.29 (m, 2H), 7.25-7.20 (m, 2H), 7.13 (t, *J* = 5.9 Hz, 1H), 7.12-7.07 (m, 1H), 3.85-3.75 (m, 2H), 3.66-3.60 (m, 4H), 3.45-3.36 (m, 2H), 3.35-3.33 (m, 2H), 2.68 (t, *J* = 6.4 Hz, 2H), 2.27-2.15 (m, 8H). <sup>13</sup>C NMR (125 MHz, DMSO-d<sub>6</sub>) δ 165.8, 159.5, 157.6, 129.7 (2C), 124.3, 120.1 (2C), 105.9, 54.8 (2C), 51.7, 49.9, 46.2, 43.5 (2C), 35.7, 31.8, 18.8. HRMS C<sub>20</sub>H<sub>28</sub>N<sub>6</sub>O<sub>4</sub>S<sub>2</sub> [M+H]<sup>+</sup> calcd: 481.1686, found: 481.1683. LC-MS: t<sub>R</sub>: 2.98, purity: > 99%, [M+H]<sup>+</sup>: 481.

**2-((2-(4-methylpiperazin-1-yl)-6,6-dioxido-7,8-dihydro-5H-thiopyrano[4,3-d]pyrimidin-4-yl)amino)-N-phenylethane-1-sulfonamide (175a).** Dichloride **187** (0.25 g, 0.99 mmol) in dioxane (2.30 mL), DIPEA (0.52 mL, 2.96 mmol) and 2-amino-N-phenylethane-1-sulfonamide (**188a**) (0.20 g, 0.99 mmol) were reacted according with the general procedure. The crude product was purified by normal phase column chromatography (ethylacetate:methanol 95:5 to 80:20) to yield the title compound as a white solid (0.21 g, 60 %). <sup>1</sup>H NMR (500 MHz, DMSO-d<sub>6</sub>) δ 9.81 (s, 1H), 7.29 (t, *J* = 7.7 Hz, 2H), 7.18 (d, *J* = 7.9 Hz, 2H), 7.08 (t, *J* = 7.3 Hz, 1H), 6.84 (t, *J* = 5.5 Hz, 1H), 3.91 (s, 2H), 3.63 (dt, *J* = 9.5 and 5.6 Hz, 2H), 3.51 (t, *J* = 5.0 Hz, 4H), 3.41-3.35 (m, 4H), 2.95 (t, *J* = 6.5 Hz, 2H), 2.21 (t, *J* = 5.0 Hz, 4H), 2.17 (s, 3H). <sup>13</sup>C NMR (125 MHz, DMSO-d<sub>6</sub>) δ 160.5, 159.9, 158.1, 138.5, 129.7 (2C), 124.2, 119.7 (2C), 95.3, 54.8 (2C), 49.6, 47.7, 47.0, 46.3, 43.6 (2C), 35.8, 32.4. HRMS: C<sub>20</sub>H<sub>28</sub>N<sub>6</sub>O<sub>4</sub>S<sub>2</sub> [M+H]<sup>+</sup> calcd: 481.1686, found: 481.1680. LC-MS: t<sub>R</sub>: 2.33 min, purity: > 99%, [M+H]<sup>+</sup>: 481.

**N-methyl-2-((2-(4-methylpiperazin-1-yl)-5,5-dioxido-7,8-dihydro-6H-thiopyrano[3,2-d]pyrimidin-4-yl)amino)-N-phenylethane-1-sulfonamide (174b).** Dichloride **186** (0.25 g, 0.99 mmol) in dioxane (2.30 mL), DIPEA (0.52 mL, 2.96 mmol) and 2-amino-N-methyl-N-phenylethane-1-sulfonamide

hydrochloride (**188b**) (0.21 g, 0.99 mmol) were reacted according with the general procedure. The crude product was purified by normal phase column chromatography (ethylacetate:methanol 95:5 to 80:20) and subsequent trituration with methanol to yield the title compound as a white solid (0.11 g, 22 %). <sup>1</sup>H NMR (500MHz, CDCl<sub>3</sub>) δ 7.39-7.34 (m, 4H), 7.31-7.27 (m, 1H), 6.77 (t, *J* = 5.6 Hz, 1H), 3.88 (dt, *J* = 9.5 and 6.1 Hz, 2H), 3.76-3.85 (m, 4H), 3.37-3.31 (m, 5H), 3.29-3.25 (m, 2H), 2.76 (t, *J* = 6.5 Hz, 2H), 2.45-2.32 (m, 9H). <sup>13</sup>C NMR (125 MHz, CDCl<sub>3</sub>) δ 165.4, 159.6, 158.1, 141.0, 129.4 (2C), 127.4, 126.2 (2C), 105.8, 54.7 (2C), 51.9, 47.4, 45.8, 43.2 (2C), 38.2, 35.5, 31.7, 18.8. HRMS: C<sub>21</sub>H<sub>30</sub>N<sub>6</sub>O<sub>4</sub>S<sub>2</sub> [M+H] calcd: 495.1843, found: 495.1834. LC-MS: t<sub>R</sub>: 3.05 min, purity: > 99%, [M+H]<sup>+</sup>: 495.

**N-methyl-2-((2-(4-methylpiperazin-1-yl)-6,6-dioxido-7,8-dihydro-5H-thiopyrano[4,3-d]pyrimidin-4-yl)amino)-N-phenylethane-1-sulfonamide**

(**175b**). Dichloride **187** (0.25 g, 0.99 mmol) in dioxane (2.30 mL), DIPEA (0.52 mL, 2.96 mmol) and 2-amino-N-methyl-N-phenylethane-1-sulfonamide hydrochloride (**188b**) (0.21 g, 0.99 mmol) were reacted according with the general procedure. The crude product was purified by normal phase column chromatography (ethylacetate:methanol 95:5 to 80:20) to yield the title compound as a white solid (0.10 g, 20 %). <sup>1</sup>H NMR (500 MHz, DMSO-d<sub>6</sub>) δ 7.44-7.36 (m, 4H), 7.32-7.26 (m, 1H), 6.97 (t, *J* = 5.5 Hz, 1H), 3.91 (s, 2H), 3.63 (ddd, *J* = 9.4, 7.3 and 5.3 Hz, 2H), 3.55 (t, *J* = 5.0 Hz, 4H), 3.44-3.38 (m, 2H), 3.38-3.35 (m, 2H), 3.25 (s, 3H), 2.96 (t, *J* = 6.5 Hz, 2H), 2.19 (t, *J* = 5.1 Hz, 4H), 2.16 (s, 3H). <sup>13</sup>C NMR (125 MHz, DMSO-d<sub>6</sub>) δ 160.2, 159.6, 158.0, 141.7, 129.2 (2C), 127.2, 126.4 (2C), 94.9, 54.5 (2C), 47.4, 46.7, 46.3, 46.1, 43.3 (2C), 37.9, 35.1, 32.1. HRMS: C<sub>21</sub>H<sub>30</sub>N<sub>6</sub>O<sub>4</sub>S<sub>2</sub> [M+H] calcd: 495.1843, found: 495.1834. LC-MS: t<sub>R</sub>: 2.71 min, purity: > 99%, [M+H]<sup>+</sup>: 495.

**N-methyl-2-((2-(4-methylpiperazin-1-yl)-5,5-dioxido-7,8-dihydro-6H-thiopyrano[3,2-d]pyrimidin-4-yl)amino)-N-(pyridin-2-yl)ethane-1-sulfonamide**

(**174c**). Dichloride **186** (0.25 g, 0.99 mmol) in dioxane (2.30 mL), DIPEA (0.52 mL, 2.96 mmol) and amine **188c** (0.21 g, 0.99 mmol) were reacted according with the general procedure. The crude product was purified by normal phase column chromatography (ethylacetate:methanol 95:5 to 80:20) and subsequent trituration with methanol to yield the title compound as a white solid

(0.10 g, 20 %). <sup>1</sup>H NMR (500 MHz, DMSO-d<sub>6</sub>) δ 8.38 (ddd, *J* = 4.8, 2.0 and 0.9 Hz, 1H), 7.84 (ddd, *J* = 8.3, 7.4 and 2.0 Hz, 1H), 7.37 (d, *J* = 8.3 Hz, 1H), 7.23 (ddd, *J* = 7.4, 4.9 and 0.9 Hz, 1H), 7.10 (t, *J* = 5.8 Hz, 1H), 3.79 (dt, *J* = 7.9 and 5.7 Hz, 2H), 3.69-3.64 (m, 6H), 3.43-3.37 (m, 2H), 3.32 (s, 3H), 2.68 (t, *J* = 6.4 Hz, 2H), 2.26-2.16 (m, 9H). <sup>13</sup>C NMR (125 MHz, DMSO-d<sub>6</sub>) δ 165.9, 159.5, 157.6, 154.1, 148.4, 138.9, 121.2, 118.1, 105.9, 54.8 (2C), 51.6, 46.2, 43.5 (2C), 35.8, 35.5, 31.8, 18.8. HRMS C<sub>20</sub>H<sub>29</sub>N<sub>7</sub>O<sub>4</sub>S<sub>2</sub> [M+H] calcd: 496.1795, found: 496.1782. LC-MS: t<sub>R</sub>: 2.77 min, purity: > 99%, [M+H]<sup>+</sup>: 496.

**N-methyl-2-((2-(4-methylpiperazin-1-yl)-6,6-dioxido-7,8-dihydro-5H-thiopyrano[4,3-d]pyrimidin-4-yl)amino)-N-(pyridin-2-yl)ethane-1-sulfonamide (175c).** Dichloride **187** (0.25 g, 0.99 mmol) in dioxane (2.30 mL), DIPEA (0.52 mL, 2.96 mmol) and amine **188c** (0.22 g, 0.99 mmol) were reacted according with the general procedure. The crude product was purified by normal phase column chromatography (ethylacetate:methanol 95:5 to 80:20) to yield the title compound as a white solid (0.14 g, 29 %). <sup>1</sup>H NMR (500 MHz, DMSO-d<sub>6</sub>) δ 8.38 (dd, *J* = 4.9 and 2.0 Hz, 1H), 7.83 (ddd, *J* = 8.3, 7.3 and 2.0 Hz, 1H), 7.38 (d, *J* = 8.3 Hz, 1H), 7.23 (ddd, *J* = 7.4, 4.8, and 0.9 Hz, 1H), 6.93 (d, *J* = 5.1 Hz, 1H), 3.89 (s, 2H), 3.67-3.60 (m, 4H), 3.54-3.58 (m, 4H), 3.40 (t, *J* = 6.4 Hz, 2H), 3.32 (s, 3H), 2.96 (t, *J* = 6.6 Hz, 2H), 2.25-2.20 (m, 4H), 2.17 (s, 3H). <sup>13</sup>C NMR (125 MHz, DMSO-d<sub>6</sub>) δ 160.5, 159.9, 158.2, 154.0, 148.4, 138.9, 121.2, 117.9, 95.3, 54.7 (2C), 50.0, 47.8, 47.0, 46.1, 43.5 (2C), 35.8, 35.5, 32.4. HRMS C<sub>20</sub>H<sub>30</sub>N<sub>7</sub>O<sub>4</sub>S<sub>2</sub> [M+H] calcd: 496.1795, found: 496.1785. LC-MS: t<sub>R</sub>: 2.77 min, purity: >99%, [M+H]<sup>+</sup>: 496.

**N-(4-iodophenyl)-2-((2-(4-methylpiperazin-1-yl)-5,5-dioxido-7,8-dihydro-6H-thiopyrano[3,2-d]pyrimidin-4-yl)amino)ethane-1-sulfonamide (174d).** Dichloride **186** (0.20 g, 0.79 mmol) in dioxane (1.80 mL), DIPEA (0.45 mL, 2.61 mmol) and amine **188d** (0.26 g, 0.79 mmol) were reacted according with the general procedure. The crude product was purified by normal phase column chromatography (ethylacetate:methanol 95:5 to 80:20) and subsequent trituration with methanol to yield the title compound as a white solid (0.08 g, 17 %). <sup>1</sup>H NMR (500 MHz, DMSO-d<sub>6</sub>) δ 7.53 (d, *J* = 8.3 Hz, 2H), 7.13 (t, *J* = 5.5 Hz, 1H), 6.94 (d, *J* = 8.3 Hz, 2H), 3.78-3.70 (m, 2H), 3.66-3.55 (m, 4H), 3.44-3.37 (m, 2H), 3.28-

3.25 (m, 2H), 2.68 (t,  $J = 6.3$  Hz, 2H), 2.25-2.15 (m, 9H).  $^{13}\text{C}$  NMR (125 MHz, DMSO- $d_6$ )  $\delta$  165.7, 159.6, 157.6, 142.2, 138.0 (2C), 122.2 (2C), 105.9, 85.4, 54.8 (2C), 51.7, 49.9, 46.2, 43.5 (2C), 36.1, 31.8, 18.8. HRMS  $\text{C}_{20}\text{H}_{27}\text{IN}_6\text{O}_4\text{S}_2$  [M+H] calcd: 607.0653, found: 607.0629. LC-MS:  $t_{\text{R}}$ : 3.32 min, purity: >99%, %, [M+H] $^+$ : 607.

**N-(4-iodophenyl)-2-((2-(4-methylpiperazin-1-yl)-6,6-dioxido-7,8-dihydro-5H-thiopyrano[4,3-d]pyrimidin-4-yl)amino)ethane-1-sulfonamide (175d).**

Dichloride **187** (0.25 g, 0.99 mmol) in dioxane (2.30 mL), DIPEA (0.52 mL, 2.96 mmol) and amine **188d** (0.32 g, 0.99 mmol) were reacted according with the general procedure. The crude product was purified by normal phase column chromatography (ethylacetate:methanol 95:5 to 80:20) to yield the title compound as a white solid (0.19 g, 32 %).  $^1\text{H}$  NMR (500 MHz, DMSO- $d_6$ )  $\delta$  7.63-7.55 (m, 2H), 6.99-6.93 (m, 2H), 6.81 (t,  $J = 5.5$  Hz, 1H), 3.92 (s, 2H), 3.60 (dt,  $J = 8.1$  and 5.7 Hz, 2H), 3.51-3.47 (m, 4H), 3.44-3.37 (m, 4H), 2.95 (t,  $J = 6.5$  Hz, 2H), 2.22-2.18 (m, 7H).  $^{13}\text{C}$  NMR (125 MHz, DMSO- $d_6$ )  $\delta$  160.6, 159.8, 158.0, 138.5, 138.3 (2C), 121.3 (2C), 95.3, 95.2, 54.9 (2C), 49.3, 47.7, 47.0, 46.4, 43.6 (2C), 36.0, 32.4. HRMS  $\text{C}_{20}\text{H}_{27}\text{IN}_6\text{O}_4\text{S}_2$  [M+H] calcd: 607.0653, found: 607.0653. LC-MS:  $t_{\text{R}}$ : 2.99 min, purity: > 99%, [M+H] $^+$ : 607.

**N-methyl-2-((2-(4-methylpiperazin-1-yl)-5,5-dioxido-7,8-dihydro-6H-thiopyrano[3,2-d]pyrimidin-4-yl)amino)ethane-1-sulfonamide (174e).**

Dichloride **186** (0.25 g, 0.99 mmol) in dioxan (2.30 mL), DIPEA (0.52 mL, 2.96 mmol) and amine **188e** (0.14 g, 0.99 mmol) were reacted according with the general procedure. The crude product was purified by normal phase column chromatography (ethylacetate:methanol 95:5 to 80:20) and subsequent trituration with methanol to yield the title compound as a white solid (0.12 g, 29 %).  $^1\text{H}$  NMR (500 MHz, DMSO- $d_6$ )  $\delta$  7.13 (t,  $J = 5.8$  Hz, 1H), 7.06 (q,  $J = 4.9$  Hz, 1H), 3.80-3.68 (m, 6H), 3.44-3.38 (m, 2H), 3.24 (dd,  $J = 8.0$  and 6.1 Hz, 2H), 2.70 (t,  $J = 6.4$  Hz, 2H), 2.57 (d,  $J = 4.7$  Hz, 3H), 2.30 (t,  $J = 5.1$  Hz, 4H), 2.23-2.12 (m, 5H).  $^{13}\text{C}$  NMR (125 MHz, DMSO- $d_6$ )  $\delta$  165.4, 159.6, 157.2, 105.5, 54.4 (2C), 51.3, 47.9,

45.8, 43.1 (2C), 35.4, 31.4, 28.6, 18.4. HRMS: C<sub>15</sub>H<sub>26</sub>N<sub>6</sub>O<sub>4</sub>S<sub>2</sub> [M+H] calcd: 419.1530, found: 419.1510. LC-MS: t<sub>R</sub>: 2.15 min, purity: > 99%, [M+H]<sup>+</sup>: 419.

**N-methyl-2-((2-(4-methylpiperazin-1-yl)-6,6-dioxido-7,8-dihydro-5H-thiopyrano[4,3-d]pyrimidin-4-yl)amino)ethane-1-sulfonamide (175e).**

Dichloride **187** (0.25 g, 0.99 mmol) in dioxane (2.30 mL), DIPEA (0.52 mL, 2.96 mmol) and amine **188e** (0.14 g, 0.99 mmol) were reacted according with the general procedure. The crude product was purified by normal phase column chromatography (ethylacetate:methanol 95:5 to 80:20) to yield the title compound as a white solid (0.11 g, 27 %). <sup>1</sup>H NMR (500 MHz, DMSO-d<sub>6</sub>) δ 7.02 (q, *J* = 4.9 Hz, 1H), 6.88 (t, *J* = 5.6 Hz, 1H), 3.94 (s, 2H), 3.64 (ddd, *J* = 14.4, 7.4 and 4.6 Hz, 6H), 3.45-3.38 (m, 2H), 3.27-3.19 (m, 2H), 2.98 (t, *J* = 6.6 Hz, 2H), 2.55 (d, *J* = 5.0 Hz, 3H), 2.29 (t, *J* = 5.0 Hz, 4H), 2.18 (s, 3H). <sup>13</sup>C NMR (125 MHz, DMSO-d<sub>6</sub>) δ 160.2, 159.6, 157.7, 94.8, 54.5 (2C), 47.9, 47.3, 46.6, 45.9, 43.3 (2C), 35.4, 32.0, 28.5. HRMS: C<sub>15</sub>H<sub>26</sub>N<sub>6</sub>O<sub>4</sub>S<sub>2</sub> [M+H]: calcd: 419.1530, found: 419.1515. LC-MS: t<sub>R</sub>: 1.01 min, purity: > 99%, [M+H]<sup>+</sup>: 419.

**N-isopropyl-2-((2-(4-methylpiperazin-1-yl)-5,5-dioxido-7,8-dihydro-6H-thiopyrano[3,2-d]pyrimidin-4-yl)amino)ethane-1-sulfonamide (174f).**

Dichloride **186** (0.15 g, 0.59 mmol) in dioxane (1.40 mL), DIPEA (0.34 mL, 1.96 mmol) and amine **188f** (0.10 g, 0.59 mmol) were reacted according with the general procedure. The crude product was purified by normal phase column chromatography (ethylacetate:methanol 95:5 to 80:20) and subsequent trituration with methanol to yield the title compound as a white solid (0.10 g, 20 %). <sup>1</sup>H NMR (500 MHz, DMSO-d<sub>6</sub>) δ 7.18-7.12 (m, 2H), 3.81-3.66 (m, 6H), 3.46-3.37 (m, 3H), 3.25-3.19 (m, 2H), 2.70 (t, *J* = 6.4 Hz, 2H), 2.33-2.29 (m, 4H), 2.23-2.13 (m, 5H), 1.11 (d, *J* = 6.5 Hz, 6H). <sup>13</sup>C NMR (125 MHz, DMSO-d<sub>6</sub>) δ 165.8, 159.6, 157.7, 105.8, 54.8 (2C), 51.7, 51.1, 46.2, 45.6, 43.6 (2C), 36.1, 31.7, 24.3 (2C), 18.7. HRMS C<sub>17</sub>H<sub>30</sub>N<sub>6</sub>O<sub>4</sub>S<sub>2</sub> calcd: 447.1843, found: 447.1837. LC-MS: t<sub>R</sub>: 2.55 min, purity: > 99%, [M+H]<sup>+</sup>: 447.

**N-isopropyl-2-((2-(4-methylpiperazin-1-yl)-6,6-dioxido-7,8-dihydro-5H-thiopyrano[4,3-d]pyrimidin-4-yl)amino)ethane-1-sulfonamide (175f).**

Dichloride **187** (0.15 g, 0.59 mmol) in dioxane (1.40 mL), DIPEA (0.34 mL, 1.96

mmol) and amine **188f** (0.10 g, 0.59 mmol) were reacted according with the general procedure. The crude product was purified by normal phase column chromatography (ethylacetate:methanol 95:5 to 80:20) to yield the title compound as a white solid (0.08 g, 30 %). <sup>1</sup>H NMR (500 MHz, DMSO-d<sub>6</sub>) δ 7.13 (d, *J* = 7.3 Hz, 1H), 6.86 (t, *J* = 5.4 Hz, 1H), 3.94 (s, 2H), 3.67-3.62 (m, 6H), 3.43-3.39 (m, 3H), 3.26-3.18 (m, 2H), 2.98 (t, *J* = 6.5 Hz, 2H), 2.31-2.26 (m, 4H), 2.18 (s, 3H), 1.10 (d, *J* = 6.5 Hz, 6H). <sup>13</sup>C NMR (125 MHz, DMSO-d<sub>6</sub>) δ 160.6, 160.0, 158.1, 95.2, 54.9 (2C), 51.4, 47.8, 47.0, 46.3, 45.5, 43.7 (2C), 36.1, 32.4, 24.3 (2C). HRMS C<sub>17</sub>H<sub>30</sub>N<sub>6</sub>O<sub>4</sub>S<sub>2</sub> [M+H] calcd: 447.1843, found: 447.1837. LC-MS: t<sub>R</sub>: 1.95 min, purity: >99 %, [M+H]<sup>+</sup>: 447.

**N,N-diethyl-2-((2-(4-methylpiperazin-1-yl)-5,5-dioxido-7,8-dihydro-6H-thiopyrano[3,2-d]pyrimidin-4-yl)amino)ethane-1-sulfonamide (174g).**

Dichloride **186** (0.25 g, 0.99 mmol) in dioxane (2.30 mL), DIPEA (0.52 mL, 2.96 mmol) and amine **188g** (0.18 g, 0.99 mmol) were reacted according with the general procedure. The crude product was purified by normal phase column chromatography (ethylacetate:methanol 95:5 to 80:20) and subsequent trituration with methanol to yield the title compound as a white solid (0.11 g, 24 %). <sup>1</sup>H NMR (500 MHz, DMSO-d<sub>6</sub>) δ 7.08 (t, *J* = 5.7 Hz, 1H), 3.81-3.76 (m, 1H), 3.74 (t, *J* = 5.4 Hz, 4H), 3.44-3.39 (m, 2H), 3.29-3.26 (m, 2H), 3.20 (q, *J* = 7.1 Hz, 4H), 2.71 (t, *J* = 6.4 Hz, 2H), 2.31 (t, *J* = 5.1 Hz, 4H), 2.23-2.11 (m, 5H), 1.11 (t, *J* = 7.1 Hz, 6H). <sup>13</sup>C NMR (125 MHz, DMSO-d<sub>6</sub>) δ 165.9, 159.6, 157.7, 105.9, 54.8 (2C), 51.7, 49.6, 46.2, 43.5 (2C), 41.8 (2C), 35.8, 31.9, 18.9, 14.9 (2C). HRMS: C<sub>18</sub>H<sub>32</sub>N<sub>6</sub>O<sub>4</sub>S<sub>2</sub> [M+H] calcd: 461.1999, found: 461.1992. LC-MS: t<sub>R</sub>: 2.69 min, purity: > 99 %, [M+H]<sup>+</sup>: 461.

**N,N-diethyl-2-((2-(4-methylpiperazin-1-yl)-6,6-dioxido-7,8-dihydro-5H-thiopyrano[4,3-d]pyrimidin-4-yl)amino)ethane-1-sulfonamide (175g).**

Dichloride **187** (0.25 g, 0.99 mmol) in dioxane (2.30 mL), DIPEA (0.52 mL, 2.96 mmol) and amine **188g** (0.18 g, 0.99 mmol) were reacted according with the general procedure. The crude product was purified by normal phase column chromatography (ethylacetate:methanol 95:5 to 80:20) to yield the title compound as a white solid (0.13 g, 29 %). <sup>1</sup>H NMR (500 MHz, DMSO-d<sub>6</sub>) δ 6.93 (t, *J* = 5.5 Hz, 1H), 3.93 (s, 2H), 3.70-3.60 (m, 6H), 3.45-3.39 (m, 2H), 3.29-3.24 (m, 2H),

3.19 (q,  $J = 7.1$  Hz, 4H), 2.98 (t,  $J = 6.5$  Hz, 2H), 2.29 (t,  $J = 5.0$  Hz, 4H), 2.18 (s, 3H), 1.10 (t,  $J = 7.1$  Hz, 6H).  $^{13}\text{C}$  NMR (125 MHz, DMSO- $d_6$ )  $\delta$  160.1, 159.5, 157.8, 94.8, 54.4 (2C), 49.2, 47.3, 46.6, 45.9, 43.2 (2C), 41.2 (2C), 35.3, 31.9, 14.4 (2C). HRMS:  $\text{C}_{18}\text{H}_{32}\text{N}_6\text{O}_4\text{S}_2$  [M+H] calcd: 461.1999, found: 461.1994. LC-MS:  $t_{\text{R}}$ : 2.30 min, purity: > 99%, [M+H] $^+$ : 461.

**2-(4-methylpiperazin-1-yl)-4-((2-(pyrrolidin-1-ylsulfonyl)ethyl)amino)-7,8-dihydro-6H-thiopyrano[3,2-d]pyrimidine 5,5-dioxide (174h).** Dichloride **186** (0.25 g, 0.99 mmol) in dioxane (2.30 mL), DIPEA (0.52 mL, 2.96 mmol) and amine **188h** (0.18 g, 0.99 mmol) were reacted according with the general procedure. The crude product was purified by normal phase column chromatography (ethylacetate:methanol 95:5 to 80:20) and subsequent trituration with methanol to yield the title compound as a white solid (0.12 g, 26 %).  $^1\text{H}$  NMR (500 MHz, DMSO- $d_6$ )  $\delta$  7.09 (t,  $J = 5.8$  Hz, 1H), 3.79 (ddd,  $J = 8.7, 7.2$  and  $5.6$  Hz, 2H), 3.73 (t,  $J = 5.0$  Hz, 4H), 3.44-3.38 (m, 2H), 3.33-3.29 (m, 2H), 3.25-3.19 (m, 4H), 2.70 (t,  $J = 6.4$  Hz, 2H), 2.30 (t,  $J = 5.0$  Hz, 4H), 2.23-2.12 (m, 5H), 1.86-1.79 (m, 4H).  $^{13}\text{C}$  NMR (125 MHz, DMSO- $d_6$ )  $\delta$  165.9, 159.6, 157.7, 105.9, 54.8 (2C), 51.7, 47.7 (2C), 46.2, 46.3, 43.5 (2C), 35.6, 31.8, 25.7 (2C), 18.9. HRMS  $\text{C}_{18}\text{H}_{30}\text{N}_6\text{O}_4\text{S}_2$  [M+H] calcd: 459.1843, found: 459.1847. LC-MS:  $t_{\text{R}}$ : 2.62 min, purity: > 99%, [M+H] $^+$ : 459.

**2-(4-methylpiperazin-1-yl)-4-((2-(pyrrolidin-1-ylsulfonyl)ethyl)amino)-7,8-dihydro-5H-thiopyrano[4,3-d]pyrimidine 6,6-dioxide (175h).** Dichloride **187** (0.25 g, 0.99 mmol) in dioxane (2.30 mL), DIPEA (0.52 mL, 2.96 mmol) and amine **188h** (0.18 g, 0.99 mmol) were reacted according with the general procedure. The crude product was purified by normal phase column chromatography (ethylacetate:methanol 95:5 to 80:20) to yield the title compound as a white solid (0.17 g, 38 %).  $^1\text{H}$  NMR (500 MHz, DMSO- $d_6$ )  $\delta$  6.96 (t,  $J = 5.5$  Hz, 1H), 3.93 (s, 2H), 3.72-3.61 (m, 6H), 3.45-3.39 (m, 2H), 3.33-3.27 (m, 3H), 3.24-3.18 (m, 4H), 2.98 (t,  $J = 6.5$  Hz, 2H), 2.38-2.27 (m, 4H), 2.20 (s, 3H), 1.85-1.78 (m, 4H).  $^{13}\text{C}$  NMR (125 MHz, DMSO- $d_6$ )  $\delta$  160.1, 159.5, 157.8, 94.8, 54.4 (2C), 47.3 (3C), 46.6,

45.7, 45.5, 43.1 (2C), 35.1, 31.9, 25.3 (2C). HRMS C<sub>18</sub>H<sub>30</sub>N<sub>6</sub>O<sub>4</sub>S<sub>2</sub> [M+H] calcd: 459.1843, found: 459.1835. LC-MS: t<sub>R</sub>: 2.06 min, purity: > 99%, [M+H]<sup>+</sup>: 459.

**2-(4-methylpiperazin-1-yl)-4-((2-(piperidin-1-ylsulfonyl)ethyl)amino)-7,8-dihydro-6H-thiopyrano[3,2-d]pyrimidine 5,5-dioxide (174i).** Dichloride **186** (0.25 g, 0.99 mmol) in dioxane (2.30 mL), DIPEA (0.52 mL, 2.96 mmol) and amine **188i** (0.19 g, 0.99 mmol) were reacted according with the general procedure. The crude product was purified by normal phase column chromatography (ethylacetate:methanol 95:5 to 80:20) and subsequent trituration with methanol to yield the title compound as a white solid (0.10 g, 21 %). <sup>1</sup>H NMR (500 MHz, DMSO-d<sub>6</sub>) δ 7.09 (t, *J* = 5.7 Hz, 1H), 3.82-3.75 (m, 2H), 3.73 (t, *J* = 5.1 Hz, 4H), 3.45-3.38 (m, 2H), 3.27-3.21 (m, 2H), 3.16-3.09 (m, 4H), 2.70 (t, *J* = 6.4 Hz, 2H), 2.30 (t, *J* = 5.1 Hz, 4H), 2.24-2.13 (m, 5H), 1.53 (q, *J* = 5.4 Hz, 4H), 1.48 (d, *J* = 6.1 Hz, 2H). <sup>13</sup>C NMR (125 MHz, DMSO-d<sub>6</sub>) δ 165.4, 159.1, 157.2, 105.5, 54.4 (2C), 51.2, 46.2, 45.8 (2C), 45.7, 43.1 (2C), 35.1, 31.4, 25.1 (2C), 23.1, 18.4. HRMS C<sub>19</sub>H<sub>32</sub>N<sub>6</sub>O<sub>4</sub>S<sub>2</sub> [M+H] calcd: 473.1999, found: 473.1987, [M+Na] calcd: 495.1819, found: 495.1833. LC-MS: t<sub>R</sub>: 2.89 min, purity: > 99%, [M+H]<sup>+</sup>: 473.

**2-(4-methylpiperazin-1-yl)-4-((2-(piperidin-1-ylsulfonyl)ethyl)amino)-7,8-dihydro-5H-thiopyrano[4,3-d]pyrimidine 6,6-dioxide (175i).** Dichloride **187** (0.25 g, 0.99 mmol) in dioxane (2.30 mL), DIPEA (0.52 mL, 2.96 mmol) and amine **188i** (0.19 g, 0.99 mmol) were reacted according with the general procedure. The crude product was purified by normal phase column chromatography (ethylacetate:methanol 95:5 to 80:20) to yield the title compound as a white solid (0.11 g, 23 %). <sup>1</sup>H NMR (500 MHz, DMSO-d<sub>6</sub>) δ 6.98 (t, *J* = 5.5 Hz, 1H), 3.94 (s, 2H), 3.69-3.64 (m, 6H), 3.42 (t, *J* = 6.6 Hz, 2H), 3.23 (dd, *J* = 8.8 and 5.8 Hz, 2H), 3.12 (t, *J* = 5.2 Hz, 4H), 2.98 (t, *J* = 6.6 Hz, 2H), 2.40-2.29 (m, 4H), 2.22 (s, 3H), 1.54 (app p, *J* = 5.3 Hz, 4H), 1.48 (q, *J* = 5.7 Hz, 2H). <sup>13</sup>C NMR (125 MHz, DMSO-d<sub>6</sub>) δ 160.1, 159.5, 157.8, 94.9, 54.3 (2C), 47.3, 46.6, 46.1, 45.8 (2C), 45.6, 43.0 (2C), 35.0, 31.9, 25.1 (2C), 23.1. HRMS C<sub>19</sub>H<sub>32</sub>N<sub>6</sub>O<sub>4</sub>S<sub>2</sub> [M+H] calcd: 473.1999, found: 473.1989. LC-MS: t<sub>R</sub>: 2.39 min, purity: > 99%, [M+H]<sup>+</sup>: 473.

**2-(4-methylpiperazin-1-yl)-4-((2-((2-methylpiperidin-1-yl)sulfonyl)ethyl)amino)-7,8-dihydro-6H-thiopyrano[3,2-d]pyrimidine 5,5-**

**dioxide (174l).** Dichloride **186** (0.25 g, 0.99 mmol) in dioxane (2.30 mL), DIPEA (0.52 mL, 2.96 mmol) and amine **188l** (0.20 g, 0.99 mmol) were reacted according with the general procedure. The crude product was purified by normal phase column chromatography (ethylacetate:methanol 95:5 to 80:20) and subsequent trituration with methanol to yield the title compound as a white solid (0.11 g, 23 %). <sup>1</sup>H NMR (500 MHz, DMSO-d<sub>6</sub>) δ 7.09 (t, *J* = 5.7 Hz, 1H), 4.00 (t, *J* = 6.1 Hz, 1H), 3.77-3.72 (m, 6H), 3.44-3.38 (m, 2H), 3.26-3.21 (m, 2H), 3.02 (td, *J* = 13.0 and 2.6 Hz, 2H), 2.70 (t, *J* = 6.4 Hz, 2H), 2.30 (t, *J* = 5.0 Hz, 4H), 2.23-2.11 (m, 5H), 1.68-1.55 (m, 2H), 1.55-1.44 (m, 2H), 1.41-1.31 (m, 2H), 1.18 (d, *J* = 6.9 Hz, 3H). <sup>13</sup>C NMR (125 MHz, DMSO-d<sub>6</sub>) δ 165.4, 159.2, 157.2, 105.5, 54.4 (2C), 51.2, 50.0, 47.9, 45.7, 43.1 (2C), 35.6, 31.4, 30.3, 25.3, 18.4, 17.8, 16.0. HRMS C<sub>20</sub>H<sub>34</sub>N<sub>6</sub>O<sub>4</sub>S<sub>2</sub> [M+H] calcd: 487.2156, found: 487.2153. LC-MS: t<sub>R</sub>: 3.10 min, purity: > 99%, [M+H]<sup>+</sup>: 487.

**2-(4-methylpiperazin-1-yl)-4-((2-((2-methylpiperidin-1-yl)sulfonyl)ethyl)amino)-7,8-dihydro-5H-thiopyrano[4,3-d]pyrimidine 6,6-dioxide (175l).** Dichloride **187** (0.25 g, 0.99 mmol) in dioxane (2.30 mL), DIPEA (0.52 mL, 2.96 mmol) and amine **188l** (0.20 g, 0.99 mmol) were reacted according with the general procedure. The crude product was purified by normal phase column chromatography (ethylacetate:methanol 95:5 to 80:20) to yield the title compound as a white solid (0.17 g, 35 %). <sup>1</sup>H NMR (500 MHz, DMSO-d<sub>6</sub>) δ 6.92 (t, *J* = 5.4 Hz, 1H), 4.04-3.97 (m, 1H), 3.93 (s, 2H), 3.69-3.62 (m, 6H), 3.41 (t, *J* = 8.2 Hz, 2H), 3.31-3.20 (m, 2H), 3.05-2.94 (m, 3H), 2.32-2.28 (m, 4H), 2.20 (s, 3H), 1.65-1.55 (m, 3H), 1.54-1.43 (m, 3H), 1.40-1.29 (m, 1H), 1.18 (d, *J* = 6.9 Hz, 3H). <sup>13</sup>C NMR (125 MHz, DMSO-d<sub>6</sub>) δ 160.6, 160.0, 158.2, 95.3, 54.8 (2C), 50.6, 48.3, 47.8, 47.0, 46.3, 43.6 (2C), 36.0, 32.4, 30.8, 26.8, 25.8, 18.2, 16.4. HRMS C<sub>20</sub>H<sub>34</sub>N<sub>6</sub>O<sub>4</sub>S<sub>2</sub> [M+H] calcd: 487.2156, found: 487.2158. LC-MS: t<sub>R</sub>: 2.58 min, purity: > 99%, [M+H]<sup>+</sup>: 487.

**2-(4-methylpiperazin-1-yl)-4-((2-(morpholinosulfonyl)ethyl)amino)-7,8-dihydro-6H-thiopyrano[3,2-d]pyrimidine 5,5-dioxide (174m).** Dichloride **186** (0.25 g, 0.99 mmol) in dioxane (2.30 mL), DIPEA (0.52 mL, 2.96 mmol) and amine **188m** (0.19 g, 0.99 mmol) were reacted according with the general procedure. The crude product was purified by normal phase column chromatography

(ethylacetate:methanol 95:5 to 80:20) and subsequent trituration with methanol to yield the title compound as a white solid (0.08 g, 17 %). <sup>1</sup>H NMR (500 MHz, DMSO-d<sub>6</sub>) δ 7.09 (t, *J* = 5.8 Hz, 1H), 3.84-3.78 (m, 2H), 3.73 (t, *J* = 4.9 Hz, 4H), 3.63 (dd, *J* = 5.9 and 3.5 Hz, 4H), 3.45-3.38 (m, 2H), 3.18-3.09 (m, 4H), 2.70 (t, *J* = 6.4 Hz, 2H), 2.30 (t, *J* = 5.0 Hz, 4H), 2.23-2.14 (m, 5H). <sup>13</sup>C NMR (125 MHz, DMSO-d<sub>6</sub>) δ 165.9, 159.7, 157.7, 106.0, 66.3 (2C), 54.8 (2C), 51.7, 46.5, 46.2, 45.7 (2C), 43.6 (2C), 35.5, 31.9, 18.9. HRMS: C<sub>18</sub>H<sub>30</sub>N<sub>6</sub>O<sub>5</sub>S<sub>2</sub> [M+H] calcd: 475.1792, found: 475.1784. LC-MS: t<sub>R</sub>: 2.44 min, purity: > 99%, [M+H]<sup>+</sup>: 475.

**2-(4-methylpiperazin-1-yl)-4-((2-(morpholinosulfonyl)ethyl)amino)-7,8-dihydro-5H-thiopyrano[4,3-d]pyrimidine 6,6-dioxide (175m).** Dichloride **187** (0.25 g, 0.99 mmol) in dioxane (2.30 mL), DIPEA (0.52 mL, 2.96 mmol) and amine **188m** (0.19 g, 0.99 mmol) were reacted according with the general procedure. The crude product was purified by normal phase column chromatography (ethylacetate:methanol 95:5 to 80:20) to yield the title compound as a white solid (0.09 g, 19 %). <sup>1</sup>H NMR (500 MHz, DMSO-d<sub>6</sub>) δ 6.98 (t, *J* = 5.6 Hz, 1H), 3.93 (s, 2H), 3.72-3.64 (m, 6H), 3.64-3.59 (m, 4H), 3.42 (t, *J* = 6.6 Hz, 2H), 3.31-3.26 (m, 2H), 3.15-3.09 (m, 4H), 2.98 (t, *J* = 6.6 Hz, 2H), 2.29 (t, *J* = 5.0 Hz, 4H), 2.18 (s, 3H). <sup>13</sup>C NMR (125 MHz, DMSO) δ 160.6, 160.0, 158.3, 95.3, 66.2 (2C), 54.9 (2C), 47.8, 47.0, 46.3, 46.3, 45.7 (2C), 43.7 (2C), 35.3, 32.4. HRMS C<sub>18</sub>H<sub>30</sub>N<sub>6</sub>O<sub>5</sub>S<sub>2</sub> [M+H] calcd: 475.1792, found: 475.1782. LC-MS (basic mode): t<sub>R</sub>: 3.99 min, purity: >99%.

**N-cyclohexyl-N-methyl-2-((2-(4-methylpiperazin-1-yl)-5,5-dioxido-7,8-dihydro-6H-thiopyrano[3,2-d]pyrimidin-4-yl)amino)ethane-1-sulfonamide (174n).** Dichloride **186** (0.25 g, 0.99 mmol) in dioxane (2.30 mL), DIPEA (0.52 mL, 2.96 mmol) and amine **188n** (0.22 g, 0.99 mmol) were reacted according with the general procedure. The crude product was purified by normal phase column chromatography (ethylacetate:methanol 95:5 to 80:20) and subsequent trituration with methanol to yield the title compound as a white solid (0.12 g, 24 %). <sup>1</sup>H NMR (500 MHz, DMSO-d<sub>6</sub>) δ 7.09 (t, *J* = 5.8 Hz, 1H), 3.81-3.67 (m, 6H), 3.56-3.45 (m, 1H), 3.44-3.39 (m, 2H), 3.29-3.23 (m, 2H), 2.71-2.68 (m, 5H), 2.30 (t, *J* = 5.1 Hz, 4H), 2.24-2.13 (m, 5H), 1.78-1.73 (m, 2H), 1.67-1.62 (m, 2H), 1.61-1.55 (m, 1H), 1.54-1.45 (m, 2H), 1.35-1.23 (m, 2H), 1.12-0.99 (m, 1H). <sup>13</sup>C NMR (125 MHz,

DMSO- $d_6$ )  $\delta$  165.9, 159.6, 157.6, 105.9, 56.4, 54.9 (2C), 51.7, 49.4, 46.2, 43.5 (2C), 35.9, 31.9, 30.7 (2C), 28.7, 25.8 (2C), 25.2, 18.9. HRMS  $C_{21}H_{36}N_6O_4S_2$  [M+H] calcd: 501.2312, found: 501.2298. LC-MS:  $t_R$ : 3.34 min, purity: > 99%, [M+H]<sup>+</sup>: 501.

**N-cyclohexyl-N-methyl-2-((2-(4-methylpiperazin-1-yl)-6,6-dioxido-7,8-dihydro-5H-thiopyrano[4,3-d]pyrimidin-4-yl)amino)ethane-1-sulfonamide (175n).** Dichloride **187** (0.25 g, 0.99 mmol) in dioxane (2.30 mL), DIPEA (0.52 mL, 2.96 mmol) and amine **188n** (0.22 g, 0.99 mmol) were reacted according with the general procedure. The crude product was purified by normal phase column chromatography (ethylacetate:methanol 95:5 to 80:20) to yield the title compound as a white solid (0.23 g, 47 %). <sup>1</sup>H NMR (500 MHz, DMSO- $d_6$ )  $\delta$  6.93 (t,  $J$  = 5.5 Hz, 1H), 3.93 (s, 2H), 3.67-3.61 (m, 6H), 3.50 (tt,  $J$  = 11.9 and 3.7 Hz, 1H), 3.44-3.40 (m, 2H), 3.29-3.22 (m, 2H), 2.98 (t,  $J$  = 6.5 Hz, 2H), 2.69 (s, 3H), 2.29 (t,  $J$  = 5.0 Hz, 4H), 2.18 (s, 3H), 1.77-1.68 (m, 2H), 1.61-1.54 (m, 3H), 1.48-1.45 (m, 2H), 1.29-1.26 (m, 2H), 1.06-1.03 (m, 1H). <sup>13</sup>C NMR (125 MHz, DMSO- $d_6$ )  $\delta$  160.6, 160.0, 158.2, 95.3, 56.4, 54.9 (2C), 49.4, 47.8, 47.1, 46.4, 43.7 (2C), 35.9, 32.4, 30.7 (2C), 28.7, 25.8 (2C), 25.2. HRMS  $C_{21}H_{36}N_6O_4S_2$  [M+H] calcd: 501.2312, found: 501.2295. LC-MS:  $t_R$ : 2.92 min, purity: > 99%, [M+H]<sup>+</sup>: 501.

**N-benzyl-2-((2-(4-methylpiperazin-1-yl)-5,5-dioxido-7,8-dihydro-6H-thiopyrano[3,2-d]pyrimidin-4-yl)amino)ethane-1-sulfonamide (174o).** Dichloride **186** (0.25 g, 0.99 mmol) in dioxane (2.30 mL), DIPEA (0.52 mL, 2.96 mmol) and 2-amino-N-benzylethane-1-sulfonamide (**188o**) (0.21 g, 0.99 mmol) were reacted according with the general procedure. The crude product was purified by normal phase column chromatography (ethylacetate:methanol 95:5 to 80:20) and subsequent trituration with methanol to yield the title compound as a white solid (0.30 g, 61 %). <sup>1</sup>H NMR (500 MHz, DMSO- $d_6$ )  $\delta$  7.76 (t,  $J$  = 6.3 Hz, 1H), 7.36-7.32 (m, 4H), 7.29-7.25 (m, 1H), 7.12 (t,  $J$  = 5.8 Hz, 1H), 4.15 (d,  $J$  = 6.3 Hz, 2H), 3.78 (dt,  $J$  = 7.5 and 5.9 Hz, 2H), 3.72 (t,  $J$  = 5.2 Hz, 4H), 3.45-3.39 (m, 2H), 3.25-3.22 (m, 2H), 2.70 (t,  $J$  = 6.4 Hz, 2H), 2.29 (t,  $J$  = 5.1 Hz, 4H), 2.22-2.17 (m, 5H). <sup>13</sup>C NMR (125 MHz, DMSO- $d_6$ )  $\delta$  165.4, 159.2, 157.2, 138.3, 128.3 (2C), 127.6 (2C), 127.2, 105.5, 54.4 (2C), 51.2, 50.1, 45.8, 45.7, 43.1 (2C), 35.4, 31.4, 18.4.

HRMS C<sub>21</sub>H<sub>30</sub>N<sub>6</sub>O<sub>4</sub>S<sub>2</sub> [M+H] calcd: 495.1843, found: 495.1852. LC-MS: t<sub>R</sub>: 2.91 min, purity: > 99%, [M+H]<sup>+</sup>: 495.

**N-benzyl-2-((2-(4-methylpiperazin-1-yl)-6,6-dioxido-7,8-dihydro-5H-thiopyrano[4,3-d]pyrimidin-4-yl)amino)ethane-1-sulfonamide (175o).**

Dichloride **187** (0.25 g, 0.99 mmol) in dioxane (2.30 mL), DIPEA (0.52 mL, 2.96 mmol) and 2-amino-N-benzylethane-1-sulfonamide (**188o**) (0.21 g, 0.99 mmol) were reacted according with the general procedure. The crude product was purified by normal phase column chromatography (ethylacetate:methanol 95:5 to 80:20) to yield the title compound as a white solid (0.34, 70 %). <sup>1</sup>H NMR (500 MHz, DMSO-d<sub>6</sub>) δ 7.72 (t, *J* = 6.3 Hz, 1H), 7.36-7.29 (m, 4H), 7.29-7.23 (m, 1H), 6.86 (t, *J* = 5.6 Hz, 1H), 4.13 (d, *J* = 6.2 Hz, 2H), 3.94 (s, 2H), 3.67-3.63 (m, 6H), 3.45-3.39 (m, 2H), 3.26-3.19 (m, 2H), 2.98 (t, *J* = 6.5 Hz, 2H), 2.28 (t, *J* = 5.0 Hz, 4H), 2.18 (s, 3H). <sup>13</sup>C NMR (125 MHz, DMSO-d<sub>6</sub>) δ 160.1, 159.6, 157.7, 138.2, 128.4 (2C), 127.5 (2C), 127.2, 94.8, 54.5 (2C), 50.3, 47.3, 46.6, 45.9, 45.9, 43.2 (2C), 35.5, 31.9. HRMS C<sub>21</sub>H<sub>30</sub>N<sub>6</sub>O<sub>4</sub>S<sub>2</sub> [M+H] calcd: 495.1843, found: 495.1839. LC-MS: t<sub>R</sub>: 2.46 min, purity: > 99%, [M+H]<sup>+</sup>: 495.

**2-((2-(4-methylpiperazin-1-yl)-5,5-dioxido-7,8-dihydro-6H-thiopyrano[3,2-d]pyrimidin-4-yl)amino)-N-(pyridin-2-ylmethyl)ethane-1-sulfonamide (174p).**

Dichloride **186** (0.15 g, 0.59 mmol) in dioxane (1.40 mL), DIPEA (0.34 mL, 1.96 mmol) and amine **188p** (0.13 g, 0.59 mmol) were reacted according with the general procedure. The crude product was purified by normal phase column chromatography (ethylacetate:methanol 95:5 to 80:20) and subsequent trituration with methanol to yield the title compound as a white solid (0.09 g, 31 %). <sup>1</sup>H NMR (500 MHz, DMSO-d<sub>6</sub>) δ 8.52-8.46 (m, 1H), 7.87 (t, *J* = 6.3 Hz, 1H), 7.82-7.78 (m, 1H), 7.45 (d, *J* = 7.9 Hz, 1H), 7.29 (dd, *J* = 7.5 and 4.8 Hz, 1H), 7.11 (t, *J* = 5.8 Hz, 1H), 4.25 (d, *J* = 6.2 Hz, 2H), 3.81-3.78 (m, 2H), 3.75-3.69 (m, 4H), 3.43-3.39 (m, 2H), 3.33-3.30 (m, 2H), 2.70 (t, *J* = 6.4 Hz, 2H), 2.32-2.25 (m, 4H), 2.23-2.13 (m, 5H). <sup>13</sup>C NMR (125 MHz, DMSO-d<sub>6</sub>) δ 165.8, 159.5, 158.3, 157.7, 149.3, 137.3, 122.9, 121.9, 105.9, 54.8 (2C), 51.7, 50.6, 48.0, 46.2, 43.4 (2C), 35.8, 31.9, 18.9. HRMS C<sub>20</sub>H<sub>29</sub>N<sub>7</sub>O<sub>4</sub>S<sub>2</sub> [M+H] calcd: 496.1795, found: 496.1789. LC-MS: t<sub>R</sub>: 2.09 min, purity: > 99%, [M+H]<sup>+</sup>: 496.

**2-((2-(4-methylpiperazin-1-yl)-6,6-dioxido-7,8-dihydro-5H-thiopyrano[4,3-d]pyrimidin-4-yl)amino)-N-(pyridin-2-ylmethyl)ethane-1-sulfonamide (175p).** Dichloride **187** (0.25 g, 0.99 mmol) in dioxane (2.30 mL), DIPEA (0.52 mL, 2.96 mmol) and amine **188p** (0.21 g, 0.99 mmol) were reacted according with the general procedure. The crude product was purified by normal phase column chromatography (ethylacetate:methanol 95:5 to 80:20) to yield the title compound as a white solid (0.12 g, 24 %). <sup>1</sup>H NMR (500 MHz, DMSO-d<sub>6</sub>) δ 8.49 (dd, *J* = 4.9 and 1.8 Hz, 1H), 7.84-7.75 (m, 2H), 7.45 (d, *J* = 7.8 Hz, 1H), 7.34-7.27 (m, 1H), 6.87 (t, *J* = 5.6 Hz, 1H), 4.24 (s, 2H), 3.94 (s, 2H), 3.70-3.61 (m, 5H), 3.41 (t, *J* = 6.5 Hz, 2H), 3.32-3.28 (m, 2H), 2.98 (t, *J* = 6.5 Hz, 2H), 2.32-2.26 (m, 4H), 2.17 (s, 3H). <sup>13</sup>C NMR (125 MHz, DMSO-d<sub>6</sub>) δ 160.6, 160.0, 158.2, 158.1, 149.3, 137.3, 122.9, 122.0, 95.3, 54.9 (2C), 50.8, 48.1, 47.8, 47.1, 46.3, 43.7 (2C), 36.0, 32.4. HRMS C<sub>20</sub>H<sub>29</sub>N<sub>7</sub>O<sub>4</sub>S<sub>2</sub> [M+H] calcd:496.1795, found: 496.1789. LC-MS: t<sub>R</sub>: 0.93 min, purity: 98%, [M+H]<sup>+</sup>: 496.

**4-((2-((3,4-dihydroquinolin-1(2H)-yl)sulfonyl)ethyl)amino)-2-(4-methylpiperazin-1-yl)-7,8-dihydro-6H-thiopyrano[3,2-d]pyrimidine 5,5-dioxide (174q).** Dichloride **186** (0.25 g, 0.99 mmol) in dioxane (2.30 mL), DIPEA (0.52 mL, 2.96 mmol) and amine **188q** (0.24 g, 0.99 mmol) were reacted according with the general procedure. The crude product was purified by normal phase column chromatography (ethylacetate:methanol 95:5 to 80:20) and subsequent trituration with methanol to yield the title compound as a white solid (0.130 g, 25 %). <sup>1</sup>H NMR (500 MHz, DMSO-d<sub>6</sub>) δ 7.52 (d, *J* = 7.8 Hz, 1H), 7.12-7.18 (m, 2H), 7.11 (t, *J* = 5.8 Hz, 1H), 7.07 (dd, *J* = 7.4 and 1.0 Hz, 1H), 3.83-3.75 (m, 2H), 3.74-3.69 (m, 2H), 3.68-3.65 (m, 4H), 3.49-3.43 (m, 2H), 3.42-3.39 (m, 2H), 2.81 (t, *J* = 6.6 Hz, 2H), 2.70 (t, *J* = 6.4 Hz, 2H), 2.30-2.25 (m, 4H), 2.23-2.13 (m, 5H), 1.97-1.88 (m, 2H). <sup>13</sup>C NMR (125 MHz, DMSO-d<sub>6</sub>) δ 165.9, 159.5, 157.6, 137.0, 130.1, 129.8, 126.7, 124.5, 122.4, 105.9, 54.8 (2C), 51.6, 50.2, 46.5, 46.2, 43.5 (2C), 35.6, 31.8, 26.8, 22.5, 18.8. HRMS C<sub>23</sub>H<sub>32</sub>N<sub>6</sub>O<sub>4</sub>S<sub>2</sub> [M+H] calcd: 521.1999, found: 521.1987. LC-MS: t<sub>R</sub>:3.32 min, purity: > 99%, [M+H]<sup>+</sup>: 521.

**4-((2-((3,4-dihydroquinolin-1(2H)-yl)sulfonyl)ethyl)amino)-2-(4-methylpiperazin-1-yl)-7,8-dihydro-5H-thiopyrano[4,3-d]pyrimidine 6,6-dioxide (175q).** Dichloride **187** (0.25 g, 0.99 mmol) in dioxane (2.30 mL), DIPEA

(0.52 mL, 2.96 mmol) and amine **188q** (0.24 g, 0.99 mmol) were reacted according with the general procedure. The crude product was purified by normal phase column chromatography (ethylacetate:methanol 95:5 to 80:20) to yield the title compound as a white solid (0.15 g, 30 %). <sup>1</sup>H NMR (500 MHz, DMSO-d<sub>6</sub>) δ 7.51 (dd, *J* = 8.2 and 1.2 Hz, 1H), 7.18-7.11 (m, 2H), 7.07-7.04 (m, 1H), 6.92 (t, *J* = 5.5 Hz, 1H), 3.88 (s, 2H), 3.74-3.67 (m, 2H), 3.66-3.63 (m, 2H), 3.61-3.52 (m, 4H), 3.46-3.36 (m, 4H), 2.96 (t, *J* = 6.5 Hz, 2H), 2.78 (t, *J* = 6.6 Hz, 2H), 2.24-2.18 (m, 7H), 1.95-1.86 (m, 2H). <sup>13</sup>C NMR (125 MHz, DMSO-d<sub>6</sub>) δ 160.1, 159.5, 157.8, 136.6, 129.7, 129.3, 126.3, 124.1, 121.9, 94.8, 54.4 (2C), 49.7, 47.3, 46.6, 46.0, 45.9, 43.1 (2C), 35.1, 31.9, 26.4, 22.1. HRMS C<sub>23</sub>H<sub>32</sub>N<sub>6</sub>O<sub>4</sub>S<sub>2</sub> [M+H] calcd: 521.1999, found: 521.1997. LC-MS: t<sub>R</sub>: 2.89 min, purity: > 99%, [M+H]<sup>+</sup>: 521.

## 5. LIST OF ABBREVIATIONS

3 $\beta$ -HSD2, 3 $\beta$ -hydroxysteroid dehydrogenase; 4-OHA, 4-hydroxyandrostenedione; AC, adenylate cyclase; AF1, independent activation function; AF2, ligand-dependent activation domain; AG, Aminoglutethimide; AIs, aromatase inhibitors; AJCC, American Joint Committee on Cancer; ALDH, aldehyde dehydrogenase; AR, aromatase; ASD, androstendione; ATAC, Arimidex, Tamoxifen, Alone or in Combination; BC, breast cancer; BCFI, breast cancer-free interval; BIG, Breast International Group; BPO, benzoyl peroxide; cAMP, cyclic adenosine monophosphate; CNS, central nervous system; CPR, NADPH-cytochrome P450 reductase; CYP19A1, cytochrome P450 hemeprotein; DAO, diamine oxidase; DBD, DNA binding domain; DCIS, ductal carcinoma in situ; DFS, disease-free survival; DHEA, dehydropiandrosterone; DIPEA, N,N-Diisopropylethylamine; DMF, dimethylformamide; E1, estrone; E2, 17 $\beta$ -estradiol; E3, 17 $\beta$ ,16 $\alpha$ -estriol; END, endoxifen; ER, estrogen receptor; ER+, estrogen receptor positive; ERE, estrogen response elements; ERK, extracellular signal-regulated kinase; ET, electronic transfer; EXE, exemestane; FAD, flavin adenine dinucleotide; FDA, Food and Drug Administration; FMN, flavin mononucleotide; GDP, guanosine diphosphate, GPCR, G protein-coupled receptor; GPER1, G protein-coupled estrogen receptor; GTP, guanosine triphosphate HER2, human epidermal growth factor receptor 2; HR, histamine receptor; HTM, histamine N-methyltransferase; ICI, Imperial Chemical Industries; LBD, ligand-binding domain; LCIS, lobular carcinoma in situ; LTFU, Long-Term Follow-Up; LTZ, letrozole; MAO B, monoamine oxidase B; MD, molecular dynamics; mERs, membrane estrogen receptors; MM-GBSA, molecular mechanics generalized born surface; MTS, medium throughput screening; NBS, *N*-bromosuccinimide; NGS, Nottingham Grading System; NST, no special type; NTD, N-terminus domain; P450c17, 17 $\alpha$ -hydroxylase; P450scc, cholesterol side-chain cleavage enzyme; P5, pregnenolone; PI3K, phosphoinositide 3-kinase; PKA, protein kinase A; PKC, protein kinase C; PPA, polyphosphoric acid; PR, progesterone receptor; PTX, pertussis toxin; QM, quantum mechanics; QM/MM, quantum mechanics/molecular mechanics; SERDs, Selective Estrogen Receptor Degraders; SERMs, Selective Estrogen Receptor Modulators; StAR, steroidogenic acute regulatory protein; TAM, tamoxifen; THF,

tetrahydrofuran; THIQ, tetrahydroisoquinoline; TM, transmembrane domain; TST, testosterone; VS, virtual screening; WHO, World Health Organization.

## 6. REFERENCES

1. American Cancer Society. Breast Cancer Facts & Figures 2019-2020. Atlanta, 2019.
2. Libson, S.; Lippman, M., A review of clinical aspects of breast cancer. *Int Rev Psychiatry* **2014**, *26* (1), 4-15.
3. Fahad Ullah, M., Breast Cancer: Current Perspectives on the Disease Status. *Adv Exp Med Biol* **2019**, *1152*, 51-64.
4. Vuong, D.; Simpson, P. T.; Green, B.; Cummings, M. C.; Lakhani, S. R., Molecular classification of breast cancer. *Virchows Arch* **2014**, *465* (1), 1-14.
5. Rakha, E. A.; Reis-Filho, J. S.; Baehner, F.; Dabbs, D. J.; Decker, T.; Eusebi, V.; Fox, S. B.; Ichihara, S.; Jacquemier, J.; Lakhani, S. R.; Palacios, J.; Richardson, A. L.; Schnitt, S. J.; Schmitt, F. C.; Tan, P. H.; Tse, G. M.; Badve, S.; Ellis, I. O., Breast cancer prognostic classification in the molecular era: the role of histological grade. *Breast Cancer Res* **2010**, *12* (4), 207.
6. Tsang, J. Y. S.; Tse, G. M., Molecular Classification of Breast Cancer. *Adv Anat Pathol* **2020**, *27* (1), 27-35.
7. Gruber, C. J.; Tschugguel, W.; Schneeberger, C.; Huber, J. C., Production and actions of estrogens. *N Engl J Med* **2002**, *346* (5), 340-52.
8. Miller, W. L., Steroidogenesis: Unanswered Questions. *Trends Endocrinol Metab* **2017**, *28* (11), 771-793.
9. Vrtačnik, P.; Ostanek, B.; Mencej-Bedrač, S.; Marc, J., The many faces of estrogen signaling. *Biochem Med (Zagreb)* **2014**, *24* (3), 329-42.
10. Ghosh, D.; Lo, J.; Egbuta, C., Recent Progress in the Discovery of Next Generation Inhibitors of Aromatase from the Structure-Function Perspective. *J Med Chem* **2016**, *59* (11), 5131-48.
11. Di Nardo, G.; Gilardi, G., Human aromatase: perspectives in biochemistry and biotechnology. *Biotechnol Appl Biochem* **2013**, *60* (1), 92-101.
12. Toda, K.; Terashima, M.; Kawamoto, T.; Sumimoto, H.; Yokoyama, Y.; Kuribayashi, I.; Mitsuuchi, Y.; Maeda, T.; Yamamoto, Y.; Sagara, Y., Structural and functional characterization of human aromatase P-450 gene. *Eur J Biochem* **1990**, *193* (2), 559-65.
13. Means, G. D.; Mahendroo, M. S.; Corbin, C. J.; Mathis, J. M.; Powell, F. E.; Mendelson, C. R.; Simpson, E. R., Structural analysis of the gene encoding

human aromatase cytochrome P-450, the enzyme responsible for estrogen biosynthesis. *J Biol Chem* **1989**, *264* (32), 19385-91.

14. Harada, N.; Yamada, K.; Saito, K.; Kibe, N.; Dohmae, S.; Takagi, Y., Structural characterization of the human estrogen synthetase (aromatase) gene. *Biochem Biophys Res Commun* **1990**, *166* (1), 365-72.

15. Bulun, S. E.; Sebastian, S.; Takayama, K.; Suzuki, T.; Sasano, H.; Shozu, M., The human CYP19 (aromatase P450) gene: update on physiologic roles and genomic organization of promoters. *J Steroid Biochem Mol Biol* **2003**, *86* (3-5), 219-24.

16. Simpson, E. R.; Clyne, C.; Rubin, G.; Boon, W. C.; Robertson, K.; Britt, K.; Speed, C.; Jones, M., Aromatase--a brief overview. *Annu Rev Physiol* **2002**, *64*, 93-127.

17. Iyanagi, T.; Xia, C.; Kim, J. J., NADPH-cytochrome P450 oxidoreductase: prototypic member of the diflavin reductase family. *Arch Biochem Biophys* **2012**, *528* (1), 72-89.

18. Ritacco, I.; Saltalamacchia, A.; Spinello, A.; Ippoliti, E.; Magistrato, A., All-Atom Simulations Disclose How Cytochrome Reductase Reshapes the Substrate Access/Egress Routes of Its Partner CYP450s. *J Phys Chem Lett* **2020**, *11* (4), 1189-1193.

19. Caciolla, J.; Bisi, A.; Belluti, F.; Rampa, A.; Gobbi, S., Reconsidering Aromatase for Breast Cancer Treatment: New Roles for an Old Target. *Molecules* **2020**, *25* (22).

20. Ghosh, D.; Griswold, J.; Erman, M.; Pangborn, W., Structural basis for androgen specificity and oestrogen synthesis in human aromatase. *Nature* **2009**, *457* (7226), 219-23.

21. Favia, A. D.; Cavalli, A.; Masetti, M.; Carotti, A.; Recanatini, M., Three-dimensional model of the human aromatase enzyme and density functional parameterization of the iron-containing protoporphyrin IX for a molecular dynamics study of heme-cysteinato cytochromes. *Proteins* **2006**, *62* (4), 1074-87.

22. Karkola, S.; Hältje, H. D.; Wähälä, K., A three-dimensional model of CYP19 aromatase for structure-based drug design. *J Steroid Biochem Mol Biol* **2007**, *105* (1-5), 63-70.

23. Ghosh, D.; Griswold, J.; Erman, M.; Pangborn, W., X-ray structure of human aromatase reveals an androgen-specific active site. *J Steroid Biochem Mol Biol* **2010**, *118* (4-5), 197-202.

24. Akhtar, M.; Wright, J. N.; Lee-Robichaud, P., A review of mechanistic studies on aromatase (CYP19) and 17 $\alpha$ -hydroxylase-17,20-lyase (CYP17). *J Steroid Biochem Mol Biol* **2011**, *125* (1-2), 2-12.
25. Sgrignani, J.; Cavalli, A.; Colombo, G.; Magistrato, A., Enzymatic and Inhibition Mechanism of Human Aromatase (CYP19A1) Enzyme. A Computational Perspective from QM/MM and Classical Molecular Dynamics Simulations. *Mini Rev Med Chem* **2016**, *16* (14), 1112-24.
26. Yoshimoto, F. K.; Guengerich, F. P., Mechanism of the third oxidative step in the conversion of androgens to estrogens by cytochrome P450 19A1 steroid aromatase. *J Am Chem Soc* **2014**, *136* (42), 15016-25.
27. Saczko, J.; Michel, O.; Chwiłkowska, A.; Sawicka, E.; Mączyńska, J.; Kulbacka, J., Estrogen Receptors in Cell Membranes: Regulation and Signaling. *Adv Anat Embryol Cell Biol* **2017**, *227*, 93-105.
28. Greene, G. L.; Gilna, P.; Waterfield, M.; Baker, A.; Hort, Y.; Shine, J., Sequence and expression of human estrogen receptor complementary DNA. *Science* **1986**, *231* (4742), 1150-4.
29. Kuiper, G. G.; Enmark, E.; Peltö-Huikko, M.; Nilsson, S.; Gustafsson, J. A., Cloning of a novel receptor expressed in rat prostate and ovary. *Proc Natl Acad Sci U S A* **1996**, *93* (12), 5925-30.
30. Saha, T.; Makar, S.; Swetha, R.; Gutti, G.; Singh, S. K., Estrogen signaling: An emanating therapeutic target for breast cancer treatment. *Eur J Med Chem* **2019**, *177*, 116-143.
31. Jia, M.; Dahlman-Wright, K.; Gustafsson, J., Estrogen receptor alpha and beta in health and disease. *Best Pract Res Clin Endocrinol Metab* **2015**, *29* (4), 557-68.
32. Heldring, N.; Pike, A.; Andersson, S.; Matthews, J.; Cheng, G.; Hartman, J.; Tujague, M.; Ström, A.; Treuter, E.; Warner, M.; Gustafsson, J. A., Estrogen receptors: how do they signal and what are their targets. *Physiol Rev* **2007**, *87* (3), 905-31.
33. Alexander, A.; Irving, A. J.; Harvey, J., Emerging roles for the novel estrogen-sensing receptor GPER1 in the CNS. *Neuropharmacology* **2017**, *113* (Pt B), 652-660.
34. Fuentes, N.; Silveyra, P., Estrogen receptor signaling mechanisms. *Adv Protein Chem Struct Biol* **2019**, *116*, 135-170.
35. Lewis-Wambi, J. S.; Jordan, V. C., Treatment of Postmenopausal Breast Cancer with Selective Estrogen Receptor Modulators (SERMs). *Breast Dis* **2005**, *24*, 93-105.

36. Riggs, B. L.; Hartmann, L. C., Selective estrogen-receptor modulators -- mechanisms of action and application to clinical practice. *N Engl J Med* **2003**, *348* (7), 618-29.
37. Patel, H. K.; Bihani, T., Selective estrogen receptor modulators (SERMs) and selective estrogen receptor degraders (SERDs) in cancer treatment. *Pharmacol Ther* **2018**, *186*, 1-24.
38. Jordan, V. C., The development of tamoxifen for breast cancer therapy: a tribute to the late Arthur L. Walpole. *Breast Cancer Res Treat* **1988**, *11* (3), 197-209.
39. Jordan, V. C., New insights into the metabolism of tamoxifen and its role in the treatment and prevention of breast cancer. *Steroids* **2007**, *72* (13), 829-42.
40. Burke, C., Endometrial cancer and tamoxifen. *Clin J Oncol Nurs* **2005**, *9* (2), 247-9.
41. Kangas, L., Introduction to toremifene. *Breast Cancer Res Treat* **1990**, *16 Suppl*, S3-7.
42. Dhingra, K., Antiestrogens--tamoxifen, SERMs and beyond. *Invest New Drugs* **1999**, *17* (3), 285-311.
43. Arpino, G.; Nair Krishnan, M.; Doval Dinesh, C.; Bardou, V. J.; Clark, G. M.; Elledge, R. M., Idoxifene versus tamoxifen: a randomized comparison in postmenopausal patients with metastatic breast cancer. *Ann Oncol* **2003**, *14* (2), 233-41.
44. Scott, J. A.; Da Camara, C. C.; Early, J. E., Raloxifene: a selective estrogen receptor modulator. *Am Fam Physician* **1999**, *60* (4), 1131-9.
45. Khovidhunkit, W.; Shoback, D. M., Clinical effects of raloxifene hydrochloride in women. *Ann Intern Med* **1999**, *130* (5), 431-9.
46. Suh, N.; Glasebrook, A. L.; Palkowitz, A. D.; Bryant, H. U.; Burris, L. L.; Starling, J. J.; Pearce, H. L.; Williams, C.; Peer, C.; Wang, Y.; Sporn, M. B., Arzoxifene, a new selective estrogen receptor modulator for chemoprevention of experimental breast cancer. *Cancer Res* **2001**, *61* (23), 8412-5.
47. Kung, A. W.; Chu, E. Y.; Xu, L., Bazedoxifene: a new selective estrogen receptor modulator for the treatment of postmenopausal osteoporosis. *Expert Opin Pharmacother* **2009**, *10* (8), 1377-85.
48. Greenberger, L. M.; Annable, T.; Collins, K. I.; Komm, B. S.; Lyttle, C. R.; Miller, C. P.; Satyaswaroop, P. G.; Zhang, Y.; Frost, P., A new antiestrogen, 2-(4-hydroxy-phenyl)-3-methyl-1-[4-(2-piperidin-1-yl-ethoxy)-benzyl]-1H-indol-5-ol hydrochloride (ERA-923), inhibits the growth of tamoxifen-sensitive and -

resistant tumors and is devoid of uterotrophic effects in mice and rats. *Clin Cancer Res* **2001**, *7* (10), 3166-77.

49. Miller, C. P.; Collini, M. D.; Tran, B. D.; Harris, H. A.; Kharode, Y. P.; Marzolf, J. T.; Moran, R. A.; Henderson, R. A.; Bender, R. H.; Unwalla, R. J.; Greenberger, L. M.; Yardley, J. P.; Abou-Gharbia, M. A.; Lyttle, C. R.; Komm, B. S., Design, synthesis, and preclinical characterization of novel, highly selective indole estrogens. *J Med Chem* **2001**, *44* (11), 1654-7.

50. Gennari, L., Lasofoxifene, a new selective estrogen receptor modulator for the treatment of osteoporosis and vaginal atrophy. *Expert Opin Pharmacother* **2009**, *10* (13), 2209-20.

51. Kaur, G.; Mahajan, M. P.; Pandey, M. K.; Singh, P.; Ramiseti, S. R.; Sharma, A. K., Design, synthesis and evaluation of Ospemifene analogs as anti-breast cancer agents. *Eur J Med Chem* **2014**, *86*, 211-8.

52. Kaur, G.; Mahajan, M. P.; Pandey, M. K.; Singh, P.; Ramiseti, S. R.; Sharma, A. K., Design, synthesis, and anti-breast cancer evaluation of new triarylethylene analogs bearing short alkyl- and polar amino-/amido-ethyl chains. *Bioorg Med Chem Lett* **2016**, *26* (8), 1963-9.

53. Elghazawy, N. H.; Engel, M.; Hartmann, R. W.; Hamed, M. M.; Ahmed, N. S.; Abadi, A. H., Design and synthesis of novel flexible ester-containing analogs of tamoxifen and their evaluation as anticancer agents. *Future Med Chem* **2016**, *8* (3), 249-56.

54. Catanzaro, E.; Seghetti, F.; Calcabrini, C.; Rampa, A.; Gobbi, S.; Sestili, P.; Turrini, E.; Maffei, F.; Hrelia, P.; Bisi, A.; Belluti, F.; Fimognari, C., Identification of a new tamoxifen-xanthene hybrid as pro-apoptotic anticancer agent. *Bioorg Chem* **2019**, *86*, 538-549.

55. Jha, A.; Yadav, Y.; Naidu, A. B.; Rao, V. K.; Kumar, A.; Parmar, V. S.; MacDonald, W. J.; Too, C. K.; Balzarini, J.; Barden, C. J.; Cameron, T. S., Design, synthesis and bioevaluation of novel 6-(4-Hydroxypiperidino)naphthalen-2-ol-based potential Selective Estrogen Receptor Modulators for breast cancer. *Eur J Med Chem* **2015**, *92*, 103-14.

56. Luo, G.; Chen, M.; Lyu, W.; Zhao, R.; Xu, Q.; You, Q.; Xiang, H., Design, synthesis, biological evaluation and molecular docking studies of novel 3-aryl-4-anilino-2H-chromen-2-one derivatives targeting ER $\alpha$  as anti-breast cancer agents. *Bioorg Med Chem Lett* **2017**, *27* (12), 2668-2673.

57. Wakeling, A. E.; Bowler, J., Biology and mode of action of pure antioestrogens. *J Steroid Biochem* **1988**, *30* (1-6), 141-7.

58. Howell, A.; Osborne, C. K.; Morris, C.; Wakeling, A. E., ICI 182,780 (Faslodex): development of a novel, "pure" antiestrogen. *Cancer* **2000**, *89* (4), 817-25.
59. Kieser, K. J.; Kim, D. W.; Carlson, K. E.; Katzenellenbogen, B. S.; Katzenellenbogen, J. A., Characterization of the pharmacophore properties of novel selective estrogen receptor downregulators (SERDs). *J Med Chem* **2010**, *53* (8), 3320-9.
60. Lu, Y.; Liu, W., Selective Estrogen Receptor Degraders (SERDs): A Promising Strategy for Estrogen Receptor Positive Endocrine-Resistant Breast Cancer. *J Med Chem* **2020**.
61. Willson, T. M.; Henke, B. R.; Momtahan, T. M.; Charifson, P. S.; Batchelor, K. W.; Lubahn, D. B.; Moore, L. B.; Oliver, B. B.; Sauls, H. R.; Triantafillou, J. A., 3-[4-(1,2-Diphenylbut-1-enyl)phenyl]acrylic acid: a non-steroidal estrogen with functional selectivity for bone over uterus in rats. *J Med Chem* **1994**, *37* (11), 1550-2.
62. Wu, Y. L.; Yang, X.; Ren, Z.; McDonnell, D. P.; Norris, J. D.; Willson, T. M.; Greene, G. L., Structural basis for an unexpected mode of SERM-mediated ER antagonism. *Mol Cell* **2005**, *18* (4), 413-24.
63. Lai, A.; Kahraman, M.; Govek, S.; Nagasawa, J.; Bonnefous, C.; Julien, J.; Douglas, K.; Sensintaffar, J.; Lu, N.; Lee, K. J.; Aparicio, A.; Kaufman, J.; Qian, J.; Shao, G.; Prudente, R.; Moon, M. J.; Joseph, J. D.; Darimont, B.; Brigham, D.; Grillot, K.; Heyman, R.; Rix, P. J.; Hager, J. H.; Smith, N. D., Identification of GDC-0810 (ARN-810), an Orally Bioavailable Selective Estrogen Receptor Degradator (SERD) that Demonstrates Robust Activity in Tamoxifen-Resistant Breast Cancer Xenografts. *J Med Chem* **2015**, *58* (12), 4888-904.
64. Joseph, J. D.; Darimont, B.; Zhou, W.; Arrazate, A.; Young, A.; Ingalla, E.; Walter, K.; Blake, R. A.; Nonomiya, J.; Guan, Z.; Kategaya, L.; Govek, S. P.; Lai, A. G.; Kahraman, M.; Brigham, D.; Sensintaffar, J.; Lu, N.; Shao, G.; Qian, J.; Grillot, K.; Moon, M.; Prudente, R.; Bischoff, E.; Lee, K. J.; Bonnefous, C.; Douglas, K. L.; Julien, J. D.; Nagasawa, J. Y.; Aparicio, A.; Kaufman, J.; Haley, B.; Giltnane, J. M.; Wertz, I. E.; Lackner, M. R.; Nannini, M. A.; Sampath, D.; Schwarz, L.; Manning, H. C.; Tantawy, M. N.; Arteaga, C. L.; Heyman, R. A.; Rix, P. J.; Friedman, L.; Smith, N. D.; Metcalfe, C.; Hager, J. H., The selective estrogen receptor downregulator GDC-0810 is efficacious in diverse models of ER+ breast cancer. *Elife* **2016**, *5*.
65. Callis, R.; Rabow, A.; Tonge, M.; Bradbury, R.; Challinor, M.; Roberts, K.; Jones, K.; Walker, G., A Screening Assay Cascade to Identify and Characterize Novel Selective Estrogen Receptor Downregulators (SERDs). *J Biomol Screen* **2015**, *20* (6), 748-59.

66. De Savi, C.; Bradbury, R. H.; Rabow, A. A.; Norman, R. A.; de Almeida, C.; Andrews, D. M.; Ballard, P.; Buttar, D.; Callis, R. J.; Currie, G. S.; Curwen, J. O.; Davies, C. D.; Donald, C. S.; Feron, L. J.; Gingell, H.; Glossop, S. C.; Hayter, B. R.; Hussain, S.; Karoutchi, G.; Lamont, S. G.; MacFaul, P.; Moss, T. A.; Pearson, S. E.; Tonge, M.; Walker, G. E.; Weir, H. M.; Wilson, Z., Optimization of a Novel Binding Motif to (E)-3-(3,5-Difluoro-4-((1R,3R)-2-(2-fluoro-2-methylpropyl)-3-methyl-2,3,4,9-tetrahydro-1H-pyrido[3,4-b]indol-1-yl)phenyl)acrylic Acid (AZD9496), a Potent and Orally Bioavailable Selective Estrogen Receptor Downregulator and Antagonist. *J Med Chem* **2015**, *58* (20), 8128-40.
67. Weir, H. M.; Bradbury, R. H.; Lawson, M.; Rabow, A. A.; Buttar, D.; Callis, R. J.; Curwen, J. O.; de Almeida, C.; Ballard, P.; Hulse, M.; Donald, C. S.; Feron, L. J.; Karoutchi, G.; MacFaul, P.; Moss, T.; Norman, R. A.; Pearson, S. E.; Tonge, M.; Davies, G.; Walker, G. E.; Wilson, Z.; Rowlinson, R.; Powell, S.; Sadler, C.; Richmond, G.; Ladd, B.; Pazolli, E.; Mazzola, A. M.; D'Cruz, C.; De Savi, C., AZD9496: An Oral Estrogen Receptor Inhibitor That Blocks the Growth of ER-Positive and ESR1-Mutant Breast Tumors in Preclinical Models. *Cancer Res* **2016**, *76* (11), 3307-18.
68. Nardone, A.; Weir, H.; Delpuech, O.; Brown, H.; De Angelis, C.; Cataldo, M. L.; Fu, X.; Shea, M. J.; Mitchell, T.; Veeraraghavan, J.; Nagi, C.; Pilling, M.; Rimawi, M. F.; Trivedi, M.; Hilsenbeck, S. G.; Chamness, G. C.; Jeselsohn, R.; Osborne, C. K.; Schiff, R., The oral selective oestrogen receptor degrader (SERD) AZD9496 is comparable to fulvestrant in antagonising ER and circumventing endocrine resistance. *Br J Cancer* **2019**, *120* (3), 331-339.
69. Tria, G. S.; Abrams, T.; Baird, J.; Burks, H. E.; Firestone, B.; Gaither, L. A.; Hamann, L. G.; He, G.; Kirby, C. A.; Kim, S.; Lombardo, F.; Macchi, K. J.; McDonnell, D. P.; Mishina, Y.; Norris, J. D.; Nunez, J.; Springer, C.; Sun, Y.; Thomsen, N. M.; Wang, C.; Wang, J.; Yu, B.; Tiong-Yip, C. L.; Peukert, S., Discovery of LSZ102, a Potent, Orally Bioavailable Selective Estrogen Receptor Degradator (SERD) for the Treatment of Estrogen Receptor Positive Breast Cancer. *J Med Chem* **2018**, *61* (7), 2837-2864.
70. Garner, F.; Shomali, M.; Paquin, D.; Lyttle, C. R.; Hattersley, G., RAD1901: a novel, orally bioavailable selective estrogen receptor degrader that demonstrates antitumor activity in breast cancer xenograft models. *Anticancer Drugs* **2015**, *26* (9), 948-56.
71. Wardell, S. E.; Nelson, E. R.; Chao, C. A.; Alley, H. M.; McDonnell, D. P., Evaluation of the pharmacological activities of RAD1901, a selective estrogen receptor degrader. *Endocr Relat Cancer* **2015**, *22* (5), 713-24.
72. Scott, J. S.; Moss, T. A.; Balazs, A.; Barlaam, B.; Breed, J.; Carbajo, R. J.; Chiarparin, E.; Davey, P. R. J.; Delpuech, O.; Fawell, S.; Fisher, D. I.; Gargica, S.; Gangl, E. T.; Grebe, T.; Greenwood, R. D.; Hande, S.; Hatoum-Mokdad, H.; Herlihy, K.; Hughes, S.; Hunt, T. A.; Huynh, H.; Janbon, S. L. M.;

Johnson, T.; Kavanagh, S.; Klinowska, T.; Lawson, M.; Lister, A. S.; Marden, S.; McGinnity, D. F.; Morrow, C. J.; Nissink, J. W. M.; O'Donovan, D. H.; Peng, B.; Polanski, R.; Stead, D. S.; Stokes, S.; Thakur, K.; Throner, S. R.; Tucker, M. J.; Varnes, J.; Wang, H.; Wilson, D. M.; Wu, D.; Wu, Y.; Yang, B.; Yang, W., Discovery of AZD9833, a Potent and Orally Bioavailable Selective Estrogen Receptor Degradator and Antagonist. *J Med Chem* **2020**, *63* (23), 14530-14559.

73. El-Ahmad, Y.; Tabart, M.; Halley, F.; Certal, V.; Thompson, F.; Filoche-Rommé, B.; Gruss-Leleu, F.; Muller, C.; Brollo, M.; Fabien, L.; Loyau, V.; Bertin, L.; Richepin, P.; Pilorge, F.; Desmazeau, P.; Girardet, C.; Beccari, S.; Louboutin, A.; Lebourg, G.; Le-Roux, J.; Terrier, C.; Vallée, F.; Steier, V.; Mathieu, M.; Rak, A.; Abecassis, P. Y.; Vicat, P.; Benard, T.; Bouaboula, M.; Sun, F.; Shomali, M.; Hebert, A.; Levit, M.; Cheng, H.; Courjaud, A.; Ginesty, C.; Perrault, C.; Garcia-Echeverria, C.; McCort, G.; Schio, L., Discovery of 6-(2,4-Dichlorophenyl)-5-[4-[(3. *J Med Chem* **2020**, *63* (2), 512-528.

74. Liang, J.; Blake, R.; Chang, J.; Friedman, L. S.; Goodacre, S.; Hartman, S.; Ingalla, E. R.; Kiefer, J. R.; Kleinheinz, T.; Labadie, S.; Li, J.; Lai, K. W.; Liao, J.; Mody, V.; McLean, N.; Metcalfe, C.; Nannini, M.; Otwine, D.; Ran, Y.; Ray, N.; Roussel, F.; Sambrone, A.; Sampath, D.; Vinogradova, M.; Wai, J.; Wang, T.; Yeap, K.; Young, A.; Zbieg, J.; Zhang, B.; Zheng, X.; Zhong, Y.; Wang, X., Discovery of GNE-149 as a Full Antagonist and Efficient Degradator of Estrogen Receptor alpha for ER+ Breast Cancer. *ACS Med Chem Lett* **2020**, *11* (6), 1342-1347.

75. Jiao, J.; Xiang, H.; Liao, Q., Recent advancement in nonsteroidal aromatase inhibitors for treatment of estrogen-dependent breast cancer. *Curr Med Chem* **2010**, *17* (30), 3476-87.

76. Dutta, U.; Pant, K., Aromatase inhibitors: past, present and future in breast cancer therapy. *Med Oncol* **2008**, *25* (2), 113-24.

77. Chumsri, S.; Howes, T.; Bao, T.; Sabnis, G.; Brodie, A., Aromatase, aromatase inhibitors, and breast cancer. *J Steroid Biochem Mol Biol* **2011**, *125* (1-2), 13-22.

78. Gobbi, S.; Rampa, A.; Belluti, F.; Bisi, A., Nonsteroidal aromatase inhibitors for the treatment of breast cancer: an update. *Anticancer Agents Med Chem* **2014**, *14* (1), 54-65.

79. Santen, R. J.; Misbin, R. I., Aminoglutethimide: review of pharmacology and clinical use. *Pharmacotherapy* **1981**, *1* (2), 95-120.

80. Santen, R. J.; Santner, S.; Davis, B.; Veldhuis, J.; Samojlik, E.; Ruby, E., Aminoglutethimide inhibits extraglandular estrogen production in postmenopausal women with breast carcinoma. *J Clin Endocrinol Metab* **1978**, *47* (6), 1257-65.

81. Siiteri, P. K.; Thompson, E. A., Studies of human placental aromatase. *J Steroid Biochem* **1975**, *6* (3-4), 317-22.
82. Cocconi, G., First generation aromatase inhibitors--aminoglutethimide and testololactone. *Breast Cancer Res Treat* **1994**, *30* (1), 57-80.
83. Thürlimann, B.; Beretta, K.; Bacchi, M.; Castiglione-Gertsch, M.; Goldhirsch, A.; Jungi, W. F.; Cavalli, F.; Senn, H. J.; Fey, M.; Löhnert, T., First-line fadrozole HCl (CGS 16949A) versus tamoxifen in postmenopausal women with advanced breast cancer. Prospective randomised trial of the Swiss Group for Clinical Cancer Research SAKK 20/88. *Ann Oncol* **1996**, *7* (5), 471-9.
84. Jordan, V. C.; Brodie, A. M., Development and evolution of therapies targeted to the estrogen receptor for the treatment and prevention of breast cancer. *Steroids* **2007**, *72* (1), 7-25.
85. Khan, Q. J.; O'Dea, A. P.; Sharma, P., Musculoskeletal adverse events associated with adjuvant aromatase inhibitors. *J Oncol* **2010**, *2010*.
86. Foglietta, J.; Inno, A.; de Iuliis, F.; Sini, V.; Duranti, S.; Turazza, M.; Tarantini, L.; Gori, S., Cardiotoxicity of Aromatase Inhibitors in Breast Cancer Patients. *Clin Breast Cancer* **2017**, *17* (1), 11-17.
87. Condorelli, R.; Vaz-Luis, I., Managing side effects in adjuvant endocrine therapy for breast cancer. *Expert Rev Anticancer Ther* **2018**, *18* (11), 1101-1112.
88. Regan, M. M.; Neven, P.; Giobbie-Hurder, A.; Goldhirsch, A.; Ejlertsen, B.; Mauriac, L.; Forbes, J. F.; Smith, I.; Láng, I.; Wardley, A.; Rabaglio, M.; Price, K. N.; Gelber, R. D.; Coates, A. S.; Thürlimann, B.; Group, B.-C.; (IBCSG), I. B. C. S. G., Assessment of letrozole and tamoxifen alone and in sequence for postmenopausal women with steroid hormone receptor-positive breast cancer: the BIG 1-98 randomised clinical trial at 8.1 years median follow-up. *Lancet Oncol* **2011**, *12* (12), 1101-8.
89. Ruhstaller, T.; Giobbie-Hurder, A.; Colleoni, M.; Jensen, M. B.; Ejlertsen, B.; de Azambuja, E.; Neven, P.; Láng, I.; Jakobsen, E. H.; Gladieff, L.; Bonnefoi, H.; Harvey, V. J.; Spazzapan, S.; Tondini, C.; Del Mastro, L.; Veyret, C.; Simoncini, E.; Gianni, L.; Rochlitz, C.; Kralidis, E.; Zaman, K.; Jassem, J.; Piccart-Gebhart, M.; Di Leo, A.; Gelber, R. D.; Coates, A. S.; Goldhirsch, A.; Thürlimann, B.; Regan, M. M.; Group, m. o. t. B.-C. G. a. t. I. B. C. S., Adjuvant Letrozole and Tamoxifen Alone or Sequentially for Postmenopausal Women With Hormone Receptor-Positive Breast Cancer: Long-Term Follow-Up of the BIG 1-98 Trial. *J Clin Oncol* **2019**, *37* (2), 105-114.
90. Baum, M.; Buzdar, A.; Cuzick, J.; Forbes, J.; Houghton, J.; Howell, A.; Sahnoud, T.; ATAC (Arimidex, T. m. A. o. i. C. T. G., Anastrozole alone or in combination with tamoxifen versus tamoxifen alone for adjuvant treatment of postmenopausal women with early-stage breast cancer: results of the ATAC

(Arimidex, Tamoxifen Alone or in Combination) trial efficacy and safety update analyses. *Cancer* **2003**, 98 (9), 1802-10.

91. Howell, A.; Cuzick, J.; Baum, M.; Buzdar, A.; Dowsett, M.; Forbes, J. F.; Hocht-Boes, G.; Houghton, J.; Locker, G. Y.; Tobias, J. S.; Group, A. T., Results of the ATAC (Arimidex, Tamoxifen, Alone or in Combination) trial after completion of 5 years' adjuvant treatment for breast cancer. *Lancet* **2005**, 365 (9453), 60-2.

92. Jelovac, D.; Macedo, L.; Goloubeva, O. G.; Handratta, V.; Brodie, A. M., Additive antitumor effect of aromatase inhibitor letrozole and antiestrogen fulvestrant in a postmenopausal breast cancer model. *Cancer Res* **2005**, 65 (12), 5439-44.

93. Zaccheo, T.; Giudici, D.; Di Salle, E., Inhibitory effect of combined treatment with the aromatase inhibitor exemestane and tamoxifen on DMBA-induced mammary tumors in rats. *J Steroid Biochem Mol Biol* **1993**, 44 (4-6), 677-80.

94. Rivera, E.; Valero, V.; Francis, D.; Asnis, A. G.; Schaaf, L. J.; Duncan, B.; Hortobagyi, G. N., Pilot study evaluating the pharmacokinetics, pharmacodynamics, and safety of the combination of exemestane and tamoxifen. *Clin Cancer Res* **2004**, 10 (6), 1943-8.

95. Love, R. R.; Hutson, P. R.; Havighurst, T. C.; Cleary, J. F., Endocrine effects of tamoxifen plus exemestane in postmenopausal women with breast cancer. *Clin Cancer Res* **2005**, 11 (4), 1500-3.

96. Hutson, P. R.; Love, R. R.; Havighurst, T. C.; Rogers, E.; Cleary, J. F., Effect of exemestane on tamoxifen pharmacokinetics in postmenopausal women treated for breast cancer. *Clin Cancer Res* **2005**, 11 (24 Pt 1), 8722-7.

97. Lézé, M. P.; Le Borgne, M.; Pinson, P.; Paluszczak, A.; Duflos, M.; Le Baut, G.; Hartmann, R. W., Synthesis and biological evaluation of 5-[(aryl)(1H-imidazol-1-yl)methyl]-1H-indoles: potent and selective aromatase inhibitors. *Bioorg Med Chem Lett* **2006**, 16 (5), 1134-7.

98. Lézé, M. P.; Paluszczak, A.; Hartmann, R. W.; Le Borgne, M., Synthesis of 6- or 4-functionalized indoles via a reductive cyclization approach and evaluation as aromatase inhibitors. *Bioorg Med Chem Lett* **2008**, 18 (16), 4713-5.

99. Wang, R.; Shi, H. F.; Zhao, J. F.; He, Y. P.; Zhang, H. B.; Liu, J. P., Design, synthesis and aromatase inhibitory activities of novel indole-imidazole derivatives. *Bioorg Med Chem Lett* **2013**, 23 (6), 1760-2.

100. Kang, H.; Xiao, X.; Huang, C.; Yuan, Y.; Tang, D.; Dai, X.; Zeng, X., Potent aromatase inhibitors and molecular mechanism of inhibitory action. *Eur J Med Chem* **2018**, 143, 426-437.

101. Di Matteo, M.; Ammazalorso, A.; Andreoli, F.; Caffa, I.; De Filippis, B.; Fantacuzzi, M.; Giampietro, L.; Maccallini, C.; Nencioni, A.; Parenti, M. D.; Soncini, D.; Del Rio, A.; Amoroso, R., Synthesis and biological characterization of 3-(imidazol-1-ylmethyl)piperidine sulfonamides as aromatase inhibitors. *Bioorg Med Chem Lett* **2016**, *26* (13), 3192-3194.
102. Fantacuzzi, M.; De Filippis, B.; Gallorini, M.; Ammazalorso, A.; Giampietro, L.; Maccallini, C.; Aturki, Z.; Donati, E.; Ibrahim, R. S.; Shawky, E.; Cataldi, A.; Amoroso, R., Synthesis, biological evaluation, and docking study of indole aryl sulfonamides as aromatase inhibitors. *Eur J Med Chem* **2020**, *185*, 111815.
103. Pingaew, R.; Prachayasittikul, V.; Mandi, P.; Nantasenamat, C.; Prachayasittikul, S.; Ruchirawat, S., Synthesis and molecular docking of 1,2,3-triazole-based sulfonamides as aromatase inhibitors. *Bioorg Med Chem* **2015**, *23* (13), 3472-80.
104. Stefanachi, A.; Favia, A. D.; Nicolotti, O.; Leonetti, F.; Pisani, L.; Catto, M.; Zimmer, C.; Hartmann, R. W.; Carotti, A., Design, synthesis, and biological evaluation of imidazolyl derivatives of 4,7-disubstituted coumarins as aromatase inhibitors selective over 17- $\alpha$ -hydroxylase/C17-20 lyase. *J Med Chem* **2011**, *54* (6), 1613-25.
105. Leonetti, F.; Favia, A.; Rao, A.; Aliano, R.; Paluszczak, A.; Hartmann, R. W.; Carotti, A., Design, synthesis, and 3D QSAR of novel potent and selective aromatase inhibitors. *J Med Chem* **2004**, *47* (27), 6792-803.
106. Yamaguchi, Y.; Nishizono, N.; Kobayashi, D.; Yoshimura, T.; Wada, K.; Oda, K., Evaluation of synthesized coumarin derivatives on aromatase inhibitory activity. *Bioorg Med Chem Lett* **2017**, *27* (12), 2645-2649.
107. Recanatini, M.; Bisi, A.; Cavalli, A.; Belluti, F.; Gobbi, S.; Rampa, A.; Valenti, P.; Palzer, M.; Paluszczak, A.; Hartmann, R. W., A new class of nonsteroidal aromatase inhibitors: design and synthesis of chromone and xanthone derivatives and inhibition of the P450 enzymes aromatase and 17  $\alpha$ -hydroxylase/C17,20-lyase. *J Med Chem* **2001**, *44* (5), 672-80.
108. Gobbi, S.; Zimmer, C.; Belluti, F.; Rampa, A.; Hartmann, R. W.; Recanatini, M.; Bisi, A., Novel highly potent and selective nonsteroidal aromatase inhibitors: synthesis, biological evaluation and structure-activity relationships investigation. *J Med Chem* **2010**, *53* (14), 5347-51.
109. Acar Çevik, U.; Sağlık, B. N.; Osmaniye, D.; Levent, S.; Kaya Çavuşoğlu, B.; Karaduman, A. B.; Özkay, Y.; Kaplancıklı, Z. A., Synthesis and docking study of benzimidazole-triazolothiadiazine hybrids as aromatase inhibitors. *Arch Pharm (Weinheim)* **2020**, *353* (5), e2000008.

110. Acar Çevik, U.; Kaya Çavuşoğlu, B.; Sağlık, B. N.; Osmaniye, D.; Levent, S.; Iğın, S.; Özkay, Y.; Kaplancıklı, Z. A., Synthesis, Docking Studies and Biological Activity of New Benzimidazole- Triazolothiadiazine Derivatives as Aromatase Inhibitor. *Molecules* **2020**, *25* (7).
111. El-Naggar, M.; El-All, A. S. A.; El-Naem, S. I. A.; Abdalla, M. M.; Rashdan, H. R. M., New Potent 5 $\alpha$ - Reductase and Aromatase Inhibitors Derived from 1,2,3-Triazole Derivative. *Molecules* **2020**, *25* (3).
112. Nussinov, R.; Tsai, C. J., The design of covalent allosteric drugs. *Annu Rev Pharmacol Toxicol* **2015**, *55*, 249-67.
113. Numazawa, M.; Watari, Y.; Yamada, K.; Umemura, N.; Handa, W., Probing the active site of aromatase with 2-methyl-substituted androstenedione analogs. *Steroids* **2003**, *68* (6), 503-13.
114. Nagaoka, M.; Watari, Y.; Yajima, H.; Tsukioka, K.; Muroi, Y.; Yamada, K.; Numazawa, M., Structure-activity relationships of 3-deoxy androgens as aromatase inhibitors. Synthesis and biochemical studies of 4-substituted 4-ene and 5-ene steroids. *Steroids* **2003**, *68* (6), 533-42.
115. Takahashi, M.; Handa, W.; Umeta, H.; Ishikawa, S.; Yamashita, K.; Numazawa, M., Aromatase inactivation by 2-substituted derivatives of the suicide substrate androsta-1,4-diene-3,17-dione. *J Steroid Biochem Mol Biol* **2009**, *116* (3-5), 191-9.
116. Yadav, M. R.; Sabale, P. M.; Giridhar, R.; Zimmer, C.; Haupenthal, J.; Hartmann, R. W., Synthesis of some novel androstanes as potential aromatase inhibitors. *Steroids* **2011**, *76* (5), 464-70.
117. Yadav, M. R.; Sabale, P. M.; Giridhar, R.; Zimmer, C.; Hartmann, R. W., Steroidal carbonitriles as potential aromatase inhibitors. *Steroids* **2012**, *77* (8-9), 850-7.
118. Takahashi, M.; Yamashita, K.; Numazawa, M., Probing the binding pocket of the active site of aromatase with 2-phenylaliphatic androsta-1,4-diene-3,17-dione steroids. *Steroids* **2010**, *75* (4-5), 330-7.
119. Komatsu, S.; Yaguchi, A.; Yamashita, K.; Nagaoka, M.; Numazawa, M., 6 $\beta$ ,19-Bridged androstenedione analogs as aromatase inhibitors. *Steroids* **2009**, *74* (12), 884-9.
120. Numazawa, M.; Handa, W.; Yamada, K., Synthesis and biochemical properties of 6-bromoandrostenedione derivatives with a 2,2-dimethyl or 2-methyl group as aromatase inhibitors. *Biol Pharm Bull* **2004**, *27* (11), 1878-82.
121. Varela, C. L.; Amaral, C.; Correia-da-Silva, G.; Carvalho, R. A.; Teixeira, N. A.; Costa, S. C.; Roleira, F. M.; Tavares-da-Silva, E. J., Design, synthesis and

biochemical studies of new 7 $\alpha$ -allylandrostanes as aromatase inhibitors. *Steroids* **2013**, 78 (7), 662-9.

122. Amaral, C.; Varela, C. L.; Maurício, J.; Sobral, A. F.; Costa, S. C.; Roleira, F. M. F.; Tavares-da-Silva, E. J.; Correia-da-Silva, G.; Teixeira, N., Anti-tumor efficacy of new 7 $\alpha$ -substituted androstanes as aromatase inhibitors in hormone-sensitive and resistant breast cancer cells. *J Steroid Biochem Mol Biol* **2017**, 171, 218-228.

123. Roleira, F. M. F.; Varela, C.; Amaral, C.; Costa, S. C.; Correia-da-Silva, G.; Moraca, F.; Costa, G.; Alcaro, S.; Teixeira, N. A. A.; Tavares da Silva, E. J., C-6 $\alpha$ - vs C-7 $\alpha$ -Substituted Steroidal Aromatase Inhibitors: Which Is Better? Synthesis, Biochemical Evaluation, Docking Studies, and Structure-Activity Relationships. *J Med Chem* **2019**, 62 (7), 3636-3657.

124. Bansal, R.; Guleria, S.; Ries, C.; Hartmann, R. W., Synthesis and antineoplastic activity of O-alkylated derivatives of 7-hydroximinoandrost-5-ene steroids. *Arch Pharm (Weinheim)* **2010**, 343 (7), 377-83.

125. Varela, C. L.; Amaral, C.; Tavares da Silva, E.; Lopes, A.; Correia-da-Silva, G.; Carvalho, R. A.; Costa, S. C.; Roleira, F. M.; Teixeira, N., Exemestane metabolites: Synthesis, stereochemical elucidation, biochemical activity and anti-proliferative effects in a hormone-dependent breast cancer cell line. *Eur J Med Chem* **2014**, 87, 336-45.

126. Bansal, R.; Guleria, S.; Thota, S.; Hartmann, R. W.; Zimmer, C., Synthesis and biological evaluation of 16E-arylidenosteroids as cytotoxic and anti-aromatase agents. *Chem Pharm Bull (Tokyo)* **2011**, 59 (3), 327-31.

127. Bansal, R.; Guleria, S.; Thota, S.; Hartmann, R.; Zimmer, C., Synthesis of imidazole-derived steroidal hybrids as potent aromatase inhibitors. *Medicinal Chemistry Research* **2013**, 22 (2), 692-698.

128. Bansal, R.; Guleria, S.; Thota, S.; Bodhankar, S. L.; Patwardhan, M. R.; Zimmer, C.; Hartmann, R. W.; Harvey, A. L., Design, synthesis and evaluation of novel 16-imidazolyl substituted steroidal derivatives possessing potent diversified pharmacological properties. *Steroids* **2012**, 77 (6), 621-9.

129. Bansal, R.; Thota, S.; Karkra, N.; Minu, M.; Zimmer, C.; Hartmann, R. W., Synthesis and aromatase inhibitory activity of some new 16E-arylidenosteroids. *Bioorg Chem* **2012**, 45, 36-40.

130. Lu, W. J.; Desta, Z.; Flockhart, D. A., Tamoxifen metabolites as active inhibitors of aromatase in the treatment of breast cancer. *Breast Cancer Res Treat* **2012**, 131 (2), 473-81.

131. Lu, W. J.; Xu, C.; Pei, Z.; Mayhoub, A. S.; Cushman, M.; Flockhart, D. A., The tamoxifen metabolite norendoxifen is a potent and selective inhibitor of

aromatase (CYP19) and a potential lead compound for novel therapeutic agents. *Breast Cancer Res Treat* **2012**, *133* (1), 99-109.

132. Sgrignani, J.; Bon, M.; Colombo, G.; Magistrato, A., Computational approaches elucidate the allosteric mechanism of human aromatase inhibition: a novel possible route to Small-molecule regulation of CYP450s activities? *J Chem Inf Model* **2014**, *54* (10), 2856-68.

133. Magistrato, A.; Sgrignani, J.; Krause, R.; Cavalli, A., Single or Multiple Access Channels to the CYP450s Active Site? An Answer from Free Energy Simulations of the Human Aromatase Enzyme. *J Phys Chem Lett* **2017**, *8* (9), 2036-2042.

134. Egbuta, C.; Lo, J.; Ghosh, D., Mechanism of inhibition of estrogen biosynthesis by azole fungicides. *Endocrinology* **2014**, *155* (12), 4622-8.

135. Ghosh, D.; Lo, J.; Morton, D.; Valette, D.; Xi, J.; Griswold, J.; Hubbell, S.; Egbuta, C.; Jiang, W.; An, J.; Davies, H. M., Novel aromatase inhibitors by structure-guided design. *J Med Chem* **2012**, *55* (19), 8464-76.

136. Spinello, A.; Martini, S.; Berti, F.; Pennati, M.; Pavlin, M.; Sgrignani, J.; Grazioso, G.; Colombo, G.; Zaffaroni, N.; Magistrato, A., Rational design of allosteric modulators of the aromatase enzyme: An unprecedented therapeutic strategy to fight breast cancer. *Eur J Med Chem* **2019**, *168*, 253-262.

137. Lv, W.; Liu, J.; Skaar, T. C.; Flockhart, D. A.; Cushman, M., Design and synthesis of norendoxifen analogues with dual aromatase inhibitory and estrogen receptor modulatory activities. *J Med Chem* **2015**, *58* (6), 2623-48.

138. Lv, W.; Liu, J.; Skaar, T. C.; O'Neill, E.; Yu, G.; Flockhart, D. A.; Cushman, M., Synthesis of Triphenylethylene Bisphenols as Aromatase Inhibitors That Also Modulate Estrogen Receptors. *J Med Chem* **2016**, *59* (1), 157-70.

139. Lubczyk, V.; Bachmann, H.; Gust, R., Investigations on estrogen receptor binding. The estrogenic, antiestrogenic, and cytotoxic properties of C2-alkyl-substituted 1,1-bis(4-hydroxyphenyl)-2-phenylethenes. *J Med Chem* **2002**, *45* (24), 5358-64.

140. Zhao, L. M.; Jin, H. S.; Liu, J.; Skaar, T. C.; Ipe, J.; Lv, W.; Flockhart, D. A.; Cushman, M., A new Suzuki synthesis of triphenylethylenes that inhibit aromatase and bind to estrogen receptors  $\alpha$  and  $\beta$ . *Bioorg Med Chem* **2016**, *24* (21), 5400-5409.

141. Caciolla, J.; Spinello, A.; Martini, S.; Bisi, A.; Zaffaroni, N.; Gobbi, S.; Magistrato, A., Targeting Orthosteric and Allosteric Pockets of Aromatase via Dual-Mode Novel Azole Inhibitors. *ACS Med Chem Lett* **2020**, *11* (5), 732-739.

142. Minami, N.; Kijima, S., Reduction of o-Acylphenols through Ethyl o-Acylphenylcarbonates to o-Alkylphenols with Sodium Borohydride. *CHEMICAL & PHARMACEUTICAL BULLETIN* **1979**, 27 (6), 1490-1494.
143. Gobbi, S.; Hu, Q.; Zimmer, C.; Belluti, F.; Rampa, A.; Hartmann, R. W.; Bisi, A., Drifting of heme-coordinating group in imidazolylmethylxanthenes leading to improved selective inhibition of CYP11B1. *Eur J Med Chem* **2017**, 139, 60-67.
144. Gobbi, S.; Cavalli, A.; Negri, M.; Schewe, K. E.; Belluti, F.; Piazzini, L.; Hartmann, R. W.; Recanatini, M.; Bisi, A., Imidazolylmethylbenzophenones as highly potent aromatase inhibitors. *J Med Chem* **2007**, 50 (15), 3420-2.
145. Gobbi, S.; Hu, Q.; Foschi, G.; Catanzaro, E.; Belluti, F.; Rampa, A.; Fimognari, C.; Hartmann, R. W.; Bisi, A., Benzophenones as xanthone-open model CYP11B1 inhibitors potentially useful for promoting wound healing. *Bioorg Chem* **2019**, 86, 401-409.
146. Brynmor, J., The Halogenation of Phenolic Ethers and Anilides. Part VIII. Alkoxy- and Dialkylbenzophenones and Dialkylmethylsulphones. *J. Chem. Soc.* **1936**, 1231-1234.
147. Caciolla, J.; Martini, S.; Spinello, A.; Pavlin, M.; Simonelli, F.; Belluti, F.; Rampa, A.; Bisi, A.; Zaffaroni, N.; Gobbi, S.; Magistrato, A., Balanced dual acting compound targeting aromatase and estrogen receptor  $\alpha$  as an emerging therapeutic opportunity to counteract estrogen responsive breast cancer. (Submitted).
148. Pavlin, M.; Spinello, A.; Pennati, M.; Zaffaroni, N.; Gobbi, S.; Bisi, A.; Colombo, G.; Magistrato, A., A Computational Assay of Estrogen Receptor  $\alpha$  Antagonists Reveals the Key Common Structural Traits of Drugs Effectively Fighting Refractory Breast Cancers. *Sci Rep* **2018**, 8 (1), 649.
149. Lemhadri, M.; Fall, Y.; Doucet, H.; Santelli, M., Palladium-Catalysed Heck Reactions of Alk-1-en-3-ones with Aryl Bromides: A Very Simple Access to (E)-1-Arylalk-1-en-3-ones. *Synthesis-Stuttgart* **2009**, (6), 1021-1035.
150. Albarran-Velo, J.; Lavandera, I.; Gotor-Fernandez, V., Sequential Two-Step Stereoselective Amination of Allylic Alcohols through the Combination of Laccases and Amine Transaminases. *Chembiochem* **2020**, 21 (1-2), 200-211.
151. Le, P. Q.; Nguyen, T. S.; May, J. A., A general method for the enantioselective synthesis of  $\alpha$ -chiral heterocycles. *Org Lett* **2012**, 14 (23), 6104-7.
152. Zhu, M.; Du, H.; Li, J.; Zou, D.; Wu, Y.; Wu, Y., Synthesis of beta-heteroaryl carbonyl compounds via direct cross-coupling of allyl alcohols with

heteroaryl boronic acids under cooperative bimetallic catalysis. *Tetrahedron Letters* **2018**, *59* (14), 1352-1355.

153. Kawakami, J.; Kimura, K.; Yamaoka, M., A convenient synthesis of 4(5)-alkylacyl-1H-imidazoles from 4(5)-imidazolecarboxaldehyde. *Synthesis-Stuttgart* **2003**, (5), 677-680.

154. Miquel, J. F.; Olsson, K.; Sundbeck, B., Synthesis of unsymmetrical diphenylalkenes. *J Med Chem* **1963**, *6*, 774-80.

155. Iwasaki, S., Photochemistry of imidazolides. I. The photo-Fries-type rearrangement of N-substituted imidazoles. *Helv Chim Acta* **1976**, *59* (8), 2738-52.

156. Goldberg, A. A.; Wragg, A. H., Xanthones: cyclization of 3'-substituted 2-carboxydiphenyl ethers. *J. Chem. Soc.* **1958**, 4227-4234.

157. Liu, C.; Zhang, M.; Zhang, Z.; Zhang, S. B.; Yang, S.; Zhang, A.; Yin, L.; Swarts, S.; Vidyasagar, S.; Zhang, L.; Okunieff, P., Synthesis and anticancer potential of novel xanthone derivatives with 3,6-substituted chains. *Bioorg Med Chem* **2016**, *24* (18), 4263-4271.

158. Dale, H. H.; Laidlaw, P. P., The physiological action of beta-iminazolylethylamine. *J Physiol* **1910**, *41* (5), 318-44.

159. Best, C. H.; Dale, H. H.; Dudley, H. W.; Thorpe, W. V., The nature of the vaso-dilator constituents of certain tissue extracts. *J Physiol* **1927**, *62* (4), 397-417.

160. Parsons, M. E.; Ganellin, C. R., Histamine and its receptors. *Br J Pharmacol* **2006**, *147 Suppl 1*, S127-35.

161. Lieberman, P., The basics of histamine biology. *Ann Allergy Asthma Immunol* **2011**, *106* (2 Suppl), S2-5.

162. Hamm, H. E., The many faces of G protein signaling. *J Biol Chem* **1998**, *273* (2), 669-72.

163. Coleman, D. E.; Sprang, S. R., How G proteins work: a continuing story. *Trends Biochem Sci* **1996**, *21* (2), 41-4.

164. Merk, H. F., Standard treatment: the role of antihistamines. *J Investig Dermatol Symp Proc* **2001**, *6* (2), 153-6.

165. Ash, A. S.; Schild, H. O., Receptors mediating some actions of histamine. *Br J Pharmacol Chemother* **1966**, *27* (2), 427-39.

166. Black, J. W.; Duncan, W. A.; Durant, C. J.; Ganellin, C. R.; Parsons, E. M., Definition and antagonism of histamine H<sub>2</sub>-receptors. *Nature* **1972**, *236* (5347), 385-90.

167. Durant, G. J.; Ganellin, C. R.; Parsons, M. E., Dimaprit, [S-[3-(N,N-dimethylamino)propyl]isothiourea]. A highly specific histamine H<sub>2</sub>-receptor agonist. Part 2. Structure-activity considerations. 1977. *Agents Actions* **1994**, *43* (3-4), 139-43.
168. Daure, E.; Ross, L.; Webster, C. R., Gastroduodenal Ulceration in Small Animals: Part 2. Proton Pump Inhibitors and Histamine-2 Receptor Antagonists. *J Am Anim Hosp Assoc* **2017**, *53* (1), 11-23.
169. Arrang, J. M.; Garbarg, M.; Schwartz, J. C., Auto-inhibition of brain histamine release mediated by a novel class (H<sub>3</sub>) of histamine receptor. *Nature* **1983**, *302* (5911), 832-7.
170. Arrang, J. M.; Garbarg, M.; Lancelot, J. C.; Lecomte, J. M.; Pollard, H.; Robba, M.; Schunack, W.; Schwartz, J. C., Highly potent and selective ligands for histamine H<sub>3</sub>-receptors. *Nature* **1987**, *327* (6118), 117-23.
171. Van der Goot, H.; Schepers, M.; Sterk, G.; Timmerman, H., Isothiourea analogues of histamine as potent agonists or antagonists of the histamine H<sub>3</sub>-receptor. *European Journal of Medicinal Chemistry* **1992**, *27* (5), 511-517.
172. Ali, S. M.; Tedford, C. E.; Gregory, R.; Handley, M. K.; Yates, S. L.; Hirth, W. W.; Phillips, J. G., Design, synthesis, and structure-activity relationships of acetylene-based histamine H<sub>3</sub> receptor antagonists. *J Med Chem* **1999**, *42* (5), 903-9.
173. Wijtman, M.; Leurs, R.; de Esch, I., Histamine H<sub>3</sub> receptor ligands break ground in a remarkable plethora of therapeutic areas. *Expert Opin Investig Drugs* **2007**, *16* (7), 967-85.
174. Schwartz, J. C., The histamine H<sub>3</sub> receptor: from discovery to clinical trials with pitolisant. *Br J Pharmacol* **2011**, *163* (4), 713-21.
175. Lovenberg, T. W.; Roland, B. L.; Wilson, S. J.; Jiang, X.; Pyati, J.; Huvar, A.; Jackson, M. R.; Erlander, M. G., Cloning and functional expression of the human histamine H<sub>3</sub> receptor. *Mol Pharmacol* **1999**, *55* (6), 1101-7.
176. Nakamura, T.; Itadani, H.; Hidaka, Y.; Ohta, M.; Tanaka, K., Molecular cloning and characterization of a new human histamine receptor, HH4R. *Biochem Biophys Res Commun* **2000**, *279* (2), 615-20.
177. Liu, C.; Ma, X.; Jiang, X.; Wilson, S. J.; Hofstra, C. L.; Blevitt, J.; Pyati, J.; Li, X.; Chai, W.; Carruthers, N.; Lovenberg, T. W., Cloning and pharmacological characterization of a fourth histamine receptor (H<sub>4</sub>) expressed in bone marrow. *Mol Pharmacol* **2001**, *59* (3), 420-6.
178. Morse, K. L.; Behan, J.; Laz, T. M.; West, R. E.; Greenfeder, S. A.; Anthes, J. C.; Umland, S.; Wan, Y.; Hipkin, R. W.; Gonsiorek, W.; Shin, N.;

Gustafson, E. L.; Qiao, X.; Wang, S.; Hedrick, J. A.; Greene, J.; Bayne, M.; Monsma, F. J., Cloning and characterization of a novel human histamine receptor. *J Pharmacol Exp Ther* **2001**, *296* (3), 1058-66.

179. Oda, T.; Morikawa, N.; Saito, Y.; Masuho, Y.; Matsumoto, S., Molecular cloning and characterization of a novel type of histamine receptor preferentially expressed in leukocytes. *J Biol Chem* **2000**, *275* (47), 36781-6.

180. Zhu, Y.; Michalovich, D.; Wu, H.; Tan, K. B.; Dytko, G. M.; Mannan, I. J.; Boyce, R.; Alston, J.; Tierney, L. A.; Li, X.; Herrity, N. C.; Vawter, L.; Sarau, H. M.; Ames, R. S.; Davenport, C. M.; Hieble, J. P.; Wilson, S.; Bergsma, D. J.; Fitzgerald, L. R., Cloning, expression, and pharmacological characterization of a novel human histamine receptor. *Mol Pharmacol* **2001**, *59* (3), 434-41.

181. Nguyen, T.; Shapiro, D. A.; George, S. R.; Setola, V.; Lee, D. K.; Cheng, R.; Rauser, L.; Lee, S. P.; Lynch, K. R.; Roth, B. L.; O'Dowd, B. F., Discovery of a novel member of the histamine receptor family. *Mol Pharmacol* **2001**, *59* (3), 427-33.

182. Cogé, F.; Guénin, S. P.; Rique, H.; Boutin, J. A.; Galizzi, J. P., Structure and expression of the human histamine H4-receptor gene. *Biochem Biophys Res Commun* **2001**, *284* (2), 301-9.

183. Jongejan, A.; Lim, H. D.; Smits, R. A.; de Esch, I. J.; Haaksma, E.; Leurs, R., Delineation of agonist binding to the human histamine H4 receptor using mutational analysis, homology modeling, and ab initio calculations. *J Chem Inf Model* **2008**, *48* (7), 1455-63.

184. Panula, P.; Chazot, P. L.; Cowart, M.; Gutzmer, R.; Leurs, R.; Liu, W. L.; Stark, H.; Thurmond, R. L.; Haas, H. L., International Union of Basic and Clinical Pharmacology. XCVIII. Histamine Receptors. *Pharmacol Rev* **2015**, *67* (3), 601-55.

185. Medina, V. A.; Rivera, E. S., Histamine receptors and cancer pharmacology. *Br J Pharmacol* **2010**, *161* (4), 755-67.

186. Massari, N. A.; Medina, V. A.; Cricco, G. P.; Martinel Lamas, D. J.; Sambuco, L.; Pagotto, R.; Ventura, C.; Ciruolo, P. J.; Pignataro, O.; Bergoc, R. M.; Rivera, E. S., Antitumor activity of histamine and clozapine in a mouse experimental model of human melanoma. *J Dermatol Sci* **2013**, *72* (3), 252-62.

187. Medina, V.; Cricco, G.; Nuñez, M.; Martín, G.; Mohamad, N.; Correa-Fiz, F.; Sanchez-Jimenez, F.; Bergoc, R.; Rivera, E. S., Histamine-mediated signaling processes in human malignant mammary cells. *Cancer Biol Ther* **2006**, *5* (11), 1462-71.

188. Medina, V. A.; Brenzoni, P. G.; Lamas, D. J.; Massari, N.; Mondillo, C.; Nunez, M. A.; Pignataro, O.; Rivera, E. S., Role of histamine H<sub>4</sub> receptor in breast cancer cell proliferation. *Front Biosci (Elite Ed)* **2011**, *3*, 1042-60.
189. Martinel Lamas, D. J.; Croci, M.; Carabajal, E.; Crescenti, E. J.; Sambuco, L.; Massari, N. A.; Bergoc, R. M.; Rivera, E. S.; Medina, V. A., Therapeutic potential of histamine H<sub>4</sub> receptor agonists in triple-negative human breast cancer experimental model. *Br J Pharmacol* **2013**, *170* (1), 188-99.
190. Smits, R. A.; Leurs, R.; de Esch, I. J., Major advances in the development of histamine H<sub>4</sub> receptor ligands. *Drug Discov Today* **2009**, *14* (15-16), 745-53.
191. Hashimoto, T.; Harusawa, S.; Araki, L.; Zuiderveld, O. P.; Smit, M. J.; Imazu, T.; Takashima, S.; Yamamoto, Y.; Sakamoto, Y.; Kurihara, T.; Leurs, R.; Bakker, R. A.; Yamatodani, A., A selective human H(4)-receptor agonist: (-)-2-cyano-1-methyl-3-[(2R,5R)-5-[1H-imidazol-4(5)-yl]tetrahydrofuran-2-yl]methylguanidine. *J Med Chem* **2003**, *46* (14), 3162-5.
192. Lim, H. D.; van Rijn, R. M.; Ling, P.; Bakker, R. A.; Thurmond, R. L.; Leurs, R., Evaluation of histamine H<sub>1</sub>-, H<sub>2</sub>-, and H<sub>3</sub>-receptor ligands at the human histamine H<sub>4</sub> receptor: identification of 4-methylhistamine as the first potent and selective H<sub>4</sub> receptor agonist. *J Pharmacol Exp Ther* **2005**, *314* (3), 1310-21.
193. Lim, H. D.; Smits, R. A.; Bakker, R. A.; van Dam, C. M.; de Esch, I. J.; Leurs, R., Discovery of S-(2-guanidylethyl)-isothiourea (VUF 8430) as a potent nonimidazole histamine H<sub>4</sub> receptor agonist. *J Med Chem* **2006**, *49* (23), 6650-1.
194. Igel, P.; Geyer, R.; Strasser, A.; Dove, S.; Seifert, R.; Buschauer, A., Synthesis and structure-activity relationships of cyanoguanidine-type and structurally related histamine H<sub>4</sub> receptor agonists. *J Med Chem* **2009**, *52* (20), 6297-313.
195. Smits, R. A.; Lim, H. D.; Stegink, B.; Bakker, R. A.; de Esch, I. J.; Leurs, R., Characterization of the histamine H<sub>4</sub> receptor binding site. Part 1. Synthesis and pharmacological evaluation of dibenzodiazepine derivatives. *J Med Chem* **2006**, *49* (15), 4512-6.
196. Sander, K.; Kottke, T.; Tanrikulu, Y.; Proschak, E.; Weizel, L.; Schneider, E. H.; Seifert, R.; Schneider, G.; Stark, H., 2,4-Diaminopyrimidines as histamine H<sub>4</sub> receptor ligands--Scaffold optimization and pharmacological characterization. *Bioorg Med Chem* **2009**, *17* (20), 7186-96.
197. Thurmond, R. L.; Desai, P. J.; Dunford, P. J.; Fung-Leung, W. P.; Hofstra, C. L.; Jiang, W.; Nguyen, S.; Riley, J. P.; Sun, S.; Williams, K. N.; Edwards, J. P.; Karlsson, L., A potent and selective histamine H<sub>4</sub> receptor antagonist with anti-inflammatory properties. *J Pharmacol Exp Ther* **2004**, *309* (1), 404-13.

198. Terzioglu, N.; van Rijn, R. M.; Bakker, R. A.; De Esch, I. J.; Leurs, R., Synthesis and structure-activity relationships of indole and benzimidazole piperazines as histamine H<sub>4</sub> receptor antagonists. *Bioorg Med Chem Lett* **2004**, *14* (21), 5251-6.
199. Venable, J. D.; Cai, H.; Chai, W.; Dvorak, C. A.; Grice, C. A.; Jablonowski, J. A.; Shah, C. R.; Kwok, A. K.; Ly, K. S.; Pio, B.; Wei, J.; Desai, P. J.; Jiang, W.; Nguyen, S.; Ling, P.; Wilson, S. J.; Dunford, P. J.; Thurmond, R. L.; Lovenberg, T. W.; Karlsson, L.; Carruthers, N. I.; Edwards, J. P., Preparation and biological evaluation of indole, benzimidazole, and thienopyrrole piperazine carboxamides: potent human histamine h<sub>4</sub> antagonists. *J Med Chem* **2005**, *48* (26), 8289-98.
200. Lane, C. A.; Hay, D.; Mowbray, C. E.; Paradowski, M.; Selby, M. D.; Swain, N. A.; Williams, D. H., Synthesis of novel histamine H<sub>4</sub> receptor antagonists. *Bioorg Med Chem Lett* **2012**, *22* (2), 1156-9.
201. Sato, H.; Tanaka, K.; Shimazaki, M.; Urbahns, K.; Sakai, K.; Gantner, F.; Bacon, K. 2-aminopyrimidine derivatives. WO 2005/054239 A1. 2005.
202. Sato, H.; Fukushima, K.; Shimazaki, M.; Urbahns, K.; Sakai, K.; Ganter, F.; Bacon, K. 2-aminopyrimidine derivatives. WO 2005/014556 A1. 2005.
203. Carceller Gonzalez, E.; Salas Solana, J.; Soliva Soliva, R.; Medina Fuentes, E. M.; Marti Via, J. 2-aminopyrimidine derivatives as modulators of the histamine H<sub>4</sub> receptor activity. WO 2007/031529. 2007.
204. Bell, A., Simon; Lane, C., Alice, Louise; Mowbray, C. E.; Selby, M., Duncan; Swain, N., Alan; Williams, D., Howard Pyrimidine derivatives. WO 2007/072163 A2. 2007.
205. Raphy, G.; Watson, R., John; Hannah, D.; Pegurier, C.; Isabelle, O.-M.; Lock, C., James; Knight, R., Laurence; Owen, D., Alan, Novel 2-aminopyrimidine derivatives, processes for preparing them, pharmaceutical compositions thereof. WO 2008/031556 A2. 2008.
206. Cowart, M. D.; Altenbach, R. J.; Liu, H.; Hsieh, G. C.; Drizin, I.; Milicic, I.; Miller, T. R.; Witte, D. G.; Wishart, N.; Fix-Stenzel, S. R.; McPherson, M. J.; Adair, R. M.; Wetter, J. M.; Bettencourt, B. M.; Marsh, K. C.; Sullivan, J. P.; Honore, P.; Esbenshade, T. A.; Brioni, J. D., Rotationally constrained 2,4-diamino-5,6-disubstituted pyrimidines: a new class of histamine H<sub>4</sub> receptor antagonists with improved druglikeness and in vivo efficacy in pain and inflammation models. *J Med Chem* **2008**, *51* (20), 6547-57.
207. Liu, H.; Altenbach, R. J.; Carr, T. L.; Chandran, P.; Hsieh, G. C.; Lewis, L. G.; Manelli, A. M.; Milicic, I.; Marsh, K. C.; Miller, T. R.; Strakhova, M. I.; Vortherms, T. A.; Wakefield, B. D.; Wetter, J. M.; Witte, D. G.; Honore, P.; Esbenshade, T. A.; Brioni, J. D.; Cowart, M. D., cis-4-(Piperazin-1-yl)-

5,6,7a,8,9,10,11,11a-octahydrobenzofuro[2,3-h]quinazolin-2-amine (A-987306), a new histamine H4R antagonist that blocks pain responses against carrageenan-induced hyperalgesia. *J Med Chem* **2008**, *51* (22), 7094-8.

208. Cai, H.; Chavez, F.; Edwards, J., P.; Fitzgerald, A., E.; Liu, J.; Mani, N., S.; Neff, D., K.; Rizzolio, M., C.; Savall, B., M.; Smith, D., M.; Venable, J., D.; Wei, J.; Wolin, R., L. 2-aminopyrimidine modulators of the histamine H4 receptor. WO 2008/100565 A1. 2008.

209. Smits, R. A.; Lim, H. D.; Hanzer, A.; Zuiderveld, O. P.; Guaita, E.; Adami, M.; Coruzzi, G.; Leurs, R.; de Esch, I. J., Fragment based design of new H4 receptor-ligands with anti-inflammatory properties in vivo. *J Med Chem* **2008**, *51* (8), 2457-67.

210. Smits, R. A.; de Esch, I. J.; Zuiderveld, O. P.; Broeker, J.; Sansuk, K.; Guaita, E.; Coruzzi, G.; Adami, M.; Haaksma, E.; Leurs, R., Discovery of quinazolines as histamine H4 receptor inverse agonists using a scaffold hopping approach. *J Med Chem* **2008**, *51* (24), 7855-65.

211. Smits, R. A.; Adami, M.; Istyastono, E. P.; Zuiderveld, O. P.; van Dam, C. M.; de Kanter, F. J.; Jongejan, A.; Coruzzi, G.; Leurs, R.; de Esch, I. J., Synthesis and QSAR of quinazoline sulfonamides as highly potent human histamine H4 receptor inverse agonists. *J Med Chem* **2010**, *53* (6), 2390-400.

212. Shionogi; Masuda, T.; Tachibana, Y.; Miyagawa, M.; Hasegawa, T.; Tobinaga, H. Pyrimidine derivatives and pharmaceutical composition containing them. WO 2011/78143 A1. 2011.